Evaluating the Impacts of Grapevine Red Blotch Virus (GRBV) on Grape Metabolism to Develop Viticultural and Enological Mitigation Strategies

By

Arran Christine Rumbaugh

DISSERTATION

Submitted in partial satisfaction of the requirements for the degree of

DOCTOR OF PHILOSOPHY

in

Agricultural and Environmental Chemistry

in the

OFFICE OF GRADUATE STUDIES

of the

UNIVERSITY OF CALIFORNIA

DAVIS

_____

Dr. Anita Oberholster, Chair

_____

Dr. Hildegarde Heymann

_____

Dr. Dario Cantu

Committee in Charge

2022

ABSTRACT

Grapevines are one of the most economically important crops around the world. Like all crops, the productivity and vitality of grapevines are threatened by pathogens such as bacteria, fungi, and viruses. Numerous viral pathogens, both RNA and DNA, impact the metabolism of the grapevine and the grape berry, resulting in downstream effects for winemakers. Grapevine fanleaf virus and grapevine leafroll virus are two of the most prominent and detrimental viruses affecting grapevines in the world. However, in 2011, a new disease termed grapevine red blotch disease (GRBD) was discovered, and shortly thereafter, the etiological agent was determined to be a new geminivirus, grapevine red blotch virus (GRBV). Since then, researchers have focused on understanding the functioning of the virus, identifying potential insect vectors, and evaluating the viral impacts on grapevine performance, grape metabolism, and resulting wine composition. The current body of knowledge regarding GRBV is described in length in Chapter 1.

The aim of this work was to investigate the extent of the pathogenicity of GRBV under genotypic and environmental factors. We evaluated grape chemical composition through ripening and at harvest of Vitis vinifera L. cv. Cabernet Sauvignon was grafted on two different rootstocks (110R and 420A) in 2016 and 2017. Our research brought to light the variable influence different rootstocks and seasons could have on disease outcome in grapevines. A more drought-resistant, vigorous rootstock (110R) experienced worsened grape composition due to GRBV infection than 420A, whereas grapevines in a warmer season with heat exceeding 35□C (2017) outperformed those grown in a cooler season under GRBV infection. This work is explained in detail in Chapter 2.

In Chapter 3, a more extensive study examined the impact of GRBV on grape metabolism on the same set of grapevines described in Chapter 2. By analyzing the

transcriptome and metabolome of the grapes, we were able to identify specific pathways and compounds that were differentially affected by GRBV infection, such as the phenylpropanoid pathway and amino acid composition. In addition, we were able to uncover conserved responses to GRBV infection across both rootstocks and seasons. Our work determined a conserved upregulation of photosynthetic processes at harvest with a simultaneous increase in malate concentrations indicating an irregularity in energy metabolism. More importantly, differential co-expression analysis revealed the enrichment of a Dicer-like (DCL) protein, specifically DCL2, which is responsible for viral-induced gene silencing. This plant immune response can decrease viral load and symptomology in plants infected with a geminivirus. DCL2 was only induced at veraison across genotypes and environments, suggesting for the first time a phenological association with this antiviral plant immune response. Additionally, in 2017 the upregulation of DCL2 was higher than 2016 with concurrent decreases in viral gene expression suggesting a warmer season led to increased viral immunity and improved grape metabolism.

Overall, the lower total soluble sugar levels and higher titratable acidity at harvest in grapes infected with GRBV suggested a delay in ripening events, which corroborated previous studies. However, no study to date has investigated the impact of GRBV on grape cell wall composition even though the cell wall plays a large role in viral transport and phenolic extractability during winemaking. Therefore, in 2019 V. vinifera L. cv. Merlot grapes were collected through ripening to investigate the impact of GRBV on grape cell wall metabolism (Chapter 4). GRBV caused the induction of several transcripts encoding for cell wall modifying enzymes at harvest; however, this was not translated into the overall composition of the cell wall. This may indicate a post-transcriptional regulation of cell wall modification processes. Interestingly, GRBV upregulated genes associated with pathogenesis-related (PR) proteins and

pectin methylesterase inhibitors which correlated to higher levels of soluble proteins and pectin in the grape cell wall. Both PR proteins and pectin are known to retain important phenolic compounds during winemaking ultimately affecting the chemical and sensorial characteristics of a final wine. This work is examined in Chapter 4 which expresses the need for further investigation into the impact of GRBV on the grape cell wall.

Finally, in Chapter 5, we utilized our understanding from the previous findings to explore potential viticulture and enological mitigation strategies to alleviate the impact of GRBV on grape and wine composition. Since GRBV causes a delay in ripening events in grapes, an extended ripening was employed in two seasons to improve primary and secondary metabolite levels in the grapes and the resulting wines. In addition, since ethanol levels are positively correlated with phenolic extractability, chaptalization of GRBV grape musts was performed in one season to increase ethanol concentration during fermentation. Interestingly, a delayed harvest of GRBV fruit did increase phenolic extractability during winemaking, yet chaptalization did not. This suggests that grape maturity plays a larger role in the phenolic extraction of GRBV fruit than ethanol concentration during winemaking. Corresponding to results obtained in Chapter 4, the maturity of the grape cell wall potentially could cause the effects observed in Chapter 5. Extended ripening did improve metabolites levels in wines made with GRBV fruit; however, this was variable depending on the rootstock and season. Although the final wine composition of GRBV chaptalized wines was similar to the wines made from healthy fruit, sensorially they were differentiated, suggesting that this technique may not sufficiently alleviate the impact of GRBV on wine composition.

ACKNOWLEDGMENTS

Firstly, I would like to acknowledge Anita Oberholster. I couldn't ask for a better mentor. Graduate school comes with its ups and downs, and you were always there to guide me in the right direction and give me the confidence to succeed.

I would like to thank all my professors and mentors and UC Davis for all their wisdom and guidance through the past four years.

I will also like to acknowledge my Red Blotch partner in crime, Raul! Thank you for showing me the ropes from day one all the way to my last day.

I would like to thank all my friends old and new, for all the memories and experiences during graduate school. I will cherish those memories forever. Without my dear friends who encouraged and pushed me along the way, graduate school would have seemed impossible. I would like to acknowledge Jordan, for the countless hours of emotional support.

And finally, I would like to thank my family. Mom, thank you for always being my best friend, the person who has always been behind me, pushing me forward. Dad, thank you for always teaching me the value of hard work and perseverance. You taught me to never give up on my ambitions. You and mom gave us the world growing up. Dani, thank you for being the best big sister who continues showing me that I can do anything I set my mind to. And Jake, my 6'4" baby brother. Thank you for always showing me what true strength is and for showing me that there is no power greater than the power of knowledge and curiosity. Without my family, friends, and mentors I would never be where I am today.

TABLE OF CONTENTS

List of Tables

List of Figures

CHAPTER 1

Grapevine red blotch disease etiology and its impact on grapevine physiology and berry and wine composition

Formatted for publication in *Horticulturae* (accepted)

1.1 Abstract:

Grapevine red blotch virus (GRBV) is widespread in the United States since its identification in 2012. GRBV is the causative agent of grapevine red blotch disease (GRBD) which has caused detrimental economic impacts to the grape and wine industry. Understanding viral function, plant-pathogen interactions, and the effects of GRBV on grapevine performance remains essential in developing potential mitigation strategies. This comprehensive review examines the current body of knowledge regarding GRBV to highlight the gaps in knowledge and potential mitigation strategies for grape growers and winemakers

1.2 Introduction:

Plant viruses detrimentally impact crops around the world by reducing yields or decreasing crop quality. Unlike other plant pathogens, viruses are obligate intracellular parasites that require the host's machinery to replicate. *Vitis vinifera* is one of the most susceptible plant hosts to viral infection, with over 80 viruses recorded that potentially impact grapevine performance [1]. Major grapevine viruses are associated with four main disease complexes: (i) viruses responsible for infectious degeneration or decline disease, (ii) viruses associated with leafroll disease, (iii) viruses associated with the rugose wood complex, and (iv) viruses associated with the fleck complex [2]. A vast majority of these viruses are comprised of an RNA genome, with DNA viruses being relatively rare. Some of the most detrimental of these viruses to the grape and wine industry are grapevine fanleaf virus (GFLV), grapevine leafroll-

associated viruses (GLRaV), and the recently recognized grapevine red blotch virus (GRBV) [3–5].

Of the known GLRaVs, GLRaV-3 is the most important etiological agent of grapevine leafroll disease (GLRD) [6]. GLRaVs affect berry ripening by decreasing sugar accumulation and anthocyanin biosynthesis [7–9]. Foliar symptoms include interveinal reddening with the veins remaining green in red cultivars, with the interveinal area of leaves of white cultivars becoming chlorotic. Currently, no sources of resistance to GLRaVs have been documented in *V. vinifera* cultivars or clones [6,10,11]. However, variable responses to GLRaV infection has been recently reported, with some rootstocks outperforming others [9].

In 2008, Cabernet Sauvignon grapevines in Oakville, California (Oakville Experimental Station, Napa County, CA) were noticed with symptoms that resembled leafroll disease. However, in laboratory tests, symptomatic vines tested negative for all known leafroll viruses; thus, this new disease was termed grapevine red blotch disease (GRBD). Simultaneously, in New York, Oregon and Washington state, other researchers experienced the same phenomena. Independently, these research groups used rolling circle amplification (RCA) or large-scale sequencing methods to identify a new circular ssDNA virus comprised of 3,206 nt [12–14]. During this time, multiple nomenclatures were used to identify this virus: grapevine cabernet franc-associated virus [12], grapevine red blotch-associated virus [13], and grapevine geminivirus [14]. The almost identical isolates in these studies indicated that the same virus was infecting grapevines in multiple states across the United States [15,16], and the name grapevine red blotch-associated virus (GRBaV) was retained. Subsequently, GRBaV was included in the family Geminiviridae family of viruses and was found to be the causative agent of GRBD [12,13,17]. Therefore, the name grapevine red blotch virus (GRBV) was adopted and will be utilized for the remainder of this review. Since its identification, GRBV presence has

been reported in vineyards worldwide [18–22] and in raisin and table grapes [23] (Table 1). Interestingly, the presence of GRBV has remained absent in Old World vineyards [24].

Currently, an increasing number of new geminiviruses are being discovered, most likely due to the increasing capabilities of high throughput sequencing technologies. Due to globalization and exchanging of planting material, geminiviruses are rapidly expanding internationally and infecting several different hosts, causing new diseases and epidemics. Grape and wine production is one of the most economically important industries globally. With the economic impact of GRBV ranging from $2,213/ha to $68,548/ha in the United States [4], recent research has focused on virus functioning, epidemiology, impact on grape metabolism, and wine quality, as well as mitigation strategies. This review examines the existing body of knowledge regarding the viral genome, virus transmission, and the impacts of GRBV on grapevine physiology, grape metabolism, and wine composition. Sensory analysis of wine made from GRBV infected fruit is also discussed. Due to the impact of GRBV on grape and wine composition, recent research has revealed potential viticultural and enological mitigation strategies. Although great advancement in our knowledge of GRBV has been achieved, several important research questions remain unanswered and are discussed here.

Table 1.1 Distribution of GBRV in the US and around the world with the cultivar(s) and date reported.

Location	Country	Cultivar	Reference
California	USA	Cabernet franc	Al Rwahnih et al. 2012, 2013 [13,25]
California	USA	Zinfandel	Al Rwahnih et al. 2012, 2013 [13,25]
New York	USA	Cabernet franc	Krenz et al. 2012 [12]
Washington	USA	Merlot	Poojari et al. 2013 [26]
Washington	USA	Cabernet franc	Poojari et al. 2013 [26]
Texas	USA	Unknown	National Clean Plant Network 2013 [27]
Pennsylvania	USA	Merlot	Krenz et al. 2014 [15]
Pennsylvania	USA	Cabernet franc	Krenz et al. 2014 [15]
New York	USA	Pinot noir	Krenz et al. 2014 [15]
California	USA	Chardonnay	Krenz et al. 2014 [15]
California	USA	Pinot noir	Krenz et al. 2014 [15]
California	USA	Cabernet Sauvignon	Krenz et al. 2014 [15]
California	USA	Malbec	Krenz et al. 2014 [15]
California	USA	Petit Verdot	Krenz et al. 2014 [15]
California	USA	Cabernet franc	Krenz et al. 2014 [15]
California	USA	Riesling	Krenz et al. 2014 [15]
California	USA	Zinfandel	Krenz et al. 2014 [15]
Maryland	USA	Merlot	Krenz et al. 2014 [15]
Maryland	USA	Cabernet franc	Krenz et al. 2014 [15]
Virginia	USA	Unknown	Krenz et al. 2014 [15]
New Jersey	USA	Cabernet franc	Krenz et al. 2014 [15]
Oregon	USA	Pinot noir	Krenz et al. 2014 [15]; Seguin et al. 2014 [14]
California (herbarium)	USA	Early Burgundy	Al Rwahnih et al. 2015 [28]
California (National Clonal Germplasm Repository)	USA	Table grapes	Al Rwahnih et al. 2015 [23]
Arkansas	USA	Unknown	Sudarshana et al. 2015 [16]
Unknown	USA	Chambourcin (interspecific hybrid)	Sudarshana et al. 2015 [16]
California	USA	Free-living *Vitis* spp.	Perry et al. 2016 [29]
California	USA	Free-living *Vitis* spp.	Bahder et al. 2016 [30]
Suwon and Gyeongsan	South Korea	Unknown	Lim et al. 2016 [18]
Ontario	Canada	Cabernet franc	Poojari et al. 2017 [22]
Ontario	Canada	Chardonnay	Poojari et al. 2017 [22]
Ontario	Canada	Riesling	Poojari et al. 2017 [22]
Ontario	Canada	Cabernet franc	Poojari et al. 2017 [22]
Ontario	Canada	Syrah	Poojari et al. 2017 [22]
British Columbia	Canada	Muscat	Poojari et al. 2017 [22]
British Columbia	Canada	Cabernet franc	Poojari et al. 2017 [22]
British Columbia	Canada	Chardonnay	Poojari et al. 2017 [22]
British Columbia	Canada	Zinfandel	Poojari et al. 2017 [22]
British Columbia	Canada	Grenache	Poojari et al. 2017 [22]
British Columbia	Canada	Petit Verdot	Poojari et al. 2017 [22]
Nyon (Agroscope grapevine virus collection)*	Switzerland	Gamay	Reynard et al. 2018 [24]
Georgia	USA	Cynthiana (Norton, interspecific hybrid)	Brannen et al. 2018 [31]
Georgia	USA	Cabernet franc	Brannen et al. 2018 [31]
Missouri	USA	Crimson Cabernet	Schoelz et al. 2018 [32]
Ontario	Canada	Cabernet Franc	Xiao et al. 2018 [33]
Ontario	Canada	Cabernet Sauvignon	Xiao et al. 2018 [33]
Ontario	Canada	Pinot noir	Xiao et al. 2018 [33]
Ontario	Canada	Merlot	Xiao et al. 2018 [33]
Ontario	Canada	Syrah	Xiao et al. 2018 [33]
Ontario	Canada	Pinot Gris	Xiao et al. 2018 [33]

Location	Country	Cultivar	Reference
Ontario	Canada	Sauvignon Blanc	Xiao et al. 2018 [33]
Ontario	Canada	Chardonnay	Xiao et al. 2018 [33]
Ontario	Canada	Riesling	Xiao et al. 2018 [33]
Ontario	Canada	Gewürz traminer	Xiao et al. 2018 [33]
San Juan and Mendoza	Argentina	Flame Seedless	Luna et al. 2019 [20]
Baja California and Ensenada	Mexico	Pinot noir	Gasperin-Bulbarela et al. 2019 [19]
Baja California and Ensenada	Mexico	Merlot	Gasperin-Bulbarela et al. 2019 [19]
Baja California and Ensenada	Mexico	Nebbiolo	Gasperin-Bulbarela et al. 2019 [19]
Punjab	India	Unknown	Marwal et al. 2019 [21]
Tennessee	USA	Several cultivars	Soltani et al. 2020 [34]
Quebec	Canada	Pinot noir	Fall et al. 2020 [35]
Nova Scotia	Canada	Chardonnay	Poojari et al. 2020 [36]
Nova Scotia	Canada	Pinot noir	Poojari et al. 2020 [36]
Nova Scotia	Canada	New York Muscat (interspecific hybrid)	Poojari et al. 2020 [36]
Nova Scotia	Canada	Marechal Foch (interspecific hybrid)	Poojari et al. 2020 [36]
Idaho	USA	Syrah	Lee et al. 2021 [37]

* GRBV was reported absent in commercial Switzerland vineyards.

1.3 GRBV genome and taxonomy:

The first group to identify GRBV used deep sequencing of dsRNA fractions extracted from symptomatic grapevines followed by RCA on total nucleic acid extracts [25]. Through sequencing of RCA product, the circular monopartite ssDNA virus was identified. Phylogenetic analyses of the coat protein and replicase-associated protein sequences revealed GRBV to group with the family Geminiviridae [12,13,15,25]. However, this was outside all seven of the recognized genera of the time. At the time of its discovery, GRBV was the second largest geminivirus genome with 3,206 nt, and the closest related sequence, only sharing 50% identity, was a dicot-infecting *Mastrevirus*, chickpea chlorotic dwarf Syria virus [12,15]. In 2017, a new genus, *Grablovirus*, was established with GRBV as the type species [38]. The genus *Grablovirus* now includes two new viruses: wild Vitis virus 1 and Prunus geminivirus A [39–41].

The GRBV genome contains the characteristic nonanucleotide sequence ('TAATATT|AC') that functions as the viral origin of replication and is found in almost all members of Geminiviridae [12,13,15,16,25,26]. Like all geminiviruses, GRBV contains bi-

directional open reading frames (ORFs). For GRBV, there are three virion-sense ORFs and three complementary-sense ORFs. Virion-sense ORF V1 was determined to be the coat protein, and V2 and V3 are putative movement proteins. In the complementary-sense, C1 and C2 show similarity with other mastreviruses, including a putative spliced transcript. The C1 and C2 spliced transcript is thought to encode for the replication protein (Rep) (Figure 1.1). C3 is in the same reading frame as C1 and is internal. However, more recently, research has uncovered a seventh ORF, V0, a small ORF upstream of V2, also thought to be associated with viral movement [39]. This second splicing event in the virion-sense was discovered through investigating evidence for C1 and C2 splicing. Although virion-sense splicing is rarer than complementary-sense splicing for geminiviruses, it does occur in mastreviruses and capulaviruses (both in the Geminiviridae family) [39,42,43]. The occurrence in GRBV is a proposed regulatory enhancement to V1 gene expression due to the arrangement of V0, V2, and V1 [39].

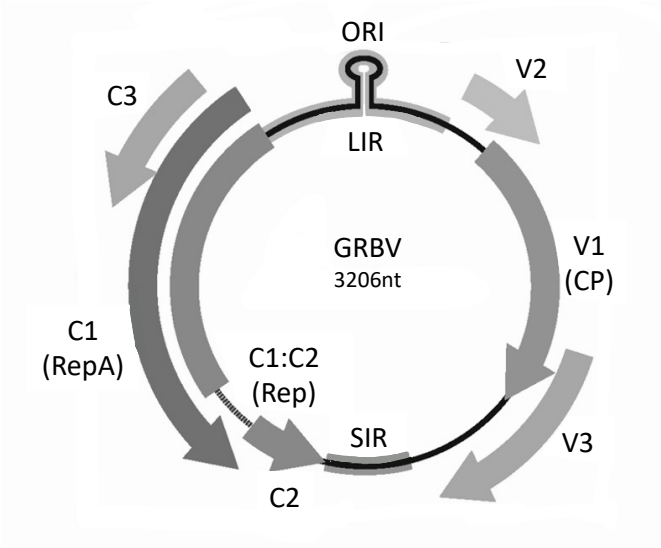

Figure 1.1. Genome organization of the genera *Grablovirus.* Adapted from International Committee on Taxonomy of Viruses [44] (upon the license agreement: https://creativecommons.org/licenses/by-sa/4.0/).

Phylogenetic analysis on genomes of known isolates of GRBV two distinct clades: clade 1 and clade 2. Clade 1 was determined to have the highest variability at 94.8% [15]. By comparing the GRBV genomes, recombination was associated with some of the variation observed that could influence the evolution of GRBV and may potentially contribute to the emergence of new virus variants [15,22]. Isolates in clade 2 showed less variability at 98.8% and contained the majority of the isolates analyzed. Between the two clades, nucleotide identity ranges from 91-93% [16]. Analysis of historical specimens of California revealed that a specific PCR product shared 97-100% nucleotide homology with GRBV. This specimen was collected from Sonoma County in 1940 and shared close nucleotide identity with clade 2 [28], indicating the presence of GRBV much earlier than 2008.

1.4 Causative role in GRBD: Symptoms, diagnosis, and transmission:

Many grapevine viruses, besides GFLV [45], have not been identified as the causal agent of their associated diseases. Although GRBV was associated with GRBD, it was not until 2018 when its etiological role in GRBD was proven. Through engineering infectious GRBV clones and agroinoculation, all four of Koch's postulates were fulfilled [17], thus establishing GRBV the causative agent of GRBD.

Symptoms of GRBD consist of red blotches on the leaf blades and margins, with reddening of the primary, secondary, and tertiary veins in red berry cultivars (as seen in Figure 1.2). In white berry cultivars, the foliar symptoms are less conspicuous and generally involve chlorotic lesions [46]. Foliar symptoms are not reported to appear until after veraison, with mature basal leaves being more symptomatic than the middle and terminal leaves and eventually dropping off prematurely when heavily symptomatic. The virus has also been detected in the roots, fruit clusters, and fruit juice [13,16]. Due to the similarity to abiotic and biotic stressors, such as nutrient deficiencies and other diseases, the most accurate method to

diagnose GRBV is DNA-based assays. However, another approach was developed using mass spectrometry to quantify GRBV in infected plants [47]. This report was the first to physically detect the predicted V1 and V2 gene products at the protein level. Based on the AAFNIFQR peptide abundance, the coat protein was consistently identified in higher amounts in petiole extracts of GRBV infected plants compared to leaf extracts.

The extent of the viral spread of GRBV in a vineyard depends on the location in North America. In New York, secondary spread via an insect vector has not been reported, and over a four-year study, no new infections were found [48]. However, other studies reported between 1-14% spread within a season in California vineyards [48,49], 11-55% in Oregon vineyards in two seasons [50], and 1% spread in British Columbia vineyards within a season [22]. Therefore, several researchers set out to determine the leading cause of new infections within a vineyard. GRBV is a graft transmissible, phloem limited virus with systemic movement detected in leaves distal to the graft site [13,26]. This, and the fact that GRBV infects several varieties, suggests that propagation material is the primary method of viral spread in the United States.

However, there is also evidence of viral spread caused by insect vectors. Research in the past five years on the spatiotemporal analysis of viral spread identified new GRBV infections near the vineyard's edge proximal to riparian habitats [49–52]. In addition, GRBV has been detected in free-living vines proximal to vineyards [29,30] but has yet to be detected in cover crops [48]. These results are consistent with short-distance spread of the virus potentially from a flying insect vector. Previous research indicates that GRBV is closely related to geminiviruses transmitted by *Auchenorrhyncha,* which are leafhoppers and treehoppers [51]. One of the first identified vectors in greenhouse settings was the Virginia creeper leafhopper, *Erythroneura ziczac* [26]. However, this insect mainly feeds on the mesophyll, not the phloem of plants, and GRBV was not reported to spread in regions of North America where *E. ziczac* is well-established [51].

Figure 1.2. Foliar symptoms of GRBD in Merlot grapevines in Napa, CA. Photo credit: Arran Rumbaugh.

The current recognized vector of GRBV is the three-cornered alfalfa hopper (*Spissistilus festinus,* Membracidae), yet successful transmission to grapevines via *S. festinus* has only been achieved in greenhouse settings [51]. Cieniewicz et al. (2017a) corroborated these results in which *S. festinus* was the only insect vector to show significant associations with the spatial pattern of infected vines. Higher numbers of *S. festinus* were found near the vineyard edges next to riparian areas, associating these habitats as potential infection sites for GRBV. Additional studies demonstrated circulative, nonpropagative transmission of GRBV by *S. festinus*, where the insect was able to successfully transmit GRBV to grapevine leaves [53]. However, other studies reveal a dissociation between *S. festinus* presence and viral spread in a vineyard, suggesting another vector may transmit GRBV [50]. To date, successful GBRV transmission by another insect has not been proven; yet, GRBV was detected in *Osbornellus borealis* (Cicadellidae), *Colladonus reductus* (Cicadellidae), and a *Melanoliarus* sp. (Cixiidae) [52], as well as *Stictocephala bisonia* and *Stictocephala basalis* [54], making them potential vector candidates.

1.5 Impacts on grapevine physiology:

Many plant viruses cause reductions in yields as well as decreases in crop quality. Grapevine viruses are no different, with many viruses detrimentally affecting the grape and wine industry. However, GRBV is the first identified geminivirus to infect grapevines, and its discovery was largely a result of poor juice wine quality in grapevines not known to have any leafroll-associated viruses. Since then, numerous studies have described the effects on grapevine performance in grapevines found to be infected by GRBV. Reports generally indicate a reduction in winter pruning weights, crop yield, as well as a change in berry weight. Pruning weights are consistently lower in GRBV infected vines, reductions ranging from 20-35% for GRBV infected vines compared to healthy vines suggesting that GRBV decreases vine vigor [24,26,46,55].

In Washington vineyards, crop yield decreased in GRBV infected Merlot and Cabernet Franc vines by 22% and 37%, respectively, which the authors attributed to a lower number of clusters per vine [26]. Similarly, in 2020, a 42% reduction in crop yield was reported, with 19% fewer clusters per vine and 47% fewer berries per cluster due to GRBV infections in Cabernet Franc grapevines in British Colombia vineyards [55]. White berried cultivars exhibited similar reductions in crop yields, with infected vines having as much as 22% lower yields compared to healthy vines [46]. Nonetheless, these results were inconsistent with data collected from Cabernet Sauvignon grapevines in California and Syrah grapevines in Idaho, where no significant differences were observed for crop yield and pruning weights [37,56]. Interestingly, increases in berry mass were also reported [46,55–57], which likely was caused by increased space due to fewer berries per cluster.

Decreased yields are potentially associated with decreased bud hardiness, photosynthesis, and stomatal conductance due to GRBV infection [24,55,56,58,59]. In healthy grapevines, higher sugar concentrations in the leaves due to decreased transportation through

phloem network into sinks (i.e. berries) can suppress photosynthesis [60]. When photosynthate production exceeds the translocation of hexoses, namely sucrose, from source-to-sink, surplus sucrose is transported to the guard cells resulting in stomatal closure [61]. Virus-infected leaves are known to have decreased photosynthesis and increased respiration and photosynthate products (i.e. sucrose), suggesting that viral infections can alter source-to-sink pathways in infected plants, where the leaves function as sinks. Higher foliar sugar levels have been reported in GRBV infected grapevines [26,56,59] similar to the leaves of sugar beets infected by beet curly top virus, a monopartite virus known to affect sugar beet production in the US for over a century [62]. Martínez-Lüscher et al. [56] proposed that GRBV impairs the translocation of sucrose from source-to-sink (leaves-to-fruit) resulting in decreases in stomatal conductance, better plant water status (stem water potential), and eventually leading to increases in foliar sugar levels. However, physical impairment of phloem unloading through callose deposits or other processes has not been observed. Levin and KC [57] proposed a similar picture on the seasonal progression of GRBD symptom development and suggests that reduction in stomatal conductance and leaf gas exchange and the onset of red-leaf foliar symptoms precedes the increase in stem water potential. Additionally, their data showed that the onset of foliar symptoms were not dependent on water status changes but on other factors such as the carbohydrate/nutrient alterations proposed by Martinez et al. [56].

Examination of foliar metabolite concentrations revealed higher concentrations of phenolic levels [59], with decreases in chlorophyll a and b, and carotenoid concentrations [24,55,58], all of which relate to premature senescence due to GRBV infection. Specific amino acid concentrations were also higher in GRBV infected leaves. Glycine, lysine, and proline were consistently higher through grape development in two cultivars [59]. A typical plant defense mechanism to stress is the accumulation of proline. Pathogen infections showed to activate the biosynthesis of proline via similar signaling components as salicylic acid (SA) [63],

the latter also being related to plant defense responses and elevated in concentration due to GRBV infections [64]. A more in-depth examination of the proteome of GRBD infected leaves clearly revealed higher expression of proteins than in healthy plants. Key enzymes in the phenylpropanoid pathway, ANS, ANR, and CHS, were all upregulated in GRBV infected leaves and petioles [47]. GLRaV infections generate similar responses at the transcriptomic level, leading to the development of red foliar symptoms of GLRD [8], which are postulated to be associated with increased foliar sugar levels [26]. Together, the induction of the flavonoid pathway and increases in proline levels in GBRV infected leaves indicates the activation of defense mechanisms.

1.6 Impairment to grape metabolism:

Like GLRD, GRBD characteristically decreases total soluble sugars (TSS) in grape berries, supporting the notion that GRBV infection impairs the translocation of sugar from the leaves to the grape berry. Concurrently, titratable acidity (TA) and malic acid levels are higher, consistent with a disruption in grape ripening events [16,24,37,46,55,56,58,65,66]. At veraison, energy utilization in the grape switches from sugar to organic acids, primarily malic acid. As sugars begin to accumulate in the vacuole, malic acid is transported into the cytosol and becomes available for energy metabolism, amino acid interconversions, and secondary metabolite synthesis, such as flavonoids. Malic acid catabolism results in a decrease in berry TA and increases pH. Interestingly, higher titratable acidity or malic acid content almost never correspond with lower pH values [46,47,55,58,65]. Higher potassium levels may cause this dissociation, yet only one study observed elevated potassium levels due to GRBV [46], where as another observed decreases [67]. It should be noted that in these studies, measurements were performed on a composite grape sample with no replications from asymptomatic and symptomatic grapevines at harvest in only one season. Like sugar, potassium is also imported

into the berry through the phloem. Since sucrose is transported in plants from source to sink via specific sucrose carriers (SoSUT1) [68], it is plausible that physical phloem impairment may inhibit the transport of sucrose, but not small ions. The positive correlation with potassium concentration and a plants resistance to pathogens is well-documented [69–71]. In addition, potassium concentrations affect hormone abundances of SA and jasmonic acid that are positively related to acquired systemic resistance to pathogens [69]. In a study evaluating genetic modulation and hormonal network alterations due to GRBV infection, SA concentrations were significantly higher towards the end of ripening [64]. Although it is plausible that GRBD may lead to higher berry potassium concentrations to fight off the infection, in less than half of viral infections studied did potassium increases lead to resistance [70]. Future studies would need to investigate the ionome of grapevines to unravel the interplay between potassium and other minerals and GRBV infection. Lastly, GRBV mainly elevates berry amino acid concentrations, hypothesized to be from a reallocation of substrates for grape energy metabolism and as a defense response [65].

During berry development, many secondary metabolites are synthesized, the majority of which are highly affected by environmental and genotypic factors. Flavonoids, synthesized via the phenylpropanoid pathway, are the most widely studied due to their important organoleptic properties [72–75]. Plant-pathogen interactions derived from viral infections commonly alter flavonoid biosynthesis [64,76–78]. GRBD imparts variable alterations to flavonoid concentrations in berries, with the most damaging being decreases in anthocyanin concentrations [16,26,37,55,56,64–66,79]; however, these results are not always statistically significant. Monomeric malvidin derivatives, the most common anthocyanin form, were found to be either higher or unimpacted due to GRBV infection [56,65] to the detriment of the less abundant anthocyanin forms. Reduction of anthocyanin accumulation in grapes has been associated with genetic suppression of the phenylpropanoid pathway (68% of genes) and

decreases in abscisic acid levels due to GRBV infection [64]. Abscisic acid is an essential hormone that positively regulates ripening in grapevines, and its accumulation correlates with anthocyanin biosynthesis [80,81]. Taken together, GRBV unfavorably alters the phenylpropanoid pathway consistent with delays in ripening events.

GRBD generally increased flavonol concentrations in white-berry cultivars [46,65], potentially related to lower vine vigor increasing sun exposure [72]. However, one study did observe lower flavonol levels in grapes [55]. The concentrations of flavan-3-ols and proanthocyanidins (condensed tannins) greatly depended on the grapevine genotype and environmental/seasonal factors [46,55,56,65,79]. However, skin proanthocyanidins were occasionally higher in GRBV infected grapes, potentially caused by a plant defense response [78].

Volatile compounds synthesized in the grape berry prior to harvest are also impacted due to GRBV infection [79]. In a two-year study evaluating the impact of GRBV on Cabernet Sauvignon grafted onto two different rootstocks, GRBV consistently decreased levels of almost all volatile compounds, except for C6 alcohols and aldehydes. These aroma compounds are synthesized in the lipoxygenase pathway and accumulate in grapes until the TSS reaches around 18 °Brix [82], with the majority of them decreasing thereafter. The impact of GRBV on the volatilome of grapes further supports evidence that the virus infection delays ripening events. Similar to other reports, the extent of these effects depend on the genotypic and environmental differences [79]. The summary of GRBV impact on grapevine physiology and grape metabolism is shown in Figure 1.3 below.

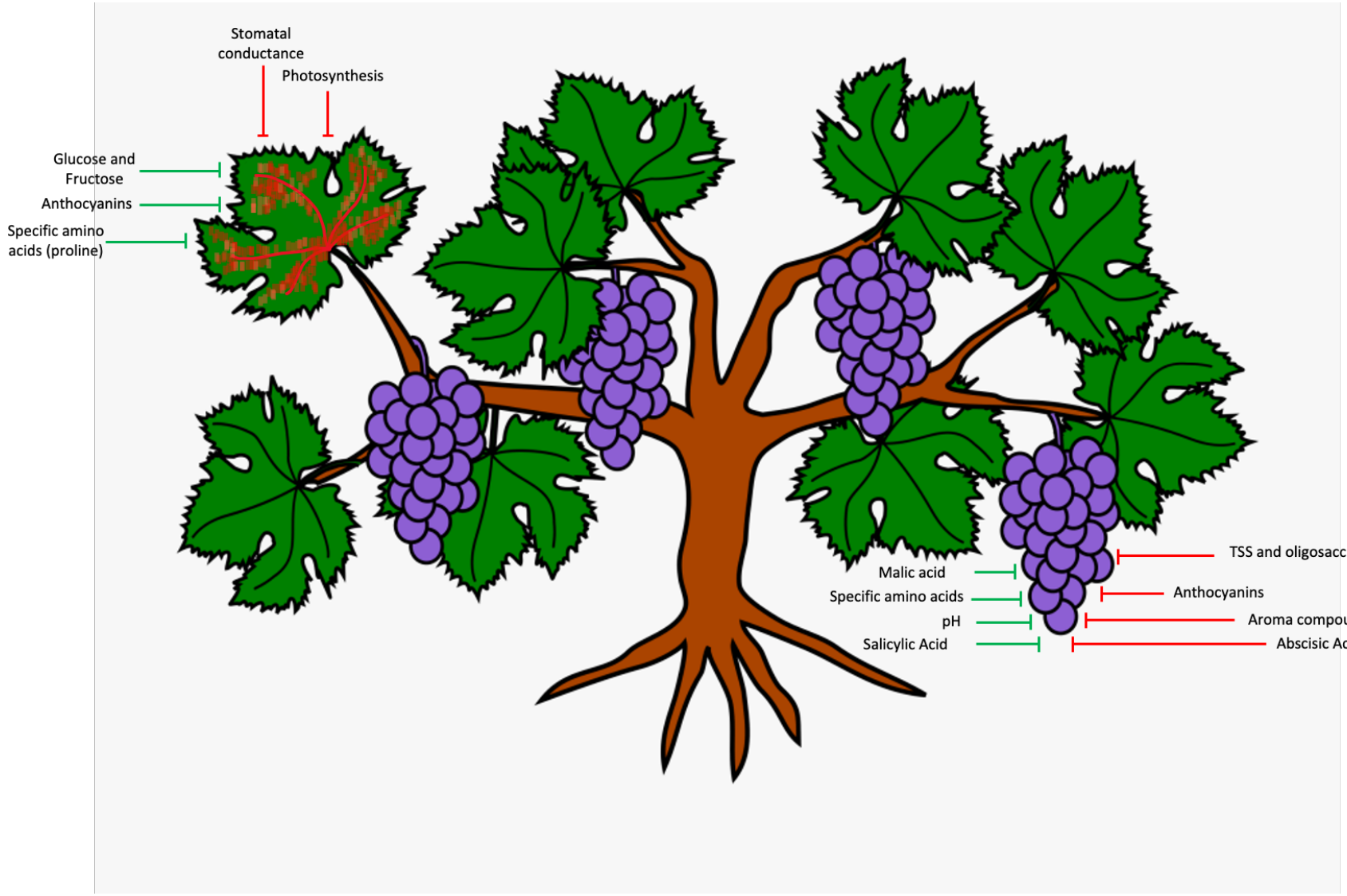

Figure 1.3. The overall impact of grapevine red blotch virus (GRBV) on grapevine physiology and grape metabolism. Green indicates an increase and red indicates a decrease in concentration. TSS= total soluble solids.

1.7 Impact on wine composition:

Currently, very few studies report how GRBV infected grapevines affect final wine composition and sensory attributes. Girardello et al. [46] not only analyzed the impact of GRBD on Chardonnay grape composition but also on wine composition over three seasons. Consistently, GRBV infected vines produced wines with reduced ethanol, correlated to the lower sugar levels at harvest. Although the TA and pH of fermenting wines were adjusted in each season using tartaric acid, the pH was generally higher in wines made from diseased fruit. Once again, the higher pH was explained by higher potassium levels where wines made from healthy fruit were 50% lower in potassium concentrations than wines made from diseased fruit [46]. However, this was only evaluated in one season, so inferences of the impact of GRBV on potassium need further confirmation. The lower ethanol content in wines made from GRBV infected grapes also seemed to affect the aroma profile of the final wines. Esterification during winemaking involves reactions of carboxylic acids and ethanol [83] to produce ethyl ester aroma compounds described as fruity and sweet (http://www.flavornet.org). As previously reported, GRBD lowers concentrations of carboxylic acids in fruit [65] and final ethanol concentrations in wines, ultimately decreasing the production of ethyl esters in the final wines. Sensorily, these panelists were able to distinguish between Chardonnay RB(+) wines and RB(-) wines, where wines made from diseased fruit were rated significantly lower than wines made from healthy fruit for hot mouthfeel, spicy and citrus aroma, and sweet taste attributes, and significantly higher for greener aromas such as apple.

Similar results were obtained in studies analyzing the impact of GRBV on final wine composition made from red-berried cultivars. Alcohol levels were consistently lower in wines made from GRBV infected fruit, which led to noticeable differences in the sensory characteristics [55,67]. Sour and green aromas were general attributes for wines made from GRBD fruit

correlating with unripe fruit. Simultaneously, these wines were rated lower for alcohol aroma, fruit aroma, and hot mouthfeel. Generally, the flavonoid grape composition differences were transferred into the resulting wines, where GRBV infected fruit produced red wines that were lighter and brighter (based on analysis of wine lightness, chroma and hue values) and more astringent [55]. These differences were attributed to the reported lower anthocyanin and polymeric pigment concentrations and higher tannin concentrations, respectively [67]. It is well accepted that flavonoid concentrations can significantly impact the overall quality of a wine, especially red wines. A research study that investigated the relationship between grape composition and perceived wine 'quality' found grapes with increased anthocyanin and skin tannin concentrations resulted in wines with increased tannin and color and better ratings by wine judges [84]. This suggests that GRBV not only detrimentally impacts grapevine performance but also wine composition and quality.

1.8 Discussion:

Geminiviruses have been causing detrimental impacts to crop production and vitality for over 100 years, yet it was only in 1995 when Geminiviridae family was established [85]. GRBV is one of the newest geminiviruses identified and is widespread in the United States and Canada affecting premium wine producing states currently. The adverse impacts of GBRV on grapevine performance, berry metabolism, and final wine composition have highlighted the importance of clean propagation material. PCR test for GRBV has helped to identify propagation material free from GRBV before sale. Researchers are pursuing studies to further investigate virus functioning, plant-pathogen interactions, as well as transmissibility of GRBV. Determining potential insect vectors of GRBV is crucial for pest management and to impede the spread of the virus. With an

increase in studies providing more information regarding GRBV, and the identification of an insect vector, *S. festinus*, an updated economic impact assessment can be made which will likely be more prominent than previously reported [4]. Mitigation strategies available to grape growers and winemakers are limited, with rogueing infected vines or complete vineyard block replacement when the disease incidence is high (>30%) being the most reliant [4].

Few studies have attempted to examine viticultural and enological techniques that potentially could alleviate the damaging impact of GRBV on a vineyard and winery [55,56]. One study extended the ripening time of GRBV infected fruit which further decreased TA levels and anthocyanin concentrations. It was concluded that a delayed harvest is not sufficient to coalesce all grape composition parameters, and results are unpredictable from season to season [56]. However, longer hang time and higher sugars does negate the impact of alcohol differences. Additionally, a later study examined the impact of water deficits on Pinot noir fruit quality in GRBV infected grapevines [57]. Authors determined that although water deficits did not impact the onset of grapevine foliar symptoms, there was an increase in symptom progression through grape ripening if the water deficits were severe. The adverse effects of water deficit on yield parameters (specifically berries per cluster) in GRBV infected vines also indicated that GRBV may impair carbohydrate partitioning to reproductive organs during water deficits. Overall, this research concluded that in some cases water deficit may worsen fruit quality and that the negative impacts of GRBV on grapevine physiology and grape metabolism cannot be alleviated by water deficit irrigation.

Alternatively, Bowen et al. [55] evaluated an enological mitigation technique to ameliorate the impact of GRBV on wine composition. They observed that small percentages of GRBV fruit included during winemaking increased the chemical and sensorial similarity to wines made from

healthy fruit. However, once 20% GRBD fruit was incorporated, the differences were noticeable and more similar to wines made from 100% GRBD fruit [55]. These findings will depend on GRBV impact in a specific season as large seasonal variability has been observed [65,67].

Together, these studies show the possibilities to mitigate GRBV effects available to grape growers and winemakers after GRBV is established in a vineyard. However, it is well documented that the impact of GRBV on grapevine performance and grape metabolism is dependent on genotypic and environmental factors [37,46,55,56,65,79]. To determine potentially resistant or susceptible genotypes and favorable seasonal factors, further research is needed to examine how plant-pathogen interactions may vary.

Besides sugar content, one of the most damaging impacts of GRBV on fruit and wine quality is phenolic composition. Many factors may influence the flavonoid concentrations in a final wine, such as interactions with cell walls, cell integrity and thickness, and initial grape flavonoid concentrations. Generally, the extractability of flavonoids into the wine matrix increases as the grape matures [86]. This is due primarily to changes in grape cell wall composition and integrity. However, there is limited research on overall plant-virus interactions regarding fruit skin cell wall metabolism, even though the cell wall plays a crucial role in the initiation of virus spread and as a defense mechanism [87]. It was postulated that GRBV alters the cell wall rigidity of leaves due to the increased yields of extracted proteins [47]; however, alterations to grape cell wall compositions are still unknown. Examining how GRBV impacts grape cell wall metabolism could lead to enological techniques to alter grape musts' composition and increase phenolic extractability and composition in a final wine.

Overall, the current body of knowledge on GRBV has dramatically expanded since 2012. Significant progress has been made in determining the impact of GRBV on grape metabolism and

how this relates to wine composition and sensory characteristics. This has guided future research to understand further viral impacts on specific metabolic pathways and plant defense mechanisms to develop mitigation strategies.

Author Contributions: Conceptualization, A.C.R., M.R.S., and A.O.; writing—original draft preparation, A.C.R.; writing—review and editing, A.C.R., M.R.S., and A.O.; supervision, A.O.; project administration, A.O.; funding acquisition, A.O. All authors have read and agreed to the published version of the manuscript.

Funding: This review received no external funding.

Acknowledgments: The authors would like to thank their respective funding bodies: American vineyard foundation (AVF), the California Department of Food and Agriculture (CDFA), and the United States Department of Agriculture (USDA). The authors would also like to thank the support of the Viticulture and Enology Department, the Plant Pathology Department, and the Agricultural and Environmental Chemistry Graduate Group at the University of California, Davis, CA, USA.

Conflicts of Interest: The authors declare no conflict of interest.

1.9 References:

1. Fuchs, M. Grapevine viruses: a multitude of diverse species with simple but overall poorly adopted management solutions in the vineyard. *J. Plant Pathol.* 2020, *102*, 643–653.
2. Dolja, V. V; Meng, B.; Martelli, G.P. Evolutionary Aspects of Grapevine Virology. In *Grapevine Viruses: Molecular Biology, Diagnostics and Management*; Meng, B., Martelli, G.P., Golino, D.A., Fuchs, M., Eds.; Springer International Publishing, 2017; pp. 659–688 ISBN 978-3-319-57706-7.
3. Martelli, G.P. DIRECTORY OF VIRUS AND VIRUS-LIKE DISEASES OF THE GRAPEVINE AND THEIR AGENTS. *J. Plant Pathol.* 2014, *96*, 1–136.
4. Ricketts, K.D.; Gómez, M.I.; Fuchs, M.F.; Martinson, T.E.; Smith, R.J.; Cooper, M.L.; Moyer, M.M.; Wise, A. Mitigating the economic impact of grapevine red blotch: Optimizing disease management strategies in U.S. vineyards. *Am. J. Enol. Vitic.* 2017, *68*, 127–135.
5. Ricketts, K.D.; Gomez, M.I.; Atallah, S.S.; Fuchs, M.F.; Martinson, T.E.; Battany, M.C.; Bettiga, L.J.; Cooper, M.L.; Verdegaal, P.S.; Smith, R.J. Reducing the economic impact of grapevine leafroll disease in california: Identifying optimal disease management strategies. *Am. J. Enol. Vitic.* 2015, *66*, 138–149.
6. Maree, H.J.; Almeida, R.P.P.; Bester, R.; Chooi, K.M.; Cohen, D.; Dolja, V. V.; Fuchs, M.F.; Golino, D.A.; Jooste, A.E.C.; Martelli, G.P.; et al. Grapevine leafroll-associated virus 3. *Front. Microbiol.* 2013, *4*, 1–21.
7. Vega, A.; Gutiérrez, R.A.; Peña-Neira, A.; Cramer, G.R.; Arce-Johnson, P. Compatible GLRaV-3 viral infections affect berry ripening decreasing sugar accumulation and anthocyanin biosynthesis in *Vitis vinifera*. *Plant Mol. Biol.* 2011, *77*, 261–274.
8. Gutha, L.R.; Casassa, L.F.; Harbertson, J.F.; Naidu, R.A. Modulation of flavonoid biosynthetic pathway genes and anthocyanins due to virus infection in grapevine (*Vitis vinifera* L.) leaves. *BMC Plant Biol.* 2010, *10*, 187.
9. Vondras, A.M.; Lerno, L.; Massonnet, M.; Minio, A.; Rowhani, A.; Liang, D.; Garcia, J.; Quiroz, D.; Figueroa-Balderas, R.; Golino, D.A.; et al. Rootstock influences the effect of grapevine leafroll-associated viruses on berry development and metabolism via abscisic acid signalling. *Mol. Plant Pathol.* 2021, 1–22.
10. Naidu, R.; Rowhani, A.; Fuchs, M.; Golino, D.; Martelli, G.P. Grapevine Leafroll: A complex viral disease affecting a high-value fruit crop. *Plant Dis.* 2014, *98*, 1172–1185.
11. Oliver, J.E.; Fuchs, M. Tolerance and resistance to viruses and their vectors in vitis sp.: A virologist's perspective of the literature. *Am. J. Enol. Vitic.* 2011, *62*, 438–451.
12. Krenz, B.; Thompson, J.R.; Fuchs, M.; Perry, K.L. Complete Genome Sequence of a New Circular DNA Virus from Grapevine. *J. Virol.* 2012, *86*, 7715–7715.
13. Al Rwahnih, M.; Dave, A.; Anderson, M.M.; Rowhani, A.; Uyemoto, J.K.; Sudarshana, M.R. Association of a DNA Virus with Grapevines Affected by Red Blotch Disease in California. *Phytopathology* 2013, *103*, 1069–1076.
14. Seguin, J.; Rajeswaran, R.; Malpica-López, N.; Martin, R.R.; Kasschau, K.; Dolja, V. V.; Otten, P.; Farinelli, L.; Pooggin, M.M. De novo reconstruction of consensus master genomes of plant RNA and DNA viruses from siRNAs. *PLoS One* 2014, *9*, 1–8.
15. Krenz, B.; Thompson, J.R.; Mclane, H.L.; Fuchs, M.; Perry, K.L. Phyto-02-14-0053-R. 2014, 1232–1240.
16. Sudarshana, M.R.; Perry, K.L.; Fuchs, M.F. Grapevine Red Blotch-Associated Virus, an

Emerging Threat to the Grapevine Industry. *Phytopathology* 2015, 1026–1032.
17. Yepes, L.M.; Cieniewicz, E.; Krenz, B.; McLane, H.; Thompson, J.R.; Perry, K.L.; Fuchs, M. Causative Role of Grapevine Red Blotch Virus in Red Blotch Disease. *Phytopathology* 2018, *108*, 902–909.
18. Lim, S.; Igori, D.; Zhao, F.; Moon, J.; Cho, I.-S.; Choi, G.-S. First report of Grapevine red blotch-associated virus on grapevine in Korea. *Plant Dis.* 2016, *100*, 1957.
19. Gasperin-Bulbarela, J.; Licea-Navarro, A.F.; Pino-Villar, C.; Hernandez-Martínez, R.; Carrillo-Tripp, J. First report of grapevine red blotch virus in Mexico. *Plant Dis.* 2019, *103*, 381.
20. Luna, F.; Debat, H.; Gomez-Talquenca, S.; Moyano, S.; Zavallo, D.; Asurmendi, S. First report of grapevine red blotch virus infecting grapevine in Argentina. *J. Plant Pathol.* 2019, *101*.
21. Marwal, A.; Kumar, R.; Paul Khurana, S.M.; Gaur, R.K. Complete nucleotide sequence of a new geminivirus isolated from *Vitis vinifera* in India: a symptomless host of Grapevine red blotch virus. *VirusDisease* 2019, *30*, 106–111.
22. Poojari, S.; Lowery, D.T.; Rott, M.; Schmidt, A.M.; Úrbez-Torres, J.R. Incidence, distribution and genetic diversity of Grapevine red blotch virus in British Columbia. *Can. J. Plant Pathol.* 2017, *39*, 201–211.
23. Al Rwahnih, M.; Rowhani, A.; Golino, D.A.; Islas, C.M.; Preece, J.E.; Sudarshana, M.R. Detection and genetic diversity of Grapevine red blotch-associated virus isolates in table grape accessions in the National Clonal Germplasm Repository in California. *Can. J. Plant Pathol.* 2015, *37*, 130–135.
24. Reynard, J.S.; Brodard, J.; Dubuis, N.; Zufferey, V.; Schumpp, O.; Schaerer, S.; Gugerli, P. Grapevine red blotch virus: Absence in Swiss vineyards and analysis of potential detrimental effect on viticultural performance. *Plant Dis.* 2018, *102*, 651–655.
25. Al Rwahnih, M.; Dave, A.; Anderson, M.M.; Uyemoto, J.K.; Sudarshana, M.R. Association of a circular DNA virus in grapevines affected by red blotch disease in California. In Proceedings of the Proc. 17th Congr. Int. Counc. Study of Virus and Virus-Like Diseases of the Grapevine (ICVG); Davis, CA, 2012.
26. Poojari, S.; Alabi, O.J.; Fofanov, V.Y.; Naidu, R.A. A Leafhopper-Transmissible DNA Virus with Novel Evolutionary Lineage in the Family *Geminiviridae* Implicated in Grapevine Redleaf Disease by Next-Generation Sequencing. *PLoS One* 2013, *8*.
27. National Clean Plant Network Fact Sheet: Grapevine Red Blotch Disease Available online: http://ucanr.edu/sites/NCPNGrapes/files/161782.pdf.
28. Al Rwahnih, M.; Rowhani, A.; Golino, D. First Report of Grapevine red blotch-associated virus in Archival Grapevine Material From Sonoma County, California. *Dis. Notes* 2015.
29. Perry, K.L.; McLane, H.; Hyder, M.Z.; Dangl, G.S.; Thompson, J.R.; Fuchs, M.F. Grapevine red blotch-associated virus is Present in Free-Living *Vitis* spp. Proximal to Cultivated Grapevines. *Phytopathology* 2016, *106*, 663–670.
30. Bahder, B.W.; Zalom, F.G.; Sudarshana, M.R. An evaluation of the flora adjacent to wine grape vineyards for the presence of alternative host plants of grapevine red blotch-associated virus. *Plant Dis.* 2016, *100*, 1571–1574.
31. Brannen, P.M.; Deom, C.M.; Alabi, O.J.; Naidu, R.A. Prevalence of viruses in commercial wine grape vineyards in Georgia. *Plant Heal. Prog.* 2018, *19*, 342–346.
32. Schoelz, J.E.; Adhab, M.; Qiu, W.; Petersen, S.; Volenberg, D. *First Report of Grapevine Red Blotch Virus in Hybrid Grapes in Missouri*; 2018; Vol. 103;.

33. Xiao, H.; Shabanian, M.; Moore, C.; Li, C.; Meng, B. Survey for major viruses in commercial *Vitis vinifera* wine grapes in Ontario. *Virol. J.* 2018, *15*, 1–11.
34. Soltani, N.; Hu, R.; Hensley, D.D.; Lockwood, D.L.; Perry, K.L.; Hajimorad, M.R. A Survery for Nine Major Viruses of Grapevines in Tennessee Vineyards. *Plant Heal. Prog.* 2020, *21*, 157–161.
35. Fall, M.L.; Xu, D.; Lemoyne, P.; Ben Moussa, I.E.; Beaulieu, C.; Carisse, O. A diverse virome of leafroll-infected grapevine unveiled by dsRNA sequencing. *Viruses* 2020, *12*.
36. Poojari, S.; Moreau, D.L.; Kahl, D.; Ritchie, M.; Ali, S.; Úrbez-Torres, J.R. Disease incidence and genetic variability of economically important grapevine viruses in Nova Scotia. *Can. J. Plant Pathol.* 2020, *42*, 584–594.
37. Lee, J.; Rennaker, C.D.; Thompson, B.D.; Karasev, A. V. Influence of Grapevine red blotch virus (GRBV) on Idaho 'Syrah' grape composition. *Sci. Hortic. (Amsterdam).* 2021, *282*.
38. Varsani, A.; Roumagnac, P.; Fuchs, M.; Navas-Castillo, J.; Moriones, E.; Idris, A.; Briddon, R.W.; Rivera-Bustamante, R.; Murilo Zerbini, F.; Martin, D.P. *Capulavirus* and *Grablovirus*: two new genera in the family *Geminiviridae*. *Arch. Virol.* 2017, *162*, 1819–1831.
39. Vargas-Asencio, J.; Liou, H.; Perry, K.L.; Thompson, J.R. Evidence for the splicing of grablovirus transcripts reveals a putative novel open reading frame. *J. Gen. Virol.* 2019, *100*, 709–720.
40. Perry, K.L.; McLane, H.; Thompson, J.R.; Fuchs, M. A novel grablovirus from non-cultivated grapevine (*Vitis* sp.) in North America. *Arch. Virol.* 2018, *163*, 259–262.
41. Al Rwahnih, M.; Alabi, O.J.; Westrick, N.M.; Golino, D. Prunus geminivirus A: A novel *grablovirus* infecting *prunus* spp. *Plant Dis.* 2018, *102*, 1246–1253.
42. Bernardo, P.; Golden, M.; Akram, M.; Naimuddin; Nadarajan, N.; Fernandez, E.; Granier, M.; Rebelo, A.G.; Peterschmitt, M.; Martin, D.P.; et al. Identification and characterisation of a highly divergent geminivirus: Evolutionary and taxonomic implications. *Virus Res.* 2013, *177*, 35–45.
43. Wright, E.A.; Heckel, T.; Groenendijk, J.; Davies, J.W.; Boulton, M.I. Splicing features in maize streak virus virion- and complementary- sense gene expression. *Plant J.* 1997, *12*, 1285–1297.
44. International Committee on Taxonomy of Viruses ICTV Available online: https://talk.ictvonline.org/.
45. Hewitt, W.B.; Goheen, A.C.; Raski, D.J.; Gooding, G. V. Studies on Virus Diseases of the Grapevine in California. *Vitis* 1962, *3*, 57–83.
46. Girardello, R.C.; Rich, V.; Smith, R.J.; Brenneman, C.; Heymann, H.; Oberholster, A. The impact of grapevine red blotch disease on *Vitis vinifera* L. Chardonnay grape and wine composition and sensory attributes over three seasons. *J. Sci. Food Agric.* 2019, jsfa.10147.
47. Buchs, N.; Braga-Lagache, S.; Uldry, A.C.; Brodard, J.; Debonneville, C.; Reynard, J.S.; Heller, M. Absolute quantification of grapevine red blotch virus in grapevine leaf and petiole tissues by proteomics. *Front. Plant Sci.* 2018, *871*.
48. Cieniewicz, E.; Flasco, M.; Brunelli, M.; Onwumelu, A.; Wise, A.; Fuchs, M.F. Differential spread of grapevine red blotch virus in California and New York vineyards. *Phytobiomes J.* 2019, *3*, 203–211.
49. Cieniewicz, E.J.; Pethybridge, S.J.; Gorny, A.; Madden, L. V.; McLane, H.; Perry, K.L.; Fuchs, M. Spatiotemporal spread of grapevine red blotch-associated virus in a California vineyard. *Virus Res.* 2017, *241*, 156–162.

50. Dalton, D.T.; Hilton, R.J.; Kaiser, C.; Daane, K.M.; Sudarshana, M.R.; Vo, J.; Zalom, F.G.; Buser, J.Z.; Walton, V.M. Spatial associations of vines infected with grapevine red blotch virus in oregon vineyards. *Plant Dis.* 2019, *103*, 1507–1514.
51. Bahder, B.W.; Zalom, F.G.; Jayanth, M.; Sudarshana, M.R. Phylogeny of Geminivirus Coat Protein Sequences and Digital PCR Aid in Identifying *Spissistilus festinus* as a Vector of Grapevine red blotch-associated virus . *Phytopathology* 2016, *106*, 1223–1230.
52. Cieniewicz, E.J.; Pethybridge, S.J.; Loeb, G.; Perry, K.; Fuchs, M. Insights Into the Ecology of Grapevine red blotch virus in a Diseased Vineyard. *Phytopathology* 2017, *108*, 94–102.
53. Flasco, M.; Hoyle, V.; Cieniewicz, E.; Roy, B.; McLane, H.; Perry, K.L.; Loeb, G.M.; Nault, B.; Cilia, M.; Fuchs, M. Grapevine red blotch virus is transmitted by the three-cornered alfalfa hopper in a circulative, nonpropagative mode with unique attributes. *Phytopathology*® 2021, 1–50.
54. Kahl, D.; Úrbez-Torres, J.R.; Kits, J.; Hart, M.; Nyirfa, A.; Lowery, D.T. Identification of candidate insect vectors of Grapevine red blotch virus by means of an artificial feeding diet. *Can. J. Plant Pathol.* 2021, *00*, 1–9.
55. Bowen, P.; Bogdanoff, C.; Poojari, S.; Usher, K.; Lowery, T.; Úrbez-Torres, J.R. Effects of grapevine red blotch disease on cabernet franc vine physiology, bud hardiness, and fruit and wine quality. *Am. J. Enol. Vitic.* 2020, *71*, 308–318.
56. Martínez-Lüscher, J.; Plank, C.M.; Brillante, L.; Cooper, M.L.; Smith, R.J.; Al-Rwahnih, M.; Yu, R.; Oberholster, A.; Girardello, R.; Kurtural, S.K. Grapevine Red Blotch Virus May Reduce Carbon Translocation Leading to Impaired Grape Berry Ripening. *J. Agric. Food Chem.* 2019, *67*, 2437–2448.
57. Levin, A.D.; KC, A.N. Water Deficits Do Not Improve Fruit Quality in Grapevine Red Blotch Virus-Infected Grapevines (*Vitis vinifera* L.). *Front. Plant Sci.* 2020, *11*, 1–13.
58. Reynard, J.; Gugerli, P. Effects of Grapevine red blotch-associated virus on vine physiology and fruit composition of field grown grapevine cv . Gamay. In Proceedings of the 18th Congress of the International Council for the Study of Virus and Virus-like Diseases of the Grapevine (ICVG).; Ankara, Turquie, 2015; pp. 234–235.
59. Wallis, C.M.; Sudarshana, M.R. Effects of Grapevine red blotch-associated virus (GRBaV) infection on foliar metabolism of grapevines. *Can. J. Plant Pathol.* 2016, *38*, 358–366.
60. Lemoine, R.; La Camera, S.; Atanassova, R.; Dédaldéchamp, F.; Allario, T.; Pourtau, N.; Bonnemain, J.L.; Laloi, M.; Coutos-Thévenot, P.; Maurousset, L.; et al. Source-to-sink transport of sugar and regulation by environmental factors. *Front. Plant Sci.* 2013, *4*, 1–21.
61. Kelly, G.; Moshelion, M.; David-Schwartz, R.; Halperin, O.; Wallach, R.; Attia, Z.; Belausov, E.; Granot, D. Hexokinase mediates stomatal closure. *Plant J.* 2013, *75*, 977–988.
62. Swiech, R.; Browning, S.; Molsen, D.; Stenger, D.C.; Holbrook, G.P. Photosynthetic responses of sugar beet and Nicotiana benthamiana Domin. infected with beet curly top virus. *Physiol. Mol. Plant Pathol.* 2001, *58*, 43–52.
63. Fabro, G.; Kovács, I.; Pavet, V.; Szabados, L.; Alvarez, M.E. Proline accumulation and AtP5CS2 gene activation are induced by plant-pathogen incompatible interactions in *Arabidopsis*. *Mol. Plant-Microbe Interact.* 2004, *17*, 343–350.
64. Blanco-Ulate, B.; Hopfer, H.; Figueroa-Balderas, R.; Ye, Z.; Rivero, R.M.; Albacete, A.; Pérez-Alfocea, F.; Koyama, R.; Anderson, M.M.; Smith, R.J.; et al. Red blotch disease alters grape berry development and metabolism by interfering with the transcriptional and hormonal regulation of ripening. *J. Exp. Bot.* 2017, *68*, 1225–1238.

65. Girardello, R.C.; Cooper, M.L.; Smith, R.J.; Lerno, L.A.; Bruce, R.C.; Eridon, S.; Oberholster, A. Impact of Grapevine Red Blotch Disease on Grape Composition of Vitis vinifera Cabernet Sauvignon, Merlot, and Chardonnay. *J. Agric. Food Chem.* 2019, *67*, 5496–5511.
66. Calvi, B.L. Effects Of Red-leaf Disease On Cabernet Sauvignon At The Oakville Experimental Vineyard And Mitigation By Harvest Delay And Crop Adjustment, University of California, Davis, 2011.
67. Girardello, R.C.; Cooper, M.L.; Lerno, L.A.; Brenneman, C.; Eridon, S.; Sokolowsky, M.; Heymann, H.; Oberholster, A. Impact of Grapevine Red Blotch Disease on Cabernet Sauvignon and Merlot Wine Composition and Sensory Attributes. *Molecules* 2020, *25*.
68. Riesmeier, J.W.; Willmitzer, L.; Frommer, W.B. Isolation and characterization of a sucrose carrier cDNA from spinach by functional expression in yeast. *EMBO J.* 1992, *11*, 4705–4713.
69. Amtmann, A.; Troufflard, S.; Armengaud, P. The effect of potassium nutrition on pest and disease resistance in plants. *Physiol. Plant.* 2008, *133*, 682–691.
70. Perrenoud, S. Potassium and plant health. *Potash Rev.* 1990, *85*, 1–5.
71. Zhou, L.; He, H.; Liu, R.; Han, Q.; Shou, H.; Liu, B. Overexpression of GmAKT2 potassium channel enhances resistance to soybean mosaic virus. *BMC Plant Biol.* 2014, *14*, 1–11.
72. Downey, M.O.; Dokoozlian, N.K.; Krstic, M.P. Cultural practice and environmental impacts on the flavonoid composition of grapes and wine: A review of recent research. *Am. J. Enol. Vitic.* 2006, *57*, 257–268.
73. Sherman, E.; Greenwood, D.R.; Villas-Boâs, S.G.; Heymann, H.; Harbertson, J.F. Impact of grape maturity and ethanol concentration on sensory properties of Washington State merlot wines. *Am. J. Enol. Vitic.* 2017, *68*, 344–356.
74. Casassa, L.F.; Beaver, C.W.; Mireles, M.; Larsen, R.C.; Hopfer, H.; Heymann, H.; Harbertson, J.F. Influence of fruit maturity, maceration length, and ethanol amount on chemical and sensory properties of Merlot wines. *Am. J. Enol. Vitic.* 2013, *64*, 437–449.
75. Bergqvist, J.; Dokoozlian, N.; Ebisuda, N. Sunlight exposure and temperature effects on berry growth and composition of Cabernet Sauvignon and Grenache in the central San Joaquin Valley of California. *Am. J. Enol. Vitic.* 2001, *52*, 1–7.
76. Alabi, O.J.; Casassa, L.F.; Gutha, L.R.; Larsen, R.C.; Henick-Kling, T.; Harbertson, J.F.; Naidu, R.A. Impacts of Grapevine Leafroll Disease on Fruit Yield and Grape and Wine Chemistry in a Wine Grape (*Vitis vinifera* L.) Cultivar. *PLoS One* 2016, *11*, e0149666.
77. Naidu, R.A.; Henick-Kling, T.; Gutha, L.R.; Harbertson, J.F.; Casassa, L.F.; Larsen, R.C.; Alabi, O.J. Impacts of Grapevine Leafroll Disease on Fruit Yield and Grape and Wine Chemistry in a Wine Grape (*Vitis vinifera* L.) Cultivar. *PLoS One* 2016, *11*, e0149666.
78. Treutter, D. Significance of flavonoids in plant resistance and enhancement of their biosynthesis. *Plant Biol.* 2005, *7*, 581–591.
79. Rumbaugh, A.C.; Girardello, R.C.; Cooper, M.L.; Plank, C.M.; Kurtural, S.K.; Oberholster, A. Impact of Rootstock and Season on Red Blotch Disease Expression in Cabernet Sauvignon (*V. vinifera*). *Plants* 2021, *10*, 1–16.
80. Gambetta, G.A.; Matthews, M.A.; Shaghasi, T.H.; McElrone, A.J.; Castellarin, S.D. Sugar and abscisic acid signaling orthologs are activated at the onset of ripening in grape. *Planta* 2010, *232*, 219–234.
81. Wheeler, S.; Loveys, B.; Ford, C.; Davies, C. The relationship between the expression of abscisic acid biosynthesis genes, accumulation of abscisic acid and the promotion of *Vitis*

vinifera L. berry ripening by abscisic acid. *Aust. J. Grape Wine Res.* 2009, *15*, 195–204.
82. Kalua, C.M.; Boss, P.K. Evolution of volatile compounds during the development of cabernet sauvignon grapes (*Vitis vinifera* l.). *J. Agric. Food Chem.* 2009, *57*, 3818–3830.
83. Waterhouse, A.L.; Sacks, G.L.; Jeffery, D.W. *Understanding Wine Chemistry*; John Wiley & Sons, Ltd: West Sussex, United Kingdom, 2016; ISBN 9781118627808.
84. Kassara, S.; Kennedy, J.A. Relationship between red wine grade and phenolics. 2. Tannin composition and size. *J. Agric. Food Chem.* 2011, *59*, 8409–8412.
85. Buck, K.W. Geminiviruses (*Geminiviridae*). In *Encyclopedia of Virology*; Granoff, A., Webster, R.G., Eds.; Academic Press, 1999; pp. 597–606.
86. Nunan, K.J.; Sims, I.M.; Bacic, A.; Robinson, S.P.; Fincher, G.B. Changes in cell wall composition during ripening of grape berries. *Plant Physiol.* 1998, *118*, 783–792.
87. Otulak-Kozieł, K.; Kozieł, E.; Lockhart, B.E.L. Plant cell wall dynamics in compatible and incompatible potato response to infection caused by Potato virus Y (PVYNTN). *Int. J. Mol. Sci.* 2018, *19*.

CHAPTER 2

Impact of rootstock and season on red blotch disease expression in Cabernet Sauvignon (V. vinifera)

Formatted for publication for *Plants* (accepted)

2.1 Abstract:

Grapevine red blotch virus (GRBV), the causative agent of grapevine red blotch disease, is widespread across the United States and causes a delay in ripening events in grapes. This study evaluates the effects of GRBV on Cabernet Sauvignon grape berry composition, grafted on two different rootstocks (110R and 420A) in two seasons (2016 and 2017). Total soluble solids, acidity, and anthocyanin concentrations were monitored through ripening and at harvest. Phenolic and volatile compounds were also analyzed at harvest to determine genotypic and environ-mental influences on disease outcome. Sugar accumulation through ripening was lower in diseased fruit (RB (+)) than healthy fruit across rootstock and season. GRBV impact was larger in 2016 than 2017, indicating a seasonal effect on disease expression. In general, anthocyanin levels and volatile compound accumulation was lower in RB (+) fruit than healthy fruit. Total phenolic composition and tannin content was higher in RB (+) fruit than healthy fruit in only 110R rootstock. Overall, GRBV impacted Cabernet Sauvignon grape composition crafted on rootstock 110R more than those crafted on rootstock 420A.

2.2 Introduction:

Grapevines are susceptible to the highest number of pathogens to infect a single crop, with over 70 viruses detected [1]. In 2008, a new virus was first observed in Napa County, California, which economically threatened grapevines: grapevine red blotch virus (GRBV) [2].

This virus is the causative agent of grapevine red blotch disease (GRBD) [3], which has been identified in vineyards across the United States, Canada, Argentina, Mexico, South Korea, and India [4–9]. Reports indicate GRBV primarily spreads through propagation material and secondarily through an insect vector [10,11]. Spissistilus festinus (Membracidae) was shown to successfully transmit GRBV in greenhouse settings, yet this has not been replicated in vineyards to date [12]. GRBV has been identified as a virus from the Geminiviridae family containing a circular single-stranded DNA genome [13,14] similar to other geminiviruses [15]. GRBD expresses symptoms of reddening of leaf blades and margins, with reddening of the primary, secondary, and tertiary veins in red grape cultivars [10].

GRBV affects grapevines in various ways. For example, leaves on infected vines show increased levels of sugar, phenolics, particular amino acids, and enzymatic activity related to plant defense, as well as a reduction in carbon fixation [16–18]. However, the most damaging are the effects on grape composition [17–20] which has been shown to be detrimental to final wine quality [21]. GRBV delays ripening by decreasing the accumulation of sugar and anthocyanin in berries, potentially due to the impairment of translocation mechanisms [17,18,20]. The virus has variable impacts on primary and secondary metabolites, specifically phenolic and aroma compounds [17,19,20]. In summary, detrimental economic impacts to vineyards in the United States could reach $68,548/ha with vine removal being the only current method of alleviation [22]. Consequently, recent research has strived to understand the effects and functioning of GRBV to establish mitigation strategies to alleviate the impact on grape composition and wine quality.

The grape berry has a double sigmoidal growth curve with three dis-tinct phases. The first phase is characterized by cell division and production of seeds, as well as synthesis of

tannins and organic acids. The second phase is characterized with the onset of veraison, which is when the grape berry begins to soften and change color. The final and third phase is berry engustment/ripening, where berries increase in size, sugar accumulates, acidity declines, and secondary metabolites such as anthocyanins and aromatic compounds are synthesized inside the berry [23]. Studies have shown that volatile compounds such as terpenoids and C6 compounds, begin to accumulate in berries after veraison, and are controlled by numerous factors [24–28]. The synthesis of these compounds in berries is also altered by ex-ternal factors such as light exposure or pathogens [29,30]. In addition, these secondary metabolites are crucial to grape growers and winemakers due to their importance in the quality of a final wine [31]. Grape maturity has shown to be a key driver in the composition of a final wine, where later harvested fruit produces wines with lower concentrations of C6 alcohols (vegetal aromas) and higher in concentration of esters (fruity aromas) [32]. However, the impacts of GRBV on volatile compound abundance in harvested grapes has not been investigated.

A plant's genetic material may influence susceptibility to viral infections [33–35]. Additionally, rootstocks can impact grapevine physiology and impact the overall composition of a grape berry. For instance, rootstock 110R (Vitis berlandieri × Vitis rupestris) causes high vigor and high drought tolerance in grapevines, whereas 420A (V. berlandieri × Vitis riparia) is a rootstock of low to moderate vigor and low drought resistance [36]. Vigor, resulting in greater shoot length and hence leaf area, may impact net carbon assimilation and the translocation of metabolites into the berry, consequently affecting the final wine composition [37]. These hydric differences affecting carbon metabolism in rootstocks can also impact the plant-pathogen interactions. Therefore, it is plausible that severity of GRBD symptoms will be dependent on the interaction between scion cultivar-rootstock. However, this has not been fully investigated.

Macro and microclimate fluctuations may also be a factor in pathogen-plant interactions [38,39], and should be considered.

This study investigated the impact of GRBV on the biosynthesis and accumulation of primary and secondary metabolites in grape berries throughout ripening and at harvest. Additionally, the influence of seasonal and genotypic factors on disease expression within grapevines were studied.

2.3 Results:

2.3.1 GRBV impacts on grape maturation

Figures 2.1 to 2.3 depict sugar accumulation, anthocyanin levels, TA, and pH through ripening. Sugar accumulation was determined by converting ºBrix to mg of sugar per berry [40]. Anthocyanin content was lower in RB (+) grapes when compared to RB (-) grapes for both years and rootstocks during ripening (Figure 2.1). However, the degree of impact varied depending on season and rootstock. In 2016, both rootstocks were equally impacted throughout ripening regarding sugar ac-cumulation and anthocyanins levels. However, in 2017 sugar accumulation was generally not significantly impacted by disease status. In 2017, grape anthocyanin levels were more significantly impacted for infected vines on 110R rootstock than 420A rootstock, whereas rootstock impact was less apparent in 2016.

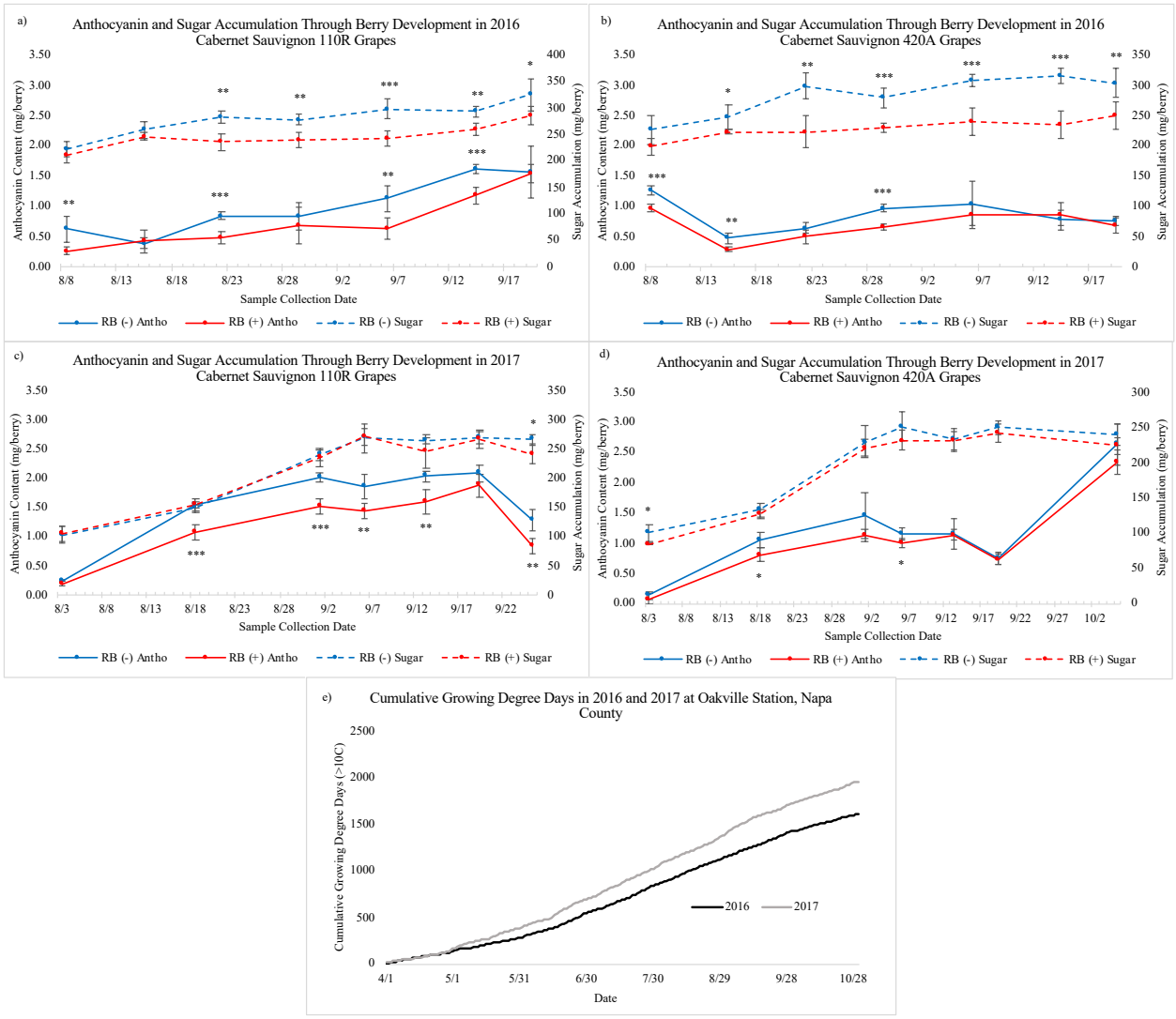

Figure 2.1 Sugar accumulation and anthocyanin content through ripening from pre-veraison to harvest for a) sugar accumulation in 2016 b) anthocyanin content in 2016 c) sugar accumulation in 2017, d) anthocyanin content in 2017 (n=5), e) cumulative growing degree days (>10°C). CS= Cabernet Sauvignon, RB=red blotch, (-)=negative, and (+)=positive. Asterisks indicate a significant difference between RB (-) and RB (+) after an ANOVA (*=p<0.05, **=p<0.01, ***=p<0.001).

At harvest in 2016 (September 20th), CS 110R and 420A rootstocks respectively had a 2% and 11% decrease in anthocyanin content (mg/berry) and a 12% and 18% decrease in sugar content (mg/berry) in RB (+) grapes when compared to RB (-) grapes.

In 2017, at harvest (September 26th and October 6th), anthocyanin content was 35% and 11% lower in RB (+) when compared to RB (-), and sugar content was 9% and 7% lower, for 110R and 420A, respectively.

By plotting ºBrix over ripening and fitting a linear trendline, it is possible to compare the rate of ripening for RB (-) and RB (+) grapevines (Figure 2.2). As indicated by the slope of the best fit line, the rate of ripening was always higher for RB (-) data vines when compared to RB (+) data vines, with the exception for CS 420A in 2017. In addition, the rate was also lower in 2016 than 2017 across virus status and rootstocks. Interestingly, the difference in the rate of ripening between RB (-) and RB (+) data vines was larger in 2016 than in 2017 which correlates to the larger differences in accumulated sugar at harvest. In 2017, the rate was lower for CS 420A than CS 110R across virus status.

Differences between RB (-) and RB (+) for pH and TA also varied between years and rootstocks (Figure 2.3). In general, RB (+) grapes had lower pH values and a higher TA when compared to RB (-), which agrees with results found by Martínez-Lüscher et al. [17]. For both TA and pH, there were more sampling dates significantly different between RB (+) and RB (-) observed in 2016 than in 2017, similar to sugar accumulation (Figure 2.1).

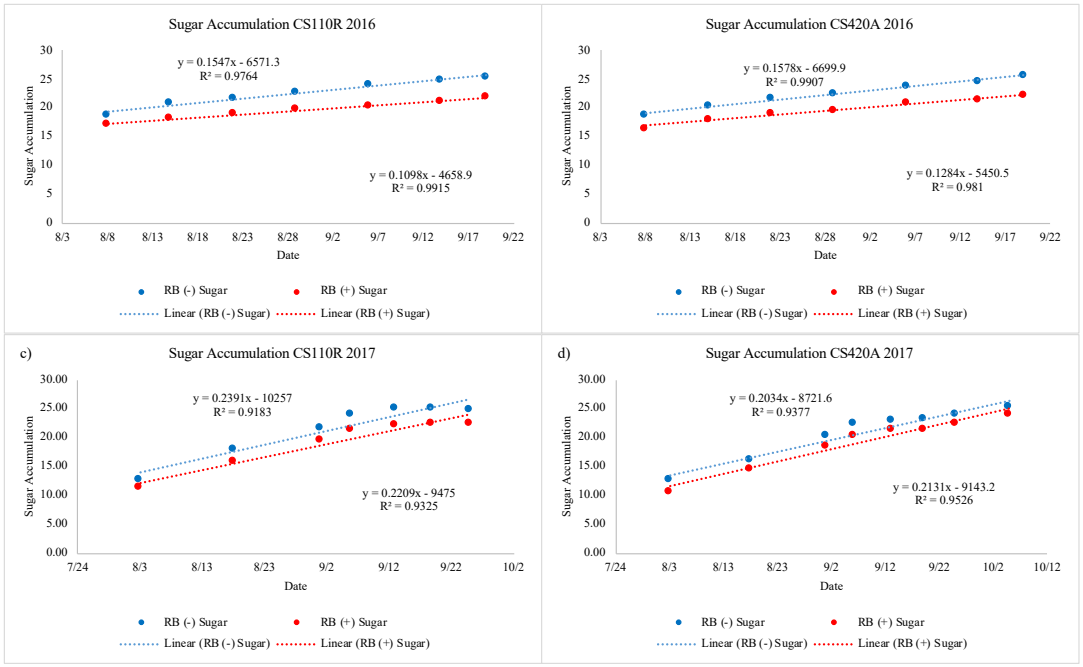

Figure 2.2 The rate of sugar accumulation as °Brix through ripening for RB (-) and RB (+) data vines. a) CS 110R in 2016, b) CS 420A in 2016, c) CS 110R in 2017, and d) CS 420A in 2017 (n=5). TA= Titratable Acidity, CS= Cabernet Sauvignon, RB= red blotch, (-)= negative, and (+)= positive.

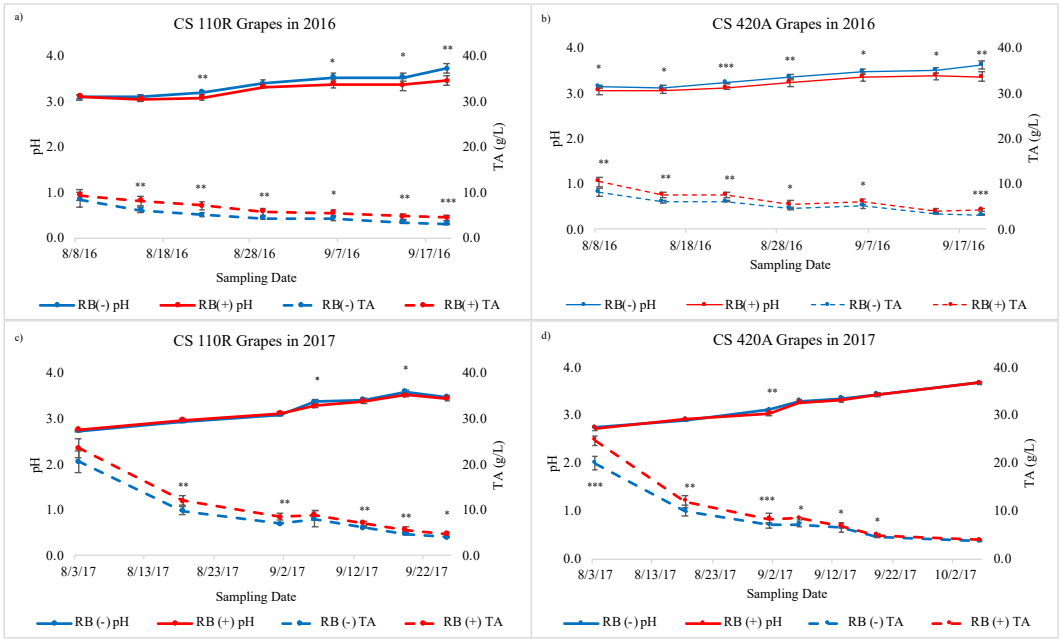

Figure 2.3 Titratable acidity and pH values from pre-veraison to harvest for a) CS 110R in 2016, b) CS 420A in 2016, c) CS 110R in 2017, and d) CS 420A in 2017 (n=5). TA= Titratable Acidity, CS= Cabernet Sauvignon, RB= red blotch, (-)= negative, and (+)= positive. Asterisks indicate a significant difference between RB (-) and RB (+) after an ANOVA (*=p<0.05, **=p<0.01, ***=p<0.001).

Table 2.1 °Brix, pH, TA (g/L), yield (kg) per vine, number of clusters per vine, and cluster mass (g) measurements from CS110R and CS420A data vines at harvest in 2016 and 2017 (n=5).

Sample	Harvest Date	°Brix	pH	TA (g/L)	Yield (kg)	Clusters/Vine	Cluster mass (g)
CS 110R RB (-)	9/20/16	25.4 ± 0.4 a	3.7 ± 0.10 a	3.1 ± 0.2 b	4.7 ± 0.6 a	36.9 ± 3.8 a	127.9 ± 6.0 a
CS 110R RB (+)	9/20/16	21.9 ± 1.0 b	3.5 ± 0.10 b	4.5 ± 0.6 a	5.5 ± 1.3 a	41.2 ± 6.74 a	130.6 ± 9.0 a
CS 420A RB (-)	9/20/16	25.6 ± 0.5 a	3.6 ± 0.0 a	3.2 ± 0.2 b	4.2 ± 0.8 a	32.5 ± 2.9 a	128.7 ± 12.6 a
CS 420A RB (+)	9/20/16	22.0 ± 0.5 b	3.34± 0.1 b	4.3 ± 0.4 a	4.9 ± 0.9 a	32.6 ± 3.6 a	142.2 ± 26.9 a
CS 110R RB (-)	9/26/17	24.6 ± 0.0 a	3.5 ± 0.0 a	4.1 ± 0.1 b	6.0 ± 0.7 b	54.79 ± 1.4 b	108.9 ± 10.7 a
CS 110R RB (+)	9/26/17	22.4 ± 0.0 b	3.5 ± 0.0 a	4.8 ± 0.1 a	7.1 ± 0.7 a	59.04 ± 3.1 a	120.2 ± 8.0 a
CS 420A RB (-)	10/6/17	25.1 ± 0.0 a	3.7 ± 0.0 a	3.6 ± 0.1 a	5.8 ± 1.3 a	50.60 ± 4.2 a	114.9 ± 21.3 a
CS 420A RB (+)	10/6/17	23.8 ± 0.0 b	3.7 ± 0.0 a	3.9 ± 0.1 a	6.2 ± 0.6 a	54.00 ± 3.1 a	113.9 ± 10.1 a
Significant Effects							
V		***	***	***	*	*	
Y				**	***	***	***
R		**	*	**		***	
V x Y		***	***	**			
V x R							
Y x R		*	***	**			
V x Y x R							

TA= Titratable Acidity, CS= Cabernet Sauvignon, RB=red blotch, (-)= negative, (+)= positive, V=virus status, Y= year, and R= rootstock. Difference in lettering indicates a significant difference between RB (-) and RB (+) for each rootstock after applying Tuckey's HSD test ($p<0.05$). Asterisks indicate a significant difference between RB (-) and RB (+) after a three-way ANOVA (*=$p<0.05$, **=$p<0.01$, ***=$p<0.001$).

2.3.2 GRBV impacts on grape composition at harvest

In general, there were no significant differences in yield and cluster number be-tween RB (+) and RB (-) grapevines, except for CS 110R in 2017. In latter case, the yield and number of clusters per vine were significantly higher in RB (+) than RB (-) (Table 2.1), contrary to findings by Martínez-Lüscher et al. [17], in which a smaller subset of data vines was used for yield components, potentially explaining the variation. As with previous findings, GRBD consistently decreased °Brix and pH values, while increasing TA values in grapes at harvest, indicating GRBD causes a delay in ripening [2,13,17,20,41,42]. In addition, malic acid concentrations in RB (-) grapes were in general significantly lower than RB (+) grapes.

There was a significant effect from virus status on °Brix, pH, TA, yield, and clusters/vine values. In addition, there was a significant interaction for virus status to year for °Brix, pH and TA values, indicating that environmental factors play a role in disease expression for these

parameters. For these values, Table 2.1 shows that grapevines in 2017 were less impacted by GRBD than in 2016, as seen during grape ripening (Figure 2.1 and 2.2).

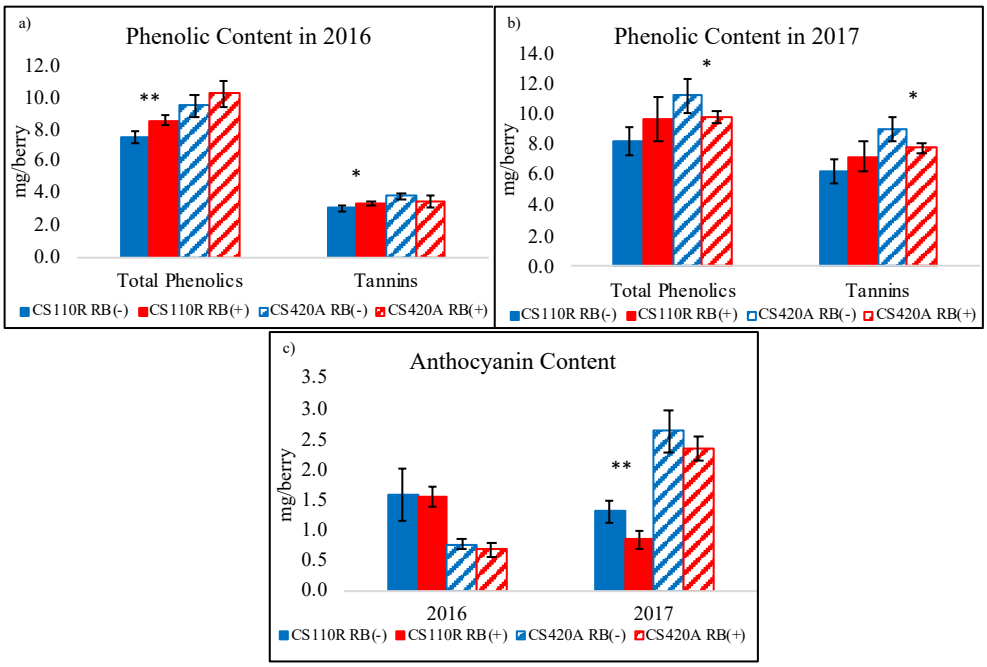

Figure 2.4 Phenolic profile of whole berry extracts at harvest through protein precipitation analysis. a) Total phenolic and total tannin composition from CS grapes on 110R and 420A rootstock in 2016, b) total phenolic and total tannin composition from CS grapes on 110R and 420A rootstock in 2017, and c) total anthocyanin concentrations in CS grapes in 2016 and 2017 (n=5). CS= Cabernet Sauvignon, RB= red blotch, (-)= negative, and (+)= positive. Asterisks indicate a significant difference between RB (-) and RB (+) after an ANOVA (*=$p<0.05$, **=$p<0.01$, ***=$p<0.001$).

2.3.3 Grape phenolic profile

The grape phenolic profile in 2016 and 2017 from the protein precipitation assay is shown in Figure 2.4. It should be noted that the phenolic content is expressed in mg/berry to observe differences in biosynthesis in the berries. Similar trends as in Figure 2.4 were observed for phenolic concentrations (mg/g of berry, Table S2.2).

In general, it was observed that RB (-) grapes were higher in anthocyanin levels than RB (+) grapes, which was only significant in 2017 for CS 110R. For CS 110R grapes, total phenolic and total tannin concentrations in RB (+) grapes were higher than in RB (-) grapes. Larger

differences between RB (-) and RB (+) in overall phenolic content was observed in 2017 when compared to 2016; however, these differences were not always significant.

Content (mg/berry) and concentration (mg/ g of berry) of total phenolics, tannins, and anthocyanins were analyzed through a three-way ANOVA with three-way inter-actions (Table S2.2). Results indicate that there was a significant virus status and virus status to year interaction for anthocyanin concentrations and content. This suggests that there was a larger interaction between disease status and season, rather than the rootstock, on final anthocyanin content in grapes. In addition, there was a significant virus status effect and virus status to rootstock effect for total tannins and total phenolics, indicating that the disease outcome is also a factor of rootstock for these parameters.

2.3.4 Volatile analysis- HS-SPME-GC-MS

The volatile compound profiles of RB (-) and RB (+) grapes were determined in both 2016 and 2017 seasons (Table S2.3). PCA was performed to plot the variability between RB (-) and RB (+) grape samples (Figure 2.5 and 2.6). Between 80.6- 94.5% of the variance is explained by the PCA in Figures 2.4 and 2.5. For CS 110R, only the significantly different volatile compounds between RB (-) and RB (+) are plotted. There were respectively ten and nine significant volatile compounds that explained the difference between treatments for CS 110R in 2016 and 2017. For CS 420A, the volatile compounds that contributed most to the variance of the PCA were plotted, due to few volatile compounds being significantly different. This selection was based on the squared cosine (cos2=0.90) which shows the importance of the volatile compounds to explain the variance in the data [43]. For CS 420A, in 2016, only cis-3-hexen-1-ol

was significantly different, and in 2017, only □-linalool and □-citronellol were significantly different with a □ level of 0.95.

In 2016, it was observed that cis-3-hexen-1-ol, hexanol, 2-hexenal, ethyl-2-methylbutyrate, and trans-2-hexen-1-ol were highly correlated with RB (+) grape extracts in CS 110R and CS 420A (Figure 2.5). Whereas, the volatile compounds hexyl acetate, ethyl acetate, ethyl hexanoate, geranial, ß-ionone, and ß-cyclocitral were correlated with CS 110R RB (-) grapes (Figure 2.5a). As for CS 420A in 2016 (Figure 2.5b), limonene, ß-linalool, ß-myrcene, acetic acid, α-terpinene, geranial, nerol, and ethyl acetate were correlated to RB (-).

The volatile profile of grapes in 2017 was similar to those in 2016. However, 110R RB (+) grapes were correlated to ethyl acetate and ß-damascenone (Figure 2.6a). On the other hand, p-cymene, ethyl butyrate, ß-myrcene, benzyl alcohol, 2-hexenal, hexanal, and nerol were correlated with CS 110R RB (-) grapes. Figure 2.6b indicates that CS 420A RB (+) grapes were only correlated with □-nonalactone, ß-caryophllene, and trans-2-hexen-1-ol, whereas, CS 420A RB (-) grapes were correlated with ethyl hexanoate, isoamyl alcohol, α-terpinene, α-pinene, p-cymene, limonene, benzyl alcohol, benzaldehyde, 2-phenylethyl alcohol, and ß-myrcene. In both years, in general it was observed that RB (+) grapes were correlated with fewer volatile compounds, apart from C6 aldehydes and alcohols.

Lastly, results from the three-way ANOVA with three-way interactions are shown in Table S2.3. It was observed that ethyl acetate, limonene, 2-hexenal, ethyl hexanoate, p-cymene, hexyl acetate, octanal, trans-2-hexen-1-ol, and ß-ionone had a significant virus status effect across years and rootstocks. Ethyl acetate, 2-hexenal, ethyl hexanoate, hexyl acetate, hexanol, trans-3-hexen-ol, cis-3-hexen-1-ol, trans-2-hexen-1-ol, geranial, ß-damascenone, and ethyl cinnamate had a significant virus status to year interaction, whereas, limonene, 2-hexenal, ethyl

hexanoate, p-cymene, cis-3-hexen-1-ol, trans-2-hexen-1-ol, nerol oxide, benzaldehyde, geranial, and benzyl alcohol had a significant virus status to rootstock effect. This suggests that the extent to which these compounds are impacted due to GRBV will vary depending on the season and the genotype of the grapevine.

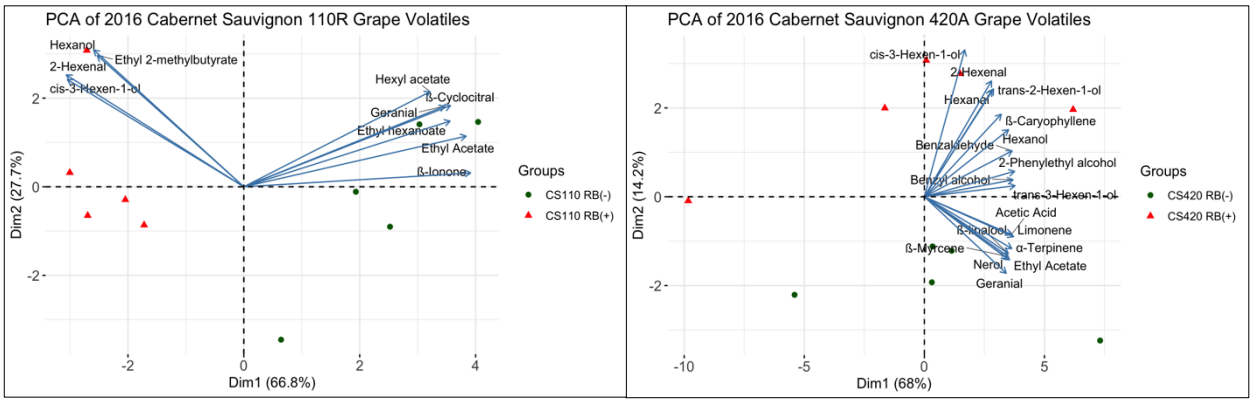

Figure 2.5 Principal component analysis of significantly different volatile compounds in whole berry extracts from CS grapes on 110R and 420A rootstock from 2016 (n=5). CS= Cabernet Sauvignon, RB=red blotch, (-)=negative, and (+)=positive.

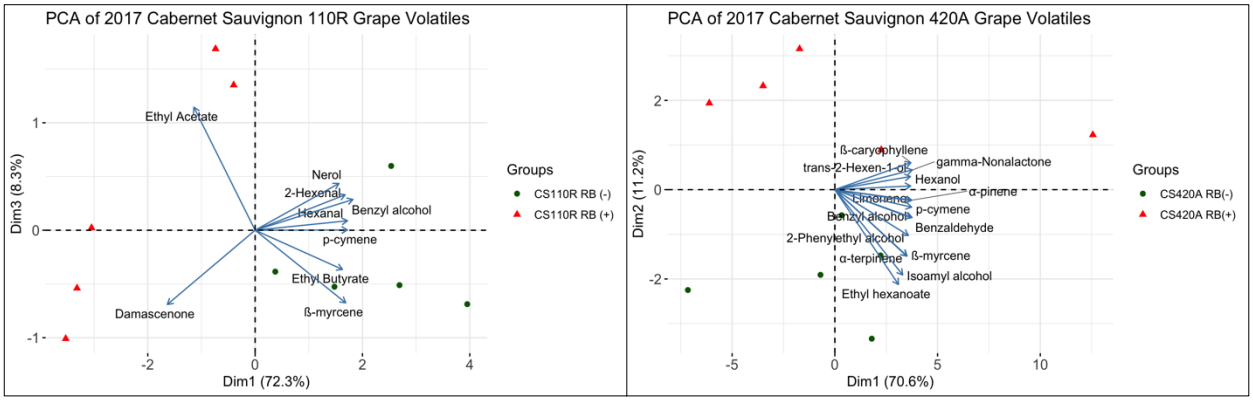

Figure 2.6 Principal component analysis of significantly different volatile compounds in whole berry extracts from CS grapes on 110R and 420A rootstock from 2017 (n=5). CS= Cabernet Sauvignon, RB= red blotch, (-)= negative, and (+)= positive.

2.4 Discussion:

2.4.1 Impact on grape volatile compounds

After veraison, volatile compound accumulation begins in grapes and changes through ripening [25,44,45]. However, the impacts of GRBV on grape volatile compounds have not been investigated. We found 35 different aromatic compounds in grapes from the two rootstocks over two seasons, of which 24 were similar between the two years studied (Table S2.3).

In 2016, across rootstock, RB (+) grapes were generally lower in volatile compound levels than RB (-), except for C6 compounds such as 2-hexenal, hexanal, cis-3-hexen-1-ol, trans-2-hexen-1-ol, and hexanol (Figure 2.5). These C6 volatile compounds are synthesized in the grape skin through the lipoxygenase pathway, are generally responsible for green or grassy aromas [24] and accumulate in CS grapes up to 18 ºBrix [25]. With the exception of hexanol, the levels of these compounds begin to significantly decrease thereafter, with a 67% decrease in grapes at 25 ºBrix when compared to grapes at 18 ºBrix [25]. These observations correlate with the common finding that GRBV causes a delay in ripening [2,10,17,18], with green aromas being present and correlated with the lower sugar ac-cumulation [25]. On the other hand, RB (-) grapes were highly correlated with mono-terpenes such as limonene, ß-myrcene, α-terpinene, geranial and p-cymene (Figures 2.4 and 2.5), which are responsible for floral and fruity aromas. These compounds have been associated with CS grapes at harvest and are known to increase through grape ripening [26] and may decrease at over ripeness [46–48].

In addition, RB (-) grapes were also highly correlated with esters such as ethyl acetate, ethyl hexanoate, hexyl acetate, and ethyl butyrate. Although ester formation is mainly related to yeast or bacteria metabolism during winemaking [49,50], grapes are also known to synthesize esters. Anthraniloyl-coenzyme A (CoA):methanol acyltransferase (AMAT) is known to be

responsible for the formation of methyl anthranilate in grapes and it is also classified as an ester-forming acyltransferase, which could be re-sponsible for the formation of esters in grapes [51]. The esters found in the current work that in general related mostly to RB (-) grapes, are known to produce red and black fruit aromas [52–54]. Collectively, these results confirm that RB (-) grapes underwent normal ripening processes [25] and produced more fruity aromas, while RB (+) grapes at harvest have aroma characteristics more related to early ripening stages.

2.4.2 Impact of season on disease expression

Results indicated that in 2016 GRBD had a larger impact regarding sugar accumulation, pH, TA, and final sugar content (ºBrix) than in 2017. In addition, the harvest dates were two to three weeks later in 2017 than in 2016. These observations can potentially be explained by the difference in temperature between the two seasons. In 2017, Napa County experienced a heat wave from August 26th- September 11th, where nine days were over 35°C, and four days were over 40°C. The cumulative growing degree days for both years can be seen in Figure 2.1e. Extreme heat conditions (>30°C) during grape maturation have been shown to inhibit enzymatic activity and halt the biosynthesis of metabolites inside the grape berry [55–58]. Inhibition of these processes due to heat leads to decreases in sugar accumulation and increases in acidity in healthy fruit [59]. This is thought to be caused from a decrease in rate of translocation of sugars from leaves to fruit, through the reduction of photosynthesis at temperatures greater than 30°C [60]. The rate of ripening in 2017 was faster than 2016 prior to the heat spike (Figures 2.1 and 2.2). However, during the heat spike in late August to harvest, sugar accumulation plateaued resulting in extended harvest times in 2017.

In addition, research has shown that temperature can alter virus-induced gene silencing (VIGS) which is triggered with the infection of a virus as a plant-derived defense mechanism to downregulate the genes of interest [61]. Previous work on other plant species infected with a geminivirus [38,61,62] has shown that the extent of gene silencing is related to temperature. Specifically, Chellappan et al. [38] showed that temperatures over 30°C induced gene silencing, which interfere with gene expression, resulting in decreases of viral DNA accumulation and decreases in symptoms. Similarly, Flores et al. [61] observed that temperatures above 22°C attenuated infection symptoms and increased gene silencing. Thus, in 2017, the infected grapevines on both rootstocks could have experienced a reduction in GRBV impacts due to the high temperatures causing viral gene silencing and a decrease in viral DNA. However, the gene expression and regulation of transcriptional factors need to be investigated further to understand the correlation between extreme heat and disease expression in GRBD infected grapevines.

At harvest, a three-way ANOVA indicated that seasonal differences play a large role in the extent of disease symptoms in terms of anthocyanin content at harvest and through ripening (for CS 110R) which was not observed for total tannin and total phenolic content. Past studies have indicated that anthocyanin accumulation in grapes is highly susceptible to variations in temperature, with high temperatures leading to anthocyanin degradation and inhibition of biosynthetic pathways [57,63]. Whereas tannin concentrations are less sensitive to environmental factors [64–67]. Therefore, regarding anthocyanin content, the temperature differences between the two seasons may have had a com-pounding effect with GRBD infection in grapevines.

2.4.3 Differences in disease expression due to rootstock

Similar to previous results [20], the severity of GRBD symptoms depends not only on season, but also on rootstock. Anthocyanin levels through ripening and at harvest in 2017 for CS 110R infected grapevines were more impacted than in 2016 which was not observed for CS 420A (Figure 2.1). Previous work described the impact GRBV has on grape metabolism and demonstrated that GRBV inhibits the phenylpropanoid pathway in grapes, which is responsible for the synthesis of flavonoids [41]. As previously mentioned, temperature plays a large role in anthocyanin content in grapes, where higher temperatures lead to lower anthocyanin levels [57,63]. Therefore, it is possible that the extreme heat in 2017 acted as a secondary stressor to infected grapevines, and potentially caused larger decreases in anthocyanin levels through ripening than in 2016. However, this was only observed for rootstock 110R, suggesting that infected grapevines on this rootstock are potentially more susceptible to temperature fluctuations. In addition, the difference in the rate of ripening between RB (-) and RB (+) data vines (Figure 2.2), was larger for CS 110R than for CS 420A.This indicates that the virus differentially impacted the rate of translocation of sugars from the leaves to the berries depending on the rootstock.

Also, at harvest CS 110R RB (+) grapevines consistently had higher levels of total tannins and phenolics than RB (-) grapes, where the opposite was observed for CS 420A (Figure 2.4). The former has been seen in prior research by Girardello et al. [20] which screened the impact of GRBD on three varieties across seven sites. One of the varieties which had significantly higher proanthocyanidin (condensed tannins) values in RB (+) grapes compared to RB (-) was CS on rootstock 110R. Flavonoid biosynthesis such as flavan-3-ols and tannins has been correlated to abiotic and biotic stress responses in the grape [68]. It is possible that the

higher content of tannin observed in CS 110R infected grapes is correlated to a plant induced defense response, which was less significant in CS 420A. Lastly, the volatile aroma profiles between RB (+) and RB (-) were more similar for grapes from rootstock CS 420A compared to rootstock CS 110R, indicating that choice of rootstock has an influence on disease expression and may have various effects on secondary metabolites.

Plant-pathogen interactions can vary depending on the genetic makeup of the plant [33–35]. Rootstock 110R has high drought tolerance and is a moderately high vigor rootstock; whereas 420A has less drought tolerant and induces lower vigor in the scion in comparison. Lower vigor can result in a change in microclimate by increasing sun exposure, overall changing berry ripening and composition [63–65,69]. Previous research that investigated the impact of GRBV on vine physiological found similarly that CS110R grapes exhibited more symptoms than CS 420A [17]. In this study, RB (+) grapevines had higher sugar content in the leaves, lower sugar content in the grapes, and higher water potential than RB (-) grapevines. These differences were more drastic for CS 110R than CS 420A grapevines. In addition, CS 110R had higher water potential than CS 420A across disease status, correlating to the high vigor of 110R. Overall, this study concluded that GRBV inhibited the translocation mechanisms of photosynthetic products from the source (leaves) to the sink (grapes). Taken together, this suggests that there is a larger impairment to translocation mechanisms in the CS 110R grapevine than CS 420A grapevines.

2.5 Materials and Methods:

2.5.1 Chemicals and reagents

All water used during extractions and other analyses was 18MΩ·cm deionized water from a Milli-Q Element system (Millipore, Bedford, MA). All ethanol was purchased from

KOPTEC (Decon Labs, King of Prussia, PA). ACS grade acetone was used during phenolic extractions, along with 37% HCl, which was purchased from Sigma Aldrich (St. Louis, MO). Ascorbic acid, maleic acid, bovine serum albumin, glacial acetic acid, ferric chloride, triethanolamine, and NaCl were purchased from Sigma Aldrich (St. Louis, MO). Urea and NaOH were purchased from Thermo Fischer (Waltham, MA), and potassium bi-tartrate and potassium metabisulfite were purchased from ACROS organics-Thermo Fischer (Fair Lawn, NJ). For headspace solid-phase microextraction-gas chromatography-mass spectrometry (HS-SPME-GC-MS) analysis, sodium citrate dehydrate was purchased from Thermo Fischer (Waltham, MA). Internal standards, 2-octanol and 2-undecanone were purchased from Sigma Aldrich (St. Louis, MO).

2.5.2 Plant material

We used Cabernet Sauvignon grapevines (clone 8, Foundation Plant Services, University of California, Davis) grafted onto 110R and 420Vineyard (Napa County, CA, USA) The grapevines were trained to a bilateral cordon, in a vertical shoot positioned system. Vineyard management followed standard commercial practices for the region. The grapevines were drip-irrigated at 50% of crop evapotranspiration as reported previously [17]. For several years prior to the initiation of this study, GRBD symptoms had been monitored for each vine in this block. Petiole samples from a subset of vines from this block were tested by qPCR analysis at Agri-Analysis LLC laboratories in Davis, CA to confirm the healthy and GRBV status of the grapevines [12]. In addition, the plant material was screened for the presence of the three most common grapevine leafroll associated virus (GLRaV-1, 3, and 4) as well as Rupestris stem pitting-associated virus.

2.5.3 Berry sampling

The field design of this project was a completely randomized design without blocking. Twenty and twenty-five data vines that tested positive (RB (+)) and negative (RB (-)) for GRBV were selected for each rootstock in 2016 and 2017, respectively. Data vines were further subdivided into four and five vines for each vineyard replicate in 2016 and 2017, respectively (n=5). Vines were sampled every two weeks pre-veraison and weekly two weeks after veraison until harvest. Fifteen berries were randomly collected from different parts of the cluster and canopy of each vine and used to determine ripening progression. At harvest, the sampling was wider to include the vines utilized for winemaking. The values from the data vines regarding ºBrix, pH, and TA (Table 2.1), were compared to the values of asymptomatic and symptomatic vines (Table S2.2), which agreed, indicating that symptomology is a strong indicator of virus status. Primary metabolites and components of harvest yield were measured from each data vines replicate (n=5). For RB (+) and RB (-), 500 berries were randomly collected from harvest lots and stored at -80°C until phenolic analysis and volatile aroma compound analysis could be performed.

2.5.4 Grape analysis through ripening

Upon sampling, 25 berries for each replicate (five berries per data vine) were immediately processed. The juice from the 25 berries was collected and centrifuged at 3,220 x g at 4°C for 15 minutes with an Eppendorf 5403 centrifuge (Westbury, NY). Juice samples were then analyzed for total soluble solids (TSS) with a refractometer RFM110 (Bellingham + Stanley Ltd,

UK), pH with an Orion-5-Star pH meter (Thermo Fisher Scientific Inc, Waltham, MA, USA) and titratable acidity (TA) with an DL50 Graphix titrator (Metter-Tolledo Inc, Columbus, Ohio, USA). The remaining berries were stored at -80oC for future analysis.

The skins were used to determine anthocyanin accumulation in the berries during ripening, since anthocyanins are localized in the pericarp of grape berries for non teinturier varieties [70]. From the berries stored at -80oC, 15 berries from each biological replicate (three berries per data vine) at each collection date were accurately weighed, and the skins of the berries were removed using a scalpel. An acidified ethanol solution (1:1 ethanol:water, 0.1% ascorbic acid (w/v), and 0.1% HCl (v/v)) was added in ratio of 1:10 w/v, and the solution homogenized for three minutes 1,355 × g using an IKA UL-TRA-TURRAX®T18 basic homogenizer (IKA® Works, Inc., NC, USA). The solution extracted overnight for 18 hours at 4°C and was then centrifuged at 3,220 x g at 4oC for 15 minutes. The supernatant was collected, concentrated under reduced pressure at 34°C, and quantitatively transferred to a 5 mL volumetric flask with acidified methanol. Anthocyanin concentration was then determined using a Genesys10S UV-Vis Spectrophotometer (Thermo Fisher Scientific, Madison, WI, USA) with similar protocols as in Harbertson et al. [71]. In summary, an aliquot of grape extract was diluted using model wine (0.5% sodium bitartrate w/v and 12% ethanol v/v adjusted to pH 3.3) to fit the absorbance limitations (0.1-1.2) of the spectrophotometer. Then, 100 µL of the diluted grape extract was added to a disposable cuvette along with 400 µL of model wine and 1mL of an anthocyanin buffer (2.3% maleic acid (w/v) and 0.99% NaCl (w/v) adjusted to pH 1.8). Anthocyanins (expressed as malvidin-3-glucoside equivalents (M3G)) were measured at 520 nm and concentrations were calculated as in Harbertson et al. [71].

2.5.5 Grape analysis at harvest

2.5.5.1 Grape phenolic profile

For the phenolic extraction, five sets of 20 berries from the RB (-) and RB (+) grapevines at harvest were randomly selected from grapes stored at -80°C and weighed. Phenolic compounds were extracted similar to that described for anthocyanins (see Section 4.4) with the addition of a subsequent extraction with an acetone solution (70:30 acetone:water and 0.1% ascorbic acid (w/v)) in the same ratio of 1:10 w/v. After an 18-hour, overnight extraction at 4°C, the solution was centrifuged, and the supernatant collected. The ethanol and acetone extractions were combined, concentrated under reduced pressure at 34°C, quantitatively transferred to a 10 mL volumetric flask with acidified methanol (1:1 methanol:water, 0.1% HCl (v/v)), and stored at -20°C for up to one month until analysis was performed.

A modified protein precipitation assay was used to determine total phenolics, total anthocyanins, and total tannins [72]. Samples were thawed and diluted to fit the limitations of the spectrophotometer (0.1-1.2). Using a Genesys10S UV-Vis Spectrophotometer, total phenolics and total tannins were measured at 510nm absorbance and expressed as catechin equivalents (CE); whereas total anthocyanins (expressed as M3G) were measured at 520nm absorbance.

2.5.5.2 Grape volatile profile

For the volatile extraction, five sets of 60 berries from the RB (-) and RB (+) grapevines collected at harvest were randomly selected from grapes stored at -80°C and weighed. Samples were prepared similar to Hendrickson et al. [73] with a few adaptations. Briefly, 6 mL of a 0.83 M sodium citrate dihydrate solution (adjusted to pH of 6 with HCl) and 60 µl of a 200 g/L

ascorbic acid solution was added to the grape berries. Each sample was spiked with 50 µl of a 10 mg/L 2-octanol internal standard solution. The grape berries were homogenized for one minute 1,355 × g using an IKA ULTRA-TURRAX®T18 basic homogenizer (IKA® Works, Inc., NC, USA). The samples were then centrifuged at 3,220 x g at 4°C for 15 minutes. Samples were analyzed in duplicate by transferring two-8 mL portions of supernatant to 20 ml amber headspace vials (Agilent Technologies, Santa Clara, CA) containing 3 g of NaCl. Each vial was spiked with 50 µl of a 10 mg/L 2-undecanone internal standard solution.

HS-SPME-GC-MS was used to analyze the volatile profiles of grape extracts. The instrument was controlled by a Gerstel Multi-Purpose Sampler (Maestro ver. 1.2.3.1 Gerstel). Headspace volatiles were extracted using a 100µm PDMS, Fused Silica Fiber from Supelco (Supelco Analytical, Bellefonte, PA, USA). Samples were heated to 30°C for five minutes under agitation, and then the PDMS fiber was introduced into the headspace of the sample vial and allowed to adsorb volatiles for 45 minutes. Once volatile adsorption was completed, the fiber was injected into the inlet which was kept at 260°C. The volatiles were allowed to desorb from the fiber onto the column for 10 minutes. Analysis was performed using an Agilent 7890A GC system equipped with a DB-WAXetr capillary column (30m length × 250µm internal diameter × 0.25µm solid phase thickness) (Agilent Technologies, Santa Clara, CA). The carrier gas, helium was kept at a constant pressure of 6.231psi. The method was retention time locked to 2-undecanone and kept at a constant pressure to avoid retention time drift. The purge flow was 50ml/min for 1.2 min, running on a splitless method. For GC analysis, the oven was kept at 40°C for five minutes, then increased to 180°C at 3°C/minute, and finally increased to 260°C at 30°C/minute for a total run time of 60 minutes. The sample was transferred to a 5975C inert XL EI MSD with a triple-axis detector purchased from Agilent Technologies and ions were

monitored using synchronous scan and selected ion monitoring (SIM). All compounds identified in this study were identified using the SIM mode as described in Hendrickson et al. [73]. Samples were analyzed using Mass Hunter software version B.07.00 (Agilent Technologies, Santa Clara, CA). Compounds were semi-quantitatively analyzed using relative peak areas by normalization with 2-undecanone as well as the berry mass. Compounds were identified by retention time and confirmation of mass spectra ion peaks using the National Institute of Standards and Technology database (NIST) (https://www.nist.gov). Each grape sample replicate was analyzed in duplicate.

2.5.6 Weather recordings

Precipitation, temperature, and growing degree days were collected from the University of California Agriculture and Natural Resources Integrated Pest Management Program (http://ipm.ucanr.edu/index.html) (Figure 2.1).

2.5.7 Statistical analysis

Statistical analysis was conducted in the R language (R, version 3.6.1). All analyses used an α of 0.05 for statistical significances. One-way analysis of variance (ANOVA) and three-way ANOVA with three-way interactions were used to determine significant differences between samples. For a three-way ANOVA with three-way interactions, only the interactions of virus status to rootstock and virus status to year were considered to determine the influence genotypic or seasonal factors had on virus status. Virus status, rootstock, and year were all considered fixed effects for the purpose of determining the genotypic and temporal effects on disease status. A

Tukey's honestly significant difference (HSD) test was used for post-hoc analysis. Principal component analysis (PCA) was used to display the variance in volatile analysis.

2.6 Conclusions:

Geminiviruses threaten the productivity and quality of crops worldwide. GRBV is the first geminivirus to be detected in grapevines and our understanding of the detrimental impacts on grape and wine composition and quality is advancing. In this study CS on 420A rootstock was less sensitive to GRBV infection then CS on 110R rootstock. This was seen in anthocyanin and sugar accumulation in 2017, as well as the grape volatile profiles. This study also clearly indicated for the first time that the aroma profiles of grapes are also impacted by GRBV. We hypothesize that the difference in vigor and drought resistance in the two rootstocks led to a difference in microclimate of the grapevine and berry composition. Moreover, it was observed that seasonal differences considerably impact disease outcome in grapevines, mainly observed on primary metabolites such as sugars and organic acids. Further research into the transcriptome and metabolome of GRBV infected grapevines is needed to elucidate how these factors affect differential gene expression. In addition, these effects need to be evaluated in overall wine composition and quality.

Author Contributions: Conceptualization, A.C.R., R.C.G, A.O. and S.K.K.; Methodology, A.C.R. and R.C.G.; Software, A.C.R. and R.C.G.; Investigation, A.C.R and R.C.G.; Formal Analysis, A.C.R. and R.C.G.; Data Curation A.C.R., R.G., and C.P; Vineyard maintenance, M.L.C.; Sample collection and data recording, A.C.R., R.C.G., M.L.C., and C.P.; Writing-

Original Draft Preparation, A.C.R.; Writing- Review & Editing, A.C.R., R.C.G, M.L.C., S.K.K., A.O.; Supervision, A.O.; Project Administration, A.O.; Funding Acquisition, A.O.

Funding: This research was funded by the American Vineyard Foundation (AVF) grant number 2017-1675. “The APC was funded by AVF and UC Davis Open Access Grant”.

Acknowledgments: This study was financially supported by the American Vineyard Foundation (AVF). Student support was received from the Department of Viticulture and Enology, the graduate group of Horticulture and Agronomy, and the graduate group of Agricultural and Environmental Chemistry at the University of California, Davis. We thank the technical staff of the Department of Viticulture and Enology from the University of California, Davis for the use and training of facility instruments. Finally, the authors acknowledge the reviewers for their productive feedback on this manuscript.

Conflicts of Interest: The authors declare no conflict of interest. The funders had no role in the design of the study; in the collection, analyses, or interpretation of data; in the writing of the manuscript, or in the decision to publish the results.

2.7 Supplementary Materials:

Table S2.1. °Brix, pH, TA (g/L), YAN (mg/L), and malic acid (mg/L) measurements from CS 110R and CS 420A symptomatic and asymptomatic vines used for winemaking in 2016 and 2017 (n=3).

Sample	Harvest Date	°Brix	pH	TA (g/L)	Malic Acid (mg/L)
CS 110R RB (-)	**9/20/16**	25.6 ± 0.1 a	3.6 ± 0.0 a	3.8 ± 0.3 b	1460.0 ± 55. b
CS 110R RB (+)	**9/20/16**	21.7 ± 0.1 b	3.5 ± 0.0 a	4.8 ± 0.1 a	2275.0 ± 48.6 a
CS 420A RB (-)	**9/20/16**	24.3 ± 0.1 a	3.5 ± 0.0 a	4.2 ± 0.1 b	1625.7 ± 48.0 b
CS 420A RB (+)	**9/20/16**	22.1 ± 0.1 b	3.5 ± 0.0 a	4.5 ± 0.1 a	1852.0 ± 13.9 a
CS 110R RB (-)	**9/26/17**	25.5 ± 0.1 a	3.6 ± 0.0 a	4.0 ± 0.0 b	2649.3 ± 45.7 a
CS 110R RB (+)	**9/26/17**	23.4 ± 0.0 b	3.6 ± 0.0 a	4.9 ± 0.1 a	2779.0 ± 68.6 a
CS 420A RB (-)	**10/6/17**	25.3 ± 0.1 a	3.6 ± 0.0 a	4.6 ± 0.1 a	2201.0 ± 34.7 b
CS 420A RB (+)	**10/6/17**	23.6 ± 0.3 b	3.5 ± 0.0 a	4.8 ± 0.0 a	2870.0 ± 21.0 a

TA= Titratable Acidity, CS110= CS 110R, CS420= CS 420A, RB=red blotch, (-)=negative, and (+)=positive. Difference in lettering indicates a significant difference between RB (-) and RB (+) after applying Tuckey's HSD test ($p<0.05$).

Table S2.2 Phenolic content (mg/berry) and concentrations (mg/ g berry) of grape extracts at harvest determined through protein precipitation assay across rootstocks and seasons. The main effects, two-way, and three-way interactions ANOVA were determined for content and concentration for each class of compounds.

mg/berry				mg/g berry			
2016	**Total Phenolics**	**Total Anthocyanins**	**Total Tannins**	**2016**	**Total Phenolics**	**Total Anthocyanins**	**Total Tannins**
CS 110R RB(-)	7.54 ± 0.41	1.57 ± 0.43	3.04 ± 0.21	**CS 110R RB(-)**	6.54 ± 0.17	1.28 ± 0.40	2.64 ± 0.15
CS 110R RB(+)	8.60 ± 0.27	1.54 ± 0.16	3.31 ± 0.13	**CS 110R RB(+)**	7.55 ± 0.20	1.31 ± 0.17	2.90 ± 0.069
CS 420A RB(-)	9.49 ± 0.68	0.76 ± 0.079	3.82 ± 0.19	**CS 420A RB(-)**	7.42 ± 0.52	0.66 ± 0.024	2.99 ± 0.15
CS 420A RB(+)	10.25 ± 0.77	0.68 ± 0.12	3.47 ± 0.33	**CS 420A RB(+)**	6.94 ± 0.77	0.60 ± 0.07	2.35 ± 0.32
2017	**Total Phenolics**	**Total Anthocyanins**	**Total Tannins**	**2017**	**Total Phenolics**	**Total Anthocyanins**	**Total Tannins**
CS 110R RB(-)	8.22 ± 0.96	1.30 ± 0.18	6.24 ± 0.79	**CS 110R RB(-)**	8.73 ± 0.61	1.37 ± 0.14	6.62 ± 0.47
CS 110R RB(+)	9.72 ± 1.46	0.84 ± 0.14	7.23 ± 1.04	**CS 110R RB(+)**	11.72 ± 0.83	0.85 ± 0.10	8.73 ± 0.65
CS 420A RB(-)	11.22 ± 1.09	2.63 ± 0.35	9.01 ± 0.84	**CS 420A RB(-)**	10.85 ± 0.68	2.81 ± 0.31	8.71 ± 0.42
CS 420A RB(+)	9.78 ± 0.43	2.33 ± 0.20	7.77 ± 0.37	**CS 420A RB(+)**	9.65 ± 0.43	2.44 ± 0.20	7.66 ± 0.31
Significant Effects				**Significant Effects**			
V		**		**V**	***	**	*
Y	**	***	***	**Y**	***	***	***
R	***	***	***	**R**	*	***	**
V x Y		*		**V x Y**		**	*
V x R	**		***	**V x R**	***		***
Y x R		***	**	**Y x R**	*	***	
V x Y x R	*		*	**V x Y x R**	***		***

CS= Cabernet Sauvignon, RB= red blotch, (-)= negative, (+)= positive, V= virus status, Y= year, and R= rootstock. Asterisks indicate a significant difference between RB (-) and RB (+) after an ANOVA (*=$p<0.05$, **=$p<0.01$, ***=$p<0.001$).

Table S2.3 HS-SPME-GC-MS analysis of volatile compound content (mg/berry) in grapes at harvest (n=5).

	2017				2016			
Compound (mg/ berry)	CS 110R RB (-)	CS 110R RB (+)	CS 420A RB (-)	CS 420A RB (+)	CS 110R RB (-)	CS 110R RB (+)	CS 420A RB (-)	CS 420A RB (+)
Ethyl Acetate †ϕ	0.92 ± 0.45	3.88 ± 1.22	0.07 ± 0.03	0.07 ± 0.05	2.27 ± 0.49	0.59 ± 0.17	1.32 ± 0.37	1.00 ± 0.29
Hexanal	4.73 ± 1.12	1.55 ± 0.99	3.94 ± 2.35	4.84 ± 2.91	0.10 ± 0.02	0.15 ± 0.04	0.11 ± 0.02	0.17 ± 0.04
β-Myrcene	0.03 ± 0.02	0.01 ± 0.00	0.03 ± 0.01	0.03 ± 0.02	0.49 ± 0.11	0.35 ± 0.08	0.40 ± 0.09	0.30 ± 0.09
Limonene#ϕ	0.12 ± 0.05	0.07 ± 0.03	0.12 ± 0.02	0.14 ± 0.05	0.29 ± 0.03	0.20 ± 0.03	0.22 ± 0.04	0.20 ± 0.04
2-Hexenal †#ϕ	1.61 ± 0.61	0.82 ± 0.39	1.98 ± 0.74	3.04 ± 1.79	7.14 ± 1.50	13.33 ± 3.09	10.78 ± 1.37	15.97 ± 2.09
Ethyl Hexanoate †#ϕ	0.18 ± 0.09	0.21 ± 0.12	0.06 ± 0.02	0.04 ± 0.04	0.49 ± 0.07	0.26 ± 0.08	0.32 ± 0.08	0.30 ± 0.11
p-Cymene #ϕ	0.01 ± 0.00	0.01 ± 0.00	0.01 ± 0.00	0.01 ± 0.00	0.04 ± 0.00	0.02 ± 0.00	0.02 ± 0.00	0.02 ± 0.00
Hexyl acetate †ϕ	0.04 ± 0.03	0.07 ± 0.03	0.03 ± 0.00	0.03 ± 0.01	0.61 ± 0.08	0.38 ± 0.07	0.46 ± 0.07	0.40 ± 0.06
Octanal ϕ	0.02 ± 0.01	0.01 ± 0.01	0.02 ± 0.00	0.03 ± 0.01	0.13 ± 0.02	0.13 ± 0.03	0.18 ± 0.04	0.18 ± 0.05
Hexanol †	1.72 ± 0.43	1.62 ± 0.60	1.52 ± 0.29	1.91 ± 1.23	10.36 ± 2.31	9.22 ± 3.40	8.19 ± 1.30	9.66 ± 1.88
trans-3-Hexen-1-ol †	0.11 ± 0.04	0.09 ± 0.03	0.11 ± 0.02	0.14 ± 0.09	1.09 ± 0.25	0.73 ± 0.20	0.78 ± 0.18	0.78 ± 0.15
cis-3-Hexen-1-ol †#	0.28 ± 0.09	0.39 ± 0.14	0.25 ± 0.06	0.59 ± 0.30	1.18 ± 0.35	2.97 ± 1.19	1.33 ± 0.19	2.86 ± 0.54
trans-2-Hexen-1-ol †#ϕ	6.11 ± 2.24	5.98 ± 2.20	6.02 ± 1.02	7.98 ± 4.96	7.03 ± 1.58	6.03 ± 2.42	5.38 ± 0.86	7.63 ± 1.27
Ethyl Octanoate	0.02 ± 0.02	0.01 ± 0.01	0.95 ± 0.05	1.36 ± 0.58	0.05 ± 0.01	0.03 ± 0.01	1.98 ± 0.35	2.42 ± 0.33
Nerol oxide #	0.02 ± 0.03	0.01 ± 0.01	0.09 ± 0.03	0.12 ± 0.07	0.17 ± 0.02	0.14 ± 0.02	0.43 ± 0.10	0.37 ± 0.16
Benzaldehyde #	0.09 ± 0.03	0.06 ± 0.02	0.003 ± 0.00	0.01 ± 0.00	0.61 ± 0.14	0.40 ± 0.10	0.14 ± 0.02	0.15 ± 0.02
β-linalool	0.01 ± 0.00	0.01 ± 0.00	0.05 ± 0.01	0.06 ± 0.03	0.08 ± 0.02	0.05 ± 0.01	0.42 ± 0.07	0.46 ± 0.10
Geranial †#	0.02 ± 0.00	0.02 ± 0.01	0.03 ± 0.01	0.04 ± 0.01	0.07 ± 0.01	0.04 ± 0.00	3.02 ± 0.13	3.02 ± 0.29
β-Damascenone †	0.01 ± 0.00	0.02 ± 0.01	0.01 ± 0.00	0.01 ± 0.00	0.03 ± 0.01	0.02 ± 0.01	0.05 ± 0.01	0.04 ± 0.01
Benzyl alcohol #	0.19 ± 0.049	0.12 ± 0.05	0.004 ± 0.00	0.01 ± 0.00	0.79 ± 0.15	0.52 ± 0.14	0.02 ± 0.01	0.03 ± 0.01
2-Phenethyl alcohol	0.22 ± 0.05	0.15 ± 0.07	0.14 ± 0.05	0.15 ± 0.06	1.14 ± 0.22	0.74 ± 0.15	0.29 ± 0.07	0.22 ± 0.07
β-Ionone ϕ	0.01 ± 0.00	0.01 ± 0.01	0.11 ± 0.03	0.11 ± 0.06	0.03 ± 0.00	0.01 ± 0.00	0.45 ± 0.09	0.46 ± 0.10
Ethyl cinnamate †	0.01 ± 0.01	0.02 ± 0.00	0.01 ± 0.00	0.01 ± 0.00	0.07 ± 0.04	0.03 ± 0.01	0.02 ± 0.00	0.02 ± 0.00

CS= Cabernet Sauvignon, RB= red blotch, (-)= negative, (+)= positive, †= volatile compound has significant virus status to year effect, #= volatile compound has significant virus status to rootstock effect, ϕ= volatile compound has significant virus status effect.

2.8 References

1. Dolja, V. V; Meng, B.; Martelli, G.P. Evolutionary Aspects of Grapevine Virology BT - Grapevine Viruses: Molecular Biology, Diagnostics and Management. **2017**, 659–688.
2. Calvi, B.L. Effects Of Red-leaf Disease On Cabernet Sauvignon At The Oakville Experimental Vineyard And Mitigation By Harvest Delay And Crop Adjustment. *MSc. Thesis. Univ. Calif.* **2011**.
3. Yepes, L.M.; Cieniewicz, E.; Krenz, B.; McLane, H.; Thompson, J.R.; Perry, K.L.; Fuchs, M. Causative Role of Grapevine Red Blotch Virus in Red Blotch Disease. *Phytopathology* **2018**, *108*, 902–909.
4. Krenz, B.; Thompson, J.R.; Mclane, H.L.; Fuchs, M.; Perry, K.L. Phyto-02-14-0053-R. **2014**, 1232–1240.
5. Poojari, S.; Lowery, D.T.; Rott, M.; Schmidt, A.M.; Úrbez-Torres, J.R. Incidence, distribution and genetic diversity of Grapevine red blotch virus in British Columbia. *Can. J. Plant Pathol.* **2017**, *39*, 201–211.
6. Luna, F.; Debat, H.; Gomez-Talquenca, S.; Moyano, S.; Zavallo, D.; Asurmendi, S. First report of grapevine red blotch virus infecting grapevine in Argentina. *J. Plant Pathol.* **2019**, *101*.
7. Lim, S.; Igori, D.; Zhao, F.; Moon, J.; Cho, I.-S.; Choi, G.-S. First report of Grapevine red blotch-associated virus on grapevine in Korea. *Plant Dis.* **2016**, *100*, 1957.
8. Marwal, A.; Kumar, R.; Paul Khurana, S.M.; Gaur, R.K. Complete nucleotide sequence of a new geminivirus isolated from Vitis vinifera in India: a symptomless host of Grapevine red blotch virus. *VirusDisease* **2019**, *30*, 106–111.
9. Gasperin-Bulbarela, J.; Licea-Navarro, A.F.; Pino-Villar, C.; Hernández-Martínez, R.; Carrillo-Tripp, J. First Report of Grapevine Red Blotch Virus in Mexico. *Plant Dis.* **2019**, *103*, 381.
10. Sudarshana, M.R.; Perry, K.L.; Fuchs, M.F. Grapevine Red Blotch-Associated Virus, an Emerging Threat to the Grapevine Industry Mysore. *Phytopathology* **2015**, 1026–1032.
11. Cieniewicz, E.; Flasco, M.; Brunelli, M.; Onwumelu, A.; Wise, A.; Fuchs, M.F. Differential spread of grapevine red blotch virus in California and New York vineyards. *Phytobiomes J.* **2019**, *3*, 203–211.
12. Bahder, B.W.; Zalom, F.G.; Jayanth, M.; Sudarshana, M.R. Phylogeny of Geminivirus Coat Protein Sequences and Digital PCR Aid in Identifying Spissistilus festinus as a Vector of Grapevine red blotch-associated virus . *Phytopathology* **2016**, *106*, 1223–1230.
13. Rwahnih, M. Al; Dave, A.; Anderson, M.M.; Rowhani, A.; Uyemoto, J.K.; Sudarshana, M.R. Association of a DNA Virus with Grapevines Affected by Red Blotch Disease in California. *Phytopathology* **2013**, *103*, 1069–1076.
14. Varsani, A.; Roumagnac, P.; Fuchs, M.; Navas-Castillo, J.; Moriones, E.; Idris, A.; Briddon, R.W.; Rivera-Bustamante, R.; Murilo Zerbini, F.; Martin, D.P. Capulavirus and Grablovirus: two new genera in the family Geminiviridae. *Arch. Virol.* **2017**, *162*, 1819–1831.
15. Shepherd, R.J. DNA Plant Viruses. *Annu. Rev. Plant Physiol.* **1979**, *30*, 405–423.
16. Buchs, N.; Braga-Lagache, S.; Uldry, A.C.; Brodard, J.; Debonneville, C.; Reynard, J.S.; Heller, M. Absolute quantification of grapevine red blotch virus in grapevine leaf and petiole tissues by proteomics. *Front. Plant Sci.* **2018**, *871*.
17. Martínez-Lüscher, J.; Plank, C.M.; Brillante, L.; Cooper, M.L.; Smith, R.J.; Al-Rwahnih,

M.; Yu, R.; Oberholster, A.; Girardello, R.; Kurtural, S.K. Grapevine Red Blotch Virus May Reduce Carbon Translocation Leading to Impaired Grape Berry Ripening. *J. Agric. Food Chem.* **2019**, *67*, 2437–2448.
18. Wallis, C.M.; Sudarshana, M.R. Effects of Grapevine red blotch-associated virus (GRBaV) infection on foliar metabolism of grapevines. *Can. J. Plant Pathol.* **2016**, *38*, 358–366.
19. Girardello, R.C.; Rich, V.; Smith, R.J.; Brenneman, C.; Heymann, H.; Oberholster, A. The impact of grapevine red blotch disease on *Vitis vinifera* L. Chardonnay grape and wine composition and sensory attributes over three seasons. *J. Sci. Food Agric.* **2019**, jsfa.10147.
20. Girardello, R.C.; Cooper, M.L.; Smith, R.J.; Lerno, L.A.; Bruce, R.C.; Eridon, S.; Oberholster, A. Impact of Grapevine Red Blotch Disease on Grape Composition of Vitis vinifera Cabernet Sauvignon, Merlot, and Chardonnay. *J. Agric. Food Chem.* **2019**, *67*, 5496–5511.
21. Girardello, R.C.; Cooper, M.L.; Lerno, L.A.; Brenneman, C.; Eridon, S.; Sokolowsky, M.; Heymann, H.; Oberholster, A. Impact of Grapevine Red Blotch Disease on Cabernet Sauvignon and Merlot Wine Composition and Sensory Attributes. *Molecules* **2020**, *25*.
22. Ricketts, K.D.; Gómez, M.I.; Fuchs, M.F.; Martinson, T.E.; Smith, R.J.; Cooper, M.L.; Moyer, M.M.; Wise, A. Mitigating the economic impact of grapevine red blotch: Optimizing disease management strategies in U.S. vineyards. *Am. J. Enol. Vitic.* **2017**, *68*, 127–135.
23. Ollat, N., Carde, J.-P., Gaudillère, J.-P., Barrieu, F., Diakou-Verdin, P., & Moing, A. Grape berry development: A review. *OENO One, 36(3), 109-131.* **2002**, *36*, 109–131.
24. Conde, C.; Silva, P.; Fontes, N.; Dias, A.C.P.; Tavares, R.M.; Sousa, M.J.; Agasse, A.; Delrot, S.; Gerós, H. Biochemical changes throughout grape berry development and fruit and wine quality. *Food* **2007**, *1*, 1–22.
25. Kalua, C.M.; Boss, P.K. Evolution of volatile compounds during the development of cabernet sauvignon grapes (Vitis vinifera l.). *J. Agric. Food Chem.* **2009**, *57*, 3818–3830.
26. Martin, D.M.; Chiang, A.; Lund, S.T.; Bohlmann, J. Biosynthesis of wine aroma: Transcript profiles of hydroxymethylbutenyl diphosphate reductase, geranyl diphosphate synthase, and linalool/nerolidol synthase parallel monoterpenol glycoside accumulation in Gewürztraminer grapes. *Planta* **2012**, *236*, 919–929.
27. Matarese, F.; Scalabrelli, G.; D'Onofrio, C. Analysis of the expression of terpene synthase genes in relation to aroma content in two aromatic Vitis vinifera varieties. *Funct. Plant Biol.* **2013**, *40*, 552–565.
28. Chang, E.H.; Jeong, S.M.; Hur, Y.Y.; Koh, S.W.; Choi, I.M. Changes of volatile compounds in vitis labrusca 'Doonuri' grapes during stages of fruit development and in wine. *Hortic. Environ. Biotechnol.* **2015**, *56*, 137–144.
29. Friedel, M.; Frotscher, J.; Nitsch, M.; Hofmann, M.; Bogs, J.; Stoll, M.; Dietrich, H. Light promotes expression of monoterpene and flavonol metabolic genes and enhances flavour of winegrape berries (Vitis vinifera L. cv. Riesling). *Aust. J. Grape Wine Res.* **2016**, *22*, 409–421.
30. Gershenzon, J.; Dudareva, N. The function of terpene natural products in the natural world. *Nat. Chem. Biol.* **2007**, *3*, 408–414.
31. Allamy, L.; Darriet, P.; Pons, A. Molecular interpretation of dried-fruit aromas in Merlot and Cabernet Sauvignon musts and young wines: Impact of over-ripening. *Food Chem.*

2018, *266*, 245–253.
32. Bindon, K.; Holt, H.; Williamson, P.O.; Varela, C.; Herderich, M.; Francis, I.L. Relationships between harvest time and wine composition in Vitis vinifera L. cv. Cabernet Sauvignon 2. Wine sensory properties and consumer preference. *Food Chem.* **2014**, *154*, 90–101.
33. Néya, B.J.; Zida, P.E.; Sérémé, D.; Lund, O.S.; Traoré, O. Evaluation of yield losses caused by cowpea aphid-borne mosaic virus (CABMV) in 21 cowpea (vigna unguiculata (L.) Walp.) Varieties in burkina faso. *Pakistan J. Biol. Sci.* **2015**, *18*, 304–313.
34. Tripathi, A.; Goswami, K.; Tiwari, M.; Mukherjee, S.K.; Sanan-Mishra, N. Identification and comparative analysis of microRNAs from tomato varieties showing contrasting response to ToLCV infections. *Physiol. Mol. Biol. Plants* **2018**, *24*, 185–202.
35. Reustle, G.M.; Ebel, R.; Winterhagen, P.; Manthey, T.; Dubois, C.; Bassler, A.; Sinn, M.; Cobanov, P.; Wetzel, T.; Krezal, G. Induction of silencing in transgenic grapevines (Vitis sp.). *ACTA Hortic.* **2005**.
36. Pongracz, D.P. *Rootstocks for grapevines*; [Barnes & Nobles Books]: [Totowa, N.J.], 1983; ISBN 9780389205678 0389205672.
37. Wang, Y.; Chen, W.K.; Gao, X.T.; He, L.; Yang, X.H.; He, F.; Duan, C.Q.; Wang, J. Rootstock-mediated effects on cabernet sauvignon performance: vine growth, berry ripening, flavonoids, and aromatic profiles. *Int. J. Mol. Sci.* **2019**, *20*.
38. Chellappan, P.; Vanitharani, R.; Ogbe, F.; Fauquet, C.M. Effect of temperature on geminivirus-induced RNA silencing in plants. *Plant Physiol.* **2005**, *138*, 1828–1841.
39. Alabi, O.J.; Casassa, L.F.; Gutha, L.R.; Larsen, R.C.; Henick-Kling, T.; Harbertson, J.F.; Naidu, R.A. Impacts of Grapevine Leafroll Disease on Fruit Yield and Grape and Wine Chemistry in a Wine Grape (Vitis vinifera L.) Cultivar. *PLoS One* **2016**, *11*, e0149666.
40. Deloire, A. The concept of berry sugar loading. **2011**, *257*, 93–95.
41. Blanco-Ulate, B.; Hopfer, H.; Figueroa-Balderas, R.; Ye, Z.; Rivero, R.M.; Albacete, A.; Pérez-Alfocea, F.; Koyama, R.; Anderson, M.M.; Smith, R.J.; et al. Red blotch disease alters grape berry development and metabolism by interfering with the transcriptional and hormonal regulation of ripening. *J. Exp. Bot.* **2017**, *68*, 1225–1238.
42. Wallis, C.M.; Sudarshana, M.R.; Girardello, R.C.; Cooper, M.L.; Smith, R.J.; Lerno, L.A.; Bruce, R.C.; Eridon, S.; Oberholster, A. Effects of Grapevine red blotch-associated virus (GRBaV) infection on foliar metabolism of grapevines. *Can. J. Plant Pathol.* **2016**, *38*, 5496–5511.
43. Abdi, H.; Williams, L.J. Principal component analysis. *Wiley Interdiscip. Rev. Comput. Stat.* **2010**, *2*, 433–459.
44. Pedneault, K.; Dorais, M.; Angers, P. Flavor of cold-hardy grapes: Impact of berry maturity and environmental conditions. *J. Agric. Food Chem.* **2013**, *61*, 10418–10438.
45. Deluc, L.G.; Grimplet, J.; Wheatley, M.D.; Tillett, R.L.; Quilici, D.R.; Osborne, C.; Schooley, D.A.; Schlauch, K.A.; Cushman, J.C.; Cramer, G.R.; et al. Transcriptomic and metabolite analyses of Cabernet Sauvignon grape berry development. *BMC Genomics* **2013**, *61*, 10418–10438.
46. Goliáš, J.; Létal, J.; Veselý, O. Evaluation of volatile compounds during the ripening in south Moravian "Gewürztraminer" and "Sauvignon Blanc" from the Pálava Region. *Mitt. Klosterneubg.* **2016**, *66*, 189–197.
47. Wilson, B.; Strauss, C.R.; Williams, P.J. Changes in Free and Glycosidically Bound Monoterpenes in Developing Muscat Grapes. *J. Agric. Food Chem.* **1984**, *32*, 919–924.

48. Coelho, E.; Rocha, S.M.; Delgadillo, I.; Coimbra, M.A. Headspace-SPME applied to varietal volatile components evolution during Vitis vinifera L. cv. “Baga” ripening. *Anal. Chim. Acta* **2006**, *563*, 204–214.
49. Bell, S.J.; Henschke, P.A. Implications of nitrogen nutrition for grapes, fermentation and wine. *Aust. J. Grape Wine Res.* **2005**, *11*, 242–295.
50. Swiegers, J.H.; Bartowsky, E.J.; Henschke, P.A.; Pretorius, I.S. Yeast and bacterial modulation of wine aroma and flavour. *Aust. J. Grape Wine Res.* **2005**, *11*, 139–173.
51. Wang, J.; Luca, V. De The biosynthesis and regulation of biosynthesis of Concord grape fruit esters, including “foxy” methylanthranilate. *Plant J.* **2005**, *44*, 606–619.
52. Escudero, A.; Campo, E.; Fariña, L.; Cacho, J.; Ferreira, V. Analytical characterization of the aroma of five premium red wines. Insights into the role of odor families and the concept of fruitiness of wines. *J. Agric. Food Chem.* **2007**, *55*, 4501–4510.
53. Lytra, G.; Tempere, S.; Revel, G. De; Barbe, J.C. Impact of perceptive interactions on red wine fruity aroma. *J. Agric. Food Chem.* **2012**, *60*, 12260–12269.
54. Pineau, B.; Barbe, J.C.; Leeuwen, C. Van; Dubourdieu, D. Examples of perceptive interactions involved in specific “Red-” and “Black-berry” aromas in red wines. *J. Agric. Food Chem.* **2009**, *57*, 3702–3708.
55. Coombe, B.G. Influence of Temperature on Composition and Quality of Grapes. *Acta Hortic.* **1987**, 23–25.
56. Jones, H.G. *Plants and Microclimate: A Quantitative Approach to Environmental Plant Physiology*; 3rd ed.; Cambridge University Press: Cambridge, 2013; ISBN 9780521279598.
57. Spayd, S.E.; Tarara, J.M.; Mee, D.L.; Ferguson, J.C. <Spayd et al_2002_Separation of light and temp on Merlot comp.pdf>. **2002**, *3*, 171–182.
58. Bergqvist, J.; Dokoozlian, N.; Ebisuda, N. Sunlight exposure and temperature effects on berry growth and composition of Cabernet Sauvignon and Grenache in the central San Joaquin Valley of California. *Am. J. Enol. Vitic.* **2001**, *52*, 1–7.
59. SEPULVEDA, G.; KLIEWER, W. Effect of high temperature on grapevines (Vitis vinifera L.). II: Distribution of soluble sugars. *Am. J. Enol. Vitic.* **1986**, *37*, 20–25.
60. Kriedemann, P.E.; Smart, R.E. Effects of irradiance, temperature, and leaf water potential on photosynthesis of vine leaves. *Photosynthetica* **1971**, *5*, 6–15.
61. Flores, M.A.; Reyes, M.I.; Robertson, D. (Niki); Kjemtrup, S. Persistent Virus-Induced Gene Silencing in Asymptomatic Accessions of Arabidopsis BT - Plant Functional Genomics: Methods and Protocols. In; Alonso, J.M., Stepanova, A.N., Eds.; Springer New York: New York, NY, 2015; pp. 305–322 ISBN 978-1-4939-2444-8.
62. Tuttle, J.R.; Idris, A.M.; Brown, J.K.; Haigler, C.H.; Robertson, D. Geminivirus-mediated gene silencing from cotton leaf crumple virus is enhanced by low temperature in cotton. *Plant Physiol.* **2008**, *148*, 41–50.
63. Mori, K.; Goto-Yamamoto, N.; Kitayama, M.; Hashizume, K. Loss of anthocyanins in red-wine grape under high temperature. *J. Exp. Bot.* **2007**, *58*, 1935–1945.
64. Downey, M.O.; Dokoozlian, N.K.; Krstic, M.P. Cultural practice and environmental impacts on the flavonoid composition of grapes and wine: A review of recent research. *Am. J. Enol. Vitic.* **2006**, *57*, 257–268.
65. Downey, M.O.; Harvey, J.S.; Robinson, S.P. The effect of bunch shading on berry development and flavonoid accumulation in Shiraz grapes. *Aust. J. Grape Wine Res.* **2004**, *10*, 55–73.

66. Blancquaert, E.H.; Oberholster, A.; Ricardo-da-Silva, J.M.; Deloire, A.J. Grape Flavonoid Evolution and Composition Under Altered Light and Temperature Conditions in Cabernet Sauvignon (Vitis vinifera L.). *Front. Plant Sci.* **2019**, *10*, 1–19.
67. Blancquaert, E.H.; Oberholster, A.; Ricardo-da-Silva, J.M.; Deloire, A.J. Effects of abiotic factors on phenolic compounds in the grape berry - A review. *South African J. Enol. Vitic.* **2019**, *40*.
68. Treutter, D. Significance of flavonoids in plant resistance and enhancement of their biosynthesis. *Plant Biol.* **2005**, *7*, 581–591.
69. Haselgrove, L.; Botting, D.; Van Heeswijck, R.; Høj, P.B.; Dry, P.R.; Ford, C.; Iland, P.G. Canopy microclimate and berry composition: The effect of bunch exposure on the phenolic composition of Vitis vinifera L. cv. Shiraz grape berries. *Aust. J. Grape Wine Res.* **2000**, *6*, 141–149.
70. Braidot, E.; Zancani, M.; Petrussa, E.; Peresson, C.; Bertolini, A.; Patui, S.; Macrì, F.; Vianello, A. Transport and accumulation of flavonoids in grapevine (Vitis vinifera L.). *Plant Signal. Behav.* **2008**, *3*, 626–632.
71. Harbertson, J.F.; Picciotto, E.A.; Adams, D.O. Measurement of Polymeric Pigments in Grape Berry Extract sand Wines Using a Protein Precipitation Assay Combined with Bisulfite Bleaching. *Am. J. Enol. Vitic.* **2003**, *54*, 301–306.
72. Harbertson, J.F.; Mireles, M.; Yu, Y. Improvement of BSA tannin precipitation assay by reformulation of resuspension buffer. *Am. J. Enol. Vitic.* **2015**, *66*, 95–99.
73. Hendrickson, D.A.; Lerno, L.A.; Hjelmeland, A.K.; Ebeler, S.E.; Heymann, H.; Hopfer, H.; Block, K.L.; Brenneman, C.A.; Oberholster, A. Impact of mechanical harvesting and optical berry sorting on grape and wine composition. *Am. J. Enol. Vitic.* **2016**, *67*, 385–397.

CHAPTER 3

Phenological Association with Virus-Induced Gene Silencing during Grapevine Red Blotch Virus Infection

Formatted for publication in *Molecular Plant*

3.1 Abstract:

Grapevine red blotch virus (GRBV) is a recently identified virus that is the causative agent of grapevine red blotch disease (GRBD). Previous research indicates primarily a substantial impact on berry ripening in all varieties studied. The current study analyzed grapes' primary and secondary metabolism across grapevine genotypes and seasons to reveal both conserved and variable impacts to GRBV infection. *Vitis vinifera* cv. Cabernet Sauvignon (CS) grapevines grafted on two different rootstocks (110R and 420A) were studied in 2016 and 2017. Metabolite profiling revealed a considerable impact on amino acid and malate acid levels, volatile aroma compounds derived from the lipoxygenase pathway, and anthocyanins synthesized in the phenylpropanoid pathway. Larger differences were found for CS 110R, specifically for anthocyanin concentrations at harvest in 2017. Conserved transcriptional responses to GRBV showed induction of auxin-mediated pathways and photosynthesis with inhibition of transcription and translation processes mainly at harvest. There was an induction of plant-pathogen interactions at pre-veraison, for all genotypes and seasons, except for CS 110R in 2017. Lastly, differential co-expression analysis revealed a transcriptional shift from metabolic synthesis and energy metabolism to transcription and translation processes associated with a virus-induced gene silencing transcript. This plant-derived defense response transcript was only significantly upregulated at veraison for all genotypes and

seasons, suggesting a phenological association with disease expression and plant immune responses.

3.2 Introduction:

Geminiviruses are responsible for detrimental effects on crop yield and quality worldwide. The international trading of agricultural materials has led to the rapid spread of geminiviruses between continents and the evolution of new virulent strains through recombination and mutation events. There are currently nine genera in the *Geminiviridae* family of viruses (*Becurtovirus, Begomovirus, Capulavirus, Curtovirus, Eragrovirus, Grablovirus, Mastrevirus, Topocuvirus,* and *Turncurtovirus*) consisting of 520 different species (Beam and Ascencio-Ibáñez, 2020). All members contain a circular single-stranded (ss) DNA genome, either mono- or bi-partite, with a distinct intergenic region that includes a nonanucleotide motif that functions as the origin of replication (Rojas et al., 2005). Geminiviruses encode viral proteins via bidirectional transcription in the virion-sense and complimentary-sense.

Like all viruses, geminiviruses must hijack and reprogram the host's cellular machinery to successfully create an infection. Upon infection, DNA viruses require DNA polymerase for replication; therefore, they must enter the nuclei of the host cells where the ssDNA is replicated through dsDNA intermediates (Hanley-Bowdoin et al., 2000). These dsDNA intermediates form dsRNAs that are well documented to be associated with antiviral RNA silencing (Blevins et al., 2006; Prasad et al., 2019). The dsRNAs are cleaved by Dicer-like (DCL) proteins to form small (~21-24 nt) RNAs (sRNAs) that mediate RNA silencing in plants and are classified into two groups: microRNAs (miRNAs) and short interfering RNAs (siRNAs) (Blevins et al., 2006). The production of siRNAs leads to several processes, such as degradation of existing RNA (post-

transcriptional gene silencing) or targeting DNA for methylation (transcriptional gene silencing) (Beam and Ascencio-Ibáñez, 2020). Tolerant or resistant plant cultivars are known to activate this silencing pathway to lower viral titer levels to achieve an antiviral state (Prasad et al., 2019). To combat this plant immune response, geminiviruses encode distinct suppressors of RNA silencing leading to abnormalities in plant development which may result in symptoms (Akbergenov et al., 2006). Revealing these plant-pathogen interactions remains crucial in understanding resistance to geminiviruses.

In 2012, the first geminivirus to infect *Vitis Vinifera* was identified: Grapevine red blotch virus (GRBV) part of the *Grablovirus* genera. GRBV is the causative agent for grapevine red blotch disease (GRBD) and has been identified in vineyards across the United States (Krenz et al., 2012; Rwahnih et al., 2013; Krenz et al., 2014; Sudarshana et al., 2015; Yepes et al., 2018), as well as several locations internationally (Lim et al., 2016; Poojari et al., 2017; Gasperin-Bulbarela et al., 2019; Luna et al., 2019; Marwal et al., 2019). Symptoms of GRBD include red blotches on leaves as well as reddening of primary, secondary, and tertiary veins for red varieties and chlorotic regions within leaf blades and marginal burning similar to potassium deficiency in white varieties. Foliar levels of specific amino acids, sugars, phenolics, and terpenoids are reported to be higher in infected grapevines (Wallis and Sudarshana, 2016). GRBV substantially impacts berry ripening in all varieties studied, causing variable impacts on primary and secondary metabolites, depending on the site and season (Blanco-Ulate et al., 2017; Girardello et al., 2019a; Girardello et al., 2019b; Martínez-Lüscher et al., 2019; Lee et al., 2021). Most notably is the impact on the phenylpropanoid pathway (Blanco-Ulate et al., 2017), responsible for flavonoid biosynthesis, which are essential compounds in wine grapes due to their organoleptic properties. The economic impact to vineyards

in the United States could reach $68,548/ha with few mitigation strategies available to the industry (Ricketts et al., 2017).

Several studies have analyzed how genotypic and environmental factors influence disease outcomes (Reustle et al., 2005; Néya et al., 2015; Tripathi et al., 2018; Honjo et al., 2020) in cassava (Chellappan et al., 2005; Kuria et al., 2017), tomatoes (Tripathi and Varma, 2003; Tripathi et al., 2018), as well as in grapevines (Blanco-Ulate et al., 2017; Vondras et al., 2021). Since grapevine rootstocks can impact grapevine physiology and metabolism, they contribute to plant-pathogen interactions (Martínez-Lüscher et al., 2019; Vondras et al., 2021). For instance, differences in vigor, resulting in greater shoot length and leaf area, may impact metabolism in the leaves and the fruit of grapevines, consequently affecting the final wine composition (Wang et al., 2019). In addition, macro and microclimate fluctuations have also been shown to contribute to pathogen-plant interactions (Chellappan et al., 2005; Flores et al., 2015; Alabi et al., 2016) and should be considered.

The present study investigated the impact of GRBV on grape metabolism through ripening across genotypic and environmental factors through transcriptomic and metabolomic approaches. This investigation set out to further understand plant-pathogen interactions in GRBV infections and uncovered a phenological association with the expression of a transcript encoding for a DCL protein. Here, we discuss the alteration of transcriptional networks associated with plant-pathogen interactions and a DCL protein in grapevines infected with GRBV.

Grape Metabolite log fold change		CS 420A							CS 110R						
Class of Compound	Compound Name	2016				2017			2016				2017		
		PV	V	PoV	H	PV	V	H	PV	V	PoV	H	PV	V	H
Carbohydrates	Arabinose	0.07	-0.03	-0.21	-0.31	**-0.42**	-0.26	-0.10	0.00	-0.14	-0.08	-0.13	0.03	-0.18	-0.10
	Fructose	0.55	-0.03	-0.30	-0.34	**-1.48**	-0.70	-0.09	0.02	-0.41	-0.07	-0.13	0.05	-0.37	-0.13
	Glucose	0.57	-0.01	-0.32	-0.41	-1.07	-0.57	-0.13	0.16	-0.37	-0.10	-0.23	0.22	-0.30	-0.16
	myo-Inositol	0.32	0.26	-0.09	-0.38	-0.19	-0.02	-0.08	-0.06	-0.14	-0.09	-0.37	-0.05	0.06	-0.20
Amino Acids	GABA	0.01	0.02	-0.01	**-0.18**	-0.13	-0.04	**-0.38**	-0.02	-0.03	0.09	-0.02	0.01	0.01	0.02
	Alanine	0.03	0.06	0.08	-0.02	-0.11	-0.07	-0.03	-0.01	0.05	**0.19**	0.08	0.07	0.06	0.09
	Arginine	0.10	0.14	0.19	0.15	-0.38	-0.12	0.04	-0.01	0.27	**0.47**	0.32	0.19	0.31	0.09
	Glutamine	0.19	0.07	0.05	-0.03	-0.05	0.02	0.01	**0.50**	0.07	0.16	0.05	0.13	0.02	0.14
	Isoleucine	0.01	0.01	0.03	-0.01	-0.03	-0.01	**-0.06**	0.00	0.01	**0.05**	0.02	0.01	0.01	**0.05**
	Leucine	0.01	0.02	0.04	-0.01	-0.04	-0.01	**-0.07**	0.00	0.01	**0.08**	0.04	0.01	0.01	**0.07**
	Phenylalanine	0.02	0.02	0.01	-0.03	-0.02	0.00	**-0.05**	0.00	0.01	0.02	-0.03	0.02	0.02	0.00
	Threonine	0.03	0.04	0.07	0.00	**-0.13**	-0.04	-0.01	0.02	0.02	**0.13**	0.10	0.04	0.04	**0.13**
	Tyrosine	0.01	0.04	-0.01	-0.04	0.01	0.02	-0.01	0.01	0.02	0.03	-0.02	0.03	0.03	0.02
	Valine	0.01	0.01	0.05	-0.03	-0.04	-0.01	**-0.07**	0.00	0.01	**0.08**	0.04	0.01	0.01	**0.07**
Secondary Amine	Proline	0.02	-0.01	-0.02	-0.18	-0.70	-0.32	0.23	0.00	-0.07	0.45	0.31	0.05	-0.13	0.44
Organic Acids	Acetate	0.00	-0.02	0.00	-0.01	-0.03	0.00	-0.02	0.00	0.00	-0.01	-0.04	0.00	0.00	0.00
	Chlorgenate	0.27	0.38	0.02	0.01	0.29	0.11	0.06	0.00	-0.17	0.10	-0.02	-0.20	-0.11	0.02
	Fumarate	0.00	0.01	0.00	0.00	-0.01	0.00	0.00	0.00	0.00	0.01	0.00	0.01	0.01	0.00
	Malate	0.47	0.50	0.39	0.03	0.28	0.17	0.42	0.16	0.08	0.62	0.64	0.22	0.53	0.46
	Pyruvate	0.04	0.03	0.00	0.00	0.01	0.01	0.00	0.01	0.00	0.01	0.01	0.02	0.03	0.01
	Succinate	0.07	0.02	0.00	-0.03	0.01	0.00	0.00	0.04	-0.03	0.01	-0.01	0.02	-0.02	0.00
	Tartrate	0.16	0.39	0.06	0.00	0.22	-0.13	0.27	-0.01	-0.32	0.18	-0.62	-0.19	-0.14	0.18
Alkaloid	Trigonelline	-0.02	0.00	0.00	0.00	**-0.09**	-0.01	0.01	-0.01	0.00	0.01	0.02	0.00	0.00	0.00
Ethanol amine	Choline	-0.02	-0.02	-0.01	0.03	**-0.09**	-0.02	0.05	-0.02	0.00	0.01	0.03	0.02	0.01	-0.03

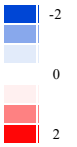

Figure 3.1. Log fold changes of primary metabolite concentrations through ripening in Cabernet Sauvignon grapes grafted onto 110R and 420A rootstocks in 2016 and 2017. Negative values (blue) indicate a decrease in concentration, positive values (red) indicate an increase in concentration in diseased grapes compared to healthy grapes. Color gradient indicates the size of log fold change. Bolded values indicate a significant difference ($p < 0.05$, FDR correction). CS= Cabernet Sauvignon, PV= pre-veraison, V=veraison, PoV= post-veraison, and H=harvest.

3.3 Results:

3.3.1 Influence of genotype and season on grape metabolism

Grapes from Cabernet Sauvignon grapevines grafted on two different rootstocks (110R and 420A) in 2016 and 2017 were sampled for metabolomic and transcriptomic analysis. Grapes were collected at four different ripeness stages in 2016 and three different ripeness stages in 2017. Further details of viticultural practices and sampling are discussed in the Section 4. A total of 78 metabolites were analyzed (24 volatile secondary metabolites, 30 secondary phenolic metabolites, and 24 primary metabolites). Multi-dimensional scaling indicated that ripeness level primarily explained the variability between samples, followed by season, genotype, and finally disease status (Figure S3.1). Figure 3.1 displays the log fold change (FC) in concentration of each primary metabolite between healthy (RB(-)) and diseased (RB(+)) grapes.

Grape Metabolite log fold change		CS 420A							CS 110R						
Class of Compound	Compound Name	2016				2017			2016				2017		
		PV	V	PoV	H	PV	V	H	PV	V	PoV	H	PV	V	H
Esters	ethyl acetate	0.21	0.04	-0.04	-0.16	0.03	-0.10	0.09	-0.15	0.02	-0.06	0.03	-0.04	-0.02	-0.16
	ethyl-2-methylpropanoate	**0.03**	0.00	0.00	-0.01	0.00	0.00	0.01	0.00	0.00	0.00	0.00	0.00	0.00	-0.01
	ethyl hexanoate	**0.08**	0.00	0.01	-0.02	0.01	-0.03	0.01	0.00	0.02	-0.01	0.02	0.01	0.01	-0.04
	ethyl octanoate	0.10	-0.03	0.00	-0.03	0.05	-0.02	0.02	0.01	0.06	-0.02	0.03	0.04	0.01	-0.02
C6 aldehyde	hexanal	**1.09**	-0.35	0.17	0.00	0.03	**-0.95**	-0.14	0.09	0.40	0.61	0.28	0.35	-0.67	0.30
	2-hexenal	0.68	-0.44	0.24	0.22	0.27	**-1.03**	0.31	0.03	0.93	0.29	0.37	0.35	-0.49	0.19
C6 alcohol	hexanol	0.27	0.08	-0.14	-0.28	0.40	**0.49**	**0.70**	0.07	0.38	-0.02	0.06	0.04	0.36	0.13
	trans-3-hexen-1-ol	0.02	0.00	-0.01	-0.01	0.01	0.02	**0.04**	0.00	0.02	0.00	0.00	0.00	0.02	-0.01
	cis-3-hexen-1-ol	0.01	0.31	-0.09	0.02	0.35	**0.45**	0.28	0.22	0.26	-0.01	0.03	-0.24	0.19	0.26
	trans-2-hexen-1-ol	0.09	0.00	0.00	-0.03	0.15	**-0.37**	-0.01	0.04	0.06	-0.02	0.05	-0.15	-0.19	-0.06
Terpenoid	alpha-pinene	0.01	0.00	0.00	0.00	0.00	0.00	0.00	0.00	-0.01	-0.01	0.01	0.00	0.01	-0.01
	beta-myrcene	0.01	0.11	-0.05	-0.06	-0.13	-0.14	-0.02	0.08	-0.14	0.05	0.02	-0.01	-0.08	-0.03
	alpha-terpinene	0.00	**0.16**	0.00	-0.04	-0.01	-0.01	0.00	0.00	-0.01	0.00	0.00	0.00	0.00	0.00
	limonene	0.00	-0.04	0.00	0.00	-0.05	-0.03	0.04	0.01	-0.04	-0.03	0.01	0.07	0.02	-0.04
	p-cymene	0.00	0.01	0.00	0.00	-0.02	0.01	0.00	0.00	-0.01	0.00	0.00	-0.01	**0.03***	-0.01
	beta-linalool	0.00	0.01	0.00	0.00	-0.01	-0.01	0.00	0.01	-0.01	0.00	0.00	0.01	0.00	0.00
	beta-cyclocitral	0.01	0.01	0.01	0.00	0.01	-0.02	0.00	-0.02	0.00	0.00	0.01	0.00	0.00	0.00
	geranial	0.00	0.00	0.00	0.00	0.00	-0.01	0.00	0.00	0.01	0.00	0.00	0.01	0.00	0.00
	beta-citronellol	0.00	-0.01	0.00	0.00	-0.01	**-0.02**	0.00	-0.01	0.00	-0.01	0.00	-0.01	-0.01	-0.01
	geraniol	-0.05	**-0.27**	0.06	0.06	0.04	-0.12	0.01	-0.18	0.24	-0.15	0.02	-0.06	-0.03	-0.08
Norisoprenoid	beta-ionone	0.02	-0.05	0.06	0.00	0.04	-0.17	0.01	-0.04	0.17	0.00	0.05	0.04	0.00	0.00
C8 aldehyde	octanal	0.01	**0.03**	0.00	0.00	0.02	**-0.03**	-0.01	0.00	0.01	0.00	0.00	0.00	-0.01	0.00
C8 alcohol	1-octen-3-ol	0.07	0.02	-0.01	-0.06	0.04	0.00	**-0.15**	0.01	0.01	0.03	0.01	0.07	-0.01	-0.03
Aromatic alcohol	guaiacol	0.00	0.01	0.00	0.01	0.02	0.00	0.00	0.00	0.01	0.00	0.00	0.02	0.00	0.00
Grape Metabolite log fold change		**CS 420A**							**CS 110R**						
Class of Compound	**Compound Name**	**2016**				**2017**			**2016**				**2017**		
		PV	**V**	**PoV**	**H**	**PV**	**V**	**H**	**PV**	**V**	**PoV**	**H**	**PV**	**V**	**H**
Benzoic Acids	Gallic Acid	0.25	-0.03	-0.23	-0.11	-0.99	-0.40	0.23	0.24	-0.16	0.32	-0.01	-1.03	-0.06	0.21
	Vanillic Acid	0.05	-0.14	-0.11	0.01	-1.00	-0.13	0.18	-0.15	-0.17	0.48	-0.48	-1.24	-0.10	0.14
Hydroxycinnamic Acid	p-Coumaric Acid	0.60	1.13	0.22	-0.44	-1.68	0.87	-0.22	0.23	0.57	2.91	-2.14	-1.28	1.40	2.11
	Caftaric Acid	0.69	**2.62**	-0.01	-0.24	-1.21	1.80	0.76	-0.13	-1.73	0.59	-0.36	**-2.54**	-1.41	-0.69
	Ferulic Acid	0.00	0.30	-0.09	0.20	-0.35	-0.46	-0.40	-0.31	0.05	-0.26	-0.24	-0.83	-0.44	0.08
Flavan-3-ols	Gallocatechin	1.32	1.07	-1.06	0.32	-0.57	1.41	0.90	0.99	-1.51	0.85	-0.95	-0.45	-0.72	0.58
	Epigallocatechin	0.87	0.46	-0.69	0.17	-0.40	-0.06	1.20	0.40	-0.55	0.35	0.24	-0.51	0.01	0.11
	Catechin	0.95	1.46	0.28	-0.38	-1.55	1.03	1.28	0.41	-0.80	2.22	0.73	-1.82	-0.17	0.46
	B1	0.54	0.15	0.33	-0.05	-0.29	2.12	1.70	-0.31	0.79	1.53	0.00	-1.71	-0.10	0.65
	Epicatechin	1.37	1.13	0.59	-1.05	-1.01	0.47	2.41	-1.09	-0.50	2.36	1.08	-1.64	-1.20	-0.12
	Epicatechin gallate	-0.27	0.32	0.25	0.06	-0.98	1.29	0.45	-1.33	0.32	1.64	0.45	-1.32	0.33	-0.04
Flavonols	Myricetin-glucoside	0.13	-0.44	-0.64	0.25	-1.04	-1.48	0.24	-0.71	-1.04	-0.09	-0.31	-0.94	-0.89	-0.37
	Quercetin-rutinoside	0.19	-0.42	-0.19	0.74	-0.73	0.21	0.37	-0.93	-1.09	0.03	-0.11	-1.50	0.23	-0.28
	Quercetin-glucoside	0.22	-0.59	-0.51	0.67	-0.94	-0.28	0.35	-0.81	-0.86	0.15	-0.17	-1.78	-0.23	-0.19
	Kaempferol glucoside	0.29	-0.59	-0.71	0.62	0.22	-0.39	0.32	-0.81	-0.85	-0.10	-0.29	-0.85	-0.26	-0.33
Anthocyanins	Delphinidin-3-glucoside	0.14	-0.58	-0.99	-0.18	-2.57	-1.98	-0.17	-0.09	-0.89	-0.19	-0.52	-3.35	-1.11	-0.96
	Cyanidin-3-glucoside	-0.31	-0.93	-1.24	-0.07	-0.72	-1.44	-0.44	0.39	-0.59	0.20	-0.50	0.00	-0.96	-1.11
	Petunidin-3-glucoside	1.38	-0.55	-0.84	0.05	-0.12	-1.80	-0.08	-1.25	-0.67	-0.15	-0.41	1.76	-1.01	-0.70
	Peonidin-3-glucoside	-0.25	-0.87	-0.76	0.26	-0.59	-1.32	-0.12	-0.40	-0.40	0.07	-0.08	-0.18	-0.57	-0.49
	Malvidin-3-glucoside	0.80	-0.49	-0.35	0.46	-2.78	-1.41	0.13	-2.74	-0.46	0.00	-0.02	-2.38	-0.63	-0.19
	Delphinidin-3-acetylglucoside	-0.11	-0.73	-1.03	-0.25	-1.01	-1.87	-0.34	-1.68	-0.82	-0.23	-0.59	-1.03	-1.26	-1.01
	Cyanidin-3-acetylglucoside	-0.33	-1.10	-1.26	-0.19	-0.16	-1.45	-0.57	0.00	-0.57	0.10	-0.61	0.00	-1.04	-1.18
	Petunidin-3-acetylglucoside	0.03	-0.83	-0.87	-0.04	-0.68	-1.78	-0.19	-1.43	-0.66	-0.20	-0.50	-0.29	-1.06	-0.88
	Peonidin-3-acetylglucoside	-0.16	-1.03	-0.44	0.39	0.00	-1.30	-0.10	-0.07	-0.37	0.00	-0.03	0.56	-0.83	-0.45
	Malvidin-3-acetylglucoside	0.00	-0.71	-0.16	0.58	-1.37	-1.40	0.14	-0.57	-0.39	-0.01	0.17	-1.26	-0.73	-0.16
	Delphinidin-3-p-coumaroyl glucoside	0.30	-0.51	-0.62	0.06	-1.15	-1.54	0.00	0.41	-0.78	-0.08	-0.43	-0.32	-0.83	-0.59
	Cyanidin-3-p-coumaroyl glucoside	0.06	-0.78	-0.79	0.25	-0.67	-1.21	-0.06	-0.80	-0.64	0.24	-0.32	-0.61	-0.75	-0.67
	Petunidin-3-p-coumaroyl glucoside	-0.13	-0.49	-0.50	0.29	-1.85	-1.62	0.15	-1.22	-0.66	-0.03	-0.34	-1.38	-0.88	-0.51
	Peonidin-3-p-coumaroyl glucoside	-0.60	-0.80	-0.26	0.75	-0.64	-1.30	0.20	0.01	-0.71	0.41	0.19	-0.87	-1.05	-0.24
	Malvidin-3-p-coumaroyl glucoside	-0.19	-0.47	-0.01	0.84	-2.16	-1.59	-2.32	-1.22	-0.58	0.25	0.27	-1.25	-0.73	-0.10

Figure 3.2. Log fold changes of secondary metabolite concentrations through ripening in Cabernet Sauvignon grapes grafted onto 110R and 420A rootstocks in 2016 and 2017. Negative values (blue) indicate a decrease in concentration, positive values (red) indicate an increase in concentration in diseased grapes compared to healthy grapes. Color gradient indicates the size of log fold change. Bolded values indicate a significant difference ($p<0.05$, FDR correction). CS= Cabernet Sauvignon, PV= pre-veraison, V=veraison, PoV= post-veraison, and H=harvest.

Generally, GRBV increased amino acids and malate concentrations and decreased carbohydrate levels. Malate concentrations were generally higher in RB(+) grapes at all ripeness levels across seasons and rootstocks. Amino acid concentrations were significantly higher in RB(+) grapes at post-veraison for CS 110R in 2016 and harvest for CS 110R in 2017. Whereas

carbohydrate concentrations at harvest were lower and malate concentrations were higher in RB(+) grapes. Proline was higher in RB(+) grapes at harvest except for CS 420A in 2016. To determine the significant seasonal and genotypic influences on grape metabolome, the differential expression analysis analyzed the interactions between season, disease statues, and rootstock. Seasonal variation played a larger role in CS 420A for primary metabolite concentrations, where fructose, glucose, arabinose, phenylalanine, threonine, and trigonelline were significantly affected by season at pre-veraison. Between CS 110R and CS 420A several amino acids were significantly affected by the difference in rootstock in 2017, but not in 2016. At pre-veraison in 2017, arabinose, alanine, arginine, phenylalanine, threonine, trigonelline, choline, and chlorogenate were significantly affected by rootstock differences, whereas gamma aminobutyric acid (GABA), leucine, isoleucine, phenylalanine, valine, and threonine were significantly affected at harvest in 2017. Amino acid concentrations were generally lower in CS420 RB(+) grapes than RB(-) at harvest, with the opposite being true for CS 110R. In addition, GRBV significantly lowered arabinose and fructose at pre-veraison for CS 420A in 2017 which was not observed in 2016 or for CS 110R rootstock.

Log FC in secondary metabolite concentrations are shown in Figure 3.2. Few significantly different volatile metabolites were observed, with the most considerable impact occurring in C6 aldehydes, C6 alcohols, and terpenes. Generally, there were increased amounts of C6 aroma compounds at pre-veraison in diseased fruit. Consistent differences were observed between CS 420A and CS 110R in 2017 at veraison, where RB(+) grapes experienced decreases in concentration for C6 aldehydes and increases in the primary C6 alcohols, hexanol, cis-3-hexen-1-ol, and trans-3-hexen-ol, although this was not always significant. In addition, transcripts encoding for alcohol dehydrogenase (ADH) were suppressed at pre-veraison in 2016 for both rootstocks.

GRBV significantly induced a transcript encoding for lipoxygenase (LOX) in both rootstocks at harvest in 2016 and post-veraison for CS 420A in 2016 (data not shown). Together, our results suggest irregular ripening events in GRBV infected fruit.

The interaction between disease statues and season indicated that seasonal differences mainly affected 420A rootstock. At veraison, α-terpinene, octanal, and trans-2-hexen-1-ol were significantly affected by season, and hexanol at harvest. Only *p*-cymene was significantly affected by season for CS 110R at veraison. Differences in rootstock significantly affected alpha-terpinene and geraniol at veraison in 2016.

The largest FC differences in phenolic compound concentrations occurred at pre-veraison and veraison, with fewer differences towards harvest. Most notably, there were large decreases in anthocyanin concentrations across season and rootstock as well as transcriptional suppression of the phenylpropanoid pathway at veraison (Figure S3.2), agreeing with previous results (Sudarshana et al., 2015; Blanco-Ulate et al., 2017; Girardello et al., 2019a; Martínez-Lüscher et al., 2019; Bowen et al., 2020). More considerable differences in metabolite concentrations were observed in 2017 than in 2016, with more consistent decreases in anthocyanin concentrations for CS 110R at harvest than CS 420A, agreeing with findings in Martinez et al. (2019). Flavan-3-ol concentrations were mainly higher in RB(+) grapes, yet consistent trends across ripeness level, season, and rootstock were not observed. The interactions between disease status and season or rootstock were not significant for any of the phenolic compounds. However, rootstock differences significantly affected caftaric acid at veraison in both seasons. Caftaric acid was higher for CS 420A in both seasons and lower for CS 110R RB(+) in 2016 grapes at veraison potentially indicating grapevine genotype affects GRBV infection (Figure 3.2).

Interestingly, phenylalanine was significantly impacted by seasonal differences for CS 420A at pre-veraison and rootstock differences in 2017 at pre-veraison and harvest. In general, at pre-veraison phenylalanine was higher in RB(+) grapes than RB(-) grapes with the exception of 420A in 2017. CS 420A RB(+) grapes in 2017 consistently had higher amounts of flavan-3-ols and by harvest very few differences in anthocyanin concentrations compared to RB(-) grapes. At harvest, phenylalanine was lower in RB(+) grapes (Figure 3.1) with transient increases in flavan-3-ols and flavonols and fewer decreases in anthocyanin concentrations (Figure 3.2). The only occurrence where phenylalanine was not lower in RB(+) grapes at harvest was in CS 110R grapes at harvest in 2017, where all anthocyanin derivatives besides malvidin and peonidin were considerably lower (FC<-0.5).

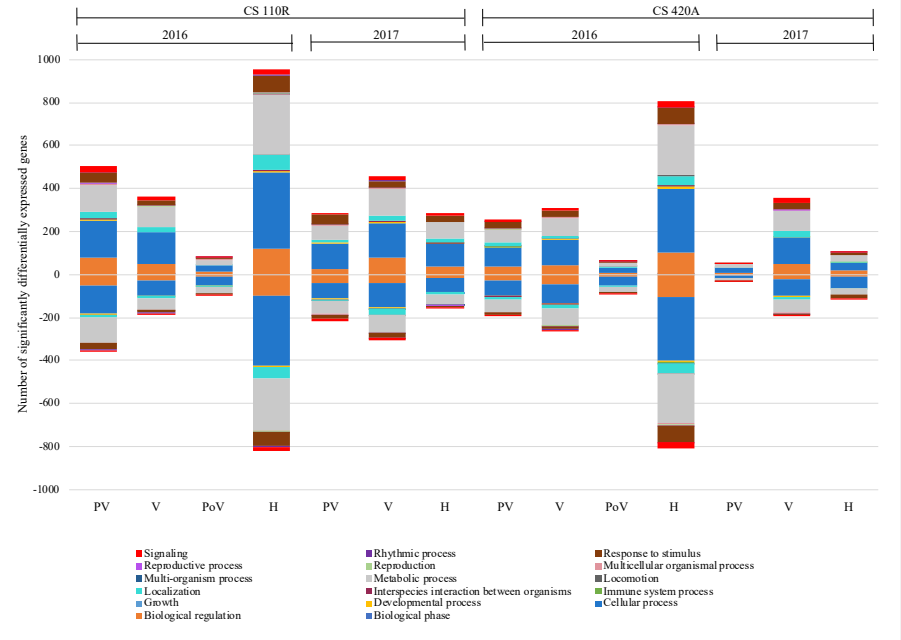

Figure 3.3. Number of significantly ($p<0.01$) differentially expressed genes at each ripeness level across genotype and season. Different coloring indicates different gene ontology classifications based on biological processes. Negative values indicate significantly down regulated genes and positive values indicated significantly upregulated genes. CS= Cabernet Sauvignon, PV= pre-veraison, V= veraison, PoV= post-veraison, H= harvest.

3.3.2 GRBV delays berry ripening through induction of defense processes, photosynthesis, and auxin pathways

RNA-seq was utilized to sequence the transcriptome of the CS grapes. Like the metabolite profiling, the differences in ripeness level predominantly explained the variance in the grape transcriptome, followed by season, rootstock, and then disease status (in descending order of effect, Figure S3.3). Differential expression (DE) analysis was performed on all trimmed and normalized genes. Significantly ($p<0.01$) differentially expressed genes (DEGs) for each rootstock, season, and ripeness level are shown in Figure 3.3. In general, there were fewer DEGs in 2017 than in 2016 for both rootstocks and fewer DEGs for CS 420A than CS 110R, concurrent with primary metabolite results. Gene ontology analysis (GO) determined the main processes impacted were biological regulation, cellular processes, localization, metabolic processes, and response to stimulus.

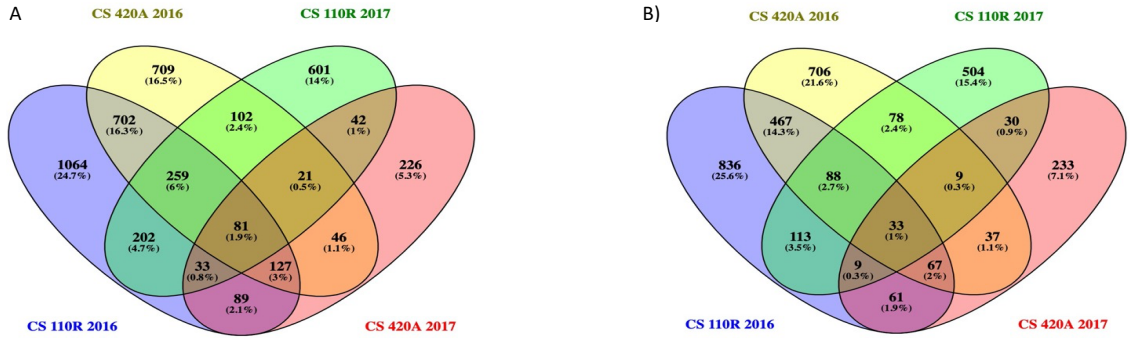

Figure 3.4. Venn Diagram of a) upregulated differentially expressed genes and b) downregulated differentially expressed genes for each rootstock and season. The genes at each ripeness level were pooled for each rootstock and season combination to find the conserved up and downregulated genes due to GRBV infection. CS= Cabernet Sauvignon.

To determine the consistent responses across genotype and season, all the significant DEGs of each rootstock/season were pooled across ripeness levels to generate a Venn Diagram (Figure

3.4). Figure 3.4a depicts all the commonly upregulated genes (81), and Figure 3.4b represents all the commonly downregulated genes (33). A dendrogram separated these 114 genes into four different clusters of 50, 14, 22, and 28 genes. The VitisNet (Grimplet et al., 2009; http://vitis-dormancy.sdstate.org) and VitisPathway (Osier, 2016; http://www.rit.edu/VitisPathways) databases were used for gene annotation, and a heatmap was used to visualize the regulation of these 114 genes due to the viral infection (Figure 3.5).

Cluster one mainly showed induction of transcripts from post-veraison to harvest (Figure 3.5). Of the 50 genes, seven were associated with energy metabolism (photosynthesis and oxidative phosphorylation), 12 were associated with transportation processes, three were associated with amino acid metabolism, and four with hormone processes. Three of the latter genes were related to auxin-mediated processes. Transcript VIT_08s0040g00800, encoding an auxin-induced protein, was highly upregulated from post-veraison to harvest, and in 2017 from veraison.

Cluster two was moderately induced at veraison to harvest and was associated with lipid metabolism, hormone signaling, and translation processes. GRBV induced one gene related to plant-pathogen interactions, VIT_19s0090g00410, at veraison in 2017 and harvest in 2016 for both rootstocks, potentially indicating that seasonal conditions may relate to the induction of plant responses to viral infection. Some of the largest differences in cluster two were transcripts encoding for currently uncharacterized proteins. The 22 genes in cluster three were mainly suppressed at harvest and related to translation, ABA signaling, and cell wall metabolism. One of the genes in this cluster was consistently upregulated at veraison, VIT_04s0023g00920, which is responsible for RNA virus-induced gene silencing (Uniprot; https://www.uniprot.org). Lastly, genes in cluster four were mainly induced at pre-veraison and associated with plant-pathogen interactions, defense responses (WRKY transcription factor), ABA signaling, and auxin signaling.

entrezgene_ID	VitisNet_gene_ID	VitisPathway	PreVeraison				Veraison				PostVeraison		Harvest				
			110R		420A		110R		420A		110R	420A	110R		420A		
			2016	2017	2016	2017	2016	2017	2016	2017	2016		2016	2017	2016	2017	
NA	VIT_05s0020g04670							1.66					2.16		1.72	1.80	Cluster 1
NA	VIT_01s0026g02710	vv60046NAC		-1.01				0.75					1.04		1.04	0.99	
100241176	VIT_09s0002g04130	vv50122Porters_cat_7_to_17						0.78		0.56			1.69				
100253780	VIT_03s0180g00070									0.65			1.01	0.47	0.65		
100241327	VIT_18s0089g00920									0.64			1.18	0.76	1.43	0.58	
100233001	VIT_02s0025g03390	vv50101Channels_and_pores								0.35			0.63	0.42	0.56		
100244742	VIT_05s0077g02080	vv10280Valine_leucine_and_isoleucine_degradation											0.66	0.56	0.66	0.64	
100241657	VIT_11s0016g00200								-0.38				0.63	0.41	0.47	0.47	
100241372	VIT_08s0040g00800	vv50122Porters_cat_7_to_17		0.82				3.15		2.78	2.80	3.46	3.63	3.03	2.87		
100243201	VIT_13s0067g01450	vv60007AS2						0.65		1.04	1.10	1.24	1.66		1.62		
100257329	VIT_03s0038g04450	vv60012BZIP							-0.89		0.70	0.72	1.05	0.79	1.36	1.12	
100854975	VIT_02s0012g00090	vv50110Protein_coat; vv34070Phosphatidylinositol_signaling_system; vv44810Regulation_of_actin_cytoskeleton; vv10562Inositol_phosphate_metabolism	-0.67					0.87	-0.59		0.66	0.49	1.23	0.70	0.98	0.81	
100263694	VIT_06s0009g03640	vv50101Channels_and_pores											1.31	1.08	2.47	1.30	
100244960	VIT_06s0004g06100	vv60044MYB; vv30009Flower_development	-0.45	-0.77									0.92	0.49	1.13	0.52	
100247918	VIT_02s0025g01450												1.06	0.81	1.56	0.90	
100259874	VIT_02s0025g01380	vv40006Cell_wall		-0.79				0.78		0.68		0.82	2.27		3.89		
100245385	VIT_18s0001g01130	vv30003Auxin_signaling											1.11	0.50	1.94	0.74	
100242802	VIT_04s0023g00410	vv10195Photosynthesis; vv50105Transport_electron_carriers							0.57	0.64	0.97		2.37	1.45	1.95		
100245459	VIT_00s0207g00210	vv10195Photosynthesis; vv50113Thylakoid_targeting_pathway; vv50135Primary_active_transporter_cat_D3_to_E2									0.60		1.27	1.03	1.14	0.77	
100266309	VIT_18s0075g00250							0.69					1.61	1.02	1.64	0.69	
100240928	VIT_05s0020g03180	vv10195Photosynthesis; vv50105Transport_electron_carriers						0.58		0.67			1.96	1.08	1.15		
100240959	VIT_00s0904g00010	vv10195Photosynthesis; vv50113Thylakoid_targeting_pathway; vv50135Primary_active_transporter_cat_D3_to_E2						0.84		0.71			2.62		1.38		
100257884	VIT_07s0104g00420			0.58						0.54	0.90		2.30		1.37		
100855239	VIT_06s0004g05430	vv10220Urea_cycle_and_metabolism_of_amino_groups		0.57			0.50	0.87		0.61	1.38	0.83	2.34		1.53		
100251147	VIT_05s0020g04800		-1.37	-0.72	-0.89					-0.59			1.12		0.78	0.60	
100247664	VIT_05s0049g00960	vv34710Circadian_rhythm						0.44			0.49	0.51	0.99		0.65	0.42	
100263807	VIT_17s0000g06370		-0.66		-0.49						0.41	0.42	0.92	0.49	0.99	0.57	
100251062	VIT_18s0164g00030	vv10195Photosynthesis; vv10190Oxidative_phosphorylation; vv50131Primary_active_transporter_cat_A2_to_A4						0.57					1.61		1.79	1.52	
100243547	VIT_03s0063g00820												1.10	1.08	1.68	1.22	
100854583	VIT_00s0371g00050	vv10051Fructose_and_mannose_metabolism											0.93	0.72	1.43	0.74	
100267459	VIT_10s0003g00890	vv10860Porphyrin_and_chlorophyll_metabolism											0.85	0.51	0.72	0.54	
100253718	VIT_19s0014g00450										0.65		1.32	1.16	1.27	1.00	
100257132	VIT_19s0090g01350		-1.08		-1.79		-0.73	-0.65		-0.89	0.70	0.72	1.24	1.22	0.78		
100254798	VIT_04s0023g02050	vv10190Oxidative_phosphorylation; vv50133Primary_active_transporter_cat_A9_to_A18								0.43	0.55	0.46	0.43	0.57	0.65	0.56	
100248784	VIT_10s0003g00140	vv30008Ethylene_signaling; vv60003AP2_EREBP		-0.82	0.66								0.88	0.70		0.68	
100258273	VIT_09s0002g05170												0.47	0.59	0.54	0.60	
100244962	VIT_06s0080g00920							0.71		0.94			2.25		1.71		
100257648	VIT_19s0093g00220	vv10480Glutathione_metabolism		0.48					0.52	0.48			1.15				
100247778	VIT_08s0007g03930	vv10100Biosynthesis_of_steroids		0.59									1.18			0.84	
100250741	VIT_03s0091g00310	vv11002Auxin_biosynthesis									1.13	1.28		1.40		0.97	
100264253	VIT_04s0023g03540		1.53		1.85						2.53	2.93		1.60	1.50	1.37	
100255226	VIT_13s0067g00260		0.81		0.71			0.75		0.86	1.62	1.15		0.90			
NA	VIT_00s0203g00150							0.46		0.47	0.62	0.64	0.54	0.45			
100262861	VIT_01s0011g00830		0.78					-0.65		0.64	0.78	0.79	1.25	1.37	1.05		
100247204	VIT_04s0023g03470	vv50132Primary_active_transporter_cat_A5_to_A8	0.68			-0.56					0.61	0.60	1.33	0.80	1.47	1.04	
100249622	VIT_01s0010g00240	vv10240Pyrimidine_metabolism									0.81	1.09	1.33	1.13	1.68	1.41	
100257113	VIT_19s0138g00140	vv50109Incompletely_characterized_transport_systems	0.88		0.52					0.61	0.52	0.69		0.55	0.85		
100233053	VIT_05s0094g01570		0.48		0.71					0.90			1.26	1.05			
100254537	VIT_08s0007g01450	vv10230Purine_metabolism	0.66						-0.75				0.70	0.68	0.55	0.57	
100266637	VIT_13s0156g00150		1.68		1.11			-0.78			1.37	0.80	1.16	1.45		1.34	

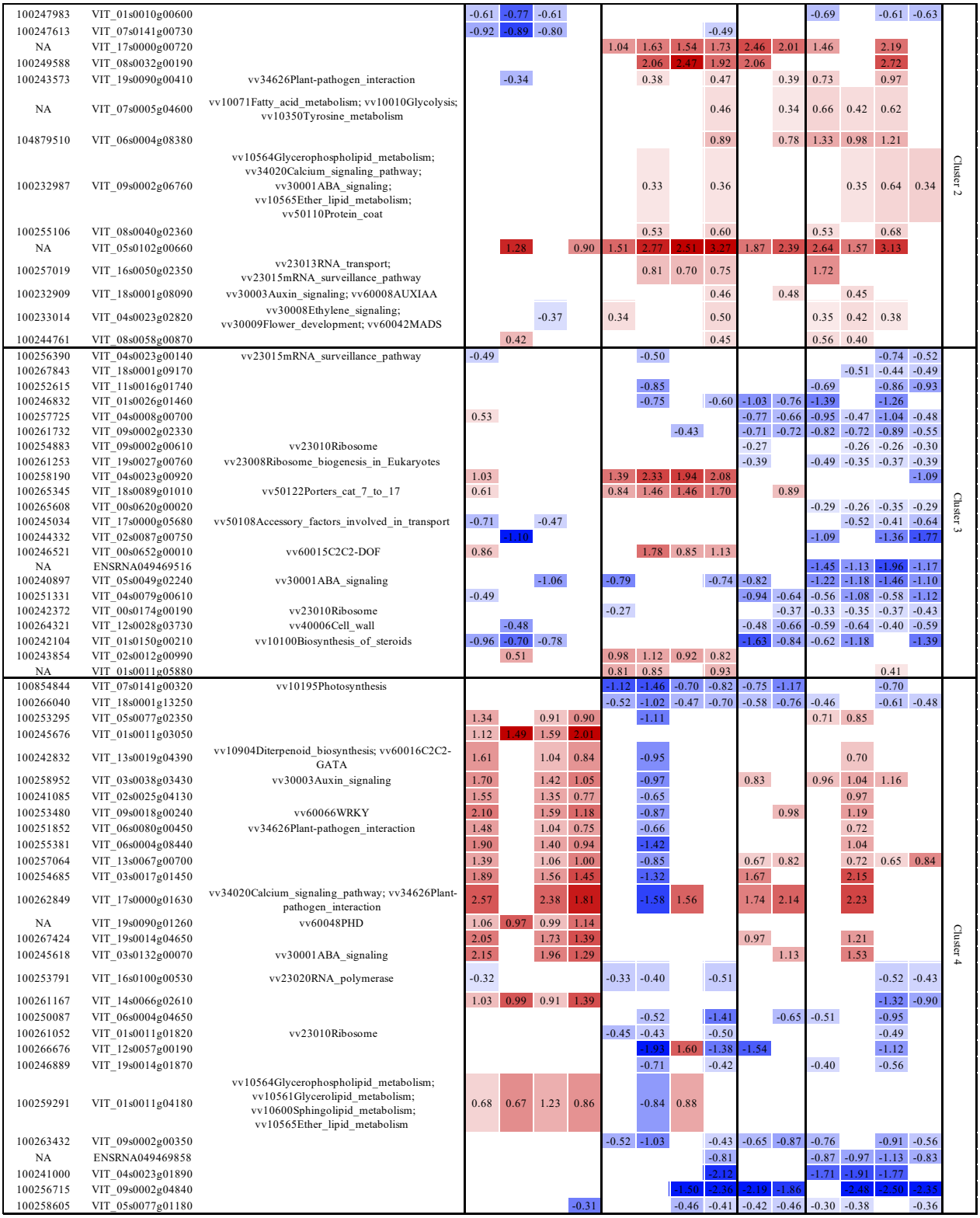

Figure 3.5. Log fold change of conserved genes affected by GRBV infection based on results from the Venn Diagram in Figure 3.4. Transcripts are grouped together in clusters based on dendrogram output. Negative values (blue) indicate a decrease in concentration, positive values (red) indicate an increase in concentration in diseased grapes. Color gradient indicates the size of log fold change. 110R = Cabernet Sauvignon on rootstock 110R and 420A = Cabernet Sauvignon on rootstock 420A.

A few genes were also suppressed at veraison to harvest and were mainly associated with translation processes. Interestingly, only CS 110R in 2017 did not follow this trend. Instead, transcripts were suppressed in the plant-pathogen interaction pathway, WRKY, and auxin signaling at veraison, followed by induction at harvest. The only time that anthocyanin concentrations were significantly impacted at harvest was for CS 110R in 2017, suggesting a differential response to GRBV for CS 110R versus CS 420A in 2017, which was not observed in 2016.

3.3.3 GRBV induces plant-pathogen interactions

All the DEGs were also used to construct a weighted gene co-expression network analysis (WGCNA). The results from the WGCNA indicated that the grouping of genes was mainly due to the difference in ripeness levels and the impact of the disease was indistinguishable (Figure S3.4). Thus, differential co-expression analysis was performed on the DEGs. Differential co-expression analysis aims to identify coordinated expression patterns that differ across conditions. Our study compared differences in gene co-expression between healthy and diseased grapes to determine networks of genes that are impacted due to the virus. Due to the entire network of correlation differences being too large to thoroughly analyze at an adjusted $p<0.05$ (FDR correction), we used adjusted p-values$< 5.0x10^{-6}$, which afforded 185 correlations.

Out of these 185 correlations, four networks contained more than four genes. Three of these networks gained co-expression, and one lost co-expression due to GRBV infection in grapes. One gaining co-expression was related to sugar metabolism, ethylene signaling, cell wall metabolism, and nucleotide sugar metabolism (Figure S3.5). Another had a centralized gene that was gaining co-expression with several genes (Figure S3.6). The transcript in the center is a calcium-binding

protein (VIT_14s0006g01400) associated with plant-pathogen interactions. The exterior transcripts encoded for transcription factors, WRKY (VIT_17s0000g01280), bHLH (VIT_17s0000g00430), and Zf-HD (VIT_14s0108g00810), glycolysis (VIT_17s0000g03280), tyrosine metabolism (VIT_17s0000g03280), fatty acid metabolism (VIT_17s0000g03280), sucrose metabolism (VIT_12s0057g00700), a SWEET sugar transporter (VIT_1s0000g00830), and auxin transport (VIT_01s0011g04640; Table S3.1).

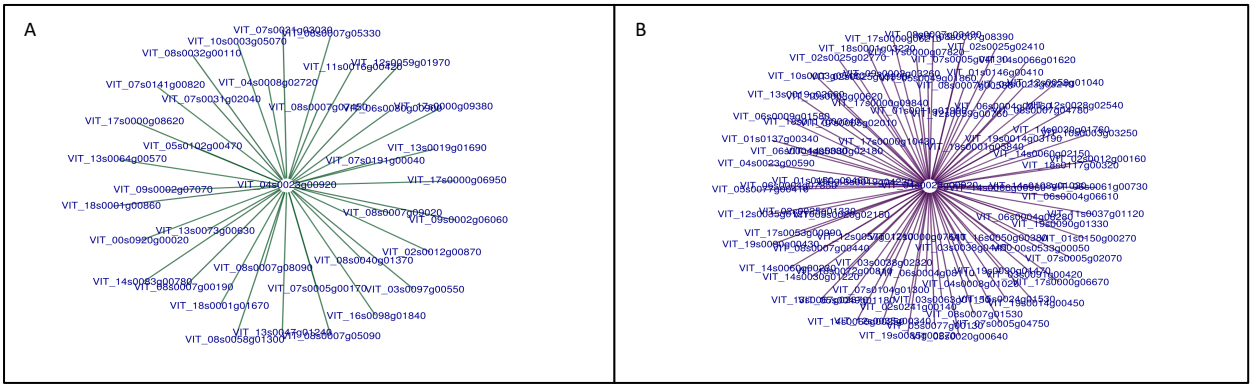

Figure 3.6. Two networks produced through differential co-expression analysis, a) one showing a gain in co-expression and b) one showing a loss in co-expression. The centralized gene is VIT_04s0023g00920, which encodes for a Dicer-like protine. The transcripts on the exterior are associated with a) transcription and translation processes or b) with metabolite synthesis and energy metabolism.

The other two networks that contained more than four genes are shown in Figure 3.6. The centralized gene gains (Figure 3.6a) or loses (Figure 3.6b) co-expression with several encompassing genes. Interestingly, the gene in the center of both figures is the same, VIT_04s0023g00920, and encodes a Dicer-like (DCL) protein, specifically DCL2. Our data suggests a transcriptional shift caused by GRBV that reallocates the co-expression of this gene in diseased grapes. Figure 3.6a demonstrates that this gene gains co-expression with genes responsible for flower development, translation, and transcription processes in GRBV fruit (Table S3.2). Simultaneously, there is a loss of co-expression (Figure 3.6b) with genes associated with plant-pathogen interactions, flavonoid biosynthesis, amino acid metabolism, carbohydrate

metabolism, transport, cell wall metabolism, and oxidative phosphorylation (Table S3.3). The one gene associated with plant-pathogen interactions is again a calcium-binding protein (VIT_02s0241g00140). The transcript in the flavonoid biosynthesis pathway encodes for the chalcone-flavanone isomerase family of proteins (VIT_13s0067g02870), which precedes the synthesis of flavonols, flavan-3-ols, anthocyanins, and proanthocyanidins in the phenylpropanoid pathway.

Table 3.1. Log fold change of VIT_04s0023g00920 which encodes for a dicer-like protein (DCL2). Bolded values indicate a significant difference (FDR adjusted p<0.05). DEG= differential expression, 110R= Cabernet Sauvignon on rootstock 110R, 420A= Cabernet Sauvignon on rootstock 420A, PV= pre-veraison, V=veraison, PoV= post-veraison, and H=harvest.

DE of VIT_04s0023g00920	Pre-veraison				Veraison				Post-veraison		Harvest			
	110R		420A		110R		420A		110R	420A	110R		420A	
	2016	2017	2016	2017	2016	2017	2016	2017	2016	2016	2016	2017	2016	2017
DCL2	1.03	0.55	0.28	-0.33	**1.39**	**2.33**	**1.94**	**2.08**	0.44	0.78	-0.02	-0.53	-0.68	-1.09

Analyzing the DE of DCL2 revealed a significant (FDR adjusted p-value <0.05) induction only at veraison for both seasons and rootstocks (Table 3.1). More considerable differences in DE were observed between 2016 than 2017. This data was compared to the viral gene expression, which was determined by overlaying the GRBV genome with the grape RNA-seq data. The six open reading frames of the GRBV genome produce five proteins, and these five proteins are thought to be translated from two mRNAs: the sense strand and the antisense strand. Therefore, the counts from open reading frames 1, 2, and 3 were combined (sense strand), and 4, 5, and 6 were combined (antisense strand) to determine viral gene expression in the diseased grapes (Figure 3.7a). Viral expression was highest at all points at pre-veraison, with a slight decrease at veraison and more drastic decreases until harvest.

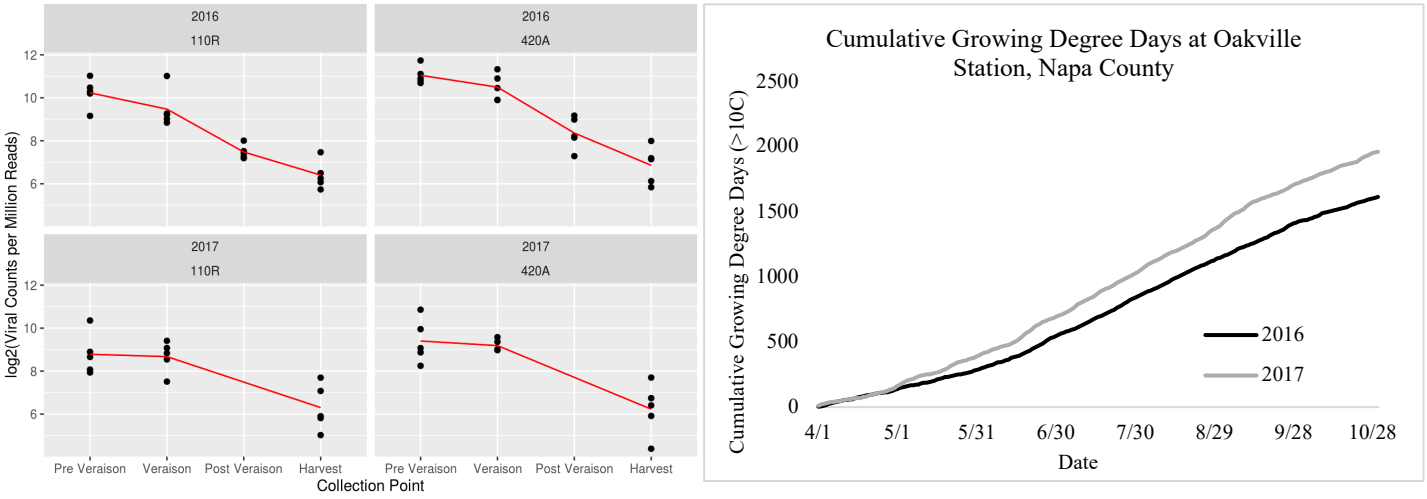

Figure 3.7. Comparison of a) viral gene expression in each season and b) cumulative growing degree days in each season. 110R= Cabernet Sauvignon on 110R rootstock and 420A= Cabernet Sauvignon on 420A rootstock.

3.4 Discussion:

GRBV is known to inhibit ripening processes in grapes leading to decreases in carbohydrate levels, increases in malic acid, and variable impacts on secondary metabolites depending on seasonal and genotypic factors (Blanco-Ulate et al., 2017; Girardello et al., 2019a; Girardello et al., 2019b; Martínez-Lüscher et al., 2019; Lee et al., 2021; Rumbaugh et al., 2021). Here, GRBV suppressed the phenylpropanoid pathway at veraison resulting in decreased anthocyanin concentrations through ripening. Phenylalanine concentrations, the amino acid that initiates the phenylpropanoid pathway and the synthesis of flavonoids, was generally higher at pre-veraison and lower by harvest in diseased fruit compared to healthy fruit. Although anthocyanins were affected through ripening, the decreases in phenylalanine accompanied with fewer anthocyanins being lower by harvest potentially indicates a delayed biosynthesis of anthocyanins in GRBV infected grapes, which was generally recovered by harvest. Our study corroborated previous results indicating that GRBV inhibits ripening events in grapes resulting in lower

carbohydrate and anthocyanin concentrations, with higher malic acid, amino acid, and C6 aroma compound concentrations (Blanco-Ulate et al., 2017; Girardello et al., 2019a; Martínez-Lüscher et al., 2019; Rumbaugh et al., 2021).

In the current study, larger differences in secondary metabolites concentrations due to GRBV infection were seen in 2017 than in 2016. This was also observed in Rumbaugh et al. (2021), where it was hypothesized that the higher temperatures in 2017 potentially increased plant defense responses, leading to fewer differences in primary metabolite concentrations. However, simultaneously it acted as a secondary stressor for RB(+) fruit in terms of secondary metabolites, such as anthocyanins, which are more sensitive to elevated temperatures, leading to larger differences (Downey et al., 2006).

GRBV infection was more impacted by seasonal differences in rootstock 420A than 110R, mainly impacting amino acids and carbohydrates suggesting that the pathogenicity of GRBV in 420A is correlated to environmental factors. Differences in rootstock mainly impacted amino acid concentrations in 2017, not in 2016 potentially suggesting that genotypic and environmental differences affect how the grapevine host will interact with GRBV. Together, our results conclude that the genotype 110R, a more drought-tolerant and vigorous rootstock than 420A, has a differential response to GRBV infection over 420A. CS 110R in 2017 did not undergo the same conserved transcriptional response to GRBV as the other rootstock/season combinations (Figure 3.5), which may have contributed to the lower anthocyanin accumulation at harvest (Figure 3.2). In addition, there were fewer significant DE genes for 420A than 110R in both seasons (Figure 3.3). Rootstock susceptibility to viral infection is an ongoing research topic (Golino, 1993; Credi and Babini, 1996; Martínez-Lüscher et al., 2019; Cabaleiro et al., 2021; Rumbaugh et al., 2021; Vondras et al., 2021), with variable conclusions. One study determined that grapevine leafroll-

associated virus-3 caused greater impacts on the rootstock 110R compared to 196.17C when grafted onto Albariño grapevines (Cabaleiro et al., 2021), which is similar to the current study. On the other hand, Vondras et al. (2021) found that Kober 5BB (*V. berlandieri* × *V. riparia,* similar to 420A) was more impacted than MGT 101- 14 during the infection of multiple grapevine leafroll-associated viruses.

GRBV infection was previously reported to generally decrease volatile aroma compound accumulation in grapes, except for C6 aldehydes and alcohols (Rumbaugh et al., 2021). C6 aroma compounds are synthesized in the lipoxygenase pathway and participate in plant defense responses and growth and development (Rosahl, 1996; Lin et al., 2019). In healthy grapes, C6 aldehydes typically increase in concentration after veraison with a decrease at harvest due to increased ADH activity. Consequently, ADH converting C6 aldehydes into C6 alcohols consistently increases hexanol levels until harvest and, to a lesser extent, trans-3-hexen-ol (Kalua and Boss, 2009). In general, transcripts encoding for LOX enzymes are upregulated before veraison and then suppressed during grape ripening (Xu et al., 2015). We observed a premature decrease in C6 aldehydes resulting in an increase in the primary C6 alcohols in diseased grapes in 2017. In addition, there was irregular induction of a LOX transcript in 2017, potentially resulting in higher levels of C6 alcohols at veraison and harvest.

GRBV decreased levels of carbohydrates and anthocyanins with increases in levels of malic acid in grapes at harvest, similar to previous findings (Girardello et al., 2019a; Martínez-Lüscher et al., 2019; Bowen et al., 2020; Girardello et al., 2020; Lee et al., 2021). Blanco-Ulate et al. (2017) demonstrated that GRBV causes an impairment to ripening events, mainly affecting the phenylpropanoid pathway in which 68% of the genes were suppressed with concurrent decreases in anthocyanin concentrations. GRBV also induced auxin metabolism while decreasing levels of

abscisic acid (ABA) and gibberellin. Auxin is involved in many grape processes, such as cell division and expansion in early fruit development and repressing fruit ripening. One of these processes is malic acid catabolism (Ziliotto et al., 2012). In healthy grapes, before veraison, malate is synthesized inside the grape berry through several pathways such as glycolysis and photosynthesis, where it is then stored in the vacuole. At veraison, sugars are no longer utilized for energy metabolism and begin to accumulate in the vacuole. In addition, photosynthetic processes drastically decrease. Thus, to accommodate the energy needs of the berry, there is a switch from carbohydrate utilization to malic acid catabolism (Sweetman et al., 2009). Malate is released from the vacuole and becomes available for energy metabolism (through the TCA cycle and oxidative phosphorylation), amino acid interconversions, and secondary metabolite synthesis, such as flavonoids. In the current study, the consistently elevated levels of malate (Figure 3.1) and the induction of auxin signaling and photosynthesis from post-veraison to harvest (Figure 3.5) potentially suggest an imbalance in energy utilization after the onset of veraison. This ultimately could have resulted in the desynchronization of ripening events in GRBV fruit that Martinez et al. (2019) theorized.

Differential co-expression analysis in the current work indicated a potential signaling control of a SWEET sugar transporter by a calcium-binding protein (Figure S3.6). SWEET transporters are known to be associated with plant-pathogen interactions, although it has been challenging to define a clear role due to variability in their responses to pathogen infection (Breia et al., 2021). The calcium-binding protein was also co-expressed with bHLH, WRKY, and Zf-HD transcription factors during GRBV infection. Basic helix-loop-helix (bHLH) proteins are a superfamily of transcription factors that have been previously associated in defense responses to tomato yellow leaf curl virus, a geminivirus (Wang et al., 2015). Both WRKY and zinc finger

homeodomain (Zf-HD) proteins have also been correlated to plant defense-signaling pathways during pathogen infections (Yoda et al., 2002; Park et al., 2007). In addition, signaling crosstalk between auxin and Ca^{2+} has been suggested (Hazak et al., 2019). Although, Ca^{2+} signals calcium-binding proteins to prompt a physiological response to survive an infection (Zhang et al., 2014), viruses are also adept at utilizing Ca^{2+} for their benefit (Zhou et al., 2009). The current work suggests that GRBV triggers an association of the calcium-binding protein with auxin transport, a hormone primarily responsible for inhibiting ripening events, and carbohydrate metabolism, sugar transport, and transcription factors involved in the plant immune system. Martínez-Lüscher et al. (2019) proposed that GRBV likely causes an impairment to carbon translocation mechanisms from source-to-sink, which our research indicates may be controlled by a calcium-binding protein mediating a defense response. Further research is needed to determine the precise role of calcium and calcium-binding proteins during GRBV infection.

Among the plant-pathogen interactions, virus-induced gene silencing (VIGS) has been widely documented in geminivirus infections (Chellappan et al., 2004; Vanitharani et al., 2005; Blevins et al., 2006; Qin et al., 2017). VIGS is a plant-derived response that regulates viral gene expression to fight the infection, mediated by sRNAs. DCL proteins are essential enzymes in this response as they produce sRNAs (Blevins et al., 2006). Most plants encode four DCL proteins (DCL 1-4), where DCL 1 encodes for miRNAs, and DCL 2-4 encodes for siRNAs (Mukherjee et al., 2013). Specifically, DCL2 triggers intercellular silencing in cells adjacent to the initial virus-infected cell, causing systematic VIGS (Qin et al., 2017). Previous literature has successfully correlated higher levels of siRNA accumulation to symptom recovery and decreases in viral titer levels (Chellappan et al., 2004).

In the current study, the antiviral transcriptional control observed with DCL2 potentially explains the irregular ripening events observed in GRBV fruit for the past ten years. For the first time, we revealed a transcriptional shift of DCL2, indicating a loss of allocation of resources for primary and secondary metabolism and energy metabolism. The loss of co-expression with the oxidative phosphorylation pathway may also explain the slight downregulation of this pathway and potentially the increase in malate concentrations previously discussed. The gaining of co-expression of this gene with transcriptional and translational processes further supports that GRBV infected grapes are potentially favoring VIGS as a defense mechanism over normal ripening processes.

Analyzing the DE of DCL2 reveals that GRBV infection led to significant induction at veraison in both seasons, which was moderate at post-veraison in 2016, and suppression at harvest in both seasons. A similar study investigating transcriptional responses to grapevine leafroll-associated virus-3 (GLRaV-3) infection observed an analogous induction of DCL2 at only veraison (Ghaffari et al., 2020). Interestingly, research indicates that the onset of foliar symptoms for GLRaVs and GRBV begins at veraison (Gutha et al., 2010; Sudarshana et al., 2015; Wallis and Sudarshana, 2016). After veraison, viral gene expression levels decreased (Figure 3.7b), which may relate to VIGS modifying viral RNAs (Unver and Budak, 2009). Taken together, our data suggests a phenological association with plant immune responses, potentially resulting in the onset of foliar symptoms.

In Chellappan et al. (2005), similar work was performed on a geminivirus infecting cassava plants. In this study, fluctuations in temperature regulated the expression of VIGS where increases in temperatures increased expression and decreased viral titer and symptoms (Chellappan et al., 2005; Flores et al., 2015). During our study, cumulative growing degree days were higher in 2017

than in 2016 (Figure 3.6a), with nine days exceeding 35°C and four days exceeding 40°C. Consistently in this study, the impact of GRBV on the grape transcriptome was lower in 2017 than in 2016 concurrently with generally lower viral gene expression and higher expression of the DCL2 transcript. Although viral titer levels were not measured in this study, our results agree with previous studies that temperature affects disease expression (Chellappan et al., 2005; Flores et al., 2015).

3.5 Methods:

3.5.1 Plant Material and sample collection

Cabernet Sauvignon grapevines (clone 8, Foundation Plant Services, University of California Davis) grafted onto 110R (*V. berlandieri* × *V. rupestris*), and 420A (*V. berlandieri* × *V. riparia*) rootstocks were used for this study. These grapevines were planted in 1999 at the Oakville Experimental Vineyard (Napa County, CA, USA). The grapevines were trained to a bilateral cordon in a vertical shoot positioned system. Viticultural practices are reported in Rumbaugh et al. (2021) and Martinez-Lüscher et al. (2019). From this vineyard block, 60 vines were tested for the presence or absence of GRBV, as well as GLRaV (types 1 to 4, and strains of 4). For this study, only healthy vines (i.e., vines that tested negative for viruses and did not show symptoms of viral disease, RB(-)) and vines which only tested positive for GRBV, and which are symptomatic (RB(+)) were used as data vines. For each treatment, 20 and 25 data vines were identified in 2016 and 2017, respectively. Data vines were randomly subdivided into five biological replicates of four and five vines, using a random sequence generator for 2016 and 2017, respectively (http://www.random.org.sequences). Five berries were collected from each data vine randomly (top, middle, and bottom of grape bunches on the outer and inner side of the canopy) for a total of

20 berries per biological replicate. Grapes were sampled four times during ripening at pre-veraison, 50% veraison (berry softening and color change), post-veraison, and harvest for 2016. For 2017, grapes were collected at all the previous points, except for post-veraison due to a heat spike and unexpected rapid increases in sugar content. Grapes sampled were immediately processed upon arrival at the laboratory, and berries were deseeded, frozen in liquid nitrogen, and stored at -80°C until further analysis.

3.5.2 Total RNA isolation

Total RNA from each biological replicate across seasons, rootstocks, and collection points was extracted and isolated. Approximately 2.00g of fresh weight grape material was mixed with lysate buffer consisting of 4M guanidine thiocyanate, 0.2M sodium acetate, 26mM EDTA, and 2.6% (w/v) PVP-40. The samples were then homogenized using a table mill, and then total RNA was isolated using the Qiagen RNeasy Plant Mini Kit in conjunction with the Qiagen PowerClean Pro Cleanup kit. DNA was removed using the Zymo Research RNA Clean & Concentrator-5 Kit. RNA integrity and purity were analyzed using a 2100 Bioanalyzer and NanoDrop 2000c spectrophotometer, respectively.

3.5.3 mRNA sequencing and analysis

Gene expression profiling was carried out using a 3' Tag-RNA-Seq protocol. Barcoded sequencing libraries were prepared using the QuantSeq FWD kit (Lexogen, Vienna, Austria) for multiplexed sequencing according to manufacturer recommendations (Lexogen). Micro-capillary gel electrophoresis was used to verify the fragment size distribution of the libraries on a Bioanalyzer 2100 (Agilent, Santa Clara, CA). The libraries were quantified by fluorometry on a Qubit

fluorometer (LifeTechnologies, Carlsbad, CA) and pooled in equimolar ratios. Up to forty-eight libraries per lane were sequenced on a HiSeq 4000 sequencer (Illumina, San Diego, CA). The sequencing was carried out by the DNA Technologies and Expression Analysis Core at the UC Davis Genome Center, supported by NIH Shared Instrumentation Grant 1S10OD010786-01.

3.5.4 Metabolite extraction and quantitation

3.5.4.1 Volatile compound analysis

The berries were finely ground in liquid nitrogen for each biological replicate using an IKA analytical mill (Wilmington, NC, USA). Approximately 0.5g of fresh weight grape powder was added to a 10mL amber headspace vial (Agilent Technologies, Santa Clara, CA) containing 1g of NaCl, 1mL of 1M sodium citrate buffer, and 25uL of ascorbic acid solution. Each vial was spiked with 25µl of a 0.5mg/L 2-undecanone internal standard solution. For a QC sample, grapes from all collection points, seasons, and rootstocks were homogenized together in liquid nitrogen and treated as a sample. A QC sample was extracted with each extraction batch and analyzed similarly to determine day-to-day instrumental drift.

Headspace solid-phase microextraction gas chromatography coupled to a mass spectrometer (HS-SPME-GC-MS) was used to analyze the volatile profiles of grape extracts, as in Rumbaugh et al. (2021). Ions were monitored using synchronous scan and selected ion monitoring (SIM). All compounds identified in this study were identified using the SIM mode described in Hendrickson et al. (2016). Samples were analyzed using Mass Hunter software version B.07.00 (Agilent Technologies, Santa Clara, CA). Compounds were semi-quantitatively analyzed using relative peak areas by normalization with 2-undecanone as well as the berry mass. The five biological replicates across all variables were analyzed in triplicate. Compounds were identified

by retention time and confirmation of mass spectra ion peaks using the National Institute of Standards and Technology database (NIST) (https://www.nist.gov). A list of 50 volatile compounds was generated from previous literature and was used for compound identification. A final list of 38 compounds was identified in the grape samples and used for quantitation.

3.5.4.2 Phenolic compound analysis

The homogenized frozen grape powder was analyzed by mixing 1g of grape material with 4mL of extraction buffer that consisted of methanol:water:chloroform in a 3:1:1 and 0.1% (v/v) formic acid. Decyl-β-glucopyranoside was used as an internal standard, and each sample was spiked with 80µL of 100mg/L solution (final concentration of 500µg/L). The sample was vortexed for 30 seconds, sonicated for 10 min at 4°C, and then centrifuged at 3,220 x g at 4°C for 10 min at 4°C. The supernatant was collected, and 1mL was diluted to 4mL using 18MΩ water. The rest of the supernatant was saved for primary metabolite analysis. The sample was mixed and centrifuged for 10 minutes at 15,000rpm. One mL of the diluted sample was transferred to a 2mL amber vial with a screw cap for analysis. QC samples, which consisted of the same grape material as described in section 4.4.1, were prepared daily in the same manner for phenolic analysis.

Analyses were carried out on an Agilent 1290 Infinity Ultra-high 150 Performance Liquid Chromatography (UHPLC) system coupled with an Agilent 6545 151 quadrupole time-of-flight (Q-TOF) LC/MS. The temperature-controlled autosampler was kept at 4°C. Chromatographic separation was carried out on an Agilent analytical column (2.1 × 150mm, particle size 2.7 µm) after 2uL of the sample was injected. Mobile phase A was LC grade water with 0.1% (v/v) formic acid, and phase B was LC grade acetonitrile with 0.1% (v/v) formic acid. The chromatographic method was 98% phase A (0-1 minute), a gradual decrease from 98% to 20% phase A (1-16

minutes), a decrease to 2% phase A (16-18 minutes), which was maintained for 2 minutes (18-20 minutes), and finally a linear increase from 2% to 98% phase A over one minute (20-21 minutes) which was then held for another four minutes (21-25 minutes). The iso pump and binary pump were set to a flow rate of 0.2mL a minute. The mass range of the detector was 100-1000 m/z, and the rate of detection was set to 2 spectra per second with a cycle time of 1 minute. The sheath gas and drying gas temperatures were at 375°C and 200°C, respectively. The capillary voltage and nozzle voltage were set to 3500V and 1000V, respectively. The nebulizer was set to 50 psi, and the fragmentor voltage set to 100 V. The internal standard eluted at 13.45 minutes with the mass of 321.2272 m/z, 343.2091 m/z, and 359.183 m/z for H+, Na+, and K+ ionized forms of the internal standard, respectively. The area of the peak of mass 343.2091 m/z was used for the normalization of all other compounds identified. A list of 51 phenolic compounds that were previously cited in literature was utilized for compound identification. The final number of identified compounds in all samples across environmental, developmental, and genotypic factors was 36 compounds which consisted of benzoic acids, hydroxycinnamic acids, flavonoids, and stilbenes.

3.5.4.3 Primary metabolite analysis

For the analysis of primary metabolites, 1mL of the supernatant from the phenolic hydroalcoholic extraction was utilized. The sample was dried under vacuum for 4 h at 35°C, suspended in 1mL of D_2O, and then dried under vacuum again for 4 h at 35°C to reduce the methanol signal (Pereira et al. 2006). The dried samples were then reconstituted with 1mL of 10mM phosphate buffer (pH 6.8), vortexed until completely homogenized, and centrifuged at 14,000 'g at 4°C for 5 min. Into a new microcentrifuge tube, 585uL of the sample was mixed with

65uL of 5 mM 3-(trimethylsilyl)-1-propane sulfonic acid-d6 (DSS-d6) as an internal standard. Each sample was adjusted to a pH of 6.8 using 1N HCl or NaOH, and 600uL was transferred to a 5mm NMR tube. Samples were stored at 4°C for no longer than 24 h until the NMR spectra were acquired. Sample acquisition and analysis were performed as in Chin et al. (2014; 2020). Briefly, the ^{1}H NMR spectra of the aqueous samples were acquired at 298 K on a Bruker 600MHz NMR spectrometer (Bruker BioSpin AG, F.llanden, Switzerland) equipped with a TCI cryoprobe and a SampleJet using the noesypr1d pulse programs. Each spectrum was acquired in approximately 10 min. Chenomx Inc. NMR suite Processor version 8.3 (Edmonton, AB, Canada) was used to identify and quantify primary metabolites in grape. A total of 26 metabolites were identified and quantified, ranging from amino acids, organic acid esters, and carbohydrates.

3.5.5 Statistical analysis

All metabolites were subjected to differential expression analysis using limma-voom. Log fold changes based on averages and p-values were calculated using R (version 4.0.1). All significant metabolite differences were determined by adjusting the p-value using a false discovery rate (FDR) test ($p<0.05$, FDR correction). Differential expression (DE) analysis was conducted using the package limma-voom in R. Significant ($p<0.01$) DEGs were analyzed for gene ontology using the PANTHER website (Thomas et al., 2003; Mi et al., 2009). The conserved responses to GRBV were determined by creating a Venn Diagram (Oliveros, 2007). The WGCNA analysis was conducted in R using log2 counts per million reads and included all genes included in the DE analyses. The analysis used a signed network and a robust biweight midcorrelation. A soft-thresholding power of 32 was chosen, using the WGCNA function pickSoftThreshold, as the smallest power for which the scale-free topology index exceeded 0.85. Differential co-expression

analyses were conducted in R using the z-score method (Zhang et al., 2007) as implemented in the Bioconductor package dcanr (Bhuva et al., 2019), version 1.6.0, which compares correlation coefficients between pairs of genes across conditions. P-values were adjusted for multiple testing using the Benjamini-Hochberg method (Yoav Benjamini and Yosef Hochberg, 2007).

3.6 Conclusions:

GRBV is the first geminivirus detected in grapevines, and our understanding of the detrimental impacts on grape and wine composition and quality is advancing. In this study, the seasonal impact was larger than the genotypic impact on GRBD expression in grapes. Seasonal differences considerably impacted disease outcomes in grapevines, where 2016 was more impacted than 2017. Fewer differences in primary metabolites and the grape transcriptome between RB(+) grapes and RB(-) grapes in 2017 were concurrent with increased induction of a VIGS transcript. CS on 420A rootstock was less sensitive to GRBV infection than CS on 110R rootstock, specifically in 2017. This was seen in anthocyanin accumulation and the grape transcriptome, specifically with plant-pathogen interactions in 2017. We hypothesize that the difference in vigor and drought resistance in the two rootstocks led to a difference in the microclimate of the grapevine and berry metabolism.

In past research, decreases in symptoms have been correlated to upregulation of VIGS. Our research reveals similar findings, where higher temperatures potentially led to induction of virus-induced RNA gene silencing in GBRV infected fruit and fewer differences in the grape transcriptome. In addition, VIGS was only significantly upregulated at veraison across genotype and season, which resulted in decreases in viral gene expression, suggesting phenological control over plant-derived immune responses. Further work on hormonal control, calcium-binding

proteins, and RNA-induced gene silencing is needed to obtain a holistic view of the plant-pathogen interactions during GRBV infection.

3.7 Supplemental Information:

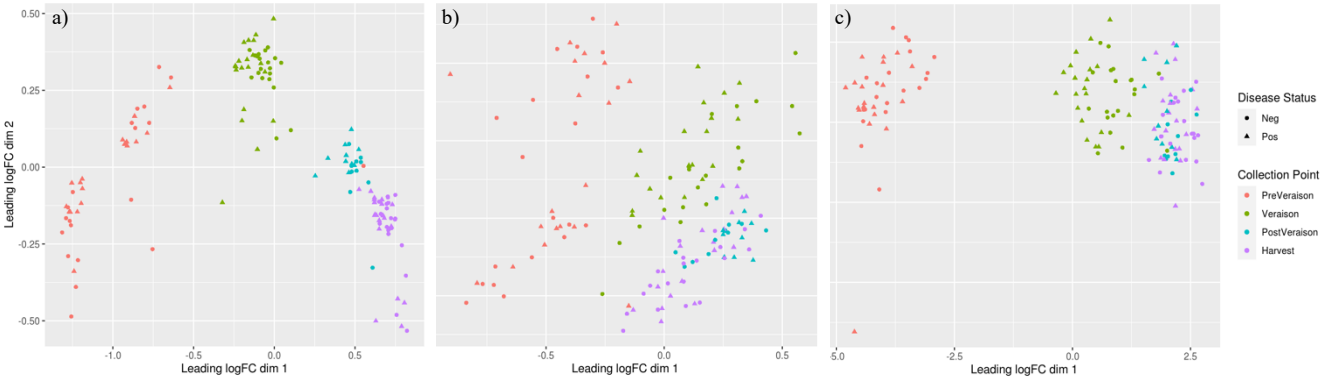

Figure S3.1. Multidimensional scaling plot of a) primary metabolites, b) volatile secondary metabolites, and c) phenolic secondary metabolites. Each plot is color coded based on the ripeness level of each sample.

Gene	Functional annotation	Pre-veraison				Veraison				Post-veraison		Harvest			
		110R		420A		110R		420A		110R	420A	110R		420A	
		2016	2017	2016	2017	2016	2017	2016	2017	2016		2016	2017	2016	2017
VIT_06s0004g02620	Phenylalanine lyase 1 (PAL1)	**1.89**	0.07	1.08	0.65	-0.28	-0.75	-0.44	**-1.29**	-0.17	-0.27	0.31	0.30	**1.48**	0.51
VIT_13s0019g04460	Phenylalanine lyase 7 (PAL7)	1.39	-0.12	-0.60	0.26	-0.46	-0.52	0.05	-1.09	-0.15	-0.19	-0.16	0.13	1.12	0.38
VIT_08s0040g01710	Phenylalanine lyase 2 (PAL2)	0.92	0.36	-0.53	0.10	-1.11	-0.85	-0.02	-0.76	-0.54	-0.45	-0.86	-0.86	-0.77	-0.46
VIT_11s0065g00350	*Trans*- cinnamate 4-monooxygenase (C4H)	0.49	0.88	0.39	0.47	-1.99	-0.23	0.15	-1.04	-0.34	-0.23	-0.22	-0.44	-0.25	-0.61
VIT_02s0025g02920	Caffeic acid 3-O-methyltransferase (COMT)	-1.09	-0.33	-0.11	0.48	-0.74	-0.18	-0.05	-0.66	0.11	0.18	-0.69	-0.02	-0.25	-0.21
VIT_16s0098g00850	Caffeic acid 3-O-methyltransferase (COMT)	0.48	-0.19	0.00	-0.11	-0.31	-0.48	-0.48	0.33	0.28	0.35	**0.83**	0.52	0.36	0.92
VIT_04s0023g02900	Ferulate-5-hydroxylase (F5H)	-0.36	-0.42	0.11	-0.02	-1.94	0.78	0.78	-0.12	0.35	-0.51	-0.93	-1.09	-0.82	-0.35
VIT_06s0061g00450	4-Coumaroyl-CoA ligase (4CL)	0.39	-0.37	0.16	0.22	-0.07	0.53	0.23	**0.78**	0.15	0.37	0.55	0.32	0.24	0.23
VIT_11s0052g01090	4-Coumaroyl-CoA ligase (4CL)	0.69	0.18	-0.05	0.04	-0.93	-0.60	0.27	-1.15	-0.06	-0.49	-0.88	-0.70	-0.66	-0.09
VIT_12s0035g02070	Cinnamoyl-CoA reductase (CCR)	-0.56	-0.22	-0.02	0.48	0.09	0.30	0.44	-0.13	1.05	0.79	0.12	0.15	0.21	0.15
VIT_14s0066g01150	Cinnamoyl-CoA reductase (CCR)	0.36	0.85	0.89	0.43	**-1.76**	-0.97	0.87	-1.32	-0.83	-0.52	-0.63	0.11	-0.30	-0.96
VIT_02s0012g01570	Cinnamoyl-CoA reductase (CCR)	-0.43	-1.11	-0.42	0.45	-0.92	-0.73	-0.07	-0.73	0.17	0.10	-0.17	0.07	0.96	0.37
VIT_03s0180g00260	Cinamyl alcohol dehydrogenase (CAD)	-0.27	-0.01	-0.54	-0.13	-0.11	-0.22	0.16	-0.06	0.08	-0.18	0.04	0.19	-0.17	0.26
VIT_08s0040g00780	*P*- Coumaroyl shikimate 3'-hydroxylase isoform	0.74	0.52	-0.21	-0.21	**-2.02**	-0.75	0.50	-1.02	0.47	-0.16	0.40	-0.66	-0.35	-0.43
VIT_16s0100g01030	Stilbene synthase (STS)	-0.27	0.37	-0.22	1.55	-1.55	-0.64	-0.16	-1.93	1.14	-0.17	1.79	-0.84	1.19	0.23
VIT_16s0100g01200	Stilbene synthase (STS)	0.58	0.92	0.50	0.45	-0.93	-0.47	0.15	-1.56	0.16	-0.04	1.83	-1.67	-2.04	-0.71
VIT_14s0068g00930	Chalcone synthase 1 (CHS1)	1.80	0.60	1.48	-0.46	-1.54	-0.91	0.00	-0.95	-0.38	-0.31	0.45	-0.23	0.73	0.42
VIT_05s0136g00260	Chalcone synthase 3 (CHS3)	**1.19**	-0.46	0.60	-0.24	-0.32	-0.57	-0.05	-0.94	0.22	0.25	0.57	0.62	**1.51**	0.42
VIT_13s0067g03820	Chalcone isomerase (CHI)	0.39	0.17	-0.01	-0.25	-0.23	-0.52	0.11	-0.86	0.27	0.01	0.49	0.36	**0.93**	0.10
VIT_13s0067g02870	Chalcone isomerase 2 (CHI2)	**0.57**	0.38	0.23	-0.04	-0.17	-0.40	-0.03	**-0.65**	0.46	0.35	1.30	0.57	**2.00**	0.33
VIT_04s0023g03370	Flavanone 3-hydroxylase (F3H)	**0.95**	0.08	0.60	-0.19	-0.17	-0.10	-0.16	-0.98	-0.15	0.06	0.05	0.26	**1.01**	0.36
VIT_18s0001g12800	Dihydroflavanol 4-reductase (DFR)	**0.82**	-0.03	-0.04	-0.09	-0.18	0.02	-0.30	-0.22	0.03	0.21	-0.29	-0.32	**0.70**	-0.13
VIT_02s0025g04720	Anthocyanidin synthase (ANS)	**1.00**	-0.33	0.51	-0.09	-0.09	-0.45	0.04	-0.61	-0.01	0.02	0.59	0.39	**1.18**	0.46
VIT_00s0361g00040	Anthocyanidin reductase (ANR)	**1.38**	0.80	0.80	-0.12	0.21	-0.62	-0.47	-0.74	-0.02	0.54	0.12	0.34	-0.92	-0.91
VIT_16s0039g02230	UDP-glucose:anthocyanidin 3-O-D-glucosyltransferase (UF3GT)	0.74	-0.77	0.40	-0.30	-0.36	0.03	0.53	-0.99	0.25	0.03	0.63	0.82	1.22	0.10
VIT_12s0034g00130	UDP-glucose:anthocyanidin 3-O-D-glucosyltransferase (UF3GT)	-0.23	0.30	-0.55	0.88	**-1.81**	0.11	-0.49	-0.55	0.23	-0.30	-0.02	0.18	**-1.19**	-0.06
VIT_12s0055g00290	UDP-glucose:anthocyanidin 3-O-D-glucosyltransferase (UF3GT)	**-1.00**	-0.34	-0.52	-0.47	-0.03	0.25	-0.08	-0.99	-0.11	-0.76	0.09	-0.07	-0.04	-0.41

Figure S3.2. Log fold change of transcripts in the phenylpropanoid pathway affected by GRBV infection. Negative values (blue) indicate a decrease in concentration, positive values (red) indicate an increase in concentration in diseased grapes. Color gradient indicates the size of log fold change. Bolded values indicate a significant difference (FDR adjusted $p<0.05$). 110R = Cabernet Sauvignon on rootstock 110R and 420A = Cabernet Sauvignon on rootstock 420A.

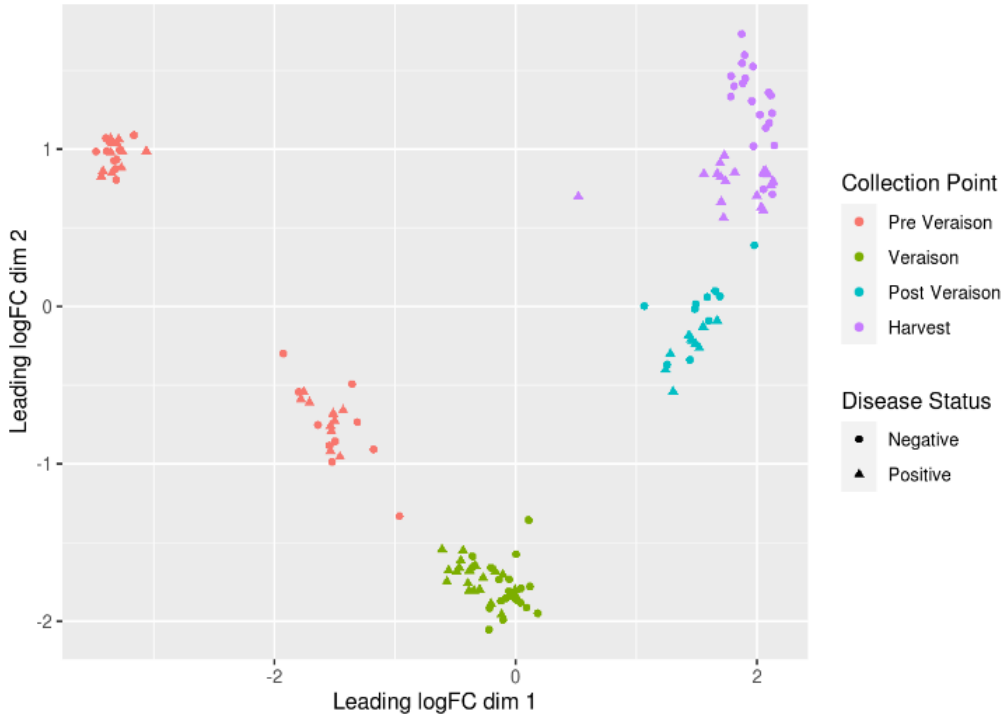

Figure S3.3. Multidimensional scaling plot of gene expression data. The plot is color coded based on the ripeness level of each sample.

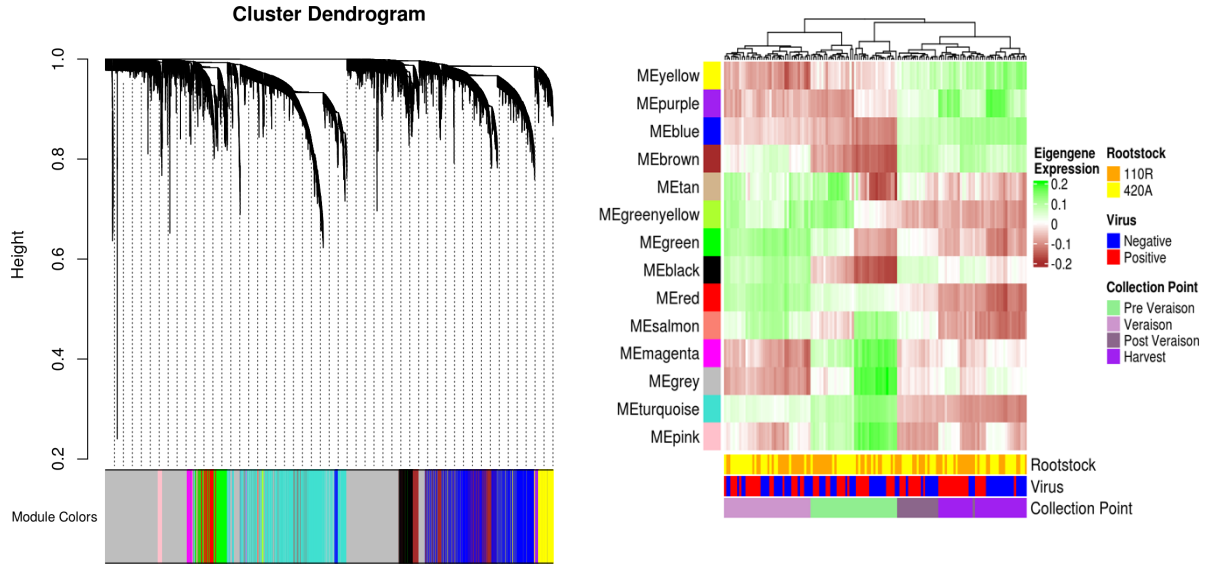

Figure S3.4. Weighted gene co-expression network analysis (WGCNA) of all differentially expressed genes from both rootstocks and seasons. Modules were created using a a) dendrogram which showed in b) a heat map that clustering was due to ripeness level.

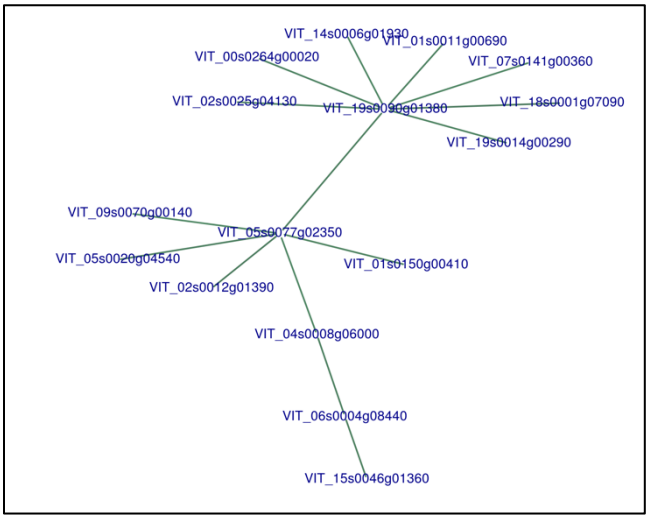

Figure S3.5. Differential co-expression analysis showing a gain of co-expression of the centralized genes with the exterior genes. The centralized genes are VIT_05s0077g02350 and VIT_19s0090g1380 whose processes are unknown. VIT_14s0006g01400. The transcripts on the exterior are associated with sugar metabolism, ethylene signaling, cell wall metabolism, and nucleotide sugar metabolism

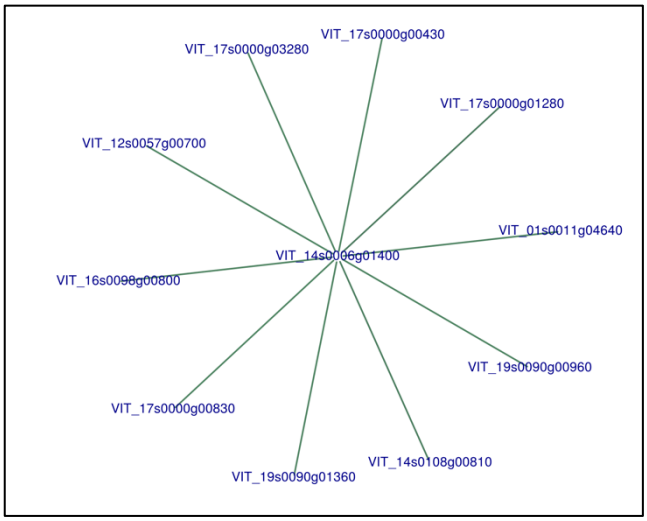

Figure S3.6. Differential co-expression analysis showing a gain of co-expression of the centralized genes with the exterior genes. The centralized gene is VIT_14s0006g01400, which encodes for a calcium binding protein. The transcripts on the exterior are associated with transcription factors related to immune responses, sugar transport, and auxin transport.

Table S3.1 Log fold change, gene IDs, and functional annotation of transcripts found through differential co-expression in **Figure S3.4**.

Table S3.2 Log fold change, gene IDs, and functional annotation of transcripts found through differential co-expression in **Figure 6a**.

Table S3.3 Log fold change, gene IDs, and functional annotation of transcripts found through differential co-expression in **Figure 6b**.

3.8 References:

Akbergenov, R., Si-Ammour, A., Blevins, T., Amin, I., Kutter, C., Vanderschuren, H., Zhang, P., Gruissem, W., Meins, F., Hohn, T., et al. (2006). Molecular characterization of geminivirus-derived small RNAs in different plant species. *Nucleic Acids Res.* **34**:462–471.

Alabi, O. J., Casassa, L. F., Gutha, L. R., Larsen, R. C., Henick-Kling, T., Harbertson, J. F., and Naidu, R. A. (2016). Impacts of Grapevine Leafroll Disease on Fruit Yield and Grape and Wine Chemistry in a Wine Grape (Vitis vinifera L.) Cultivar. *PLoS One* **11**:e0149666.

Beam, K., and Ascencio-Ibáñez, J. T. (2020). Geminivirus Resistance: A Minireview. *Front. Plant Sci.* **11**:1–9.

Bhuva, D. D., Cursons, J., Smyth, G. K., and Davis, M. J. (2019). Differential co-expression-based detection of conditional relationships in transcriptional data: Comparative analysis and application to breast cancer. *Genome Biol.* **20**:1–21.

Blanco-Ulate, B., Hopfer, H., Figueroa-Balderas, R., Ye, Z., Rivero, R. M., Albacete, A., Pérez-Alfocea, F., Koyama, R., Anderson, M. M., Smith, R. J., et al. (2017). Red blotch disease alters grape berry development and metabolism by interfering with the transcriptional and hormonal regulation of ripening. *J. Exp. Bot.* **68**:1225–1238.

Blevins, T., Rajeswaran, R., Shivaprasad, P. V., Beknazariants, D., Si-Ammour, A., Park, H. S., Vazquez, F., Robertson, D., Meins, F., Hohn, T., et al. (2006). Four plant Dicers mediate viral small RNA biogenesis and DNA virus induced silencing. *Nucleic Acids Res.* **34**:6233–6246.

Bowen, P., Bogdanoff, C., Poojari, S., Usher, K., Lowery, T., and Úrbez-Torres, J. R. (2020). Effects of grapevine red blotch disease on cabernet franc vine physiology, bud hardiness, and fruit and wine quality. *Am. J. Enol. Vitic.* **71**:308–318.

Breia, R., Conde, A., Badim, H., Fortes, A. M., Gerós, H., and Granell, A. (2021). Plant Sweets: From sugar transport to plant–pathogen interaction and more unexpected physiological roles. *Plant Physiol.* **186**:836–852.

Cabaleiro, C., Pesqueira, A. M., and García-Berrios, J. J. (2021). Influence of Grapevine Leafroll-associated Virus-3 in Mature Plants of Vitis vinifera L. cv Albariño on 110R and 196.17C Rootstocks. *South African J. Enol. Vitic.* **42**:165–174.

Chellappan, P., Vanitharani, R., Pita, J., and Fauquet, C. M. (2004). Short Interfering RNA Accumulation Correlates with Host Recovery in DNA Virus-Infected Hosts, and Gene Silencing Targets Specific Viral Sequences. *J. Virol.* **78**:7465–7477.

Chellappan, P., Vanitharani, R., Ogbe, F., and Fauquet, C. M. (2005). Effect of temperature on geminivirus-induced RNA silencing in plants. *Plant Physiol.* **138**:1828–1841.

Chin, E. L., Mishchuk, D. O., Breksa, A. P., and Slupsky, C. M. (2014). Metabolite signature of candidatus liberibacter asiaticus infection in two citrus varieties. *J. Agric. Food Chem.* **62**:6585–6591.

Chin, E. L., Ramsey, J. S., Mishchuk, D. O., Saha, S., Foster, E., Chavez, J. D., Howe, K., Zhong, X., Polek, M. Lou, Godfrey, K. E., et al. (2020). Longitudinal Transcriptomic, Proteomic, and Metabolomic Analyses of Citrus sinensis (L.) Osbeck Graft-Inoculated with " Candidatus Liberibacter asiaticus." *J. Proteome Res.* **19**:719–732.

Credi, R., and Babini, A. R. (1996). Effect of virus and virus-like infections on the growth of grapevine rootstocks. *Adv. Hortic. Sci.* **10**:95–98.

Downey, M. O., Dokoozlian, N. K., and Krstic, M. P. (2006). Cultural practice and environmental impacts on the flavonoid composition of grapes and wine: A review of recent

research. *Am. J. Enol. Vitic.* **57**:257–268.

Flores, M. A., Reyes, M. I., Robertson, D. (Niki), and Kjemtrup, S. (2015). Persistent Virus-Induced Gene Silencing in Asymptomatic Accessions of Arabidopsis BT - Plant Functional Genomics: Methods and Protocols. In (ed. Alonso, J. M.) and Stepanova, A. N.), pp. 305–322. New York, NY: Springer New York.

Gasperin-Bulbarela, J., Licea-Navarro, A. F., Pino-Villar, C., Hernandez-Martínez, R., and Carrillo-Tripp, J. (2019). First report of grapevine´ red blotch virus in Mexico. *Plant Dis.* **103**:381.

Ghaffari, S., Reynard, J. S., and Rienth, M. (2020). Single berry sampling reveals novel insights into transcriptomic changes induced by leafroll virus infections in grapevine (V. vinifera). *Res. Sq.* Advance Access published 2020, doi:10.21203/rs.2.22668/v1.

Girardello, R. C., Cooper, M. L., Smith, R. J., Lerno, L. A., Bruce, R. C., Eridon, S., and Oberholster, A. (2019a). Impact of Grapevine Red Blotch Disease on Grape Composition of Vitis vinifera Cabernet Sauvignon, Merlot, and Chardonnay. *J. Agric. Food Chem.* **67**:5496–5511.

Girardello, R. C., Rich, V., Smith, R. J., Brenneman, C., Heymann, H., and Oberholster, A. (2019b). The impact of grapevine red blotch disease on *Vitis vinifera* L. Chardonnay grape and wine composition and sensory attributes over three seasons. *J. Sci. Food Agric.* Advance Access published 2019, doi:10.1002/jsfa.10147.

Girardello, R. C., Cooper, M. L., Lerno, L. A., Brenneman, C., Eridon, S., Sokolowsky, M., Heymann, H., and Oberholster, A. (2020). Impact of Grapevine Red Blotch Disease on Cabernet Sauvignon and Merlot Wine Composition and Sensory Attributes. *Molecules* **25**.

Golino, D. A. (1993). Potential Interactions Between Rootstocks and Grapevine Latent Viruses. *Am. J. Enol. Vitic.* **44**:148–152.

Grimplet, J., Cramer, G. R., Dickerson, J. A., Mathiason, K., van Hemert, J., and Fennell, A. Y. (2009). Vitisnet: "Omics" integration through grapevine molecular networks. *PLoS One* **4**.

Gutha, L. R., Casassa, L. F., Harbertson, J. F., and Naidu, R. A. (2010). Modulation of flavonoid biosynthetic pathway genes and anthocyanins due to virus infection in grapevine (Vitis vinifera L.) leaves. *BMC Plant Biol.* **10**:187.

Hanley-Bowdoin, L., Settlage, S. B., Orozco, B. M., Nagar, S., and Robertson, D. (2000). *Geminiviruses: Models for plant DNA replication, transcription, and cell cycle regulation*.

Hazak, O., Mamon, E., Lavy, M., Sternberg, H., Behera, S., Schmitz-Thom, I., Bloch, D., Dementiev, O., Gutman, I., Danziger, T., et al. (2019). *A novel Ca2+-binding protein that can rapidly transduce auxin responses during root growth*.

Hendrickson, D. A., Lerno, L. A., Hjelmeland, A. K., Ebeler, S. E., Heymann, H., Hopfer, H., Block, K. L., Brenneman, C. A., and Oberholster, A. (2016). Impact of mechanical harvesting and optical berry sorting on grape and wine composition. *Am. J. Enol. Vitic.* **67**:385–397.

Honjo, M. N., Emura, N., Kawagoe, T., Sugisaka, J., Kamitani, M., Nagano, A. J., and Kudoh, H. (2020). Seasonality of interactions between a plant virus and its host during persistent infection in a natural environment. *ISME J.* **14**:506–518.

Kalua, C. M., and Boss, P. K. (2009). Evolution of volatile compounds during the development of cabernet sauvignon grapes (vitis vinifera l.). *J. Agric. Food Chem.* **57**:3818–3830.

Krenz, B., Thompson, J. R., Fuchs, M., and Perry, K. L. (2012). Complete Genome Sequence of a New Circular DNA Virus from Grapevine. *J. Virol.* **86**:7715–7715.

Krenz, B., Thompson, J. R., Mclane, H. L., Fuchs, M., and Perry, K. L. (2014). Phyto-02-14-0053-R Advance Access published 2014.

Kuria, P., Ilyas, M., Ateka, E., Miano, D., Onguso, J., Carrington, J. C., and Taylor, N. J. (2017). Differential response of cassava genotypes to infection by cassava mosaic geminiviruses. *Virus Res.* **227**:69–81.

Lee, J., Rennaker, C. D., Thompson, B. D., and Karasev, A. V. (2021). Influence of Grapevine red blotch virus (GRBV) on Idaho 'Syrah' grape composition. *Sci. Hortic. (Amsterdam).* **282**.

Lim, S., Igori, D., Zhao, F., Moon, J., Cho, I.-S., and Choi, G.-S. (2016). First report of Grapevine red blotch-associated virus on grapevine in Korea. *Plant Dis.* **100**:1957.

Lin, J., Massonnet, M., and Cantu, D. (2019). The genetic basis of grape and wine aroma. *Hortic. Res.* **6**.

Luna, F., Debat, H., Gomez-Talquenca, S., Moyano, S., Zavallo, D., and Asurmendi, S. (2019). First report of grapevine red blotch virus infecting grapevine in Argentina. *J. Plant Pathol.* **101**.

Martínez-Lüscher, J., Plank, C. M., Brillante, L., Cooper, M. L., Smith, R. J., Al-Rwahnih, M., Yu, R., Oberholster, A., Girardello, R., and Kurtural, S. K. (2019). Grapevine Red Blotch Virus May Reduce Carbon Translocation Leading to Impaired Grape Berry Ripening. *J. Agric. Food Chem.* **67**:2437–2448.

Marwal, A., Kumar, R., Paul Khurana, S. M., and Gaur, R. K. (2019). Complete nucleotide sequence of a new geminivirus isolated from Vitis vinifera in India: a symptomless host of Grapevine red blotch virus. *VirusDisease* **30**:106–111.

Mi, H., Dong, Q., Muruganujan, A., Gaudet, P., Lewis, S., and Thomas, P. D. (2009). PANTHER version 7: Improved phylogenetic trees, orthologs and collaboration with the Gene Ontology Consortium. *Nucleic Acids Res.* **38**:204–210.

Mukherjee, K., Campos, H., and Kolaczkowski, B. (2013). Evolution of animal and plant dicers: Early parallel duplications and recurrent adaptation of antiviral RNA binding in plants. *Mol. Biol. Evol.* **30**:627–641.

Néya, B. J., Zida, P. E., Sérémé, D., Lund, O. S., and Traoré, O. (2015). Evaluation of yield losses caused by cowpea aphid-borne mosaic virus (CABMV) in 21 cowpea (vigna unguiculata (L.) Walp.) Varieties in burkina faso. *Pakistan J. Biol. Sci.* **18**:304–313.

Oliveros, J. C. (2007). An Interactive Tool for Comparing Lists with Venn's Diagrams. *Venny* Advance Access published 2007.

Osier, M. V. (2016). VitisPathways: Gene pathway analysis for V. vinifera. *Vitis - J. Grapevine Res.* **55**:129–133.

Park, H. C., Kim, M. L., Lee, S. M., Bahk, J. D., Yun, D. J., Lim, C. O., Hong, J. C., Lee, S. Y., Cho, M. J., and Chung, W. S. (2007). Pathogen-induced binding of the soybean zinc finger homeodomain proteins GmZF-HD1 and GmZF-HD2 to two repeats of ATTA homeodomain binding site in the calmodulin isoform 4 (GmCaM4) promoter. *Nucleic Acids Res.* **35**:3612–3623.

Poojari, S., Lowery, D. T., Rott, M., Schmidt, A. M., and Úrbez-Torres, J. R. (2017). Incidence, distribution and genetic diversity of Grapevine red blotch virus in British Columbia. *Can. J. Plant Pathol.* **39**:201–211.

Prasad, A., Sharma, N., Muthamilarasan, M., Rana, S., and Prasad, M. (2019). Recent advances in small RNA mediated plant-virus interactions. *Crit. Rev. Biotechnol.* **39**:587–601.

Qin, C., Li, B., Fan, Y., Zhang, X., Yu, Z., Ryabov, E., Zhao, M., Wang, H., Shi, N., Zhang, P., et al. (2017). Roles of dicer-like proteins 2 and 4 in intra- and intercellular antiviral

silencing. *Plant Physiol.* **174**:1067–1081.

Reustle, G. M., Ebel, R., Winterhagen, P., Manthey, T., Dubois, C., Bassler, A., Sinn, M., Cobanov, P., Wetzel, T., and Krezal, G. (2005). Induction of silencing in transgenic grapevines (Vitis sp.). *ACTA Hortic.* Advance Access published 2005.

Ricketts, K. D., Gómez, M. I., Fuchs, M. F., Martinson, T. E., Smith, R. J., Cooper, M. L., Moyer, M. M., and Wise, A. (2017). Mitigating the economic impact of grapevine red blotch: Optimizing disease management strategies in U.S. vineyards. *Am. J. Enol. Vitic.* **68**:127–135.

Rojas, M. R., Hagen, C., Lucas, W. J., and Gilbertson, R. L. (2005). Exploiting chinks in the plant's armor: Evolution and emergence of geminiviruses. *Annu. Rev. Phytopathol.* **43**:361–394.

Rosahl, S. (1996). Lipoxygenases in Plants - Their Role in Development and Stress Response. *Zeitschrift fur Naturforsch. - Sect. C J. Biosci.* **51**:123–138.

Rumbaugh, A. C., Girardello, R. C., Cooper, M. L., Plank, C. M., Kurtural, S. K., and Oberholster, A. (2021). Impact of Rootstock and Season on Red Blotch Disease Expression in Cabernet Sauvignon (V. vinifera) **10**:1–16.

Rwahnih, M. Al, Dave, A., Anderson, M. M., Rowhani, A., Uyemoto, J. K., and Sudarshana, M. R. (2013). Association of a DNA Virus with Grapevines Affected by Red Blotch Disease in California. *Phytopathology* **103**:1069–1076.

Sudarshana, M. R., Perry, K. L., and Fuchs, M. F. (2015). Grapevine Red Blotch-Associated Virus, an Emerging Threat to the Grapevine Industry Mysore. *Phytopathology* Advance Access published 2015, doi:10.1094/PHYTO-12-14-0369-FI.

Sweetman, C., Deluc, L. G., Cramer, G. R., Ford, C. M., and Soole, K. L. (2009). Regulation of malate metabolism in grape berry and other developing fruits. *Phytochemistry* **70**:1329–1344.

Thomas, P. D., Campbell, M. J., Kejariwal, A., Mi, H., Karlak, B., Daverman, R., Diemer, K., Muruganujan, A., and Narechania, A. (2003). PANTHER: A library of protein families and subfamilies indexed by function. *Genome Res.* **13**:2129–2141.

Tripathi, S., and Varma, A. (2003). Identification of sources of resistance in Lycopersicon species to Tomato leaf curl geminivirus (ToLCV) by agroinoculation. *Euphytica* **129**:43–52.

Tripathi, A., Goswami, K., Tiwari, M., Mukherjee, S. K., and Sanan-Mishra, N. (2018). Identification and comparative analysis of microRNAs from tomato varieties showing contrasting response to ToLCV infections. *Physiol. Mol. Biol. Plants* **24**:185–202.

Unver, T., and Budak, H. (2009). Virus-induced gene silencing, A post transcriptional gene silencing method. *Int. J. Plant Genomics* **2009**.

Vanitharani, R., Chellappan, P., and Fauquet, C. M. (2005). Geminiviruses and RNA silencing. *Trends Plant Sci.* **10**:144–151.

Vondras, A. M., Lerno, L., Massonnet, M., Minio, A., Rowhani, A., Liang, D., Garcia, J., Quiroz, D., Figueroa-Balderas, R., Golino, D. A., et al. (2021). Rootstock influences the effect of grapevine leafroll-associated viruses on berry development and metabolism via abscisic acid signalling. *Mol. Plant Pathol.* Advance Access published 2021, doi:10.1111/mpp.13077.

Wallis, C. M., and Sudarshana, M. R. (2016). Effects of Grapevine red blotch-associated virus (GRBaV) infection on foliar metabolism of grapevines. *Can. J. Plant Pathol.* **38**:358–366.

Wang, J., Hu, Z., Zhao, T., Yang, Y., Chen, T., Yang, M., Yu, W., and Zhang, B. (2015). Genome-wide analysis of bHLH transcription factor and involvement in the infection by

yellow leaf curl virus in tomato (Solanum lycopersicum). *BMC Genomics* **16**:1–14.

Wang, Y., Chen, W. K., Gao, X. T., He, L., Yang, X. H., He, F., Duan, C. Q., and Wang, J. (2019). Rootstock-mediated effects on cabernet sauvignon performance: vine growth, berry ripening, flavonoids, and aromatic profiles. *Int. J. Mol. Sci.* **20**.

Xu, X. Q., Cheng, G., Duan, L. L., Jiang, R., Pan, Q. H., Duan, C. Q., and Wang, J. (2015). Effect of training systems on fatty acids and their derived volatiles in Cabernet Sauvignon grapes and wines of the north foot of Mt. Tianshan. *Food Chem.* **181**:198–206.

Yepes, L. M., Cieniewicz, E., Krenz, B., McLane, H., Thompson, J. R., Perry, K. L., and Fuchs, M. (2018). Causative Role of Grapevine Red Blotch Virus in Red Blotch Disease. *Phytopathology* **108**:902–909.

Yoav Benjamini and Yosef Hochberg (2007). Controlling the False Discovery Rate : A Practical and Powerful Approach to Multiple Testing Yoav Benjamini ; Yosef Hochberg Journal of the Royal Statistical Society . Series B (Methodological) , Vol . 57 , No . 1 . (1995), pp . *R. Stat. Soc.* **57**:289–300.

Yoda, H., Ogawa, M., Yamaguchi, Y., Koizumi, N., Kusano, T., and Sano, H. (2002). Identification of early-responsive genes associated with the hypersensitive response to tobacco mosaic virus and characterization of a WRKY-type transcription factor in tobacco plants. *Mol. Genet. Genomics* **267**:154–161.

Zhang, J., Ji, Y., and Zhang, L. (2007). Extracting three-way gene interactions from microarray data. *Bioinformatics* **23**:2903–2909.

Zhang, L., Du, L., and Poovaiah, B. W. (2014). Calcium signaling and biotic defense responses in plants. *Plant Signal. Behav.* **9**.

Zhou, Y., Frey, T. K., and Yang, J. J. (2009). Viral calciomics: Interplays between Ca2+ and virus. *Cell Calcium* **46**:1–17.

Ziliotto, F., Corso, M., Rizzini, F. M., Rasori, A., Botton, A., and Bonghi, C. (2012). Grape berry ripening delay induced by a pre-véraison NAA treatment is paralleled by a shift in the expression pattern of auxin- and ethylene-related genes. *BMC Plant Biol.* **12**.

CHAPTER 4

Grapevine red blotch virus alters grape skin cell wall composition impacting phenolic extractability during winemaking

Formatted for publication in *Agriculture*

4.1 Abstract:

Grapevine red blotch virus (GRBV) is the causal agent of grapevine red blotch disease and is known to delay grape ripening. However, grape cell wall modifications during GRBV infection are largely unknown, even though the cell wall plays a large roll in pathogenicity, viral interactions with host plants, and phenolic extractability during winemaking. Understanding the impact of GRBV infection on cell wall metabolism is important for the development of potential mitigations strategies. In this study, high-throughput transcriptome sequencing was conducted on *Vitis vinifera L.* Merlot grapes during ripening. The cell wall composition, phenolic content, and phenolic extractability at two different commercial harvest points were also determined. Log fold changes indicated a strong induction in diseased grapes at harvest of several transcripts involved in cell wall solubilization and degradation. However, these observations did not translate to changes in cell wall composition at either harvest point in diseased grapes potentially suggesting post-transcriptional regulation. Moderate induction of pectin methylesterase inhibitor transcripts and transcripts associated with pathogenesis-related proteins coincided with increases in pectin and soluble proteins in diseased grapes at harvest. Both components are known to retain polymeric phenolic compounds during winemaking. Our study confirmed this when significantly lower levels of polymeric pigments were measured in wines made from GRBV infected fruit, even though these levels were similar between diseased and healthy grape extracts.

4.2 Introduction:

Grapevine red blotch virus (GRBV), the causative agent of red blotch (RB) disease, has been prevalent in the United States since its identification in 2012 [1]. GRBV, a member of the Geminiviridae family, genus *Grablovirus* [2,3], is comprised of a circular, single stranded DNA molecule [1]. The primary method of dissemination is through propagation material; however, *Spissistilus festinus,* a three-cornered alfalfa hopper, is recognized as a potential insect vector of GRBV [4]. An economic impact study of the disease indicated that damages could range from $2,213/ha to $68,548/ha in the United States, however this cost analysis was done prior to the knowledge of potential insect vectors [5].

GRBV detrimentally impacts grape and wine composition by delaying ripening in grapes, resulting in significant decreases in total soluble solids (TSS) levels and anthocyanin concentrations, with higher amounts of titratable acidity (TA) [6–9]. Recent research suggests that the inhibition of translocation of carbon (hexoses) from leaves to the grapes results in the impairment of ripening in GRBV infected grapes, instead of decreases in carbon assimilation [8]. The restriction in the biosynthesis and accumulation of flavonoids, such as anthocyanins, has been linked to transcriptional suppression of the central and peripheral phenylpropanoid pathways [9]. These alterations are translated into the resulting wines, making wines with less fruit aromas, color, and mouthfeel [10].

Phenolic extractability during winemaking is affected by multiple factors: grape cell wall composition, cell wall integrity and porosity, grape phenolic concentration, and the interactions with each other [11–14]. It is well known that grape cell walls are made up of cellulose, hemicellulose, lignin, and pectin, that intertwine proteins and polyphenols [15]. During ripening, grape cell walls change in composition and integrity. Reports indicate significant decreases of type

I arabinogalactan, galactose, pectin methylation and acylation, as well as increases in the solubility of galacturonan [15,16]. Generally, the degradation and solubilization of cell walls that occurs as the grape matures results in higher phenolic extractability [17]. In addition, it has been shown that abiotic factors alter cell wall modifications by impeding methylesterification of cell wall pectins, increasing cell wall thickening (increasing lignin and cellulose), and increasing cell wall derived proteins. On the other hand, biotic factors have been shown to produce enzymes that degrade cell wall polysaccharides [18–20]. Consequently, these changes in the grape cell wall can directly impact the extractability and final concentrations of phenolics in wines.

However, there is little known about the impact of GRBV on cell wall composition and structure. Through transcriptomic studies involving GRBV infected grapes, Blanco-Ulate et al. [9] found an upregulation of invertase/ pectin methylesterase inhibitors at late stages of berry ripening. These enzymes are known to impede the dimethylesterification of cell wall pectins in early berry ripening to control berry enlargement and softening. Further insight on overall cell wall metabolism in GRBV infected grapes is needed to fully understand the impact on phenolic extractability during winemaking.

Prior research determined that an extended hangtime of RB(+) grapes improved phenolic extractability resulting in wine with improved phenolic content [21]. Although higher sugar content, and therefore higher ethanol content in a fermenting wine, has shown to increase phenolic extractability [11,12], our previous work has indicated the same is not true for GRBV fruit with a pre-fermitative sugar addition [21]. This work suggested that another factor affected phenolic extractability during winemaking with GRBV infected fruit. Thus, the aim of the current study was to investigate the impact of GRBV and grape maturity on phenolic extractability by determining the changes in grape cell wall composition and how this relates to the release of

phenolics under winemaking conditions. This is the first known study to evaluate the impact of GRBV infection on cell wall metabolism in grapes.

4.3 Methods and Materials:

4.3.1 Biological sampling

Vitis Vinifera L. cv. Merlot grapevines, clone 12, were used for this study in 2019 from a vineyard in Paso Robles (Paso Robles, CA, USA). Viticulture practices are described in Girardello et al. (unpublished work, referred to in Appendix A). This vineyard has been tested since 2016 for the presence of grapevine leafroll associated-virus (GLRaV) species (GLRaV-1, GLRaV-3, and GLRaV-3) as well as Rupestris stem pitting-associated virus (GRSPaV) (Girardello et al. unpublished work, referred to in Appendix A) (Agri-Analysis LLC laboratories, Davis, CA). Vines were tested for the presence or absence of GRBV by analyzing petiole samples using qPCR techniques. Twenty-five healthy vines that tested negative for all viruses tested including GRBV (RB(-)) and twenty-five symptomatic vines that tested positive for only GRBV (RB(+)) were selected for the current study. Five biological replicates of five vines each were randomly assigned for sampling for RNA extraction. Samples were collected for transcriptomic analysis at four different phenological stages to track the metabolism of the cell wall: pre-veraison which corresponds to green berries (June 29th), veraison when 50% of the berries have begun to develop color and soften (August 13th), post-veraison when 100% of the berries have accumulated color and are soft (September 4th), and harvest when the berries are fully mature referring to commercial harvest (25°Brix for the current study, September 18th). Samples were immediately flash frozen upon arrival and stored at -80°C until analysis.

In addition, samples were collected once the healthy grapes reached 25 and 27°Brix (September 18th and October 4th respectively) to analyze cell wall composition, phenolic content through exhaustive extractions, and for micro-fermentations to emulate phenolic extraction efficiency at harvest relating to winemaking. Two clusters from each vine (50 clusters per disease status) were randomly selected, removed, and pooled together for each treatment at each collection point. Samples for cell wall analysis and phenolic content were stored at -20°C until analysis, whereas microfermentations were immediately performed (Section 4.3.6).

4.3.2 Total RNA isolation

From the four different phenological time points, two berries from each vine for a total of ten berries was combined and a total of 2.00g of grape material was used for RNA extraction (n=5). Grape material was then homogenized with 9mL of a guanidine thiocyanate lysate buffer (4M guanidine thiocyanate, 0.2M sodium acetate, 26mM EDTA, and 2.6% (w/v) PVP-40) to extract total RNA. A Qiagen RNeasy Plant Mini Kit in conjunction with the Qiagen PowerClean Pro Cleanup kit was used to further isolate the total RNA. To 1000ng of each sample, 5µl NEB DNase reaction buffer (10X), 0.5µl of NEB DNaseI, and up to a final volume of 50µl of RNase-free water was mixed. Samples were incubated at 37°C for 10 minutes and then cleaned with 1.6X (80µl) Beckman-Coulter RNAClean XP Beads at room temperature for 10 minutes. The samples were washed twice with 200µl of 80% ethanol, dried and eluted with 30µl of RNase-free water. Sample integrity and quantity was checked with the Labchip GX RNA HIT assay.

4.3.3 Library preparation and RNA sequencing

Library preparation and gene expression profiling was carried out using a 3' Tag-RNA-Seq protocol as described in Rumbaugh et al (2021). The libraries were sequenced in one lane on a HiSeq 4000 sequencer (Illumina, San Diego, CA). The sequencing was carried out by the DNA Technologies and Expression Analysis Core at the UC Davis Genome Center, supported by NIH Shared Instrumentation Grant 1S10OD010786-01.

4.3.4 Cell wall material preparation and analysis

Cell wall material (CWM) was prepared similar to that of CWM5 in Medina et al. [11] based on a modified method from Vidal et al. [22]. Total cell wall material isolated per disease status and collection point was weighed (n=1). Cellulose, non-cellulosic glucose, soluble polysaccharides, uronic acid (expressed as galacturonic acid equivalents), protein (expressed as bovine serum albumin equivalents), total phenolic content (TPC, expressed as gallic acid equivalents), soluble protein, and total soluble solids (TPP) were all measured as in Medina et al. [11].

4.3.5 Grape phenolic content

Exhaustive extractions to determine phenolic content in grape material was performed as in Girardello et al. [7]. Briefly, five sets of 15 berries were randomly selected from each collection point and disease status and homogenized in a solution of 1:1 ethanol:water, 0.1% hydrochloric acid (HCl) and 0.1% ascorbic acid (1mL/0.1g of tissue) for 3 min with a IKA ULTRA-TURRAXT18 basic homogenizer (IKA Works, Inc., NC, USA). After an overnight extraction (14hrs) at 4°C, the samples were centrifuged at 3200g at 4°C for 15min, the supernatant was

collected and stored at −20°C. The grape material was sequentially extracted with a solution of 70:30 acetone:water and 0.1% ascorbic acid at the same ratio, overnight at 4°C. After centrifugation, supernatant fractions were separately concentrated under reduced pressure at 35°C and quantitatively transferred to a 10mL and 5mL volumetric flask respectively with 50% methanol (0.1% HCl). Each fraction was analyzed separately, and values were combined after analysis.

4.3.6 Microfermentations

Micro-ferments were performed in Bodum coffee plungers as described in Sparrow and Smart [23]. Titratable acidity (TA) was adjusted to 6g/L and yeast assimilable nitrogen (YAN) was adjusted to 250mg/L. Micro-ferments were inoculated with 1 g/gallon of EC1118 yeast and fermented at 25 ± 1°C. Fermented wines were pressed after eight days, stored at 4°C for 14 days, racked with an addition of 80 mg/L of SO_2, and stored at 4°C until phenolic analysis.

4.3.7 HPLC-DAD analysis

Both grape phenolic extractions and microfermentations were analyzed for their phenolic content using HPLC-DAD as in Girardello et al. [7] based on a method from Peng et al. [24]. All phenolic concentrations are calculated based on calibration curves described in Girardello et al. [7]. For grape berry extractions, units are expressed as mg/berry or mg/g of berry, and microfermentations are expressed as mg/L.

4.3.8 Statistical Analysis

Statistical analysis was conducted in the R language (R, version 3.6.1). For cell wall composition and phenolic analysis, a one-way ANOVA was used to determine significance between RB(+) and RB(-) samples at an α of 0.05. A box and whiskers plot was used for visualization for cell wall components. Genes with fewer than ten counts per million reads in all samples were filtered prior to analysis. Differential expression (DE) analysis was conducted using the package limma-voom in R for all filtered genes. Only significant ($p<0.01$) DEGs were used to create the heatmap in Table 4.1.

Table 4.1. Genes significantly altered by GRBV infection from the phenylpropanoid metabolic pathways, hexose transporters, pathogenesis related proteins, and cell wall metabolism *n*=5. Functional annotations, gene accession numbers, and NCBI IDs are provided. All reported fold changes correspond to significant up- (gold) or down-regulation (purple) (p<0.01).

Gene	NCBI ID	Functional Annotation	PV	V	POV	H
VIT_06s0061g00450	100267198	4-coumarate-CoA ligase (4CL)[a]				**0.45**
VIT_11s0052g01090	100254698	4-coumarate-CoA ligase (4CL)[a]				**-0.92**
VIT_12s0035g02070	100245372	Cinnamoyl-CoA reductase (CCR)[a]				**0.75**
VIT_14s0066g01150	100262839	Cinnamoyl-CoA reductase (CCR)[a]		**-1.17**		
VIT_08s0040g00780	100263633	p-Coumaroyl shikimate 3'-hydroxylase isoform[a]				**-1.28**
VIT_15s0048g01000	100264323	Dihydroflavanol 4-reductase (DFR)[a]	**0.44**			**0.84**
VIT_12s0034g00130	100242982	UDP-glucose:anthocyanin 3-O-D-glucosyltransferase (UF3GT)[a]			**1.05**	**-0.91**
VIT_12s0055g00290	100255538	UDP-glucose:anthocyanin 3-O-D-glucosyltransferase (UF3GT)[a]		**-0.34**		
VIT_13s0067g02870	100255217	Chalcone isomerase (CHI)[b]		**0.33**	**0.61**	**0.52**
VIT_01s0011g03110	100257723	MYB family transcription factor EFM[c]	**-0.70**			**0.81**
VIT_08s0007g07230	100233122	MYB transcription factor (MYBCS1)[c]		**-0.36**	**-0.74**	
VIT_00s0181g00010	100233083	Hexose transporter (HT1)[d]			**1.33**	**2.20**
VIT_18s0001g05570	100232961	Hexose transporter (HT2)[d]				**1.13**
VIT_11s0149g00050	100232971	Hexose transporter (HT3)[d]				**0.68**
VIT_18s0122g00850	100232977	Hexose transporter (HT6)[c]				**0.49**
VIT_11s0016g03400	100262713	Putative hexose transporter (HT13)[b]				**0.94**
VIT_05s0077g01580	100249884	Pathogenesis-related protein (PR10.2)[c]				**0.92**
VIT_03s0088g00810	100258414	Pathogenesis-related protein (PR1)[c]	**1.95**			
VIT_14s0081g00030	100255405	Pathgenesis related protein PR-4[c]				**1.06**
VIT_06s0004g08190	100246641	Pathogenesis-related genes transcriptional activator PTI6[c]				**0.79**
VIT_01s0011g05110	100232890	Ripening-related protein-like[c]	**0.88**		**-1.33**	**-0.82**
VIT_01s0011g05140	100245649	MLP-like protein 43[c]	**0.76**		**-1.08**	
VIT_04s0023g03540	100264253	Thaumatin-like protein 1b[c]				**2.02**
VIT_03s0038g02170	100265907	Thaumatin-like protein 1b[c]		**-0.61**		**1.85**
VIT_18s0001g14480	100257373	Thaumatin-like protein 1b[c]		**-0.47**		
VIT_04s0023g03550	100247111	Thaumatin-like protein 1b[c]				**2.02**
VIT_17s0000g02470	100261232	Thaumatin-like protein[c]	**0.47**			
VIT_18s0001g01130	100245385	Expansin (Exp1)[e]		**-0.44**		**0.69**
VIT_13s0067g02930	100244917	Expansin (Exp2)[e]				**1.35**
VIT_01s0026g02620	100260158	Expansin[b]				**1.56**
VIT_14s0108g01020	100244103	Expansin[b]	**1.82**		**1.43**	
VIT_17s0053g00990	100261426	Expansin[b]				**1.82**

Phenylpropanoid Pathway

Hexose transporters

Pathogenesis-related protein synthesis

Cell wall metabolism

3

NS

-3

Gene	NCBI ID	Functional Annotation	PV	V	POV	H
VIT_17s0000g09800	NA	Pectate lyase (PL)[e]				2.48
VIT_01s0137g00240	100242302	Pectate lyase[b]	1.12			2.54
VIT_16s0039g00260	100247757	Pectate lyase[b]				2.74
VIT_13s0019g04910	100246124	Pectate lyase[b]			0.90	2.12
VIT_05s0051g00590	100232902	Pectate lyase[b]				2.46
VIT_08s0040g02740	100255011	Pectate lyase[b]			0.47	0.66
VIT_16s0050g00570	100247339	Pectin acetylesterase[b]				1.27
VIT_14s0060g00230	100264849	Pectin acetylesterase[b]			-0.92	-0.83
VIT_13s0047g00230	100262623	Pectinesterase[b]				2.31
VIT_10s0116g00590	100253692	Pectinesterase[b]		1.12		
VIT_11s0016g00300	NA	Pectinesterase[b]		1.01		
VIT_09s0002g00320	100251413	Pectinesterase[c]			-2.66	
VIT_07s0005g00730	100245304	Pectinesterase[c]		0.44		0.65
VIT_12s0035g01900	100233113	Pectin methylesterase (PME)[e]	0.39			0.44
VIT_11s0016g00590	100267888	PME inhibitor[a]				0.99
VIT_15s0021g00540	100251390	PME inhibitor[a]			0.83	
VIT_16s0022g00960	100232884	PME inhibitor[a]	0.49			
VIT_16s0022g00870	100260301	PME inhibitor[b]	0.40			
VIT_00s0323g00050	100253894	PME inhibitor[b]	-0.97			
VIT_00s0323g00060	100248802	PME inhibitor[b]	-0.69			
VIT_00s0340g00050	100257176	Endoglucanase[b]				-1.42
VIT_02s0025g01380	100259874	Endoglucanase[b]				1.98
VIT_07s0005g00740	100232904	Endoglucanase[b]				2.59
VIT_18s0001g14040	100262603	Endoglucanase[b]			-0.86	
VIT_01s0011g06250	100266368	Xyloglucan endotransglucosylase/hydrolase[b]				0.74
VIT_11s0052g01280	100241056	Xyloglucan endotransglucosylase/hydrolase[b]	1.15			
VIT_11s0052g01250	100256457	Xyloglucan endotransglucosylase/hydrolase[b]		-0.85		
VIT_11s0052g01220	100241119	Xyloglucan endotransglucosylase/hydrolase[b]	1.45			
VIT_01s0150g00460	100232906	Xyloglucan endotransglucosylase/hydrolase[b]			-0.77	
VIT_07s0005g04420	100854532	Exostosin domain-containing protein[b]				-0.89
VIT_16s0022g02080	100263561	Exostosin domain-containing protein[b]				-2.00
VIT_13s0064g00890	100256811	Cellulose Synthase[b]				-0.28
VIT_18s0072g00370	100255463	Cellulose Synthase[b]			0.67	-0.40
VIT_18s0122g00120	100242715	Cellulose Synthase[b]				-0.77

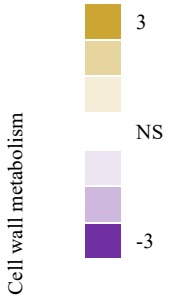

Abbreviations in paratheses indicate gene name. NS= not significant (p< 0.01), PV= Pre-veraison, V= Veraison, POV= Post-veraison, H= Harvest, purple indicates dowregulated gene, yellow indicates upregulated gene, degree of coloring indicates degree of log fold change. Functional annotations came from the following sources: [a]= Blanco-Ulate et al. 2017, [b]= UniProt (https://www.uniprot.org), [c]= NCBI Gene Bank (https://www.ncbi.nlm.nih.gov/gene), [d]= Hayes et al. 2007, [e]= Schlosser et al. 2008

4.4 Results:

4.4.1 GRBV alters cell wall metabolism in grapes

Differentially expressed genes (DEGs) between RB(+) and RB(-) grapes were determined and the log fold changes of significant ($p<0.01$) DEGs are displayed in Table 4.1. Transcripts involved with cell wall degradation during ripening were mainly significantly upregulated in GRBV infected fruit at harvest. The most considerable upregulation involved four expansin transcripts (VIT_18s0001g01130, VIT_13s0067g02930, VIT_01s0026g02620, and VIT_17s0053g00990) and six pectate lyase (PL) transcripts (VIT_17s0000g09800, VIT_01s0137g00240, VIT_16s0039g00260, VIT_13s0019g04910, VIT_05s0051g00590, and VIT_08s0040g02740). Other transcripts included one pectin acetylesterase (VIT_16s0050g00570), two pectinesterases (VIT_13s0047g00230 and VIT_07s0005g00730), one pectin methylesterase (PME) (VIT_12s0035g01900), two endoglucanases (VIT_02s0025g01380 and VIT_07s0005g00740), and one xyloglucan endotransglucosylase/hydrolase transcripts (VIT_01s0011g06250). In addition, PME inhibitors were moderately induced at pre-veraison, post-veraison, and harvest; however, two of these transcripts were also suppressed at pre-veraison. Synchronous downregulation to cell wall biogenesis transcripts occurred at harvest, most notably in two exotosin protein transcripts (VIT_07s0005g04420 and VIT_16s0022g02080) and three cellulose synthase transcripts (VIT_13s0064g00890, VIT_18s0072g00370, and VIT_18s0122g00120).

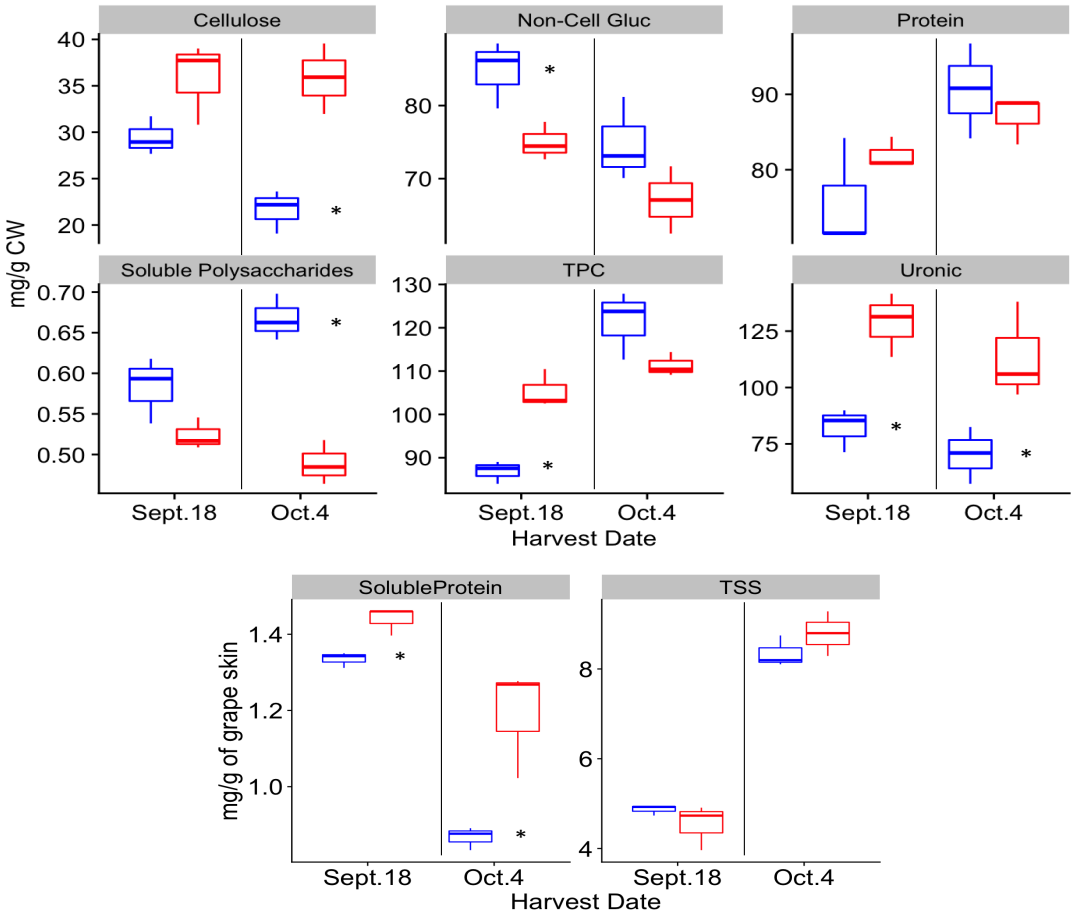

Figure 4.1. Cell wall composition of healthy and diseased grapes collected at 25 and 27°Brix from Paso Robles (n=3). Asterisks indicate a significant difference between disease status at each harvest after applying a one-way ANOVA ($p < 0.05$). Healthy grapes are shown in blue and diseased grapes are shown in red. CW= cell wall, Non-Cell Gluc= non cellulose glucose, TPC= total phenolic content, and TSS= total soluble solids.

Even though cell wall degradation processes were enriched for RB(+) grapes on Sept. 18th (25°Brix), these alterations were not seen in the grape cell wall material between Sept. 18th (25°Brix) and Oct. 4th (27°Brix) (Figure 4.1). Between the two harvest points, cellulose and polysaccharide content was not significantly different for RB(+) grapes, and non-cellulosic glucose was moderately lower for RB(+) grapes (Table S4.1). For RB(-) grapes, cellulose and non-cellulosic glucose content decreased, with significant increases in soluble polysaccharides indicating typical solubilization of the grape skin cell wall (Figure 4.1). Both RB(-) and RB(+) grapes decreased in the total mass of isolated CWM between harvest dates suggesting

solubilization and degradation of the cell wall, yet RB(+) grapes were higher than RB(-) grapes at both collection points (Figure 4.2). Total isolated CWM for RB(+) grapes was 139.3g and 103.03g, whereas 125.95g and 84.75g of CWM were isolated for RB(-) grapes at 25°Brix and 27°Brix, respectively.

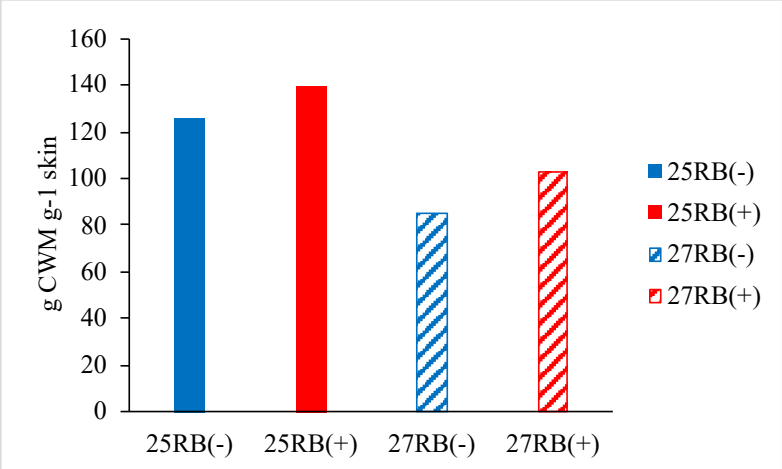

Figure 4.2. Amount of cell wall material (CWM) extracted from grape skins at 25 and 27°Brix from Paso Robles (*n*=1). Blue indicates healthy grapes and red indicates diseased grapes. 25= 25°Brix, 27= 27°Brix, RB(-)= healthy grapes, RB(+)= GRBV infected grapes, and CWM= cell wall material.

Cell wall protein was not significantly different between RB(-) and RB(+) grapes at either ripeness level, whereas TPC was significantly lower in RB(-) grapes compared to RB(+) on Sept. 18th. This was observed by Oct. 4th indicating that RB(-) grapes incorporated more phenolics into the cell wall than RB(+) between the two harvest points. Interestingly, pectin, measured as uronic acid, was significantly higher in RB(+) grapes at both ripeness points, which may be explained by the induction of PME inhibitors at post-veraison and harvest.

4.4.2 GRBV induces the production of pathogenesis related proteins

GRBV induced the transcription of four genes associated with pathogenesis-related (PR) protein synthesis at pre-veraison (VIT_03s0088g00810, VIT_01s0011g05110,

VIT_01s0011g05140, and VIT_17s0000g02470) with moderate suppression of four genes (VIT_01s0011g05110, VIT_01s0011g05140, VIT_03s0038g02170, and VIT_18s0001g14480) at veraison and post-veraison (Table 4.1). Following, six genes (VIT_05s0077g01580, VIT_14s0081g00030, VIT_06s0004g08190, VIT_04s0023g03540, VIT_03s0038g02170, VIT_04s0023g03550) were induced at harvest (Sept. 18th) in RB(+) grapes. This included three thaumatin-like proteins. These findings correlate with significantly higher amounts of soluble proteins observed in GRBV infected grapes on Sept. 18th and Oct. 4th (Figure 4.1). Soluble proteins are measured

Table 4.2. Phenolic profile of healthy and diseased grapes collected at 25 and 27°Brix from Paso Robles in content (ug/berry) and concentration (ug/g of berry) (n=5). Difference in lettering indicates a significant difference across disease status and ripeness level for each parameter after applying Tukey's HSD test ($p < 0.05$).

ug/berry	Gallic Acid	Polymeric Phenols	Flavan-3-ols	HA	Flavonols	Polymeric Pigments	Total Anth glucoside	Total Anth acetyl	Total Anth p-coumaryl	Total ANTH
RB(-) 25	8.22 c	2285.66 b	487.82 a	36.52 a	101.64 a	12.79 b	872.36 a	196.11 a	185.69 a	1254.16 a
RB(+) 25	10.82 b	2028.07 b	659.64 a	48.2 a	77.11 a	11.61 b	613.89 b	183.85 a	195.33 a	993.07 a
RB(-) 27	12.41 ab	4890.28 a	495.23 a	39.28 ab	83.84 a	25.1 a	635.91 ab	147.35 a	174.36 ab	957.61 a
RB(+) 27	14.3 a	4942.27 a	639.52 a	31.02 b	89.06 a	23.46 a	323.59 c	81.11 b	111.86 b	516.56 b
ug/g berry	**Gallic Acid**	**Polymeric Phenols**	**Flavan-3-ols**	**HA**	**Flavonols**	**Polymeric Pigments**	**Total Anth glucoside**	**Total Anth acetyl**	**Total Anth p-coumaryl**	**Total ANTH**
RB(-) 25	7.5±0.69 c	2081.64 b	445.77 a	33.32 a	92.81 a	11.63 b	795.10 a	179.69 a	169.24 a	1144.03 a
RB(+) 25	9.04±0.58 c	1699.56 b	549.46 a	39.85 a	64.17 b	9.72 b	511.31 bc	153.05 a	162.73 ab	827.1 a
RB(-) 27	11.2±1.38 b	4413.04 a	445.44 a	35.32 a	75.07 ab	22.69 a	575.46 ab	133.47 a	157.78 ab	866.7 a
RB(+) 27	13.62±1.57 a	4699.01 a	609.18 a	29.49 a	84.28 ab	22.26 a	305.91 c	76.64 b	105.73 b	488.27 b

RB= red blotch, (+)= positive, (-)= negative, 25= 25°Brix, 27= 27°Brix, HA= hydroxycinnamic acids, and Anth=anthocyanins.

Table 4.3. Phenolic profile of microfermentations made from healthy and diseased grapes collected at 25 and 27°Brix from Paso Robles (n=3). Difference in lettering indicates a significant difference across disease status and ripeness level for each parameter after applying Tukey's HSD test ($p < 0.05$).

mg/L	Gallic Acid	Polymeric Phenols	Flavan-3-ols	HA	Flavonols	Polymeric Pigments	Total Anth. glucoside	Total Anth acetyl	Total Anth. p-coumaryl	Total Anth.
25RB(-)	11.26 bc	158.11 ab	72.39 c	33.41 a	55.64 ab	294.17 b	126.46 a	11.98 a	53.46 b	474.1 ab
25RB(+)	13.02 a	137.05 b	96.92 ab	24.97 a	24.97 c	142.95 c	67.41 b	9.80 a	26.96 c	237.31 c
27RB(-)	9.85 c	181.35 ab	78.76 bc	42.87 a	61.26 a	362.61 a	127.27 a	13.89 a	71.59 a	561.47 a
27RB(+)	12.96 ab	191.86 a	111.66 a	38.33 a	49.88 b	268.41 b	113.83 a	13.5 a	64.56 ab	446.8 b

RB= red blotch, (+)= positive, (-)= negative, 25= 25°Brix, 27= 27°Brix, HA= hydroxycinnamic acids, and Anth=anthocyanins.

4.4.3 GRBV decreases phenolic extractability

Table 4.2 and 4.3 show flavonoid concentrations in both grape extracts and microfermentatsions, respectively. Similar trends were observed between phenolic content (μg/berry) and phenolic concentrations (μg/g berry). RB(+) and RB(-) grape extract phenolic concentrations, besides anthocyanins, were statistically similar at the second harvest point which was not observed at the first harvest point (Table 4.2). The same trend was not observed in the microfermentations (Table 4.3). In general, at both harvest dates, there were significant differences between RB(+) and RB(-) wines. Overall, there were significantly higher levels of gallic acid and total flavan-3-ols with significantly lower total flavonols, lower polymeric pigments and total anthocyanins in RB(+) wines compared to RB(-) wines. This shows the discrepancy between phenolic availability and phenolic extractability between healthy and diseased grapes.

Figure 4.3 and 4.4 compares the difference in phenolic availability in the grape to the microfermentations which simulated phenolic extractability under winemaking conditions. Anthocyanin concentrations present in whole berry extractions did not reflect the extractability of anthocyanins during winemaking (Figure 4.3). Even though, for whole berry extractions anthocyanin concentrations at the first harvest (25°Brix) point were higher than the second collection point, irrespective of disease status, the opposite was true for microfermentations. This indicates that the maximum extractability of anthocyanins is not primarily a factor of the total anthocyanin concentrations available in the berry, but also the ripeness stage of the berry.

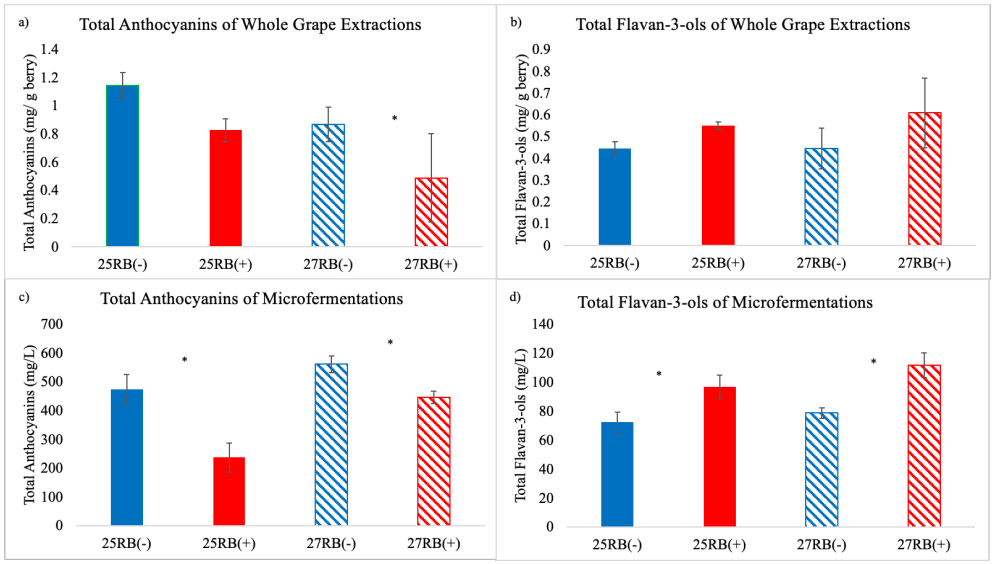

Figure 4.3. Total anthocyanin and total flavan-3-ol concentrations in whole berry extractions and microfermentations of data vine grapes collected at 25 and 27°Brix from Paso Robles in 2019. For whole berry extractions *n*=5 and for microfermentations *n*=3. Asterisks indicate a significant difference between disease status at each harvest after applying a one-way ANOVA ($p < 0.05$). Healthy grapes are shown in blue and diseased grapes are shown in red. The first harvest (Sept. 18th) is shown in solid bars and the second harvest (Oct. 4th) is shown in dashed bars. Total anthocyanins= sum of monomeric anthocyanin glucosides, acetylglucosides, and p-coumaroyl glucosides (Table 4.2 and 4.3), total flavan-3-ols= sum of catechin, B1, epicatechin, B2, and epicatgallate (Table 4.2 and 4.3), 25= 25°Brix, 27= 27°Brix, RB(-)= healthy grapes, RB(+)= GRBV infected grapes.

Figure 4.4. Total polymeric pigments and total polymeric phenols concentrations in whole berry extractions and

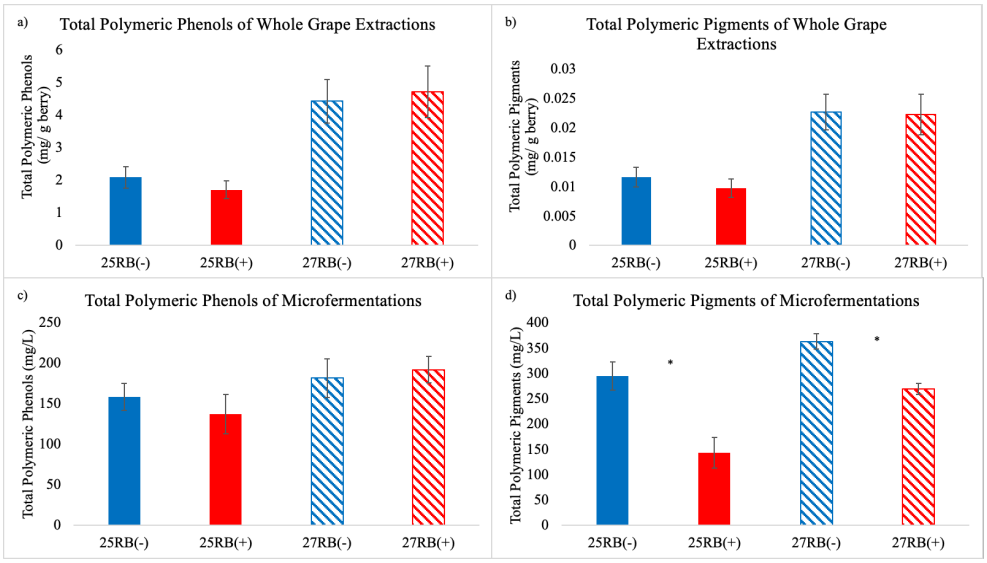

microfermentations of data vines grapes collected at 25 and 27°Brix from Paso Robles in 2019. For whole berry extractions *n*=5 and for microfermentations *n*=3. Asterisks indicate a significant difference between disease status at each harvest after applying a one-way ANOVA ($p < 0.05$). Healthy grapes are shown in blue and diseased grapes are shown in red. The first harvest (Sept. 18th) is shown in solid bars and the second harvest (Oct. 4th) is shown in dashed bars. 25= 25°Brix, 27= 27°Brix, RB(-)= healthy grapes, RB(+)= GRBV infected grapes.

In general anthocyanin concentrations were significantly lower in RB(+) compared to RB(-) grapes and microfermentations. In contrast, flavan-3-ol concentrations were significantly higher in RB(+) compared to RB(-) microfermentations at both harvest dates (Figure 4.3). In general, polymeric phenol concentrations between microfermentations and grape extracts followed similar trends, where significantly higher concentrations were observed at the second harvest compared to the first harvest, irrespective of disease status. However, in the case of polymeric pigments a significant decrease were observed in RB(+) compared to RB(-) wines at each harvest date even though grape extract concentrations were similar between disease status (Figure 4.4). This also seemed to occur with flavonol concentrations (Table 4.2 and 4.3). This indicates that there is either a decrease in extraction of polymeric pigments from RB(+) grapes or there is a potential loss of polymeric pigments during winemaking of RB(+) grapes.

4.5 Discussion:

In addition to sugar and organic acids, cell wall integrity and composition are important factors when choosing when to harvest grapes for winemaking (Gao et al. 2019). Overall ripening events are affected by pathogen invasion which alter the cell wall metabolism in ripening fruits. In order to overcome the cell wall barrier, pathogens alter the plant cell wall metabolism to convert the polysaccharides into substrates utilized for energy and nutrition [25]. As a defense response, plants can overexpress certain key enzymes to hinder the pathogenicity. The overexpression of pectin methylesterase inhibiting (PMEI) genes in *Arabidopsis* was found to decrease susceptibility to infection by *Botrytis* by enhancing the pectin methyl esterification [25]. In the current study, the impact of GRBV on grape cell wall metabolism was studied as it can ultimately affect grape phenolic extraction during winemaking.

Research indicates that the amount of isolated CWM in fruit is cultivar dependent. Studies regarding the isolation of CWM from strawberries reported that the firmest cultivars had the highest amount of isolated CWM per gram of skin [26]. Furthermore, significantly more CWM was isolated from Monastrell grapes than Merlot, Cabernet Sauvignon, and Syrah grape cultivars [15]. In the latter study this was linked to an increase in skin cell layers. The current study did not include microscopy of the collected grapes; therefore, it is unknown whether this increase in CWM in GRBV infected grapes is due to an increase in the skin cell layers, as a result of a delay in the degradation of the cell walls, or due to differences in skin cell volume and cell wall thickness. However, since grape skin cell wall material is known to decrease through ripening, it could be related to the delay in ripening effects [15,27].

Cellulose is the major component of plant cell walls and is synthesized through cellulose synthase enzymes, while cellulases and endoglucanases are responsible for its degradation, the latter playing a role in secondary cell wall development [28,29]. Concentrations of cellulose in grape skin cell walls vary inconsistently through ripening, depending on season and variety [15,30]. In the current study, induction of two endoglucanases with simultaneous suppression of cellulose synthase at harvest suggests degradation of the cell wall due to GRBV infection. However, cellulose concentrations of RB(+) grapes did not alter between Sept. 18th and Oct. 4th, possibly suggesting a post-transcriptional regulation for these enzymes. In fact, cellulose concentrations were higher in RB(+) grapes compared to RB(-) grapes which could explain the higher amount of isolated cell wall material in RB(+) grapes. Another explanation could be that the two week between harvest points did not provide enough time for transcriptional regulation to translate into alterations in cell wall composition.

In our study, non-cellulosic glucose accounts for the glucose derived from primarily hemicellulose. Hemicellulose is comprised of glucose, mannose, galactose, xylose and arabinose. Non-cellulosic glucose concentrations decreased between the two harvest points, regardless of disease status, but were generally lower in RB(+) grapes than healthy grapes. This could suggest an alteration in the synthesis of the grape skin cell wall, decreasing the amount of glucose in the hemicellulose. Enrichment at harvest of transcripts encoding two mannosidase enzymes suggest a breakdown of mannan in the hemicellulose of RB(+) grapes. In addition, the overexpression of expansin related genes at harvest would further suggest cell wall degradation since these enzymes have been repeatedly associated with fruit softening [31]. However, cell wall monosaccharides and the differences in the enzymatic activity related to cell wall metabolism were not measured in this study. With normal degradation and solubilization of the cell wall, soluble polysaccharides are known to increase with advanced ripening stages in grapes [15,27,30,32,33]. Our study indicated that soluble polysaccharides are higher in RB(-) than RB(+) grapes which was significant at the second harvest. This may indicate that RB(-) grape skin cell walls were going through normal ripening events; whereas RB(+) grapes cell walls were delayed in the solubilization of the polysaccharides that are incorporated into the cell wall.

On the other hand, grape cell wall phenolic concentrations in grapes strongly increase after veraison and then decrease towards harvest [15,30,32,34]. In addition, high concentrations of cell wall polyphenols have been positively correlated to anthocyanin extraction [32,33]. In the current study, we observed an increase in TPC between the two ripeness levels for RB(-), with little change occurring in RB(+) grape skin cell walls. However, these higher TPC levels in the CWM were not correlated with increases in anthocyanin concentrations in the microfermentations. This may be due several factors. First, anthocyanin extractability is negatively correlated with cellulose levels

[30]; therefore, the lower cellulose levels in RB(-) grapes may have led to higher anthocyanin extractability. Second, the higher ethanol concentration in the second harvest wines compared to the first harvest wines may have impacted extractability. Higher ethanol concentration during fermentation causes a loss of the hydrophobic interactions between anthocyanins and cell walls, consequently increasing anthocyanin extractability during winemaking [14].

Research has consistently indicated that pectin (measured as uronic acid) concentrations substantially decrease through ripening in grapes as a result of demethylesterification, depolymerization, and solubilization [15,32,35]. Primarily pectate lyase (PL), pectin methylesterase (PME), pectin esterase, and polygalacturonase (PG) are key enzymes responsible for pectin degradation during ripening. Pectin demethylesterification through PME enzymes allows for the hydrolysis of pectin by PG enzymes. On the other hand, PMEI are expressed in early berry development to regulate PME activity and berry enlargement [36]. A phytoplasma infecting lime trees was reported to induce PME, PMEI, PG, PL and pectinesterase related genes [28], which is in agreement with our findings. Similarly, a study investigating the transcriptome of watermelon infected with *Cucumber green mottle mosaic virus*, determined that pectinesterase and PG related genes were upregulated in diseased fruit [37]. Although the degradation of pectin showed increased transcriptional levels due to GRBV infection, RB(+) grapes at both harvest points were significantly higher in pectin than RB(-) grapes. This potentially could have been caused by induction of PMEI from veraison to harvest (Table 4.1). Three of the same genes in this study (VIT_11s0016g00590, VIT_15s0021g0054, and VIT_16s0022g00960) were also found to be enriched during GRBV infection [38], suggesting transcriptional regulation of pectin degradation during grape ripening resulting in higher levels of pectin in GRBV fruit.

Interestingly, soluble proteins were also significantly higher in RB(+) than RB(-) grapes.

Soluble proteins are known to increase through grape ripening [39,40]. High quantities of pectin and PR proteins (which make up a portion of soluble proteins) have been reported to decrease extractability of phenolics, specifically tannins [13,14,41]. Springer and Sacks [41] found that higher amounts of cell wall pectin and soluble proteins correlated to increased binding of tannins in finished wines. These authors later published work indicating that some of these proteins responsible for retention of tannins were PR proteins (thaumatin-like proteins and chitinases) that can be formed due to abiotic and biotic stressors [42]. In this current study, several genes related to PR proteins were enriched during grape ripening in RB(+) grapes. This indicates that the increase in soluble proteins observed in RB(+) grapes could be derived from the induction of transcripts associated with PR proteins. Although specific PR proteins, such as chitinases and thaumatin-like proteins, were not directly measured, higher amounts of soluble proteins in the grapes could potentially lead to retention of phenolics during winemaking. The RB(+) grapes during fermentation showed to retain polymeric pigments (Figure 4.4) even though concentrations in the RB(+) grape extracts were statistically similar to RB(-) grapes at each ripeness level. Polymeric pigments are formed through the interactions of anthocyanins and tannins [43]. Previous research has indicated that tannins can bind to the cell wall through hydrogen bonding and hydrophobic interactions [44]. Our study indicates that GRBV altered grape skin cell wall pectin levels as well as soluble protein concentrations which potentially lead to hydrophobic interactions with polymeric pigments, or the tannins used in their formation.

4.6 Conclusion:

For the first time, our study evaluated the impact of GRBV on grape cell wall metabolism to determine potential cascading effects during winemaking such as phenolic retention.

Transcriptomic analysis suggested that induction of cell wall degradation processes during GRBV infection is attempting to solubilize the cell wall polysaccharides to support the energy demands of the virus. However, although transcriptional regulation shows to degrade the overall grape cell wall, this did not translate into the measured composition of the grape exocarp. Wines made from GRBV infected fruit contained less polymeric pigments then expected from grape content. This was potentially due to the significantly higher amounts of pectin and soluble proteins in GRBV grape cell walls. To enhance our understanding of these findings, a more in-depth study is needed into the impact of GRBV infection on grape cell wall changes during ripening. Specifically, potential differences in the degree of methylesterification or acylation of the pectin in GRBV fruit should be further investigated. Furthermore, it should be determined whether transcriptional induction of PR protein synthesis led to higher levels of chitinases and thaumatin-like proteins. It will also be interesting to determine the differences in the cell wall composition of the mesocarp versus the exocarp.

4.7 Supplemental Information

Table S4.1. Cell wall composition of healthy and diseased grapes collected at 25 and 27°Brix from Paso Robles. For TSS, soluble proteins, protein, TPC, uronic acid, soluble polysaccharides, non-cellulosic glucose, and cellulose *n*=3. For lipids *n* =2 and for lignin *n*=4. Difference in lettering indicates a significant difference across disease status and ripeness level for each parameter after applying Tukey's HSD test ($p < 0.05$).

Sample	TSS (mg/ g GS)	Soluble Protein (mg/ g GS)	Protein (mg/ g CWM)	TPC (mg/ g CWM)	Lipids (mg/ g CWM)	Uronic Acid (mg/ g CWM)	Lignin (mg/ g CWM)	Soluble Polysaccharides (mg/ g CWM)	Non-Cellulosic Glucose (mg/ g CWM)	Cellulose (mg/ g CWM)
25RB(+)	4.54 b	1.44 a	81.98 ab	105.39 b	39.57 a	128.85 a	466.43 a	0.52 bc	74.96 ab	35.85 a
25RB(-)	4.87 b	1.33 ab	75.77 b	86.86 c	43.17 a	82.19 bc	461.35 a	0.58 b	84.76 a	29.44 ab
27RB(+)	8.79 a	1.19 b	87.02 ab	111.31 ab	30.39 b	113.64 ab	433.53 a	0.49 c	67.08 c	35.82 a
27RB(-)	8.35 a	0.87 c	90.57 a	121.43 a	36.37 ab	70.25 c	489.27 a	0.67 a	74.79 ab	21.63 b

RB= red blotch, (+)= positive, (-)= negative, 25= 25°Brix, 27= 27°Brix, GS= grape skin, CWM= cell wall material, TSS= total soluble solids, and TPC= total phenolic content.

4.8 References:

1. Al Rwahnih, M.; Dave, A.; Anderson, M.M.; Rowhani, A.; Uyemoto, J.K.; Sudarshana, M.R. Association of a DNA Virus with Grapevines Affected by Red Blotch Disease in California. *Phytopathology* **2013**, *103*, 1069–1076.
2. Varsani, A.; Roumagnac, P.; Fuchs, M.; Navas-Castillo, J.; Moriones, E.; Idris, A.; Briddon, R.W.; Rivera-Bustamante, R.; Murilo Zerbini, F.; Martin, D.P. Capulavirus and Grablovirus: two new genera in the family Geminiviridae. *Arch. Virol.* **2017**, *162*, 1819–1831.
3. Vargas-Asencio, J.; Liou, H.; Perry, K.L.; Thompson, J.R. Evidence for the splicing of grablovirus transcripts reveals a putative novel open reading frame. *J. Gen. Virol.* **2019**, *100*, 709–720.
4. Bahder, B.W.; Zalom, F.G.; Jayanth, M.; Sudarshana, M.R. Phylogeny of Geminivirus Coat Protein Sequences and Digital PCR Aid in Identifying Spissistilus festinus as a Vector of Grapevine red blotch-associated virus . *Phytopathology* **2016**, *106*, 1223–1230.
5. Ricketts, K.D.; Gómez, M.I.; Fuchs, M.F.; Martinson, T.E.; Smith, R.J.; Cooper, M.L.; Moyer, M.M.; Wise, A. Mitigating the economic impact of grapevine red blotch: Optimizing disease management strategies in U.S. vineyards. *Am. J. Enol. Vitic.* **2017**, *68*, 127–135.
6. Sudarshana, M.R.; Perry, K.L.; Fuchs, M.F. Grapevine Red Blotch-Associated Virus, an Emerging Threat to the Grapevine Industry Mysore. *Phytopathology* **2015**, 1026–1032.
7. Girardello, R.C.; Cooper, M.L.; Smith, R.J.; Lerno, L.A.; Bruce, R.C.; Eridon, S.; Oberholster, A. Impact of Grapevine Red Blotch Disease on Grape Composition of Vitis vinifera Cabernet Sauvignon, Merlot, and Chardonnay. *J. Agric. Food Chem.* **2019**, *67*, 5496–5511.
8. Martínez-Lüscher, J.; Plank, C.M.; Brillante, L.; Cooper, M.L.; Smith, R.J.; Al-Rwahnih, M.; Yu, R.; Oberholster, A.; Girardello, R.; Kurtural, S.K. Grapevine Red Blotch Virus May Reduce Carbon Translocation Leading to Impaired Grape Berry Ripening. *J. Agric. Food Chem.* **2019**, *67*, 2437–2448.
9. Blanco-Ulate, B.; Hopfer, H.; Figueroa-Balderas, R.; Ye, Z.; Rivero, R.M.; Albacete, A.; Pérez-Alfocea, F.; Koyama, R.; Anderson, M.M.; Smith, R.J.; et al. Red blotch disease alters grape berry development and metabolism by interfering with the transcriptional and hormonal regulation of ripening. *J. Exp. Bot.* **2017**, *68*, 1225–1238.
10. Girardello, R.C.; Cooper, M.L.; Lerno, L.A.; Brenneman, C.; Eridon, S.; Sokolowsky, M.; Heymann, H.; Oberholster, A. Impact of Grapevine Red Blotch Disease on Cabernet Sauvignon and Merlot Wine Composition and Sensory Attributes. *Molecules* **2020**, *25*.
11. Medina-Plaza, C.; Beaver, J.W.; Lerno, L.; Dokoozlian, N.; Ponangi, R.; Blair, T.; Block, D.E.; Oberholster, A. Impact of temperature, ethanol and cell wall material composition on cell wall-anthocyanin interactions. *Molecules* **2019**, *24*, 8–11.
12. Beaver, J.W.; Medina-Plaza, C.; Miller, K.; Dokoozlian, N.; Ponangi, R.; Blair, T.; Block, D.; Oberholster, A. Effects of the Temperature and Ethanol on the Kinetics of Proanthocyanidin Adsorption in Model Wine Systems. *J. Agric. Food Chem.* **2019**.
13. Bindon, K.A.; Bacic, A.; Kennedy, J.A. Tissue-specific and developmental modifications of grape cell walls influence the adsorption of proanthocyanidins. *J. Agric. Food Chem.* **2012**, *60*, 9249–9260.
14. Bindon, K.A.; Madani, S.H.; Pendleton, P.; Smith, P.A.; Kennedy, J.A. Factors affecting skin tannin extractability in ripening grapes. *J. Agric. Food Chem.* **2014**, *62*, 1130–1141.

15. Ortega-Regules, A.; Ros-Garcia, J.M.; Bautista-Ortin, A.B.; Lopez-Roca, J.M.; Gomez-Plaza, E. Changes in skin cell wall composition during the maturation of four premium wine grape varieties. *J. Sci. Food Agric.* **2008**, *88*, 420–428.
16. Nunan, K.J.; Davies, C.; Robinson, S.P.; Fincher, G.B. Expression patterns of cell wall-modifying enzymes during grape berry development. *Planta* **2001**, *214*, 257–264.
17. Nunan, K.J.; Sims, I.M.; Bacic, A.; Robinson, S.P.; Fincher, G.B. Changes in cell wall composition during ripening of grape berries. *Plant Physiol.* **1998**, *118*, 783–792.
18. Le Gall, H.; Philippe, F.; Domon, J.M.; Gillet, F.; Pelloux, J.; Rayon, C. Cell wall metabolism in response to abiotic stress. *Plants* **2015**, *4*, 112–166.
19. Otulak-Kozieł, K.; Kozieł, E.; Lockhart, B.E.L. Plant cell wall dynamics in compatible and incompatible potato response to infection caused by Potato virus Y (PVYNTN). *Int. J. Mol. Sci.* **2018**, *19*.
20. Blanco-Ulate, B.; Morales-Cruz, A.; Amrine, K.C.H.; Labavitch, J.M.; Powell, A.L.T.; Cantu, D. Genome-wide transcriptional profiling of Botrytis cinerea genes targeting plant cell walls during infections of different hosts. *Front. Plant Sci.* **2014**, *5*, 1–16.
21. Rumbaugh, A.; Girardello, R.C.; Cantu, A.; Brenneman, C.; Heymann, H.; Oberholster, A. Mitigating Grapevine Red Blotch Virus Impact on Final Wine Composition. *Beverages* **2021**, *7*.
22. Vidal, S.; Williams, P.; O'Neill, M.A.; Pellerin, P. Polysaccharides from grape berry cell walls. Part I: Tissue distribution and structural characterization of the pectic polysaccharides. *Carbohydr. Polym.* **2001**, *45*, 315–323.
23. Sparrow, A.M.; Smart, R.E.; Dambergs, R.G.; Close, D.C. Skin particle size affects the phenolic attributes of pinot noir wine: Proof of concept. *Am. J. Enol. Vitic.* **2016**, *67*, 29–37.
24. Peng, Z.; Iland, P.G.; Oberholster, A.; Sefton, M.A.; Waters, E.J. Analysis of pigmented polymers in red wine by reverse phase HPLC. *Aust. J. Grape Wine Res.* **2002**, *8*, 70–75.
25. Cantu, D.; Vicente, A.R.; Labavitch, J.M.; Bennett, A.B.; Powell, A.L.T. Strangers in the matrix: plant cell walls and pathogen susceptibility. *Trends Plant Sci.* **2008**, *13*, 610–617.
26. Rosli, H.G.; Civello, P.M.; Martínez, G.A. Changes in cell wall composition of three Fragaria x ananassa cultivars with different softening rate during ripening. *Plant Physiol. Biochem.* **2004**, *42*, 823–831.
27. Ortega-Regules, A.; Romero-Cascales, I.; Ros-García, J.M.; López-Roca, J.M.; Gómez-Plaza, E. A first approach towards the relationship between grape skin cell-wall composition and anthocyanin extractability. *Anal. Chim. Acta* **2006**, *563*, 26–32.
28. Mardi, M.; Karimi Farsad, L.; Gharechahi, J.; Salekdeh, G.H. In-depth transcriptome sequencing of Mexican lime trees infected with Candidatus Phytoplasma aurantifolia. *PLoS One* **2015**, *10*, 1–23.
29. Glass, M.; Barkwill, S.; Unda, F.; Mansfield, S.D. Endo-β-1,4-glucanases impact plant cell wall development by influencing cellulose crystallization. *J. Integr. Plant Biol.* **2015**, *57*, 396–410.
30. Ortega-Regules, A.; Ros-García, J.M.; Bautista-Ortín, A.B.; López-Roca, J.M.; Gómez-Plaza, E. Differences in morphology and composition of skin and pulp cell walls from grapes (Vitis vinifera L.): Technological implications. *Eur. Food Res. Technol.* **2008**, *227*, 223–231.
31. Li, Y.; Jones, L.; McQueen-Mason, S. Expansins and cell growth. *Curr. Opin. Plant Biol.* **2003**, *6*, 603–610.

32. Hernández-Hierro, J.M.; Quijada-Morín, N.; Martínez-Lapuente, L.; Guadalupe, Z.; Ayestarán, B.; Rivas-Gonzalo, J.C.; Escribano-Bailón, M.T. Relationship between skin cell wall composition and anthocyanin extractability of Vitis vinifera L. cv. Tempranillo at different grape ripeness degree. *Food Chem.* **2014**, *146*, 41–47.
33. Apolinar-Valiente, R.; Gómez-Plaza, E.; Terrier, N.; Doco, T.; Ros-García, J.M. The composition of cell walls from grape skin in Vitis vinifera intraspecific hybrids. *J. Sci. Food Agric.* **2017**, *97*, 4029–4035.
34. Delgado, R.; Martín, P.; Del Álamo, M.; González, M.R. Changes in the phenolic composition of grape berries during ripening in relation to vineyard nitrogen and potassium fertilisation rates. *J. Sci. Food Agric.* **2004**, *84*, 623–630.
35. Vicens, A.; Fournand, D.; Williams, P.; Sidhoum, L.; Moutounet, M.; Doco, T. Changes in polysaccharide and protein composition of cell walls in grape berry skin (Cv. Shiraz) during ripening and over-ripening. *J. Agric. Food Chem.* **2009**, *57*, 2955–2960.
36. Lionetti, V.; Raiola, A.; Mattei, B.; Bellincampi, D. The grapevine VvPMEI1 gene encodes a novel functional pectin methylesterase inhibitor associated to grape berry development. *PLoS One* **2015**, *10*, 1–19.
37. Li, X.; An, M.; Xia, Z.; Bai, X.; Wu, Y. Transcriptome analysis of watermelon (Citrullus lanatus) fruits in response to Cucumber green mottle mosaic virus (CGMMV) infection. *Sci. Rep.* **2017**, *7*, 1–12.
38. Blanco-Ulate, B.; Hopfer, H.; Figueroa-Balderas, R.; Ye, Z.; Rivero, R.M.; Albacete, A.; Pérez-Alfocea, F.; Koyama, R.; Anderson, M.M.; Smith, R.J.; et al. Red blotch disease alters grape berry development and metabolism by interfering with the transcriptional and hormonal regulation of ripening. *J. Exp. Bot.* **2017**, *68*, 1225–1238.
39. Pocock, K.F.; Hayasaka, Y.; McCarthy, M.G.; Waters, E.J. Thaumatin-like proteins and chitinases, the haze-forming proteins of wine, accumulate during ripening of grape (Vitis vinifera) berries and drought stress does not affect the final levels per berry at maturity. *J. Agric. Food Chem.* **2000**, *48*, 1637–1643.
40. Tian, B.; Harrison, R.; Morton, J.; Jaspers, M. Changes in pathogenesis-related proteins and phenolics in Vitis vinifera L. cv. 'Sauvignon Blanc' grape skin and pulp during ripening. *Sci. Hortic. (Amsterdam).* **2019**, *243*, 78–83.
41. Springer, L.F.; Sacks, G.L. Protein-precipitable tannin in wines from Vitis vinifera and interspecific hybrid grapes (Vitis ssp.): Differences in concentration, extractability, and cell wall binding. *J. Agric. Food Chem.* **2014**, *62*, 7515–7523.
42. Springer, L.F.; Sherwood, R.W.; Sacks, G.L. Pathogenesis-Related Proteins Limit the Retention of Condensed Tannin Additions to Red Wines. *J. Agric. Food Chem.* **2016**, *64*, 1309–1317.
43. Bindon, K.; Kassara, S.; Hayasaka, Y.; Schulkin, A.; Smith, P. Properties of wine polymeric pigments formed from anthocyanin and tannins differing in size distribution and subunit composition. *J. Agric. Food Chem.* **2014**, *62*, 11582–11593.
44. Le Bourvellec, C.; Guyot, S.; Renard, C.M.G.C. Non-covalent interaction between procyanidins and apple cell wall material: Part I. Effect of some environmental parameters. *Biochim. Biophys. Acta - Gen. Subj.* **2004**, *1672*, 192–202.

CHAPTER 5

Mitigating the Impacts of Grapevine Red Blotch Virus on Cabernet Sauvignon Final Wine Composition

Formatted for publication in *Beverages* (accepted)

5.1 Abstract:

Grapevine red blotch virus (GRBV), the causative agent of red blotch disease, causes significant decreases in sugar and anthocyanin accumulation in grapes, suggesting a delay in ripening events. Two mitigation strategies were investigated to alleviate the impact of GRBV on wine composition. Wines were made from Cabernet Sauvignon (CS) (*Vitis vinifera)* grapevines, grafted onto 110R and 420A rootstocks, in 2016 and 2017. A delayed harvest and chaptalization of diseased grapes were employed to decrease chemical and sensory impacts on wines caused by GRBV. Extending the ripening of the diseased fruit produced wines that were overall higher in aroma compounds such as esters and terpenes and alcohol-related (hot and alcohol) sensory attributes compared to wines made from diseased fruit harvested at the same time as healthy fruit. In 2016 only, a longer hangtime of GRBV infected fruit resulted in wines with increased anthocyanin concentrations compared to wines made from GRBV diseased fruit that was harvested at the same time as healthy fruit. Chaptalization of the diseased grapes in 2017 produced wines chemically more similar to wines made from healthy fruit. However, this was not supported by sensory analysis, potentially due to high alcohol content masking aroma characteristics.

5.2 Introduction:

Grapevines (*Vitis* spp.) are among the most widely grown fruit crops globally, with the United States being one of the top grape-growing and wine-producing countries. Like many other crops, pathogens threaten the economic status of grapevines by lowering yields or decreasing the quality of the grapes and the resulting wines. Currently, with over 70 viruses identified, grapevines contain the highest number of pathogens to infect a single crop [1]. In 2012, a new circular, single-stranded DNA virus was identified in grapevines and is currently known as grapevine red blotch virus (GRBV) [2,3].

GRBV has been identified in the United States, Canada, Switzerland, South Korea, Mexico, India, and Argentina [4–10] and is known to infect white and red wine grape cultivars and table and raisin grapes, and it is interspecific of hybrids and rootstocks. GRBV is the causative agent of grapevine red blotch disease (GRBD) [11], with foliar symptoms consisting of red blotches on leaf blades and margins and reddening of the primary, secondary, and tertiary veins in red grape cultivars [12–14]. GRBV causes increases in sugar and anthocyanin concentrations in leaves of red grape cultivars, with consistent decreases of both in the grape berry [14–16]. The impact of GRBV on the secondary metabolites in grapes is variable and dependent on genotypic and environmental factors [14,17]. However, little research has been done on the impact of GRBV on the final wine composition and quality.

Previous studies observed that GRBD causes a delay in grape maturation and can potentially impact the final wine quality, producing wines with lower ethanol, phenolic, and aroma content. Research indicated that a trained sensory panel was able to differentiate between wines made from GRBV infected fruit and wines made from healthy fruit, which was driven by differences in alcohol and mouthfeel attributes [18]. Recently, a study indicated that the low

inclusion of GRBD fruit during winemaking still impacted the chemical and sensorial parameters of the final wine [19]. However, no mitigation strategies have been investigated to alleviate the effects of GRBV on final wine composition.

It is well known that when the grape berry has reached full maturation, flow from the phloem decreases, slowing down the transport of water and solutes from leaves to the berry [20]. Therefore, extending ripening past the typical ripening point of grapes correlates to decreases in metabolite biosynthesis in the berry [21]. Instead, metabolites, such as sugars and phenolics, begin to concentrate in the berry through transpiration [20,22,23]. Although research has indicated that a longer hangtime can increase phenolic concentration in the berry through dehydration [24], other studies have demonstrated a decrease in anthocyanin levels in overripe berries due to degradation [25]. However, the maximum level of anthocyanins in the grape did not correlate with maximum extractability in the final wines, where a longer hangtime resulted in greater anthocyanin extractability during winemaking [25]. Additionally, fruit maturity impacts volatile accumulation in grapes such as terpenes and esters [26–28]. Bindon et al. investigated the relationship between fruit maturity, wine composition, and sensory characteristics. They found that later harvested fruit correlated to dark fruit attributes, whereas earlier picked fruit correlated with vegetative characteristics [29].

Phenolic extraction during fermentation is also impacted by ethanol production [30]. In general, higher ethanol concentrations during fermentation increase phenolic content in final wines [31,32], which have been correlated to higher sensory quality scores by wine judges [33]. However, additional studies have indicated that higher ethanol concentrations during fermentation do not increase the extraction of monomeric phenolics but increase polymerization and produce darker wines that are perceived by a sensory panel [34]. This study indicated that wine alcohol

content is positively correlated to fruity characteristics in final wines and negatively correlated to green or vegetal aromas [28,34].

As previous research has shown that GRBV has led to delay ripening events in grapes, resulting in wines with lower ethanol content and phenolic concentrations, the current study investigated two mitigation strategies to reduce the impact of GRBV on resulting wine quality. In 2016 and 2017, diseased fruit was harvested first when the healthy fruit reached 25 °Brix, and a second time once the diseased fruit reached 25 °Brix. Additionally, in 2017, a sub-portion of the first harvested diseased fruit was also chaptalized to match the sugar content of healthy fruit must. Both mitigation strategies increase the sugar content of grape musts, consequently increasing the ethanol content of final wines. Therefore, it is hypothesized that the two mitigation strategies employed in this project will result in a wine made from diseased fruit being chemically and sensorially similar to a wine made from healthy fruit.

5.3 Methods and Materials:

5.3.1 Grape harvest and winemaking

Cabernet Sauvignon (*Vitis vinifera)*, grafted onto 110R and 420A rootstocks, grapevines were used for this investigation, from Oakville Experimental Station (Napa County, CA, USA). Details of the vineyard and viticultural practices were previously described in Rumbaugh et al. [17] and Martínez-Lüscher et al. [15]. GRBV symptoms in this vineyard block were monitored for several years prior to this study. A 100% correlation between qPCR testing for GRBV and symptoms in grapevines was shown. Due to the number of vines needed for winemaking, only a subset of vines was retested for GRBV [17]. At harvest, 240 symptomatic (RB(+)) vines and 120 asymptomatic (RB(–)) vines were harvested simultaneously once RB(–) reached 25 °Brix. In

addition, a second harvest of diseased fruit (RB(+) 2H) was performed once they reached 25 °Brix. In general, this harvest occurred one to two weeks after the first harvest (Table 5.1). However, the second harvest of CS 420A grapevines on 17 October 2017, occurred after the Northern California wildfires and heavy smoke exposure. Therefore, these wines were excluded from the sensory analysis due to smoke impact.

Table 5.1. Chemical analysis of grape musts after destemming–crushing and sugar addition (when applicable) across years and rootstocks (n = 3).

Sample	Harvest Date	°Brix	pH	TA (g/L)	YAN (mg/L)	Malic Acid (mg/L)
CS110 RB(–)	9/20/16	25.6 ± 0.1 a	3.62 ± 0.0 a	3.84 ± 0.3 b	81.1 ± 7.1 b	1460.0 ± 55.1 c
CS110 RB(+)	9/20/16	21.7 ± 0.1 c	3.45 ± 0.0 b	4.75 ± 0.1 a	121.8 ± 9.8 a	2275.0 ± 48.6 a
CS110 RB(+) 2H	9/27/16	23.8 ± 0.1 b	3.59 ± 0.0 a	4.49 ± 0.2 a	127.2 ± 7.1 a	1970.3 ± 29.5 b
CS420 RB(–)	9/20/16	24.3 ± 0.1 a	3.50 ± 0.0 b	4.23 ± 0.1 b	99.7 ± 2.5 a	1625.7 ± 48.0 c
CS420 RB(+)	9/20/16	22.1 ± 0.1 b	3.48 ± 0.0 b	4.53 ± 0.1 a	83.6 ± 17.8 a	1852.0 ± 13.9 b
CS420 RB(+) 2H	9/27/16	23.7 ± 0.1 a	3.55 ± 0.0 a	4.56 ± 0.2 a	104.3 ± 3.2 a	1953.3 ± 56.3 a
CS110 (–)	9/26/17	25.5 ± 0.1 b	3.62 ± 0.0 b	3.97 ± 0.0 c	145.9 ±0.6 b	2649.3 ± 45.7 b
CS110 (+)	9/26/17	23.4 ± 0.0 d	3.57 ± 0.0 b	4.87 ± 0.1 a	150.2 ±1.8 b	2779.0 ± 68.6 ab
CS110 (+) S	9/26/17	28.2 ± 0.5 a	3.57 ± 0.1 b	4.83 ± 0.1 a	143.7 ±6.8 b	2831.7 ± 140.4 ab
CS110 (+) 2H	10/6/17	24.7 ± 0.2 c	3.86 ± 0.0 a	4.18 ± 0.1 b	164.0 ±1.4 a	2971.7 ± 47.7 a
CS420 (–)	10/6/17	25.3 ± 0.1 a	3.56 ± 0.0 b	4.62 ± 0.2 a	127.9 ±15.9 a	2201.0 ± 34.7 c
CS420 (+)	10/6/17	23.6 ± 0.3 b	3.51 ± 0.0 b	4.82 ± 0.0 a	106.3 ± 4.1 a	2870.0 ± 21.0 a
CS420 (+) S	10/6/17	25.9 ± 0.6 a	3.51 ± 0.0 b	4.82 ± 0.1 a	111.0 ± 13.5 a	2823.7 ± 16.4 a
CS420 (+) 2H	10/17/17	24.2 ± 0.1 b	3.70 ± 0.0 a	4.05 ± 0.0 b	117.1 ± 2.4 a	2477.0 ± 39.0 b

TA = titratable acidity, YAN = yeast assimilable nitrogen, CS110 = Cabernet Sauvignon 110R, CS420 = Cabernet Sauvignon 420A, RB = red blotch, (–) = negative, (+) = positive, 2H = second harvest, S = chaptalization. Difference in lettering indicates a significant difference between treatments in each rootstock/season combination after applying Tukey's HSD test ($p < 0.05$).

Wines were made at the UC Davis LEED Platinum Teaching and Research Winery (University of California, Davis, CA, USA) using standard experimental protocols for red wines in 200 L research fermenters [18]. In 2016, the following fermentations were performed in triplicate: RB(–), RB(+), and RB(+) 2H. In 2017, due to observed differences between RB(+) and RB(+) 2H in 2016, chaptalization was performed to determine if sugar content (therefore ethanol content) was the main driver of phenolic extraction in wines. Thus, during the first harvest, RB(+) grapes either had no sugar added or sugar (sucrose) added aiming for similar total soluble-solids (TSS measured in °Brix) of RB(–) grape must. The following fermentations were performed in

2017 in triplicate: RB(–), RB(+), RB(+) sugar addition (S), and RB(+) 2H. Prior to yeast inoculation, °Brix, titratable acidity (TA measured as tartaric acid equivalents), pH, malic acid concentration, and yeast assimilable nitrogen (YAN) were measured for all treatments and are shown in Table 5.1. Fermentations were performed as in Girardello et al.[18].

Upon completion of primary fermentation (eight to nine days to reach <2.0 g/L residual sugar), wines were pressed using a basket press and returned to the research fermenters to settle. According to the manufacturer's protocol, the wines were inoculated for malolactic fermentation (MLF) with Viniflora® *Oenococcus oeni* (Chr. Hansen A/S, Hørsholm, Denmark). When needed, re-inoculation with Lalvin MBR VP 41 *Oenococcus oeni* (Lallemand, Bakersfield, CA, USA) was performed. This was the case with RB(–) and RB(+) S in 2017 due to higher final ethanol content. These wines took around two to three months longer to finish, potentially causing differences in secondary metabolites [35,36]. Once MLF was complete, the wines were racked into stainless steel containers, adjusted to 30 mg/L of free SO_2, and stored at 15 °C. Before bottling, ethanol concentrations were measured using an infrared spectrophotometer (Anton Paar USA Inc., Ashland, VA, USA), whereas residual sugar, acetic acid, free and bound SO_2, pH, and TA were measured as in Iland and coworkers [37]. During bottling, wines were sterile filtered in Bordeaux-style bottles with Saranex screw caps (Saranex/Transcendia, Franklin Park, IL, USA). Wines were stored at 14 °C until further analysis. Three months after bottling, two bottles from each fermenter replicate were randomly selected for a total of six replicates for each analysis.

5.3.2 Phenolic Analysis

5.3.2.1 Phenolic Extraction through Fermentation

The progression of phenolic extraction was analyzed for each of the wine treatments for each rootstock. A 2 mL sample was taken each day of alcoholic fermentation to track the extraction of total phenolics, total anthocyanins, and total tannins. Samples were centrifuged at 4 °C at 4000 rpm for 15 min with an Eppendorf 5403 centrifuge (Westbury, NY, USA). An aliquot was taken and placed into a 1.5 mL tube and shaken to minimize CO_2 production. Samples were analyzed based on a modified protein precipitation method [38–40] using a Genesys10S UV–Vis Spectrophotometer (Thermo Fisher Scientific, Madison, WI, USA) at 280–520 nm, and data were processed using the program Wine-XRAY with VESUVVIO software (Napa, CA, USA).

5.3.2.2 Wine Phenolic Analysis

Wine samples were collected at the time of sensory analysis and frozen until chemical analysis. Samples were thawed and centrifuged at 15,000 rpm for 5 min with an Eppendorf 5424 centrifuge (Westbury, NY, USA). Large polymeric pigments (LPP) and small polymeric pigments (SPP) were measured as in Harbertson et al. [40], whereas a modified protein precipitation assay [41] was used to determine total tannins. Using a Genesys10S UV–Vis Spectrophotometer, total tannins were measured at 510 nm absorbance and expressed as catechin equivalents (CE); SPP and LPP were measured at 520 nm absorbance. Relative concentrations of tannins were expressed as CE, and absorbance units of SPP and LPP were calculated as in Harbertson et al. [41].

Wine phenolic profiles were determined by RP-HPLC using an Agilent 1260 Infinity (Agilent Technologies, Santa Clara, CA, USA) equipped with a diode array detector, with a temperature controlled autosampler maintained at 8 °C. Chromatographic separation was carried

out with a PLRP-S 100 A 3 μM 150 × 4.6 mm column stored at 35 °C. The sample (20 μL) was injected onto the column with the mobile phase flow rate set at 1 mL/min. The chromatographic method is described in Peng et al. [42]. To monitor the eluted compounds, the wavelengths 280 nm, 320 nm, 360 nm, and 520 nm were used. Calibrations curves were constructed for gallic acid, (+)-catechin, (−)-epicatechin, caffeic acid, quercetin, quercetin-rhamnoside, *p*-coumaric acid, and malvidin-3-*O*-glucoside chloride to quantify compounds. Other compounds identified were quantified as described in Girardello et al. [18]. All data processing was completed with Agilent® CDS ChemStation software version D.04 (Agilent Technologies, Santa Clara, CA, USA).

5.3.3 Volatile Profile Analysis

Two bottles were randomly selected from each fermentation replicate for each treatment (a total of six bottles per treatment). To an amber vial containing 3 g of NaCl, 10 mL of the wine sample was added. In 2016, each vial was spiked with 50 μL of 50 mg/L 2-octanol, and in 2017, each vial was spiked with 50 μL 10 mg/L of 2-undecanone as an internal standard. The vials were capped with crimp caps (Supelco Analytical, Bellefonte, PA, USA). Each bottle replicate from each fermentation replicate was analyzed in triplicate. The volatile profiles of each wine treatment were analyzed via HS-SPME-GC–MS. The wine samples were extracted and injected onto the GC-MS model 7890A (Agilent Technologies, Santa Clara, CA, USA) via a Gerstel Muli-purpose Sampler (version 1.2.3.1, Gerstel Inc, Linthicum, MD, USA). The analysis was carried out similarly as in Hendrickson et al.[43], with the exception that the carrier gas, helium, was set at a constant pressure of 5.53 psi in 2016 (retention-time locked to 2-octanol) and 7.03 psi in 2017 (retention-time locked to 2-undecanone). Each sample was semi-quantitatively analyzed using relative peak areas by normalizing with the peak area of the internal standard. Compounds were

analyzed using Mass Hunter software version B.07.00 (Agilent Technologies) and identified by retention time and confirmation of mass spectra ion peaks using the National Institute of Standards and Technology database (NIST) (https://www.nist.gov (accessed on 9 July 2020)).

5.3.4 Sensory Evaluation

In 2016, for both rootstocks and all treatments, three fermenter replicates were evaluated for a total of 18 wines. Due to noticeable differences in one of the fermenter replicates in each treatment, only two replicates were chosen in 2017. Cabernet Sauvignon 420A RB(+) 2H wines were not evaluated through descriptive analysis (DA) due to a smoky and ashy aftertaste from the wildfires in 2017, leaving seven treatments and 14 wines to be analyzed in 2017. DA was performed in triplicate for aroma, taste, mouthfeel, and color in May 2017 and June 2018, three months after bottling, in the J. Lohr Wine Sensory Room, at the University of California in Davis, California. Eleven panelists (five male and six female) were recruited for sensory analysis of both 2016 and 2017 wines by advertising within the University of California, Davis. Panelists gave informed consent before the study and were not aware of the research purpose or how many different samples they were evaluating. For DA and color evaluation of the wines, similar methods as in Lawless and Heymann [44] and Casassa et al. [24] were used, respectively.

Training for the panel consisted of seven one-hour sessions over four weeks. Panelists saw each wine at least three times. In those sessions, panelists generated a list of sensory attributes with related reference standards (Tables S5.5 and S5.6) after blindly tasting the wines. Following the training sessions, panelists assessed the wines in triplicate in one-hour evaluation sessions over two weeks in individual sensory booths. In 2016, panelists evaluated six wines in each of the nine evaluation sessions, with a 30-s break between each wine evaluated. A five-minute break was

given between wines three and four. Similarly, in 2017 panelists evaluated seven wines in each of the six sessions with a five-minute break between wines four and five. Prior to each evaluation session, panelists completed a reference standard test where they were asked to identify aroma standards blindly. The wines were served (40 mL) in a black ISO (ISO-3591:1977) wine tasting glass coded with a randomly generated three-digit code. Wine samples were randomly presented in a Williams Latin Square complete block design calculated by the FIZZ software (FIZZ network, version 2.47 B, Biosystèmes, Couternon, France). The evaluation sessions were performed in a booth with red lighting at room temperature, where the panelists were asked to evaluate each wine in attribute intensity on a 10 cm anchored line scale ("not present" and "high" for all attributes besides viscosity, for which the anchors were "watery" and "very viscous"). Panelists expectorated each wine and cleansed their palates with ambient temperature water and unsalted crackers during a 1-min break between wine samples to limit carry over.

Afterward, panelists were directed to another booth to evaluate the color of each wine. The wine poster *Les couleurs du vin* (Bouchard Ainé & Fils) was used to assess each wine as described in Casassa et al. [24]. The panelists were asked to blindly match each wine with one of the 42 red wine color examples on the poster. Wines were analyzed under vertically mounted halogen lights at a 45° angle and in the direct line of sight. Panelists were asked to compare each wine side by side with the poster. All sensory data were collected using FIZZ software.

5.3.5 Statistical Analysis

Sample means and standard deviations were calculated using Microsoft Excel (Microsoft, Redmond, Washington, DC, USA), and all other statistical analysis was performed using R (RStudio version 1.2.5042, R version 3.6.1 https://www.rstudio.com (accessed on 26 November

2021)) with an alpha of 0.05. Chemical analysis was conducted through a one-way analysis of variance (ANOVA) and a post-hoc Tukey Honest significance (HSD) test. For sensory analysis, significance was tested by multivariate analysis of variance (MANOVA) for the overall treatment effect, and then by a three-way ANOVA with two-way interactions. If there was a significant wine to judge interaction and wine to replication interaction, a pseudo-mixed model ANOVA was performed to determine if the wine effect was truly significant in the sensory analysis. Principal component analysis (PCA) was used to determine the variance in the volatile analysis. Multiple factor analysis (MFA) was used to determine the variance between samples for chemical and sensory analysis.

5.4 Results:

5.4.1 Basic Grape Chemical Composition at Harvest

In Table 5.1, the harvest dates and basic chemical composition for each treatment (RB(–), RB(+), RB(+) S and, RB(+) 2H) are shown. In 2017, CS 420A RB(+) 2H grapes were harvested after the Northern California wildfires and 10 days of smoke exposure, which potentially led to smoke impacted wines. It was observed that in all cases but CS 420A in 2017, RB(+) 2H grapes were significantly higher in TSS than RB(+) grapes, which were harvested at the same time as healthy fruit (RB(–)). However, CS 110R RB(+) 2H grapes in both years were not able to meet similar TSS as RB(–) grapes. In general, pH was lower, and TA and malic acid were higher in RB(+) compared to RB(–) grape juice, corresponding to a delay in ripening. The RB(+) 2H grape juice, in general, showed higher pH values and decreased TA and malic acid concentrations when compared to RB(+). No significant trend for YAN levels was observed.

5.4.2 Phenolic Extractability

The graphs of total anthocyanin and total tannin concentrations are respectively shown in Figures 5.1a,b for all wine treatments for CS 110R and 420A in 2016. Figures 5.1c,d respectively portray total anthocyanin and total tannin concentrations for CS 110R and 420A in 2017. Significant differences among treatments were calculated for anthocyanin concentrations (Table S5.1) and tannin concentrations (Table S5.2). In general, total anthocyanin concentrations in RB(–) grape musts were significantly higher than the other treatments towards the end of fermentation across season and rootstock (Figures 5.1a,c and Table S5.1). The anthocyanin profile of fermenting grape musts (Figure 5.1 and Tables S5.1 and S5.2) indicated that a delayed harvest of diseased fruit increased the extractability of anthocyanins when compared to RB(+) fruit.

It was observed for RB(+) 2H grapes that dehydration in the berry led to significantly smaller berry mass and increases in sugar content (data not shown). It was hypothesized that the higher sugar concentration, resulting in higher alcohol content during fermentation, led to higher extraction of anthocyanins into the final wines. Therefore, in 2017, chaptalization was performed, aiming for the TSS of the RB(–) grapes, to investigate this possibility. However, as indicated by Figure 5.1, chaptalization of diseased grape must did not increase anthocyanin extraction and was statistically similar to RB(+) wines at the end of fermentation.

Overall, RB(–) wines were significantly higher in tannin concentrations at the end of fermentation when compared to the other treatments, which were all similar. Although the harvest date was one to two weeks later, tannin concentrations for RB(+) 2H and RB(+) wines were generally statistically similar through fermentation, except for CS 110R in 2016.

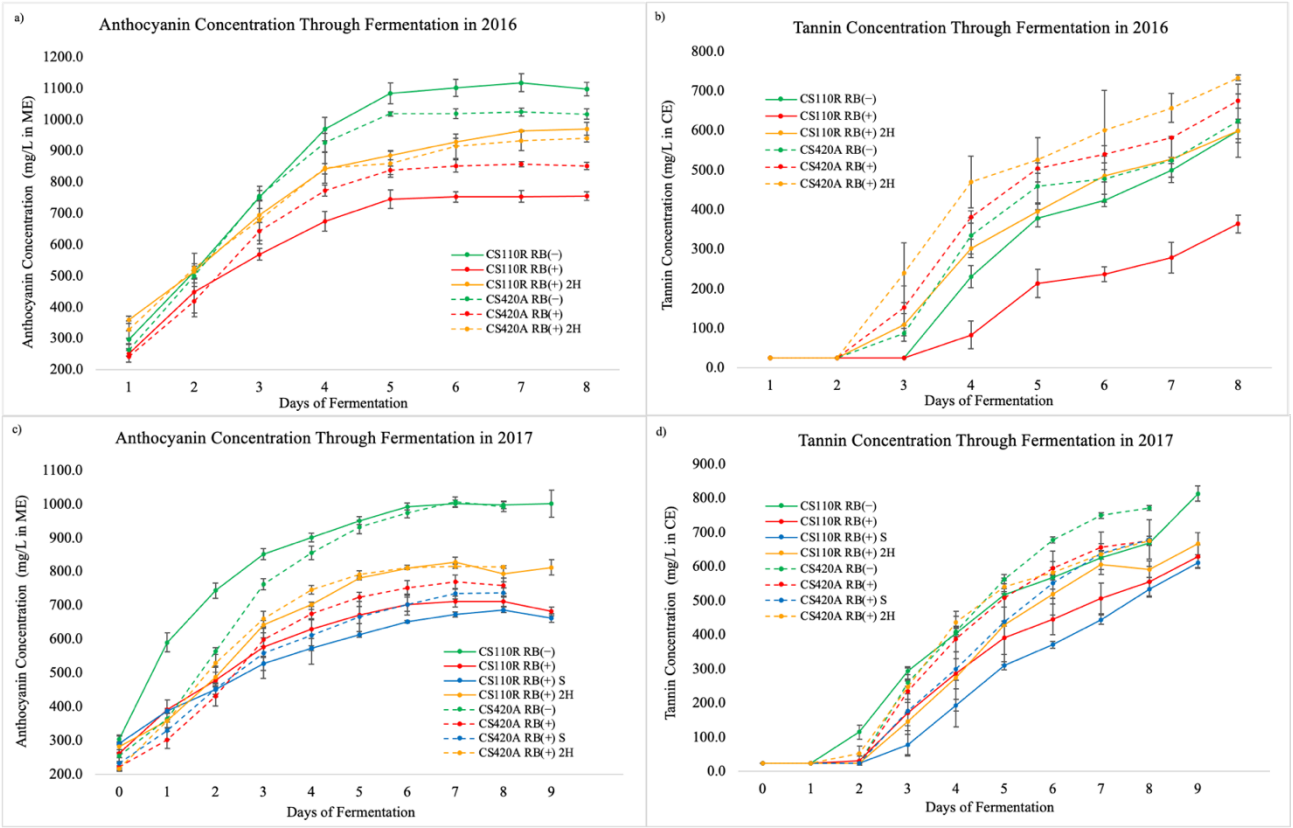

Figure 5.1. Total anthocyanin and tannin concentrations during fermentation via Wine X-ray analysis for wines in 2016 and 2017 (n = 3). (**a**) Total anthocyanin concentrations through fermentation in 2016; (**b**) total tannin concentrations through fermentation in 2016; (**c**) total anthocyanin concentrations through fermentation in 2017, and (**d**) total tannin concentrations through fermentation in 2017. CS110 = Cabernet Sauvignon 110R, CS420 = Cabernet Sauvignon 420A, RB = red blotch, (–) = negative, (+) = positive, 2H = second harvest, S = chaptalization, ME = malvidin-3-glucoside equivalents, and CE = catechin equivalents.

5.4.3 Final Wine Composition

5.4.3.1 Chemical Parameters at Bottling

Table 5.2 depicts the percentage alcohol (% *v*/*v*), pH, TA, and residual sugar (RS) for all wine treatments in both years. As expected, with the starting TSS values of the grape must, RB(–) was highest in alcohol content in 2016, followed by RB(+) 2H and then RB(+). Similar observations were made in 2017; however, RB(+) S wines were significantly higher in percentage alcohol than all other treatments. In general, RS was significantly lower in RB(+) than other treatments except for CS 420A in 2017.

Table 5.2. Chemical compositions of final wines in 2016 and 2017 (n = 6).

	2016					
	110R			420A		
Bottling Chemical Parameters	RB(–)	RB(+)	RB(+) 2H	RB(–)	RB(+)	RB(+) 2H
% Alcohol (% *v*/*v*)	15.10 ± 0.20 a	11.99 ± 0.24 c	13.54 ± 0.09 b	14.07 ± 0.18 a	12.12 ± 0.18 c	13.66 ± 0.09 b
pH	3.55 ± 0.07 b	3.6 ± 0.01 ab	3.65 ± 0.03 a	3.44 ± 0.04 b	3.47 ± 0.01 b	3.59 ± 0.05 a
TA (g/L)	6.79 ± 0.21 a	6.45 ± 0.12 a	6.61 ± 0.13 a	7.13 ± 0.21 a	6.86 ± 0.04 ab	6.51 ± 0.20 b
RS (g/L)	0.27 ± 0.03 a	0.17 ± 0.01 c	0.22 ± 0.00 b	0.20 ± 0.01 a	0.19 ± 0.01 b	0.20 ± 0.01 a

	2017							
	110R				420A			
Bottling Chemical Parameters	RB(–)	RB(+)	RB(+) S	RB(+) 2H	RB(–)	RB(+)	RB(+) S	RB(+) 2H
% Alcohol (% *v*/*v*)	15.42 ± 0.12 b	13.77 ± 0.15 d	16.06 ± 0.03 a	14.72 ± 0.06 c	15.01 ± 0.09 b	14.02 ± 0.18 c	15.51 ± 0.16 a	14.30 ± 0.02 c
pH	3.78 ± 0.05 b	3.88 ± 0.01 a	3.92 ± 0.04 a	3.88 ± 0.03 ab	3.58 ± 0.02 b	3.67 ± 0.03 a	3.71 ± 0.02 a	3.70 ± 0.03 a
TA (g/L)	6.74 ± 0.12 a	5.83 ± 0.11 b	6.06 ± 0.11 b	5.94 ± 0.10 b	6.41 ± 0.16 a	6.05 ± 0.21 a	6.42 ± 0.16 a	6.21 ± 0.21 a
RS (g/L)	0.74 ± 0.15 a	0.23 ± 0.10 b	0.96 ± 0.03 a	0.42 ± 0.10 b	0.87 ± 0.45 a	0.47 ± 0.15 a	0.61 ± 0.18 a	0.24 ± 0.02 a

TA = Titratable Acidity, RS = residual sugar, 110R = Cabernet Sauvignon 110R, 420A = Cabernet Sauvignon 420A, RB = red blotch, (–) = negative, and (+) = positive, 2H = second harvest, S = chaptalization. Difference in lettering indicates a significant difference between treatments of 110R and 420A respectively, after applying Tukey's HSD test ($p < 0.05$).

5.4.3.2 Phenolic Compound Composition

Tables 5.3 and 5.4 portray the phenolic profiles of the individual wine treatments. Total tannin, SPP, and LPP values from the protein precipitation assay are supplemental to the values of polymeric pigments and phenols from RP-HPLC analysis. In 2016, it was observed that total flavan-3-ols were significantly higher in RB(+) and RB(+) 2H wines than RB(–) wines for both rootstocks. The concentrations of flavanols and anthocyanins were generally lower in RB(+) wines than in other wine treatments. Additionally, polymeric pigment, polymeric phenol, and SPP values were significantly higher in RB(–) and RB(+) 2H wines than RB(+) wines for both rootstocks in 2016.

Overall, in 2017 the phenolic profiles of chaptalized wines were more similar to RB(–) wines than RB(+) or RB(+) 2H wines. For CS 110R, flavan-3-ol, flavanol, and anthocyanin concentrations were higher in RB(+) and RB(+) 2H wines compared to RB(–) and RB(+) S wines. In addition, RB(–) and RB(+) S wines generally were higher in concentration for polymeric pigments, polymeric phenols, and SPP values than RB(+) 2H and RB(+). For CS 420A, RB(+) S was the only treatment significantly different and lower than other wine treatments for anthocyanin concentrations.

Table 5.3. Phenolic profile of wines in 2016 analyzed using HPLC-DAD and spectrophotometrically (n = 6). Values for SPP, LPP, and Tannin were obtained through a modified protein precipitation assay. All other values were obtained through HPLC-DAD.

	2016					
	110R			**420A**		
Phenolic Compound	RB(–)	RB(+)	RB(+) 2H	RB(–)	RB(+)	RB(+) 2H
Total Flavan-3-ols (mg/L)	29.14 ± 0.60 b	32.93 ± 0.95 a	33.99 ± 0.96 a	30.00 ± 0.77 b	33.86 ± 0.65 a	34.47 ± 0.29 a
Total HCA (mg/L)	33.34 ± 0.50c	35.57 ± 0.06 b	38.58 ± 0.92a	42.79 ± 2.84 b	47.68 ± 3.74 a	45.41 ± 1.64 ab
Total Flavonols (mg/L)	70.64 ± 5.37 a	47.66 ± 2.45 b	75.74 ± 1.76 a	82.45 ± 1.38 a	73.00 ± 2.41 b	79.16 ± 1.89 a
Total Anthocyanins (mg/L)	334.42 ± 16.07 b	295.61 ± 15.86 c	365.64 ± 8.56 a	370.96 ± 4.96 a	329.98 ± 20.1 b	346.31 ± 23.24 ab
Gallic Acid (mg/L)	7.73 ± 0.28 c	10.03 ± 0.20 b	10.88 ± 0.44 a	7.22 ± 0.37 b	9.29 ± 0.06 a	9.63 ± 0.47 a
Polymeric Pigments (mg/L)	20.97 ± 4.12 a	10.16 ± 2.07 b	18.03 ± 1.90 a	18.48 ± 0.22 a	14.03 ± 0.06 c	16.29 ± 1.44 b
Polymeric Phenols (mg/L)	233.81 ± 44.59 a	136.41 ± 24.48 b	250.05 ± 32.61 a	232.59 ± 10.83 a	198.46 ± 9.55 b	237.22 ± 22.76 a
SPP (Au_{520})	2.34 ± 0.08 a	1.30 ± 0.11 c	1.64 ± 0.01 b	1.60 ± 0.06 a	1.15 ± 0.05 c	1.39 ± 0.06 b
LPP (Au_{520})	0.72 ± 0.21 a	0.29 ± 0.18 a	0.70 ± 0.12 a	0.55 ± 0.21 a	0.50 ± 0.06 a	0.55 ± 0.05 a
Tannin (mg/L CE)	173.53 ± 77.14 ab	154.77 ± 19.76 b	405.14 ± 87.81 a	386.77 ± 41.76 a	456.08 ± 26.96 a	488.43 ± 41.87 a

HCA = hydroxycinnamic acids, SPP = short polymeric pigments, LPP = long polymeric pigments, CE = catechin equivalents, 110R = Cabernet Sauvignon 110R, 420A = Cabernet Sauvignon 420A, RB = red blotch, (–) = negative, and (+) = positive, 2H = second harvest, S=chaptalization. Difference in lettering indicates a significant difference between treatments after applying Tukey's HSD test ($p < 0.05$).

Table 5.4. Phenolic profile of wines in 2017 analyzed using HPLC-DAD and spectrophotometrically (n = 6). Values for SPP, LPP, and tannin were obtained through a modified protein precipitation assay. All other values were obtained through HPLC-DAD.

	2017							
	110R				**420A**			
Phenolic Compound	RB(–)	RB(+)	RB(+) S	RB(+) 2H	RB(–)	RB(+)	RB(+) S	RB(+) 2H
Total Flavan-3-ols (mg/L)	37.98 ± 1.05 c	46.45 ± 1.28 a	37.93 ± 0.29 c	42.26 ± 1.66 b	41.94 ± 1.20 a	42.14 ± 0.86 a	37.65 ± 1.90 b	42.01 ± 1.43 a
Total HCA (mg/L)	26.89 ± 1.41 a	27.39 ± 0.46 a	26.22 ± 1.25 a	17.17 ± 1.59 b	28.99 ± 1.45 a	24.03 ± 1.99 b	21.55 ± 2.25 b	16.40 ± 1.64 c
Total Flavonols (mg/L)	36.51 ± 2.71 ab	41.38 ± 2.29 a	34.04 ± 2.38 b	41.70 ± 7.43 a	45.60 ± 3.27 ab	47.36 ± 1.90 a	44.14 ± 1.26 ab	38.79 ± 4.47 b
Total Anthocyanins (mg/L)	92.74 ± 26.48 b	214.11 ± 11.70 a	100.47 ± 28.10 b	189.61 ± 29.54 a	170.35 ± 11.66 a	185.50 ± 5.43 a	143.27 ± 28.5 b	182.85 ± 16.75 a
Gallic Acid (mg/L)	16.38 ± 0.17 c	19.71 ± 0.86 a	19.11 ± 0.11 a	17.83 ± 0.17 b	14.69 ± 0.19 b	15.89 ± 0.39 a	15.05 ± 0.69 b	15.79 ± 0.44 a
Polymeric Pigments (mg/L)	38.05 ± 11.50 a	19.54 ± 0.65 b	40.46 ± 4.45 a	17.43 ± 6.63 b	27.22 ± 5.40 ab	22.17 ± 0.73 bc	31.85 ± 2.64 a	19.94 ± 5.57 c
Polymeric Phenols (mg/L)	379.98 ± 98.00 a	253.26 ± 2.36 b	417.65 ± 25.17 a	217.08 ± 81.58 b	341.40 ± 38.37 ab	298.81 ± 16.46 bc	380.55 ± 31.61 a	245.89 ± 68.18 c
SPP (Au_{520})	3.14 ± 0.30 a	1.50 ± 0.01 c	2.53 ± 0.07 b	1.74 ± 0.35 c	2.49 ± 0.24 a	1.47 ± 0.03 c	2.00 ± 0.06 b	2.00 ± 0.40 b
LPP (Au_{520})	1.06 ± 0.72 ab	0.54 ± 0.03 bc	1.42 ± 0.12 a	0.29 ± 0.28 c	0.85 ± 0.25 ab	0.65 ± 0.03 ab	1.07 ± 0.09 a	0.19 ± 0.32 b
Tannin (mg/L CE)	297.99 ± 171.60 ab	440.52 ± 33.49 a	460.33 ± 25.76 a	175.89 ± 133.11 b	379.17 ± 61.19 b	452.88 ± 37.89 ab	542.14 ± 17.27 a	230.01 ± 128.61 c

HCA = hydroxycinnamic acids, SPP = short polymeric pigments, LPP = long polymeric pigments, CE = catechin equivalents, 110R = Cabernet Sauvignon 110R, 420A = Cabernet Sauvignon 420A, RB = red blotch, (–) = negative, and (+) = positive, 2H = second harvest, S = chaptalization. Difference in lettering indicates a significant difference between treatments after applying Tukey's HSD test ($p < 0.05$).

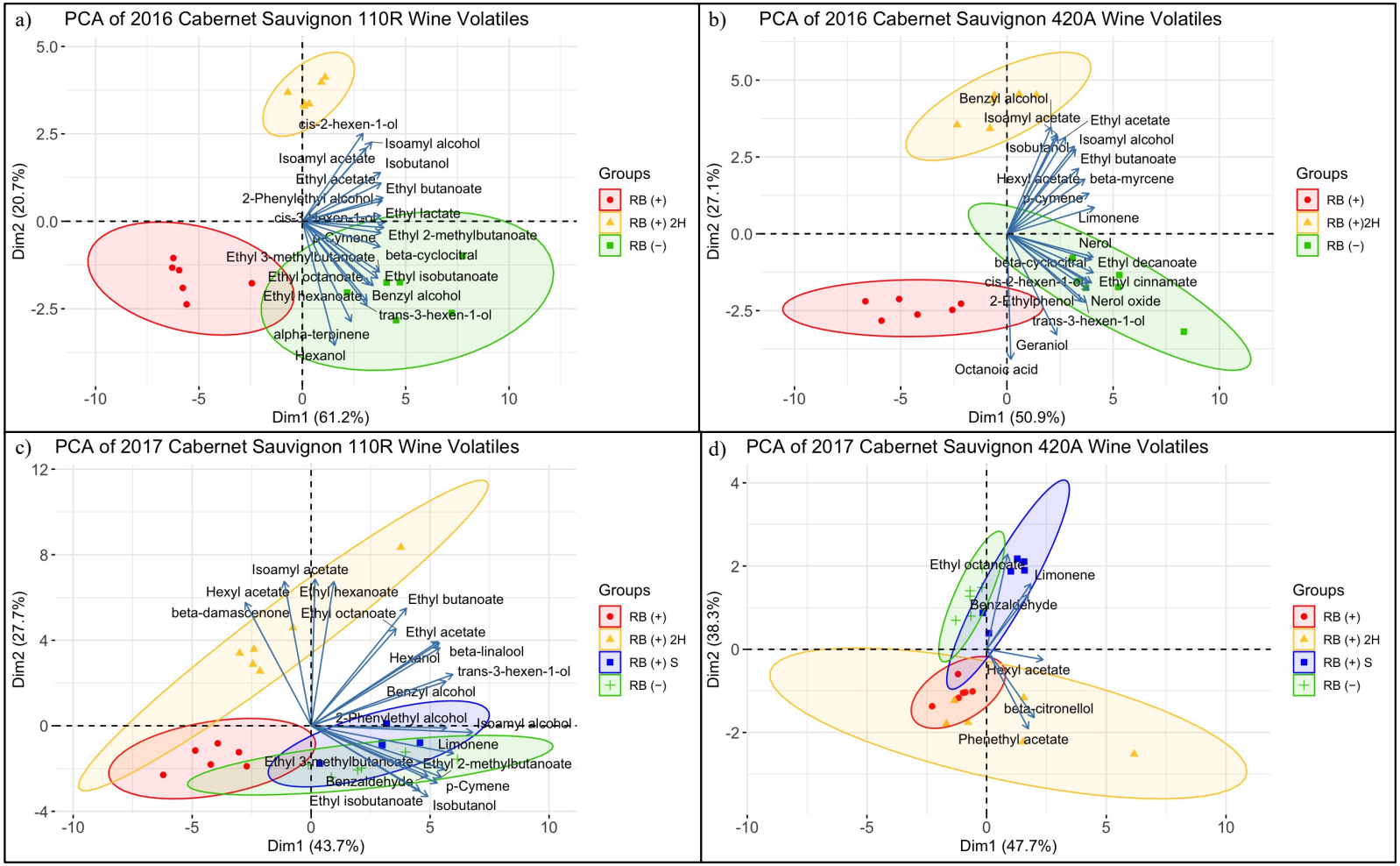

Figure 5.2. Principal component analysis of volatile compounds in wines: (**a**) CS 110R wines made in 2016, (**b**) CS 420A wines made in 2016, (**c**) CS 110R wines made in 2017, and (**d**) CS 420A wines made in 2017. Ellipses are drawn to 95% confidence with $n = 6$ for two bottle replicates for each fermenter replicate. Only the highest 20 significant volatile compounds that contribute to the variance are plotted. However, 2d shows only the six volatiles that were significantly different. CS110 = Cabernet Sauvignon 110R, CS420 = Cabernet Sauvignon 420A, RB = red blotch, (–) = negative, and (+) = positive, 2H = second harvest, S = chaptalization.

5.4.3.3 Volatile Compound Composition

In 2016, 34 and 39 volatile aroma compounds were identified, and 31 and 27 were significantly different for CS 110R and CS 420A, respectively. For CS 110R and CS 420A in 2017, there was a total of 31 and 29 volatiles identified, 26 and 6 of them being significantly different, respectively. Figure 5.2 depicts the PCA of the volatile profiles of wines made in 2016 and 2017, with ellipses to show 95% confidence intervals. Across seasons and rootstocks, 71–86% of the variance of the volatile profiles between treatments was explained. The third principal component (PC) was able to further separate the treatments only in the case of CS 110R 2017, in which an additional 12% of the variance was explained (Figure S5.1). For the PCA in Figure 2a–c and Figure S5.1, the 20 highest significantly different volatile compounds that contribute to the variance between the treatments are shown. The separation between sample treatments is well displayed by plotting the variables that contribute the most variance explained in the PCA, and the separation between sample treatments is well displayed [45]. For CS 420A wines in 2017 (Figure 5.2d), only the six significantly different volatile compounds are plotted to show the highest degree of separation between the treatments.

In general, across season and rootstocks, RB(+) wines were negatively correlated with most of the volatile compounds. In 2016, the PCA of the volatile profiles of wines in Figure 5.2a,b showed that RB(+) 2H wines were differentiated from RB(+) and RB(–) wines. Esters, terpenoids, and higher alcohols (HAs), which are responsible for fruity and floral aromas, were negatively correlated with RB(+) wines and positively correlated with RB(+) 2H and RB(–) wines.

For CS 110R wines in 2017, Figure 5.2c indicates that RB(+) 2H and RB(+) wines were similar and were separated from RB(–) wines at the 95% confidence level. RB(+) 2H was correlated with esters and terpenoids. By plotting the third PC (Figure S5.1), RB(+) S wines were

separated from RB(–) wines and were positively correlated with HAs, whereas RB(–) wines were correlated with the esters, ethyl 2-methylbutanoate and ethyl 3-methylbutanoate, as well as p-cymene, and cis-2-hexen-1-ol.

For CS 420A in 2017 (Figure 5.2d) only RB(–) and RB(+) wines were separated on the PCA at a 95% confidence interval. RB(+) S and RB(–) wines were both highly correlated with the volatile compounds ethyl octanoate, limonene, and benzaldehyde. The confidence ellipses suggest that RB(+) and RB(+) 2H wines were not distinguishable; however, the volatile aroma compound profile of CS 420A RB(+) 2H may have been affected by the Northern California wildfires, and, therefore, no conclusions can be drawn.

5.4.4 Descriptive Analysis of Final Wines

A MANOVA determined significant wine effects for all sensory evaluations, except for CS 420A in 2017. An ANOVA and MFA were still applied to analyze CS 420A data in 2017; however, this observation indicates that the panel could not distinguish between the CS 420A wines made in 2017. All sensory attributes that had a significant wine effect in the final wines in 2016 and 2017 are shown in Table S5.3. In general, it was observed that panelists could distinguish between RB(–) wines and RB(+) wines, across season and rootstock. A hot mouthfeel or an alcohol aroma was higher for RB(–) wines than RB(+) wines, which was mainly significant.

For CS 110R wines in 2016, RB(–) had significantly higher values for hot mouthfeel and visual color than RB(+) wines. At the same time, RB(+) wines were rated significantly higher for sour. Panelists rated RB(+) 2H higher for dry mouthfeel than other treatments and statistically similar to RB(–) for color. RB(+) 2H wines were also found to be significantly hotter than RB(+) wines, but still lower than RB(–) wines. In the case of CS 420A wines made in 2016, RB(–) and

RB(+) 2H wines were statistically similar for alcohol aroma and sweet taste, which were both higher than RB(+) wines.

In 2017, RB(–) wines were rated significantly higher for dark fruit and red cherry aromas. They were higher, although not significant for the vanilla aroma and hot mouthfeel compared to RB(+) wines. On the other hand, RB(+) wines were rated higher for barnyard, soil, savory, and black pepper aromas, as well as astringency mouthfeel than RB(–) wines, although only barnyard was significant. The panelists rated RB(+) 2H wines as statistically similar to RB(–) wines for all attributes, and RB(+) S wines as statistically similar to RB(+) wines for all attributes besides hot mouthfeel (Table S5.3). For the hot mouthfeel, RB(+) S wines were significantly higher than RB(+) wines but similar to RB(–) and RB(+) 2H wines.

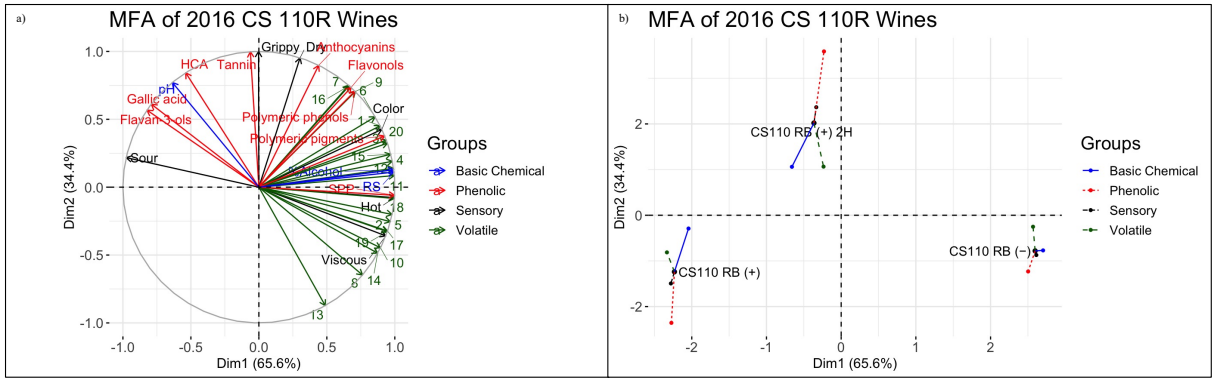

Figure 5.3. Multifactor analysis of 2016 Cabernet Sauvignon 110R wines which (**a**) displays the significant basic chemical parameters at bottling, phenolic profile, volatile profile, and sensory attributes on a loadings plot and how they separate and correlate to (**b**) the wine treatments plotted on a partial axes plot. For bottling values, phenolic compound values, and volatile compound values n = 6, and for sensory data *n* = 9. CS110 = Cabernet Sauvignon 110R, RS = residual sugar, HCA = hydroxycinnamic acids, SPP = small polymeric pigments, 1 = ethyl acetate, 2 = ethyl isobutanoate, 3 = ethyl butanoate, 4 = ethyl 2-methylbutanoate, 5 = ethyl 3-methylbutanoate, 6 = isobutanol, 7 = isoamyl acetate, 8 = α-terpinene, 9 = isoamyl alcohol, 10 = ethyl hexanoate, 11 = p-cymene, 12 = ethyl lactate, 13 = hexanol, 14 = trans-3-hexen-1-ol, 15 = cis-3-hexen-1-ol, 16 = cis-2-hexen-1-ol, 17 = ethyl octanoate, 18 = β-cyclocitral, 19 = benzyl alcohol, 20 = 2-phenylethyl alcohol, RB = red blotch, (+) = positive, (–) = negative, 2H = second harvest.

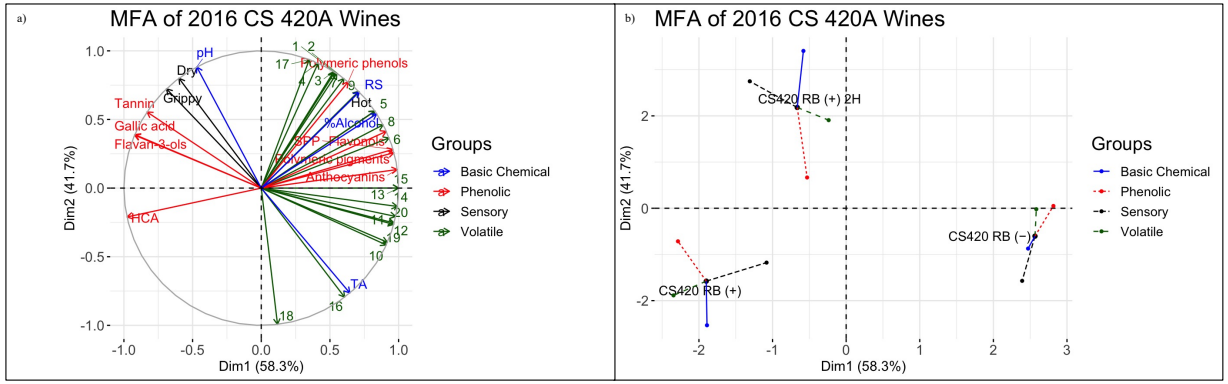

Figure 5.4. Multifactor analysis of 2016 Cabernet Sauvignon 420A wines which (**a**) displays the significant basic chemical parameters at bottling, phenolic profile, volatile profile, and sensory attributes on a loadings plot and how they separate and correlate to (**b**) the wine treatments plotted on a partial axes plot. For bottling values, phenolic compound values, and volatile compound values n = 6, and for sensory data n = 9. CS 420 = Cabernet Sauvignon 420A, RS = residual sugar, TA = titratable acidity, HCA = hydroxycinnamic acids, SPP = small polymeric pigments, 1 = ethyl acetate, 2 = ethyl butanoate, 3 = isobutanol, 4 = isoamyl acetate, 5 = β-myrcene, 6 = limonene, 7 = isoamyl alcohol, 8 = p-cymene, 9 = hexyl acetate, 10 = trans-3-hexen-1-ol, 11 = cis-2-hexen-1-ol, 12 = nerol oxide, 13 = β-cycolcitral, 14 = ethyl decanoate, 15 = nerol, 16 = geraniol, 17 = benzyl alcohol, 18 = octanoic acid, 19 = 2-ethylphenol, 20 = ethyl cinnamate, RB = red blotch, (+) = positive, (–) = negative, 2H = second harvest.

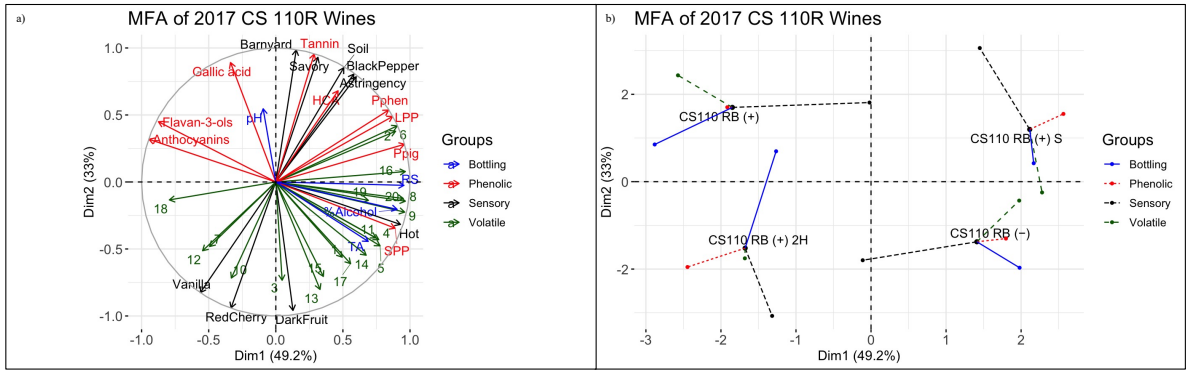

Figure 5.5. Multifactor analysis of 2017 Cabernet Sauvignon 110R wines which (**a**) displays the significant basic chemical parameters at bottling, phenolic profile, volatile profile, and sensory attributes on a loadings plot and how they separate and correlate to (**b**) the wine treatments plotted on a partial axes plot. Since a fermenter replicate was removed for each treatment for DA (n = 6), the same fermenter was removed when plotting the MFA for bottling values, phenolic compound values, and volatile compound values (n = 4). CS110 = Cabernet Sauvignon 110R, RS = residual sugar, TA = titratable acidity, HCA = hydroxycinnamic acids, SPP = small polymeric pigments, LPP = large polymeric pigments, 1 = ethyl acetate, 2 = ethyl isobutanoate, 3 = ethyl butanoate, 4 = ethyl 2-methylbutanoate, 5 = ethyl 3-methylbutanoate, 6 = isobutanol, 7 = isoamyl acetate, 8 = limonene, 9 = isoamyl alcohol, 10 = ethyl hexanoate, 11 = p-cymene, 12 = hexyl acetate, 13 = hexanol, 14 = trans-3-hexen-1-ol, 15 = ethyl octanoate, 16 = benzaldehyde, 17 = β-linalool, 18 = β-damascenone, 19 = benzyl alcohol, 20 = 2-phenylethyl alcohol, RB = red blotch, (+) = positive, (–) = negative, 2H = second harvest.

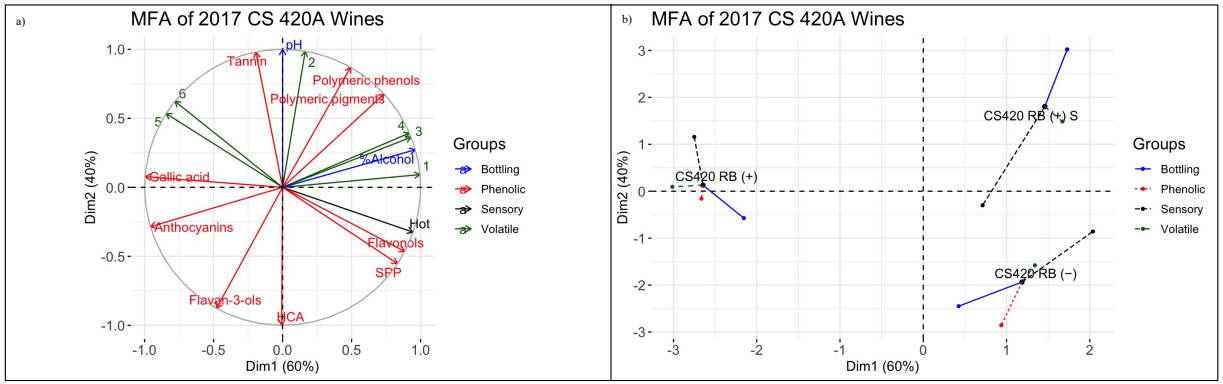

Figure 5.6. Multifactor analysis of 2017 Cabernet Sauvignon 420A wines which (**a**) displays the significant basic chemical parameters at bottling, phenolic profile, volatile profile, and sensory attributes on a loadings plot and how they separate and correlate to (**b**) the wine treatments plotted on a partial axes plot. Since a fermenter replicate was removed for each treatment for DA (*n* = 6), the same fermenter was removed when plotting the MFA for bottling values, phenolic compound values, and volatile compound values (*n* = 4). In addition, since the second harvest was not analyzed for sensory, it is not shown here, consequently changing what values were significant. CS 420 = Cabernet Sauvignon 420A, RS = residual sugar, TA = titratable acidity, HCA = hydroxycinnamic acids, ANTH = anthocyanins, Pphen = polymeric phenols, Ppig = polymeric pigments, SPP = small polymeric pigments, 1 = limonene, 2 = hexyl acetate, 3 = ethyl octanoate, 4 = β-citronellol, 5 = phenethyl acetate, RB = red blotch, (+) = positive, (–) = negative, 2H = second harvest**.**

5.5 Discussion:

5.5.1 Phenolic Extractability

The current study indicated that extending the ripening of GRBV infected grapes did increase anthocyanin extractability during winemaking. Chaptalization of diseased grape musts in 2017 did not show a similar trend, suggesting another factor besides ethanol concentration influences anthocyanin extractability. Similar findings were observed in Bautista-Ortin et al. [25], where a longer hangtime of grapes resulted in increased anthocyanin extractability during winemaking. In this work, the authors correlated their findings to changes in the grape skin cell wall. Research has shown that dehydration of berries and a longer hangtime can lead to degradation of the grape skin cell wall [46]. It is commonly accepted that pectolytic enzyme activity that degrades the cell wall increases during ripening and is positively correlated to the enhanced extractability of anthocyanins from grape skins [47]. GRBV delays grape ripening events, one potentially being cell wall metabolism, resulting in more rigid cell walls, consequently decreasing phenolic extractability. Our work potentially suggests that changes in the integrity and composition of the grape skin cell wall through a longer hangtime drive extractability during fermentation for GRBV infected grapes. Another explanation is that extended ripening concentrates secondary metabolites through dehydration, leading to a higher concentration of anthocyanins in RB(+) 2H wines compared to RB(+) and RB(+) S wines. However, an investigation into the changes in the cell wall of GRBV infected grapes through ripening and how this may impact phenolic extractability is needed.

Results in the current study indicate that RB(+) wines were significantly lower in tannin concentrations than RB(–) wines by the end of primary fermentation. This is contrary to findings in Rumbaugh et al. [17], where tannin content and concentration were higher in RB(+) grapes

when compared to RB(–) grapes, which was potentially due to a host defense mechanism stimulated by GRBV infection. This suggests that although tannin grape content is higher in RB(+) grapes than RB(–), the extractability during winemaking is much lower. Previous work has indicated that tannins can bind to grape skin cell walls during fermentation [48], and that tannin extraction can increase with increases in ethanol and temperature [49]. However, in 2017 for RB(+) S wines, the concentration of tannins was similar to RB(+) and RB(+) 2H wines, indicating that a higher alcohol content did not afford higher extraction of tannins in GRBV infected fruit. Collectively these observations indicate that ethanol production during fermentation is not the only factor increasing tannin extraction of RB(–) grape musts when compared to RB(+) and RB(+) S. Research indicates that pectin and soluble proteins, namely pathogenesis-related (PR) proteins, can bind to tannins during fermentation, decreasing extraction during winemaking [31,48,50]. The impact of GRBV on grape skin cell wall composition and PR proteins has yet to be elucidated.

5.5.2 The Effect of Ethanol and Ripeness Stage on Wine Chemical Composition

In 2016, the extended ripening of diseased grapes showed the potential to mitigate some of the effects of GRBV on the chemical composition of the wines. RB(+) 2H wines were generally higher in phenolic concentrations than RB(+) wines, agreeing with previous work that investigated the impact of a longer hangtime of grapes on phenolic composition in wines [24,25,34]. However, unlike results in 2016, tannin levels in 2017 were significantly lower in RB(+) 2H when compared to RB(+) and RB(+) S, which were previously similar during fermentation (Figure 5.1). In 2017, RB(+) 2H grapes were harvested one to two weeks later than in 2016, potentially increasing cell wall degradation [47,51–53]. Increased berry senescence can increase the binding of large polymeric compounds to the grape cell wall. Therefore, although extended ripening can potentially

alleviate the impact of GRBV on final wine composition, this is highly dependent on the ripening stage, where over-ripening can cause decreases in desired polymeric phenols in wines.

Overall, RB(+) wines were lower in volatile aroma compound concentrations than RB(–) wines, agreeing with previous results regarding the volatile profile of grapes [17]. The current study indicates that the volatile profile of RB(+) 2H wines were generally different than those of both RB(+) and RB(–). Previous research has shown that volatile accumulation is correlated with ripening in grapes [26,27,54,55]. Studies also indicated that alcohol content plays a significant role in the production of volatiles during winemaking, through yeast metabolism and chemical reactions, as well as the volatility of aroma compounds in a final wine [56,57]. The differences in alcohol content among these wines would contribute to a difference in volatility of aroma compounds and the formation of volatile compounds during fermentation, leading to all three wines being differentiated based on volatile composition.

On the other hand, chaptalizing the GRBV grape must in 2017 increased the chemical similarity between RB(+) S and RB(–) wines. In the case of CS 110R, the increase in polymerized phenolics in these two treatments most likely is a result of the higher alcohol content, leading to a longer malolactic fermentation (MLF). Previous work investigating the effects of the duration of MLF on secondary metabolite concentrations has shown that a longer duration of MLF caused decreases in anthocyanin concentrations while increasing polymerization [36]. In addition, research indicates that a higher prefermentative Brix, and therefore higher alcohol content, did not lead to higher anthocyanin extraction, but it did increase concentrations of polymeric phenols and pigments [24,34].

The alcohol content also largely impacted the volatile profiles of the final wines. For both rootstocks in 2017, the chaptalization of wine differentiated the volatile compound profile from

RB(+) wines. PCA results indicated that CS 110R RB(+) S wines positively correlated with HAs (Figure S5.1). HAs are formed through yeast metabolism of either sugar or amino acids (Ehrlich mechanism). Their production is increased with higher amounts of suspended solids, such as augmented sugar due to chaptalization [58]. Depending on their concentration, these compounds are responsible for fusel oil and solvent aromas in wines [59]. On the other hand, RB(–) wines were correlated to esters formed through enzymatic or acid-catalyzed condensation reactions of carboxylic acids and alcohols, and responsible for fruity and floral aromas [58]. In the current study, the chaptalization of CS 110R diseased grape musts increased HA formation during fermentation, differentiating RB(+) S wines from RB(–) wines (Figure S5.1).

5.5.3 Integrating Chemical and Sensorial Observations

MFA was used to visualize the correlations between chemical and sensorial observations (Figures 5.3–5.6). Between 82 and 100% of the variance was explained in the first two dimensions across seasons and rootstocks. CS 110R in 2016 had the best correlation between chemical and sensory data, although CS 420A in 2016 and 2017 also showed correlations between sensory and basic chemical and volatile data, while CS 110R in 2017 only exhibited correlations between sensory and phenolic datasets (Figure S5.2 and Table S5.4) [60].

In 2016, RB(–) and RB(+) 2H were positively correlated to alcohol content, hot mouthfeel, alcohol aroma, and many of the volatile compounds responsible for the fruity or floral aromas, such as esters and terpenes. This agrees with the previous research that showed higher alcohol content is associated with fruity and floral aromas [34]. For CS 110R in 2016, the color sensory attribute was highly correlated with anthocyanin concentrations and polymeric pigments, all of which were well correlated with RB(–) and, to a lesser degree, RB(+) 2H wines. The RB(+) wines

in 2016 were negatively correlated with the majority of aroma compounds, anthocyanins, and alcohol content compared to RB(–) wine and was rated lower in the related sensory attributes (Figure 5.3). On the other hand, in RB(+) 2H wines, total tannin concentrations and polymeric phenol concentrations were highly correlated with a dry mouthfeel, indicating a delayed harvest can lead to higher tannin levels and higher astringency in wines [22]. For CS 420A in 2016 (Figure 5.4a,b), RS and sweet taste were positively correlated with RB(–) and RB(+) 2H, and negatively correlated with RB(+) wines. All wines were dry with less than 0.2 g/L of RS. Therefore, the perceived sweet taste in the wines could have been related to higher ethanol concentrations, which are associated with darker fruits and perceived sweetness in wines [24,31,61].

The MFA for 110R wines in 2017 (Figure 5.5) could not separate the wine treatments well, which potentially is explained by their volatile and sensory profiles. RB(+) S wines were similar to RB(–) wines in terms of the volatile compound profile, yet different in terms of their sensory characteristics (Figure 5.2c and Table S5.3), whereas RB(+) S and RB(+) wines were positively correlated with soil, barnyard, savory, and black pepper attributes and negatively correlated with vanilla, red cherry, and dark fruit (Figure 5.5). The latter attributes were generally rated higher by panelists for RB(–) and RB(+) 2H than for RB(+) S and RB(+) wines. Previous findings suggest an increase in ethanol concentration can be detrimental to the aromatic profile of a wine, by the overwhelming alcohol aroma masking the fruity aromas contributed by esters [56,57,62,63]. Higher ethanol concentrations have also been associated with spicy flavors, astringency, and hot mouthfeel [34]. In addition, the higher concentration of HAs in RB(+) S wines are known to suppress fruity characteristics in wines [64]. These results suggest that although chemically the chaptalization of first harvested GRBV impacted grapes produced wines similar to RB(–) wines, the alcohol content may have been high enough to mask aromas from panelists' perceptions.

5.6 Conclusion:

This study investigated two potential mitigation strategies for GRBV: chaptalization and extending the ripening time of GRBV impacted grapes. Through chemical and sensorial analysis of the wines, it was determined that although chaptalization was able to increase the concentration of esters, terpenes, and HAs, this did not translate into fruitier aromas detected by sensory panelists. Overall, the chaptalized wines led to a decrease in anthocyanin concentrations, but an increase in polymeric pigments, which were similar to RB(–) wines. Therefore, although chemically the chaptalization of first harvested diseased grapes produced wines that were similar to RB(–) wines, panelists did not rate them similarly.

On the other hand, the sensory analysis found that a delayed harvest was able to increase the similarities between healthy and diseased grapes. Moreover, delayed harvest consistently increased concentrations of volatile and phenolic compounds compared to RB(+) wines. However, it is unknown whether this was driven by changes in the grape skin cell wall integrity and composition. Further research is needed to understand how GRBV alters grape skin cell walls during ripening.

Author Contributions: C.B, H.H, and A.O. conceived and planned experiments. A.R., R.C.G., C.B., and A.O. processed the grape and made the wines. A.R. and R.C.G carried out sample collection, and data acquisition for grapes and wines. A.C, H.H., and A.O. designed sensory evaluations. A.R., R.C.G, and A.C. conducted sensory evaluations. A.R., R.C.G, H.H., and A.O., contributed to interpretation of the results. A.R. took lead in writing manuscript. All authors provided critical feedback and helped shape the research, analysis, and manuscript.

Funding: The authors thank the American Vineyard Foundation (AVF, Grant number 2017-1675) and the Henry A. Jastro Scholarship for funding this work.

Acknowledgments: The authors thank the Agricultural and Environmental graduate group, the Horticulture and Agronomy graduate group, and the Viticulture and Enology Department at UC Davis. In addition, employees of the LEED Platinum Teaching and Research Winery at UC Davis for their help in winemaking.

Conflicts of Interest: The authors declare no conflict of interest.

Ethics Statement: All subjects gave their informed consent for inclusion prior to participating in this study. They study was conducted in accordance with the Declaration of Helsinki and the Institutional Review Board (IRB 699890-1) approved this study as exempt with project number HRP-213.

5.7 Supplemental Information:

Table S5.1 Total anthocyanin concentrations (mg/L) during fermentation via Wine X-ray analysis for wines in 2016 and 2017 (n=3).

Total Anthocyanins	2016							
Day of Fermentation	CS110 RB (-)	CS110 RB (+)	CS110 RB (+) 2H	CS420 RB (-)	CS420 RB (+)	CS420 RB (+) 2H		
0	--	--	--	--	--	--		
1	295.33 ± 28.15 b	251.00 ± 28.58 b	359.00 ± 12.53 a	263.33 ± 19.66 b	242.00 ± 18.38 b	327.67 ± 28.01 a		
2	512.67 ± 24.66 a	447.67 ± 67.02 a	512.33 ± 18.50 a	498.67 ± 20.60 ab	417.67 ± 48.60 b	524.00 ± 47.03 a		
3	750.67 ± 34.85 a	568.67 ± 19.40 b	693.33 ± 22.48 a	755.33 ± 17.01 a	642.00 ± 40.00 b	677.67 ± 64.63 ab		
4	968.67 ± 37.5 a	673.67 ± 31.66 c	842.00 ± 17.06 b	925.33 ± 29.26 a	772.00 ± 17.35 b	844.67 ± 49.24 ab		
5	1084.00 ± 33.42 a	744.00 ± 29.51 c	884.33 ± 14.01 b	1018.00 ± 7.00 a	837.33 ± 13.05 b	858.00 ± 41.58 b		
6	1100.67 ± 27.74 a	752.33 ± 16.65 c	927.33 ± 11.72 b	1017.67 ± 16.01 a	851.00 ± 19.52 b	914.33 ± 39.27 b		
7	1117.00 ± 28.35 a	753.33 ± 18.23 c	963.33 ± 2.08 b	1023.67 ± 13.32 a	857.00 ± 7.55 c	932.00 ± 30.79 b		
8	1097.33 ± 22.14 a	755.00 ± 14.11 c	970.00 ± 20.78 b	1017.00 ± 16.46 a	851.00 ± 11.27 c	938.67 ± 11.37 b		
Total Anthocyanins	2017							
Day of Fermentation	CS110R RB (-)	CS110R RB (+)	CS110R RB (+) S	CS110R RB (+) 2H	CS420A RB (-)	CS420A RB (+)	CS420A RB (+) S	CS420A RB (+) 2H
0	304.00 ± 8.54 a	261.00 ± 25.54 a	291.00 ± 25.06 a	282.33 ± 10.12 a	255.00 ± 6.56 a	221.00 ± 11.79 b	232.00 ± 6.24 b	215.67 ± 3.21 b
1	590.00 ± 27.73 a	391.67 ± 29.02 b	388.00 ± 6.00 b	358.67 ± 23.18 b	362.67 ± 26.27 a	302.33 ± 25.38a	328.67 ± 25.72 a	358.33 ± 20.84 a
2	743.00 ± 22.91a	478.00 ± 41.94 b	450.00 ± 21.00 b	486.67 ± 29.09 b	564.33 ± 9.61 a	431.00 ± 30.05 b	452.00 ± 15.62 b	528.33 ± 26.63 a
3	851.67 ± 16.26 a	576.00 ± 27.22 c	526.67 ± 19.30 c	642.67 ± 11.68 b	762.00 ± 16.37 a	598.33 ± 19.66 b	557.67 ± 74.54 b	659.67 ± 23.18 ab
4	900.33 ± 13.43 a	629.33 ± 28.02 c	573.33 ± 7.23 d	702.67 ± 6.81 b	855.00 ± 19.97 a	674.00 ± 13.08 bc	611.33 ± 85.24 c	745.33 ± 13.20 ab
5	950.33 ± 11.93 a	671.00 ± 25.51 c	613.00 ± 8.19 d	780.67 ± 5.13 b	931.00 ± 20.52 a	724.67 ± 14.47 bc	666.33 ± 55.08 c	791.33 ± 10.97 b
6	992.00 ± 9.54 a	702.67 ± 20.84 c	650.67 ± 3.21 d	808.67 ± 2.08 b	973.33 ± 15.57 a	751.33 ± 22.01 c	702.33 ± 30.62 c	812.00 ± 6.93 b
7	1000.33 ± 11.59 a	711.33 ± 16.80 c	673.00 ± 7.00 d	828.33 ± 13.65 b	1006.00 ± 14.73 a	769.00 ± 20.95 c	734.00 ± 14.73 c	815.33 ± 5.86 b
8	996.33 ± 10.97 a	711.67 ± 15.28 c	685.67 ± 8.14 c	792.33 ± 23.76 b	991.67 ± 14.29 a	757.67 ± 23.03 c	737.00 ± 13.45 c	812.67 ± 3.06 b
9	1000.00 ± 40.15 a	682.00 ± 13.45 c	661.33 ± 12.66 c	812.00 ± 22.52 b	--	--	--	--

Difference in letters indicates a significant difference between treatments for each rootstock after applying Tuckey's HSD test ($p<0.05$). CS110= Cabernet Sauvignon 110R, CS420= Cabernet Sauvignon 420A, RB=red blotch, (-)=negative, and (+)=positive, 2H= second harvest, NS= no sugar, S= chaptalization, ME=malvidin-3-glucoside equivalents, and CE=catechin equivalents.

Table S5.2 Total tannin concentrations during fermentation by Wine X-ray analysis for wines in 2016 and 2017 (n=3).

Total Tannins	2016							
Day of Fermentation	CS110 RB (-)	CS110 RB (+)	CS110 RB (+) 2H	CS420 RB (-)	CS420 RB (+)	CS420 RB (+) 2H		
0	--	--	--	--	--	--		
1	24.00 ± 0.00 a	24.00 ± 0.00 a	24.00 ± 0.00 a	24.00 ± 0.00 a	24.00 ± 0.00 a	24.00 ± 0.00 a		
2	24.00 ± 0.00 a	24.00 ± 0.00 a	24.00 ± 0.00 a	24.00 ± 0.00 a	24.00 ± 0.00 a	24.00 ± 0.00 a		
3	24.00 ± 0.00 b	24.00 ± 0.00 b	109.00 ± 28.35 a	87.00 ± 19.67 b	153.00 ± 53.08 ab	240.00 ± 75.48 a		
4	229.67 ± 28.29 a	83.00 ± 35.16 b	301.67 ± 24.01 a	333.67 ± 45.37 b	380.33 ± 15.37 ab	469.33 ± 65.59 a		
5	377.67 ± 21.22 a	212.33 ± 35.70 b	395.00 ± 19.29 a	458.67 ± 42.15 a	504.33 ± 13.01 a	525.33 ± 56.32 a		
6	422.33 ± 15.70 b	235.67 ± 18.58 c	485.33 ± 15.31a	476.67 ± 58.23 a	539.67 ± 21.73 a	601.00 ± 99.80 a		
7	499.00 ± 17.32 a	278.33 ± 38.80 b	527.67 ± 4.51a	524.00 ± 55.57 b	582.33 ± 2.52 ab	657.00 ± 35.93 a		
8	598.67 ± 19.66 a	363.67 ± 22.50 b	599.00 ± 29.51a	623.67 ± 92.51 a	674.33 ± 17.62 a	733.00 ± 7.00 a		
Total Tannins	2017							
Day of Fermentation	CS110R RB (-)	CS110R RB (+)	CS110R RB (+) S	CS110R RB (+) 2H	CS420A RB (-)	CS420A RB (+)	CS420A RB (+) S	CS420A RB (+) 2H
0	24.00 ± 0.00 a	24.00 ± 0.00 a	24.00 ± 0.00 a	24.00 ± 0.00 a	24.00 ± 0.00 a	24.00 ± 0.00 a	24.00 ± 0.00 a	24.00 ± 0.00 a
1	24.00 ± 0.00 a	24.00 ± 0.00 a	24.00 ± 0.00 a	24.00 ± 0.00 a	24.00 ± 0.00 a	24.00 ± 0.00 a	24.00 ± 0.00 a	24.00 ± 0.00 a
2	115.00 ± 20.30 a	31.67 ± 13.28 b	24.00 ± 0.00 b	24.00 ± 0.00 b	24.00 ± 0.00 a	24.00 ± 0.00 a	24.00 ± 0.00 a	51.67 ± 22.50 a
3	293.67 ± 10.02 a	172.00 ± 38.97 b	77.33 ± 31.72 c	146.00 ± 27.18 bc	259.33 ± 10.41 a	235.00 ± 33.60 a	177.33 ± 129.25 a	246.67 ± 19.09 a
4	404.00 ± 3.00 a	286.00 ± 44.40 b	193.67 ± 17.67 c	274.67 ± 7.51 b	408.33 ± 13.65 a	387.67 ± 37.07 a	299.00 ± 169.58 a	435.67 ± 18.18 a
5	517.67 ± 8.14 a	391.00 ± 48.87 b	309.33 ± 11.93 c	428.67 ± 4.04 b	563.00 ± 13.45 a	507.67 ± 27.32 a	438.67 ± 126.62 a	540.00 ± 19.47 a
6	568.00 ± 8.00 a	444.67 ± 45.21 b	371.00 ± 10.00 c	519.33 ± 13.50 a	677.67 ± 9.07 a	594.00 ± 21.00 a	551.33 ± 93.60 a	581.67 ± 14.84 a
7	625.33 ± 4.04 a	505.67 ± 45.08 b	444.00 ± 13.89 b	606.33 ± 15.57 a	749.33 ± 8.08 a	656.67 ± 10.02 b	638.33 ± 62.40 b	636.67 ± 8.50 b
8	669.00 ± 7.81 a	554.67 ± 44.60 b	534.00 ± 20.30 b	592.00 ± 24.58 b	771.67 ± 7.37 a	676.00 ± 4.36 b	679.33 ± 57.55 b	675.33 ± 12.66 b
9	813.33 ± 22.14 a	629.00 ± 33.81 b	611.33 ± 15.14 b	667.00 ± 32.45 b	--	--	--	--

Difference in letters indicates a significant difference between treatments after applying Tuckey's HSD test ($p<0.05$). CS110= Cabernet Sauvignon 110R, CS420= Cabernet Sauvignon 420A, RB=red blotch, (-)=negative, and (+)=positive, 2H= second harvest, NS= no sugar, S= chaptalization, ME=malvidin-3-glucoside equivalents, and CE=catechin equivalents.

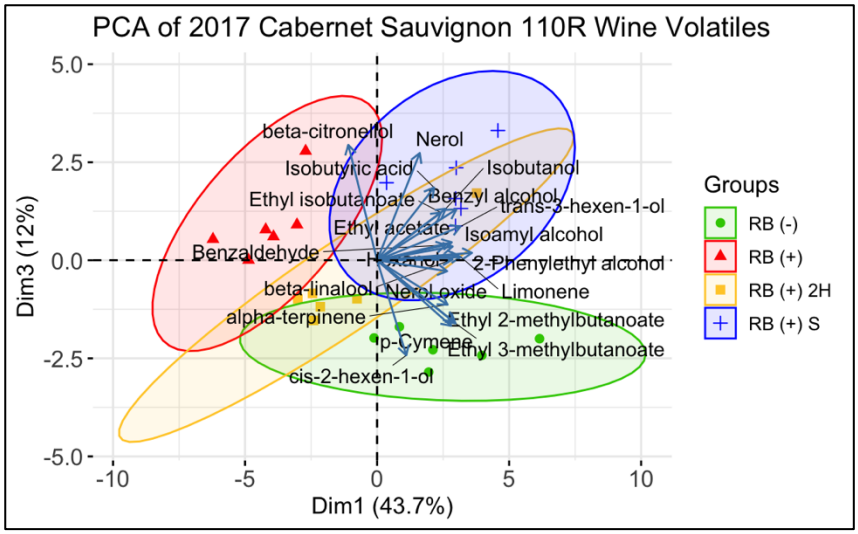

Figure S5.1 Principal component analysis of the first and third dimension for volatile compounds in CS 110R wines made in 2017. Ellipses are drawn to 95% confidence with an n=6 for two bottle replicates for each fermentor replicate. Only the highest 20 significant volatile compounds that contribute to the variance are plotted. CS110= Cabernet Sauvignon 110R, RB=red blotch, (-)=negative, and (+)=positive, 2H= second harvest, S=chaptalization.

Table S5.3 Significantly different sensory attributes of wines made in 2016 and 2017 as determined through descriptive analysis.

	2016						
	CS110R				CS420A		
Sensory Attribute	RB (-)	RB (+)	RB (+) 2H	Sensory Attribute	RB (-)	RB (+)	RB (+) 2H
Sour	1.88 ± 0.38 b	2.35 ± 0.43 a	2.27 ± 0.17 ab	Alcohol	2.75 ± 0.32 a	2.32 ± 0.28 b	2.84 ± 0.34 a
Hot	2.29 ± 0.23 a	1.48 ± 0.22 c	1.74 ± 0.17 b	Sweet	1.93 ± 0.37 ab	1.57 ± 0.39 b	2.03 ± 0.34 a
Dry	1.86 ± 0.30 b	1.65 ± 0.19 b	2.15 ± 0.22 a	Viscous	2.17 ± 0.34 b	2.24 ± 0.41 ab	2.58 ± 0.24 a
Viscous	2.58 ± 0.27 a	2.21 ± 0.46 a	2.22 ± 0.35 a				
Color	23.19 ± 0.97 a	18.36 ± 1.64 b	22.11 ± 1.35 a				
	2017						
	CS110R				CS420A		
Sensory Attribute	RB (-)	RB (+)	RB (+) S	RB (+) 2H	Sensory Attribute	RB (-)	RB (+)	RB (+) S
Dark Fruit	3.59 ± 0.31 a	2.27 ± 0.55 c	2.37 ± 0.80 bc	3.20 ± 0.51 ab	Hot	4.60 ± 0.58 a	3.28 ± 0.54 b	4.23 ± 0.45 a
Red Cherry	2.59 ± 0.44 a	1.61 ± 0.77 b	1.22 ± 0.43 b	2.93 ± 0.63 a				
Vanilla	1.51 ± 0.22 a	1.26 ± 0.30 ab	0.90 ± 0.49 b	1.84 ± 0.42 a				
Black Pepper	1.20 ± 0.47 ab	1.45 ± 0.47 a	1.79 ± 0.50 a	0.63 ± 0.31 b				
Barnyard	1.79 ± 0.74 b	2.74 ± 0.53 a	2.80 ± 0.52 a	1.69 ± 0.51 b				
Soil	0.71 ± 0.37 a	0.92 ± 0.44 a	1.16 ± 0.50 a	0.55 ± 0.31 a				
Savory	1.56 ± 0.68 bc	2.59 ± 0.82 ab	3.08 ± 0.80 a	1.40 ± 0.51 c				
Astringency	3.62 ± 0.75 ab	3.97 ± 0.41 a	4.54 ± 0.89 a	2.55 ± 0.71 b				
Hot	4.15 ± 1.21 ab	2.98 ± 0.67 b	4.27 ± 0.51 a	3.56 ± 0.55 ab				

CS110= Cabernet Sauvignon 110R, CS 420A= Cabernet Sauvignon 420A, RB=red blotch, (-)=negative, and (+)=positive, 2H= second harvest, S=chaptalization.

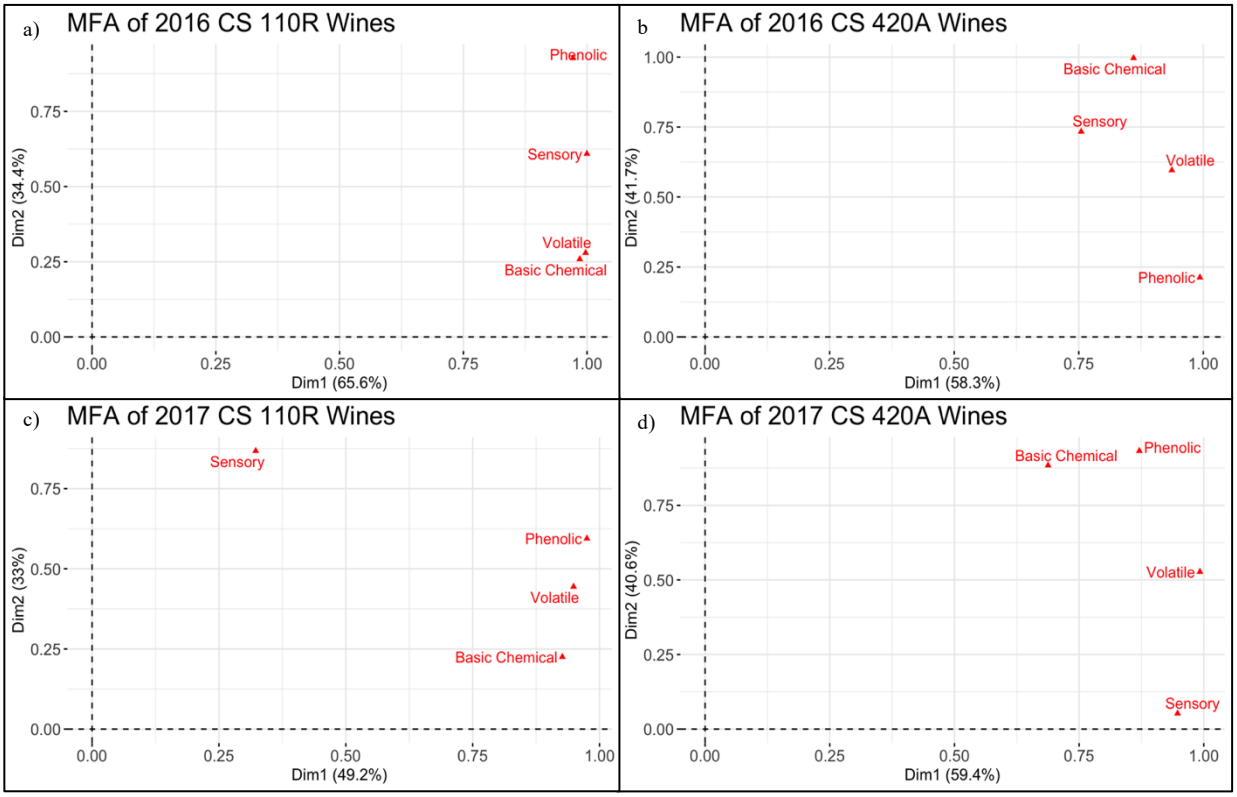

Figure S5.2. Multifactor analysis of the groups of variables that were used to analyze the wines: sensory profile volatile profile, phenolic profile, and basic chemical parameters at bottling. a) CS 110R wines made in 2016, b) CS 420A wines made in 2016, c) CS 110R wines made in 2017, and d) CS 420A wines made in 2017. CS110= Cabernet Sauvignon 110R, and CS420= Cabernet Sauvignon 420A.

Table S5.4 RV coefficients to compare each data set in the multifactor analysis of each rootstock and season. Significant RV coefficients are indicated in bold lettering.

Comparison	RV Coefficient			
	CS 110R 2016	CS 420A 2016	CS 110R 2017	CS 420A 2017
Sensory vs. Phenolic	0.28	0.43	**0.81**	0.09
Sensory vs. Volatile	**0.80**	0.47	0.28	0.51
Sensory vs. Basic Chemical	**0.76**	**0.51**	0.18	**0.68**
Phenolic vs. Volatile	**0.80**	0.22	0.24	0.19
Phenolic vs. Basic Chemical	0.10	0.33	0.16	0.04
Volatile vs. Basic Chemical	**0.91**	**0.86**	**0.56**	**0.82**

CS= Cabernet Sauvignon, phenolic= phenolic profile of wines, volatile= volatile profile of wines, basic chemical= chemical data from bottling

Table S5.5 List of sensory attributes that were used in 2016 and the recipes to make each standard.

	Aroma	Recipe
1	dark fruit	three thawed crushed blackberry plus 1 frozen dark cherry
2	strawberry	2 small pieces of frozen strawberry + 10 ml wine
3	banana -fresh	1 x 1cm circle of fresh banana, no peel
4	pear	20 mL R.W. Knudsen Pear juice + 10 grams of fresh pear
5	apple	15 g sliced fresh Grannysmith green apple, 20 mL base wine
6	citrus	0.15 g fresh tangerine peel + 0.1 g fresh lemon peel + 0.1 g fresh grapefruit peel
7	fresh veg	10 g McCains Frozen Sliced Green Beans + 10 g McCains Frozen Green Peas + 1 g bell pepper NO WINE
8	vegetation	0.1 g "birdsfoot trefoil green" +0.1 g "assorted green leves"
9	floral	1/2 tspn Rose water (Monin) + Few Dry petals + 1/2 tspn Violet water
10	spice	1/2 tsp all spice
11	leather	20 mL base wine plus 2 leather show lace strips, 3 inches brown, 3 inches tan
12	vanilla	2ml McCormick Pure Vanilla extract + 25 ml wine
13	earthy	0.3 g dried mushroom 1 tps potting soil + 2 drops of water
14	oak	1 Am Oak cube M+ with 1 French Oak Cube Light + 1 Fench Oak Cube M in 20 mL wine
15	alcohol	20 mL Everclear 30 mL base wine
16	yeasty	1/8 teaspoon active dry yeast + 10 mL demineralized water
17	mineral	1 tbsp gravel in 5 mL mineral water (investigate other rocks and decarbonated sparkling water)
18	black pepper	two turns of black pepper mill
	Taste	**Recipe**
1	sour	3.5 g/L tartaric acid
2	bitter	1.25 g/L caffein
3	sweet	20 g/L sucrose
	Mouthfeel	**Recipe**
1	hot	Alcohol Hotness (300 mL/L seagrams vodka)
2	dry	Dry (1.3 g/L alum)
3	viscous	Viscous (3 g/L CMC)
4	grippy	Drawing or tightening sensation felt in the mouth, lips and/or cheeks, lack of slip between mouth surfaces resulting in the inability to easily move mouth surfaces across each other
5	puckery	white vinegar (200 mL/L)
6	effervescent	sparkling mineral water

Table S5.6 List of sensory attributes used in 2017 and the recipes to make each sensory standard.

	Aroma	**Recipe**
1	dark fruit	3 thawed crushed blackberries + 1 thawed dark cherry + 5ml of black currant juice+1 teaspoon of black currant jam+10ml of base wine
2	strawberry	1 small, cut, thawed strawberry
3	red cherry	3 crushed, fresh cherries + 1/2 tablespoon of black cherry jam +10 ml of black cherry juice
4	dried fruit	2g of raisins + 2g of dates + 2g of appricots all crushed
5	green	5 g Frozen Sliced Green Beans + 4 blades of grass + 5 g bell pepper
6	chocolate	10g of dark chocolate (baking chocolate)
7	soil/earthy	1 teaspoon of potting soil + 2.5g of fresh chopped mushroom + 10ml of mineral water
8	musty	1g of ripped cardboard + 5mL of tap water
9	wood cedar	1 piece of ceddar + 10ml of base wine
10	black pepper	2 pinches of black peppper
11	mulling spice +vanilla	1/8 teaspoon cinnamon + 1/8 teaspoon whole all spice + 1/8 teaspoon ground cloves + 1 drop of vanilla + 40ml of base wine
12	barnyard	1/8 teaspoon white pepper + 20ml base wine
13	floral	(3 drops) of rose water+ 3 drops of orange blossom+20ml of base wine
14	flint/mineral	5 rocks + 10mL of tap water
15	savory	1 drop of liquid smoke+ 50ml of base wine
16	alcohol	20 mL Everclear Vodka + 30 mL base wine
	Taste	**Recipe**
1	Sour	3 g/L tartaric acid
2	Bitter	1.5 g/L Caffein
3	Sweet	15g/L sucrose
4	Salty	2 g/L table salt
	Mouthfeel	**Recipe**
1	Hot/Burning	350ml/L of Vodka in water; 150ml/L of Vodka; 50ml/L of Vodka
2	Viscous	3g/L of CMC in water; 1.5g/L of CMC; pure water
3	Astringent	3g/L of Alum in water; 1.5g/L of Alum; 0.5/L Alum

5.8 References:

1. Dolja, V. V; Meng, B.; Martelli, G.P. Evolutionary Aspects of Grapevine Virology. In *Grapevine Viruses: Molecular Biology, Diagnostics and Management*; Meng, B., Martelli, G.P., Golino, D.A., Fuchs, M., Eds.; Springer International Publishing, 2017; pp. 659–688 ISBN 978-3-319-57706-7.
2. Krenz, B.; Thompson, J.R.; Fuchs, M.; Perry, K.L. Complete Genome Sequence of a New Circular DNA Virus from Grapevine. *J. Virol.* 2012, *86*, 7715–7715.
3. Rwahnih, M. Al; Dave, A.; Anderson, M.M.; Rowhani, A.; Uyemoto, J.K.; Sudarshana, M.R. Association of a DNA Virus with Grapevines Affected by Red Blotch Disease in California. *Phytopathology* 2013, *103*, 1069–1076.
4. Krenz, B.; Thompson, J.R.; Mclane, H.L.; Fuchs, M.; Perry, K.L. Phyto-02-14-0053-R. 2014, 1232–1240.
5. Poojari, S.; Lowery, D.T.; Rott, M.; Schmidt, A.M.; Úrbez-Torres, J.R. Incidence, distribution and genetic diversity of Grapevine red blotch virus in British Columbia. *Can. J. Plant Pathol.* 2017, *39*, 201–211.
6. Reynard, J.; Gugerli, P. Effects of Grapevine red blotch-associated virus on vine physiology and fruit composition of field grown grapevine cv . Gamay. 2014.
7. Lim, S.; Igori, D.; Zhao, F.; Moon, J.; Cho, I.-S.; Choi, G.-S. First report of Grapevine red blotch-associated virus on grapevine in Korea. *Plant Dis.* 2016, *100*, 1957.
8. Gasperin-Bulbarela, J.; Licea-Navarro, A.F.; Pino-Villar, C.; Hernandez-Martínez, R.; Carrillo-Tripp, J. First report of grapevine´ red blotch virus in Mexico. *Plant Dis.* 2019, *103*, 381.
9. Luna, F.; Debat, H.; Gomez-Talquenca, S.; Moyano, S.; Zavallo, D.; Asurmendi, S. First report of grapevine red blotch virus infecting grapevine in Argentina. *J. Plant Pathol.* 2019, *101*.
10. Marwal, A.; Kumar, R.; Paul Khurana, S.M.; Gaur, R.K. Complete nucleotide sequence of a new geminivirus isolated from Vitis vinifera in India: a symptomless host of Grapevine red blotch virus. *VirusDisease* 2019, *30*, 106–111.
11. Yepes, L.M.; Cieniewicz, E.; Krenz, B.; McLane, H.; Thompson, J.R.; Perry, K.L.; Fuchs, M. Causative Role of Grapevine Red Blotch Virus in Red Blotch Disease. *Phytopathology* 2018, *108*, 902–909.
12. Calvi, B.L. Effects Of Red-leaf Disease On Cabernet Sauvignon At The Oakville Experimental Vineyard And Mitigation By Harvest Delay And Crop Adjustment, University of California, Davis, 2011.
13. Sudarshana, M.R.; Perry, K.L.; Fuchs, M.F. Grapevine Red Blotch-Associated Virus, an Emerging Threat to the Grapevine Industry Mysore. *Phytopathology* 2015, 1026–1032.
14. Girardello, R.C.; Cooper, M.L.; Smith, R.J.; Lerno, L.A.; Bruce, R.C.; Eridon, S.; Oberholster, A. Impact of Grapevine Red Blotch Disease on Grape Composition of Vitis vinifera Cabernet Sauvignon, Merlot, and Chardonnay. *J. Agric. Food Chem.* 2019, *67*, 5496–5511.
15. Martínez-Lüscher, J.; Plank, C.M.; Brillante, L.; Cooper, M.L.; Smith, R.J.; Al-Rwahnih, M.; Yu, R.; Oberholster, A.; Girardello, R.; Kurtural, S.K. Grapevine Red Blotch Virus May Reduce Carbon Translocation Leading to Impaired Grape Berry Ripening. *J. Agric. Food Chem.* 2019, *67*, 2437–2448.
16. Wallis, C.M.; Sudarshana, M.R.; Girardello, R.C.; Cooper, M.L.; Smith, R.J.; Lerno, L.A.;

Bruce, R.C.; Eridon, S.; Oberholster, A. Effects of Grapevine red blotch-associated virus (GRBaV) infection on foliar metabolism of grapevines. *Can. J. Plant Pathol.* 2016, *38*, 5496–5511.
17. Rumbaugh, A.C.; Girardello, R.C.; Cooper, M.L.; Plank, C.M.; Kurtural, S.K.; Oberholster, A. Impact of Rootstock and Season on Red Blotch Disease Expression in Cabernet Sauvignon (V. vinifera). 2021, *10*, 1–16.
18. Girardello, R.C.; Cooper, M.L.; Lerno, L.A.; Brenneman, C.; Eridon, S.; Sokolowsky, M.; Heymann, H.; Oberholster, A. Impact of Grapevine Red Blotch Disease on Cabernet Sauvignon and Merlot Wine Composition and Sensory Attributes. *Molecules* 2020, *25*.
19. Bowen, P.; Bogdanoff, C.; Poojari, S.; Usher, K.; Lowery, T.; Úrbez-Torres, J.R. Effects of grapevine red blotch disease on cabernet franc vine physiology, bud hardiness, and fruit and wine quality. *Am. J. Enol. Vitic.* 2020, *71*, 308–318.
20. Coombe, B.G.; Mccarthy, M.G. Dynam ics of grape berry grow th and physiology of ripening. *Aust. J. Grape Wine Res.* 2000, *6*, 131–135.
21. Keller, M. *The Science of Grapevines: Anatomy and Physiology*; 2nd ed.; Elsevier Science: San Diego, 2015;
22. Bondada, B.; Harbertson, E.; Shrestha, P.M.; Keller, M. Temporal extension of ripening beyond its physiological limits imposes physical and osmotic challenges perturbing metabolism in grape (Vitis vinifera L.) berries. *Sci. Hortic. (Amsterdam).* 2017, *219*, 135–143.
23. Coombe, B.G. The Grape Berry as a Sink. *Acta Hortic.* 1989, *239*, 149–158.
24. Casassa, L.F.; Beaver, C.W.; Mireles, M.; Larsen, R.C.; Hopfer, H.; Heymann, H.; Harbertson, J.F. Influence of fruit maturity, maceration length, and ethanol amount on chemical and sensory properties of Merlot wines. *Am. J. Enol. Vitic.* 2013, *64*, 437–449.
25. Bautista-Ortín, A.B.; Fernández-Fernández, J.I.; López-Roca, J.M.; Gómez-Plaza, E. The effect of grape ripening stage on red wine color. *J. Int. des Sci. la Vigne du Vin* 2006, *40*, 15–24.
26. Canuti, V.; Conversano, M.; Calzi, M.L.; Heymann, H.; Matthews, M.A.; Ebeler, S.E. Headspace solid-phase microextraction-gas chromatography-mass spectrometry for profiling free volatile compounds in Cabernet Sauvignon grapes and wines. *J. Chromatogr. A* 2009, *1216*, 3012–3022.
27. Kalua, C.M.; Boss, P.K. Evolution of volatile compounds during the development of cabernet sauvignon grapes (vitis vinifera l.). *J. Agric. Food Chem.* 2009, *57*, 3818–3830.
28. Palomo, E.S.; Díaz-Maroto, M.C.; Viñas, M.A.G.; Soriano-Pérez, A.; Pérez-Coello, M.S. Aroma profile of wines from Albillo and Muscat grape varieties at different stages of ripening. *Food Control* 2007, *18*, 398–403.
29. Bindon, K.; Holt, H.; Williamson, P.O.; Varela, C.; Herderich, M.; Francis, I.L. Relationships between harvest time and wine composition in Vitis vinifera L. cv. Cabernet Sauvignon 2. Wine sensory properties and consumer preference. *Food Chem.* 2014, *154*, 90–101.
30. Lerno, L.; Reichwage, M.; Panprivech, S.; Ponangi, R.; Hearne, L.; Oberholster, A.; Block, D.E. Chemical gradients in pilot-scale cabernet sauvignon fermentations and their effect on phenolic extraction. *Am. J. Enol. Vitic.* 2017, *68*, 401–411.
31. Bindon, K.A.; Madani, S.H.; Pendleton, P.; Smith, P.A.; Kennedy, J.A. Factors affecting skin tannin extractability in ripening grapes. *J. Agric. Food Chem.* 2014, *62*, 1130–1141.
32. Medina-Plaza, C.; Beaver, J.W.; Lerno, L.; Dokoozlian, N.; Ponangi, R.; Blair, T.; Block,

D.E.; Oberholster, A. Impact of temperature, ethanol and cell wall material composition on cell wall-anthocyanin interactions. *Molecules* 2019, *24*, 8–11.
33. Kassara, S.; Kennedy, J.A. Relationship between red wine grade and phenolics. 2. Tannin composition and size. *J. Agric. Food Chem.* 2011, *59*, 8409–8412.
34. Sherman, E.; Greenwood, D.R.; Villas-Boâs, S.G.; Heymann, H.; Harbertson, J.F. Impact of grape maturity and ethanol concentration on sensory properties of Washington State merlot wines. *Am. J. Enol. Vitic.* 2017, *68*, 344–356.
35. Costello, P.J.; Francis, I.L.; Bartowsky, E.J. Variations in the effect of malolactic fermentation on the chemical and sensory properties of cabernet sauvignon wine: Interactive influences of oenococcus oeni strain and wine matrix composition. *Aust. J. Grape Wine Res.* 2012, *18*, 287–301.
36. López, R.; López-Alfaro, I.; Gutiérrez, A.R.; Tenorio, C.; Garijo, P.; González-Arenzana, L.; Santamaría, P. Malolactic fermentation of Tempranillo wine: Contribution of the lactic acid bacteria inoculation to sensory quality and chemical composition. *Int. J. Food Sci. Technol.* 2011, *46*, 2373–2381.
37. Iland, P.; Bruer, N.; Edwards, G.; Weeks, S.; Wilkes, E. *Chemical Analysis of Grapes and Wine: Techniques and Concepts.*; Patrick Iland Wine Promotions PTY LTD: Campbelltown SA, Australia, 2004;
38. Harbertson, J.F.; Mireles, M.; Yu, Y. Improvement of BSA tannin precipitation assay by reformulation of resuspension buffer. *Am. J. Enol. Vitic.* 2015, *66*, 95–99.
39. Harbertson, J.F.; Picciotto, E.A.; Adams, D.O. Measurement of Polymeric Pigments in Grape Berry Extract sand Wines Using a Protein Precipitation Assay Combined with Bisulfite Bleaching. *Am. J. Enol. Vitic.* 2003, *54*, 301–306.
40. Peng, Z.; Iland, P.G.; Oberholster, A.; Sefton, M.A.; Waters, E.J. Analysis of pigmented polymers in red wine by reverse phase HPLC. *Aust. J. Grape Wine Res.* 2002, *8*, 70–75.
41. Hendrickson, D.A.; Lerno, L.A.; Hjelmeland, A.K.; Ebeler, S.E.; Heymann, H.; Hopfer, H.; Block, K.L.; Brenneman, C.A.; Oberholster, A. Impact of mechanical harvesting and optical berry sorting on grape and wine composition. *Am. J. Enol. Vitic.* 2016, *67*, 385–397.
42. Lawless, H.; Heymann, H. *Sensory evaluation of food: Principles and practices*; Springer New York: New York, NY, 1998;
43. Kassambara, A. Practical guide to principal component methods in R Available online: Stdha.com.
44. Marquez, A.; Perez-Serratosa, M.; Varo, M.A.; Merida, J. Effect of temperature on the anthocyanin extraction and color evolution during controlled dehydration of tempranillo grapes. *J. Agric. Food Chem.* 2014, *62*, 7897–7902.
45. Hernández-Hierro, J.M.; Quijada-Morín, N.; Martínez-Lapuente, L.; Guadalupe, Z.; Ayestarán, B.; Rivas-Gonzalo, J.C.; Escribano-Bailón, M.T. Relationship between skin cell wall composition and anthocyanin extractability of Vitis vinifera L. cv. Tempranillo at different grape ripeness degree. *Food Chem.* 2014, *146*, 41–47.
46. Bindon, K.A.; Bacic, A.; Kennedy, J.A. Tissue-specific and developmental modifications of grape cell walls influence the adsorption of proanthocyanidins. *J. Agric. Food Chem.* 2012, *60*, 9249–9260.
47. Beaver, J.W.; Medina-Plaza, C.; Miller, K.; Dokoozlian, N.; Ponangi, R.; Blair, T.; Block, D.; Oberholster, A. Effects of the Temperature and Ethanol on the Kinetics of Proanthocyanidin Adsorption in Model Wine Systems. *J. Agric. Food Chem.* 2019.

48. Springer, L.F.; Sacks, G.L. Protein-precipitable tannin in wines from Vitis vinifera and interspecific hybrid grapes (Vitis ssp.): Differences in concentration, extractability, and cell wall binding. *J. Agric. Food Chem.* 2014, *62*, 7515–7523.
49. Bautista-Ortín, A.B.; Molero, N.; Marín, F.; Ruiz-García, Y.; Gómez-Plaza, E. Reactivity of pure and commercial grape skin tannins with cell wall material. *Eur. Food Res. Technol.* 2014, *240*, 645–654.
50. Bautista-Ortín, A.B.; Molero, N.; Marín, F.; Ruiz-García, Y.; Gómez-Plaza, E. Reactivity of pure and commercial grape skin tannins with cell wall material. *Eur. Food Res. Technol.* 2015, *240*, 645–654.
51. Pedneault, K.; Dorais, M.; Angers, P. Flavor of cold-hardy grapes: Impact of berry maturity and environmental conditions. *J. Agric. Food Chem.* 2013, *61*, 10418–10438.
52. Deluc, L.G.; Grimplet, J.; Wheatley, M.D.; Tillett, R.L.; Quilici, D.R.; Osborne, C.; Schooley, D.A.; Schlauch, K.A.; Cushman, J.C.; Cramer, G.R.; et al. Transcriptomic and metabolite analyses of Cabernet Sauvignon grape berry development. *BMC Genomics* 2013, *61*, 10418–10438.
53. Goldner, M.C.; Zamora, M.C.; Lira, P.D.L.; Gianninoto, H.; Bandoni, A. Effect of ethanol level in the perception of aroma attributes and the detection of volatile compounds in red wine. *J. Sens. Stud.* 2009, *24*, 243–257.
54. Robinson, A.L.; Ebeler, S.E.; Heymann, H.; Boss, P.K.; Solomon, P.S.; Trengove, R.D. Interactions between wine volatile compounds and grape and wine matrix components influence aroma compound headspace partitioning. *J. Agric. Food Chem.* 2009, *57*, 10313–10322.
55. Waterhouse, A.L.; Sacks, G.L.; Jeffery, D.W. *Understanding Wine Chemistry*; 2016; ISBN 9781118627808.
56. Cameleyre, M.; Lytra, G.; Tempere, S.; Barbe, J.C. Olfactory Impact of Higher Alcohols on Red Wine Fruity Ester Aroma Expression in Model Solution. *J. Agric. Food Chem.* 2015, *63*, 9777–9788.
57. Josse, J.; Pagès, J.; Husson, F. Testing the significance of the RV coefficient. *Comput. Stat. Data Anal.* 2008, *53*, 82–91.
58. Heymann, H.; Licalzi, M.; Conversano, M.R.; Bauer, A.; Skogerson, K.; Matthews, M. Effects of extended grape ripening with or without must and wine alcohol manipulations on cabernet sauvignon wine sensory characteristics. *South African J. Enol. Vitic.* 2013, *34*, 86–99.
59. Escudero, A.; Campo, E.; Fariña, L.; Cacho, J.; Ferreira, V. Analytical characterization of the aroma of five premium red wines. Insights into the role of odor families and the concept of fruitiness of wines. *J. Agric. Food Chem.* 2007, *55*, 4501–4510.
60. Villamor, R.R.; Evans, M.A.; Ross, C.F. Effects of ethanol, tannin, and fructose concentrations on sensory properties of model red wines. *Am. J. Enol. Vitic.* 2013, *64*, 342–348.
61. De-La-Fuente-Blanco, A.; Sáenz-Navajas, M.P.; Ferreira, V. On the effects of higher alcohols on red wine aroma. *Food Chem.* 2016, *210*, 107–114.

CHAPTER 6

CONCLUSION

Geminiviruses detrimentally impact crops around the world by reducing yields or decreasing crop quality. Currently, deep sequencing and other technological advancements are increasing the number of new geminiviruses discovered worldwide. Factors associated with globalization, such as exchanging crop material, are potentially initiating new occurrences of diseases and epidemics correlated to geminiviruses in crops. *Vitis vinifera* is one of the most susceptible crops to viral infection. Prior to the identification of GRBV, the most damaging viruses to the grape and wine industry were grapevine fanleaf virus (GFLV) and grapevine leafroll-associated viruses (GLRaV).

Since its identification, GRBV presence has been reported in vineyards worldwide and raisin and table grapes. Overall, GRBV and GLRaV cause similar foliar symptoms in grapevines with analogous effects on grape and wine composition. However, unlike GLRaV, GRBV is a single-stranded (ss)-DNA geminivirus. GRBV foliar symptoms consist of interveinal reddening with the veins becoming red in red cultivars and interveinal area of leaves of white cultivars becoming chlorotic. Since these symptoms are also like some nutrient deficiencies, molecular testing is recommended to accurately test for the presence of GRBV in a vineyard. Currently, no sources of GRBV resistance have been documented. Nevertheless, variable responses to GRBV infection have been reported elsewhere as well as in the work detailed in this dissertation. Since the economic impact of GRBV currently is reported to range from $2,213/ha to $68,548/ha in the United States, research has focused on identifying important plant-pathogen interactions, the viral impact on grape metabolism and wine composition, and developing mitigation strategies.

This work evaluated how grapevine genotype and environment influence the disease outcome in grapevines infected with GRBV. We examined GRBV infected grapevines across multiple

rootstocks, varieties, sites as well as seasons. This work indicated that seasonal differences considerably impact GRBD outcome in grapevines, whereas genotypic influences are less apparent. Specifically, fewer differences in primary metabolites and the grape transcriptome between RB(+) grapes and RB(-) grapes were observed in 2017 than in 2016. This was concurrent with increased induction of a VIGS transcript, DCL2. Since 2017 was a warmer season than 2016, we suggest that transcription of DCL2 is potentially dependent and positively correlated with temperature increases.

Interestingly, we uncovered a transcriptional shift in GRBV infected grapes, causing a gain in co-expression between DCL2 and several transcripts related to transcription and translation processes. Consequently, DCL2 loses co-expression with transcripts related to primary and secondary metabolism. This work potentially uncovered a connection between the observed impairment to ripening events in GRBV infected grapes and the transcription of DCL2. In addition, DCL2 was only significantly enriched at veraison. For the first time, our study identified a key antiviral plant response potentially associated with a specific phenological stage and dependent on growing temperature.

Furthermore, we determined that CS on 420A rootstock was less sensitive to GRBV infection than CS on 110R rootstock. This was seen in secondary metabolite levels, sugar accumulation, and the grape transcriptome in 2017. Specifically, in 2017 GRBV infection impacted anthocyanin accumulation in CS 110R grapes more than CS 420A. In conjunction, GRBV enriched specific plant-pathogen interactions at pre-veraison in CS 420A in both seasons and CS in 2016. These same pathways were not induced until harvest for CS 110R in 2017, suggesting a differential response to GRBV infection. We hypothesize that the difference in vigor

and drought resistance in the two rootstocks led to a difference in the microclimate of the grapevine and berry composition.

Due to differences in phenolic extractability, our research analyzed the impact GRBV has on grape cell wall metabolism. Transcriptomic analysis suggested that induction of cell wall degradation processes during GRBV infection is attempting to solubilize the cell wall polysaccharides to support the energy demands of the virus. However, translatable differences in the cell wall composition of the grape exocarp were not observed. Alternatively, the significantly higher amounts of pectin and soluble proteins in GRBV fruit did correlate to the enrichment of related transcripts and decreases in polymeric pigment extraction. These differences can potentially explain the decreases in phenolic extractability during winemaking.

Finally, this study investigated two potential mitigation strategies for GRBV: extending the ripening time and chaptalization of GRBV impacted grapes. Although chaptalization increased the production of esters, terpenes, and higher alcohols, this did not translate to fruitier aromas detected by sensory panelists. On the other hand, sensory analysis found that a delayed harvest could increase the similarities between healthy and diseased grapes. Moreover, delayed harvest consistently increased concentrations of volatile and phenolic compounds compared to RB (+) wines. Although, extending the ripening time of GRBV infected grapes was dependent on seasonal conditions, and, therefore, may not be the most robust mitigation method.

This work revealed several factors about GRBV infections in grapevines that were previously unknown and uncovered new questions that need to be answered. Although this work was essential in understanding some of the plant-pathogen interactions, future work is needed to expand our knowledge of GRBV infections in grapevines. A deeper analysis of the grape cell wall metabolism, analysis of specific pathogenesis related proteins, and the methylation of cell wall

pectin under GRBV infections needs to be investigated. In addition, further analysis of how temperature can impact the expression of DCL2 and how this relates to symptom development is needed. Finally, continual exploration for potential resistant genotypes is necessary to aid the grape and wine industry. The work detailed in this project led to these future research questions and increased our understanding of the interactions between GRBV and the grapevine.

Appendix A

Longer cluster hanging time improves grape and wine quality of *Vitis vinifera* L. Merlot impacted by grapevine red blotch disease

Formatted for publication in *Food Science International* (submitted)

Raul C. Girardello[1], Arran Rumbaugh [1,] Anji Perry[2], Hildegarde Heymann[1], Charles Brenneman[1] and Anita Oberholster[1*].

[1]Department of Viticulture and Enology, University of California, Davis, CA 95616-8749, USA

[2]J Lohr Vineyards and Wines, Paso Robles, CA 93446, USA.

*Correspondent Author: aoberholster@ucdavis.edu

1136 Robert Mondavi Institute North - 595 Hilgard Lane. Davis, CA 95616-5270 U.S.A

A.1 Abstract:

Grapevine red blotch virus (GRBV) is a recently discovered virus that has become a major concern for the grape and wine industry in California. GRBV has been confirmed in several states in the US, Canada, Mexico, South Korea, and Switzerland. Prior research indicated that GRBV delays grape ripening resulting in reduced °Brix and anthocyanin concentrations, with variable impacts on other phenolic compounds when compared to fruit from healthy vines. The difference in sugar concentration at harvest resulted in significantly higher ethanol concentrations in wines made with fruit from healthy vines compared to diseased vines, which strongly impacted sensory properties. In the current study, chaptalization and sequential harvesting were employed utilizing *Vitis vinifera* L. cv Merlot (Paso Robles, CA) in the 2016 and 2017 seasons. GRBV infected grapevines were harvested at the same time as healthy vines as well as at a later date when they reached the total soluble solids (TSS, mostly sugars expressed in °Brix) content of the healthy vines. Basic chemical parameters (°Brix, pH, titratable acidity (TA), ethanol percentage (wine)), phenolic and volatile

profiles of grapes and their subsequent wines were measured. Additionally, wine sensory properties were determined by descriptive analyses. Chemical analysis demonstrated that GRBV increased TA and decreased sugar accumulation and anthocyanin synthesis in grapes. Wines made from GRBV grapes harvested at a later ripening stage showed less impact of the disease, producing wines with chemical, phenolic and volatile profiles as well as sensory properties more similar to wines made from healthy fruit when compared to wines made from GRBV fruit harvested earlier. The longer hang time of GRBV grapes was shown to be a potential strategy to mitigate the impacts of grapevine red blotch disease.

Key Words: Red Blotch disease, sequential harvest, grape, wine, phenolics, volatiles, sensory.

A.2 Introduction:

It is well known that grapes go through several physical, physiological and biochemical changes during ripening that directly impact berry composition (Adams, 2006; Castellarin et al., 2015; Pirie & Mullins, 1977). From the winemaking point of view, grape composition at harvest is one of the most critical factors in order to make quality wines. Several parameters are taken into consideration by viticulturists and winemakers to decide the ideal harvest time. Berry sugar concentration, especially glucose and fructose, increases during berry ripening and influences wine style since it is proportional to final ethanol concentration (B. G. Coombe, 1992). Ethanol concentration influences the extraction of phenolic compounds during fermentation, the formation of volatile compounds, and the perception of wine sensory attributes (Canals, Llaudy, Valls, Canals, & Zamora, 2005; Fischer & Noble, 1994; Ellena S. King, Dunn, & Heymann, 2013; Lerno et al., 2015a; Waterhouse, Sacks, & Jeffery, 2016). On the other hand, titratable acidity (TA) concentration decreases during grape ripening, impacting wine style due to its correlation with

wine pH and sensory characteristics such as sourness (Fontoin, Saucier, Teissedre, & Glories, 2008; Lamikanra, Inyang, & Leong, 1995).

The composition of secondary metabolites such as phenolic and volatile compounds also changes during ripening. Anthocyanins accumulate during berry ripening in the vacuoles of the skin cells of the berry in non-tentureir cultivars and are responsible for the color in red grapes. Anthocyanin concentration at harvest is an important harvest indicator and can influence winemaking decisions (Boss, Davies, & Robinson, 1996). Flavonols are phenolic compounds found in the epidermal layer of the grape skin cells. Their biosynthesis is dependent on sunlight exposure, and they can play an important role in wine co-pigmentation together with anthocyanins (Price, Breen, Valladao, & Watson, 1995). Flavan-3-ols are the most abundant class of phenol present in the grape berry, and they accumulate in the skins and seeds before veraison. Oligomers and polymers of flavan-3-ols, also known as tannin or proanthocyanidins, are the main contributors to astringency and bitterness in grapes and wines (Adams, 2006; Kennedy, 2008). Finally, grape-derived volatile compounds are present in wines. Their accumulation during ripening is variable and dependent on the cultivar and viticultural practices (González-Barreiro, Rial-Otero, Cancho-Grande, & Simal-Gándara, 2015; Keller, 2015; Song, Shellie, Wang, & Qian, 2012). The phenolic and volatile compound compositions of grapes and wines play a crucial role in wine style.

However, several biotic and abiotic factors influence grape composition during ripening, which ultimately impacts wine quality. Grapevines are exposed to many diseases caused by viruses, resulting in economic losses by reducing plant vigor and yield as well as grape quality by altering grape biochemistry and composition (Gutha, Casassa, Harbertson, & Naidu, 2010; Martelli, 2014). Grapevine red blotch virus (GRBV) was recently identified as the agent responsible for causing grapevine red blotch disease (GRBD) (Sudarshana, Perry, & Fuchs, 2015).

GRBD has been found not only in California but also in many states throughout the US as well as in Canada, Mexico, Argentina, and South Korea (Gasperin-Bulbarela, Licea-Navarro, Pino-Villar, Hernández-Martínez, & Carrillo-Tripp, 2018; Krenz, Thompson, McLane, Fuchs, & Perry, 2014; Lim et al., 2016; Luna et al., 2019). It has been demonstrated that GRBV infection was able to compromise regulation of grape ripening in Zinfandel by suppressing specific ripening events, altering the expression patterns of transcription factors, and causing hormonal imbalances (Blanco-Ulate et al., 2017; Cieniewicz et al., 2018). Studies conducted on Cabernet Sauvignon, Cabernet Franc, and Merlot found that fruit from vines infected with GRBD showed reduced sugar accumulation when compared to healthy controls (Calvi, 2011; Martínez-Lüscher et al., 2019; Poojari, Alabi, Fofanov, & Naidu, 2013). A more detailed study conducted on Cabernet Sauvignon, Merlot, and Chardonnay in seven different locations found that GRBD can impact grape composition by decreasing sugar and anthocyanin content, mostly increasing TA, proanthocyanidin, and flavonol content, which suggest a delay in normal grape ripening processes (Cauduro Girardello et al., 2019). As a result, wines made from grapes affected by GRBD were demonstrated to have lower ethanol and in some cases, lower anthocyanin concentrations, and higher proanthocyanidin concentrations when compared to wines made from healthy vines (Cauduro Girardello, Cooper, et al., 2020; Cauduro Girardello, Rich, et al., 2020).

The prior work demonstrated that sugar differences between grapes from GRBD infected and healthy vines at harvest resulted in significantly higher ethanol content in wines made with fruit from healthy vines, which strongly affected wine chemical and phenolic composition as well as sensory properties (Cauduro Girardello, Cooper, et al., 2020; Cauduro Girardello, Rich, et al., 2020). The ethanol content of the wines mainly drove the sensorial differences between wines made with fruit from healthy or infected grapevines. This study aims to determine whether

sequential harvesting of GRBD grapevines can be a potential strategy to mitigate the negative impacts of the disease on grape and wine composition. Moreover, chaptalization was employed as another potential mitigation strategy in the 2017 season. Both mitigation strategies were performed in other to increase the sugar content of grape musts and consequently increase ethanol content of final wines. This will allow us to understand if the main differences between wines made from healthy and GRBD vines are due to berry secondary metabolite differences or berry sugar content and the resulting ethanol content of the wines.

A.3 Materials and Methods

A.3.1 Experimental Design and Berry Sampling

The study was carried out during the 2016 and 2017 seasons in a commercial vineyard of *Vitis vinifera* L. Merlot, clone 12, conducted on a vertical shoot positioned (VSP) trellis system in a bilateral cordon, grafted on 1103P rootstock located in Paso Robles, CA, U.S.A. Approximately 120 asymptomatic grapevines "RB (-)" and 360 symptomatic grapevines "RB (+)" grapevines for GRBD were selected for this study based on mapping of the vineyard over several seasons for the presence of GRBD through visual symptoms. After selection, grapevines were weekly evaluated for GRBD symptoms until the completion of the study. Among RB (-) and RB (+) plants, leaves and petioles from 20 and 25 grapevines were respectively tested (data vines) in 2016 and 2017 for each of the treatments for the presence of GRBV by qPCR analysis to confirm the healthy and GRBD status of the grapevines. Additionally, the plant material was tested for the presence of grapevine leafroll associated-virus (GLRaV) species (GLRaV-1, GLRaV-3, and GLRaV-3) as well as Rupestris stem pitting-associated virus (GRSPaV) (Bahder, Zalom, Jayanth, & Sudarshana, 2016; Dalton et al., 2019) (Agri-Analysis LLC laboratories, Davis, CA) as they commonly

coincide. RB (-) and RB (+) data vines were composed of 5 biological replicates of 4 vines each (N=20) in 2016, and of 5 biological replicates of 5 vines each (N=25) in 2017. Berry samples from RB (-) and RB (+) data vines were taken weekly from veraison to harvest. For each sampling date, 10 berries were collected randomly from each vine from the bottom, middle, and top of the clusters located in the inside and outside areas of the canopy. Following sample collection, a subset of berries representing each biological replicate was immediately analyzed for °Brix with a refractometer RFM110 (Bellingham + Stanley Ltd, UK), pH with an Orion-5-Star pH meter (Thermo Fisher Scientific Inc, Waltham, MA, USA), and titratable acidity (TA) with an DL50 Graphix titrator (Metter-Tolledo Inc, Columbus, Ohio, USA), while the remaining berries were stored at -80^{o}C for future analysis.

A.3.2 Harvest and Winemaking

Asymptomatic vines are vines that show no sign of diseases whereas symptomatic vines are vines that show clear disease symptoms. These vines have been tracked for several years. Data vines refer to the subset (20 %) of asymptomatic and symptomatic vines that we test by qPCR to confirm GRBV status. We have 100% correlation between symptomatic and asymptomatic vines and those testing positive and negative respectively for GRBV. Approximately 120 asymptomatic "RB (-)" and 240 symptomatic grapevines for GRBD were harvested once RB (-) grapevines reached 25 °Brix. Grapes harvested from symptomatic grapevines were split into two sets: those destined to be fermented as controls without chaptalization "RB (+)" and those which the must was chaptalized to 25 °Brix "RB (+) S" (chaptalization was performed only in the 2017 season). Additionally, another set of 120 symptomatic grapevines was harvested week(s) later when grapes reached 25 °Brix in the field "RB (+) 2H".

For each RB (-), RB (+), RB (+) S, and RB (+) 2H treatment, approximately 400 kg of grapes were harvested, transported to the UC Davis Teaching and Research Winery (Davis, CA), and kept refrigerated until the next day when they were processed following standard research protocols (Lerno et al., 2015a). Grapes were destemmed and crushed using a Bucher Vaslin Delta E2 (Santa Rosa, CA, USA) and the must was placed into 200 L stainless steel research fermentors. Fermentations were carried out in triplicate (n=3).

Fermentation conditions were controlled by an Integrated Fermentation Control System (IFCS) unit (Cypress Semiconductor San Jose, CA, USA). Before yeast inoculation, 50 mg/L of sulfur dioxide was added as a potassium metabisulfite solution (15%). Tartaric acid (American Tartaric Products, Windsor, CA, USA) and diammonium phosphate (DAP) (Omnisal GmBH, Lutherstadt Wittenberg, Germany) were adjusted to achieve 6 g/L and 250 mg/L, respectively. Must was inoculated with *Saccharomyces cerevisiae* strain EC-1118 (Lallemand, Montreal, Canada) according to the procedure of rehydration described by the manufacturer. Management of the cap was done by performing one tank volume pump-over twice a day, and fermentation temperatures were controlled at 25ºC. Wine samples were collected daily during fermentation and immediately analyzed for total anthocyanin and tannin concentration using models based on the protein precipitation assay (James F. Harbertson, Mireles, & Yu, 2015) developed by Wine X Ray LLC (Napa, CA, USA) using a Genesys10S UV-Vis Spectrophotometer (Thermo Fisher Scientific, Medison, WI, USA). After eight days of maceration, the wines were dry (<2 g/L of sugar) and pressed using a basket press. The wines were then inoculated with *Oenococcus oeni* (Chr. Hansen A/S, Hørsholm, Denmark) to induce malolactic fermentation (MLF). After MLF was completed, the wines were racked, free SO_2 adjusted to 35 mg/L, and stored at 13ºC until bottling.

Finally, the wines were bottled in Bordeaux-style bottles with Saranex screw caps (Saranex/Transcendia, Franklin Park, IL, USA) and stored at 14ºC until analysis.

A.3.3 Whole Berry and Skin Phenolic Extraction

For the phenolic extraction, five sets of 20 berries from RB (-), RB (+), and RB (+) 2H grapevines were randomly selected from clusters collected at harvest stored at -80°C and weighed. Grape berries were homogenized for 3 minutes at 1,355 x g using an IKA ULTRA-TURRAX®T18 basic homogenizer (IKA® Works, Inc., NC, USA). A solution of 1:1 ethanol:water containing 0.1% hydrochloric acid (HCl) and 0.1% of ascorbic acid was added to the homogenized tissue at a ratio of 1 ml of solvent to 0.1 g of tissue and extracted overnight for 22 hours at 4ºC. The samples were centrifuged at 3,200 x g at 4ºC for 15 minutes, and the supernatant was collected and stored at -20ºC. The homogenized tissue was subsequently extracted with a solution of 70:30 acetone:water containing 0.1% ascorbic acid at the same ratio (1 ml/0.1 g of tissue), overnight at 4ºC. After centrifugation, supernatants were combined and concentrated under reduced pressure to approximately 5 ml at 35ºC, quantitatively transferred to a 10 ml volumetric flask, and made up the volume with model wine (14% ethanol, 5g/L of potassium bitartrate, and pH 3.4). The protocol used for skin extraction from berries collected during ripening was the same as described above. To separate skins from pulp and seeds, semi-frozen berries were peeled using a scalpel, and the skins were immediately dried using paper towels and subsequently weighed prior to extractions. The anthocyanin accumulation was measured in RB (-) and RB (+) berry skins during ripening.

A.3.4 Analysis of Total Phenolics, Total Anthocyanins, and Total Tannins

Whole berry extracts and final wines were analyzed for total iron-reactive phenolics, total anthocyanins, and total tannins by the modified protein precipitation assay (James F Harbertson, Mireles, & Yu, 2014). Total iron-reactive phenolics and total tannins were measured at 510 nm absorbance and expressed as catechin equivalents (CE), while total anthocyanins (expressed as malvidin-3-glucosides (M3G) equivalents), was measured at 520 nm absorbance using a Genesys10S UV-Vis Spectrophotometer (Thermo Fisher Scientific, Medison, WI, USA).

A.3.5 Phenolic Profiling

Reversed-phase high-performance liquid chromatography (RP-HPLC) was performed to determine the phenolic profiles of berry and wine samples. Frozen berry extractions and wine samples were thawed and centrifuged for 5 minutes at 3,200 x g prior to analysis. Samples analyzed by RP-HPLC using an Agilent 1260 Infinity equipped with a PLRP-S 100A 3µM 150x4.6 mm column (Agilent Technologies, Santa Clara, CA, USA) at 35^{o}C, an autosampler with temperature control at 8^{o}C and diode array detector. Two mobile phases were used: mobile phase A (water containing 1.5% phosphoric acid v/v) and mobile phase B (80% acetonitrile and 20% mobile phase A). Twenty µl of sample was injected with the mobile phase flow rate set at 1 ml/min. The gradient for separation used was described by Peng, et al (Peng, Iland, Oberholster, Sefton, & Waters, 2002). The eluted compounds were monitored and identified by spectral and retention time comparisons to standards at four different wavelengths: 280 nm (gallic acid, (+)-catechin, dimer B, (-)-epicatechin, dimer B2, epicatechin gallate and polymeric phenols), 320 nm (caftaric acid, caffeic acid, coutaric acid, *p*-coumaric acid), 360 nm (quercetin-3-galactoside, quercetin-3-glucuronide, quercetin-3-glucoside and quercetin-3-rhamnoside) and 520 nm (anthocyanins and polymeric pigments). The identified compounds were quantified by external calibration curves.

All data processing was completed with Agilent® CDS ChemStation software version D.04 (Agilent Technologies, Santa Clara, CA, USA).

Calibrations curves were constructed for gallic acid, (+)-catechin, (−)-epicatechin, caffeic acid, quercetin, *p*-coumaric acid, purchased from Sigma Aldrich (St. Louis, MO), quercetin-rhamnoside and malvidin-3-*O*-glucoside chloride purchased from Extrasynthese (Genay, France). These compounds were quantified by themselves while other compounds were quantified as the following: B1, B2, epicatechin gallate and polymeric phenols as (+)-catechin equivalents; caftaric acid as caffeic acid equivalents; coutaric acid as *p*-coumaric acid equivalents; quercetin-3-galactoside, quercetin-3-glucuronide, quercetin-3-glucoside as quercetin-3-rhamnoside equivalents; and anthocyanins and polymeric pigments as malvidin-3-*O*-glucoside chloride equivalents. Five biological replicates of whole berry extracts and bottle duplicates of each wine fermentation replicate were analyzed by RP-HPLC.

A.3.6 Analysis of Volatile Compounds

Grape and wine volatile compounds were determined by an automated headspace solid-phase microextraction-gas chromatography-mass spectrometry (HS-SPME-GC-MS). Analysis were carried out using an Agilent 7890A gas chromatography coupled to a 5975C inert XL EI MSD with a triple-axis detector (Agilent Technologies, Santa Clara, CA, USA) controlled by Maestro (ver. 1.2.3.1, Gerstel Inc, Linthicum, MD, USA) by a method described by Hendrickson et al. (Hendrickson et al., 2016). For grape samples, volatile compounds from four sets of 60 berries collected at harvest were extracted and prepared following Hendrickson et al (Hendrickson et al., 2016), with few adaptations. For wines, bottle duplicates of each wine treatment replicate were analyzed in triplicate. Ten ml of sample were transferred to a 20 ml amber glass headspace

vial (Agilent Technologies, Santa Clara, CA, USA) containing 3g of NaCl (Sigma-Aldrich, St. Louis, MO, USA) and 50 µl of an internal standard (IS) solution of 2-undecanone (10mg/L prepared in 100% ethanol). Each sample was analyzed randomly using the following parameters: five minutes agitation at 500 rpm after reaching 30°C followed by sample exposure to a 1 cm polydimethylsiloxane/divinylbenzene/carboxen (PDMS/DVB/CAR) (Supelco Analytical, Bellefonte, PA, USA), 23-gauge SPME fiber for 45 minutes. The initial oven temperature was kept at 40°C, while gas helium was used as carrier gas at a flow of 0.8636 ml/min, in a DB-Wax 231 ETR capillary column (30 m, 0.25 mm, 0.25 µm film thickness) (J&W Scientific, Folsom, CA) column, with constant pressure at 5.5311 psi. After oven temperature was kept at 40°C for 5 min, an increment of 3°C/min was performed up to 180°C, and then another increase of 30°C/min until reach 260°C, when it was kept for 7.67 min. The SPME fiber was desorbed in split mode with a 10:1 split ratio and it was held in the inlet for 10 min to prevent carryover effects. The method was retention time-locked to the internal standard, 2-undecanone. Total run time was 61.67 min. Electron ionization source was used, with a source temperature of 230°C and the quadrupole at 150°C. The samples were measured using synchronous scan and selected ion monitoring (SIM mode). The scan range was from 40 m/z to 300 m/z, and compounds were detected using between two and six selected ions with a scan rate of 5.80 scans/sec.

Data was analyzed by MassHunter Qualitative Analysis software Version B.07.00 (Agilent Technologies, Santa Clara, CA, USA). Results are expressed as peak areas and were determined after normalization with 2-octanol and 2-undecanone as internal standard as well as the berry mass for grapes samples, and 2-undecanone as internal standard for wine samples. Compounds were identified by comparison with standards and the mass spectrometry spectrum of the peaks at the

determined retention times. For confirmation, peaks were compared to the National Institute of Standards and Technology database (NIST) (https://www.nist.gov).

A.3.7 Sensorial Descriptive Analysis

The sensory panel consisted of nine volunteer panelists (five females and four males) in 2016 and 10 (six females and four males) in 2017. In the training sessions, the panelists generated the relevant wine attributes by consensus as well as the related reference standards (Supplementary Materials - Tables S6 and S7). Panelists were trained by discussion and consensus on the attributes and use of a 15 cm anchored ("not present" and "very intense", besides for viscosity which the anchors were "watery" and "very viscous") line scale with the help of the reference standards. The panel rated the wines in three replicates over three evaluation sessions with seven wines each and one evaluation session of six wines. Panelists rated the wines monadically, first for aroma attributes, then for taste and mouthfeel attributes. Before beginning a session, judges familiarized themselves with aroma reference standards by recognizing them blindly and reevaluating those that they could not detect immediately. Intensities of the attributes were scored on a 15-cm anchored line scales that were similar to those used during training sessions. The presentation order of the wines was randomized according to a Williams Latin Square Design created by FIZZ software (FIZZ network, version 2.47 B, Biosystems, Courtenon, France). Wines were served in black ISO wine tasting glasses coded with a randomly generated three-digit codes and covered with plastic Petri dishes. In each evaluation, 40 mL of each wine was poured no less than 15 minutes before tasting. Panelists were instructed to expectorate the wine and cleanse their palate during a one-minute break with ambient temperature water, and unsalted crackers to limit potential carryover.

The color evaluation was recorded directly after the descriptive analysis. Another 40 mL of wine was served in clear Bordeaux style glasses coded with a three-digit randomly generated code. The panelists were asked to match the color of the wines with the color on a poster (Les Couleurs du Vin) showing different shades of wine color from brown to purple in 42 graduations, respectively. The color samples on the poster were marked with increasing indices. The panelists were asked to hold the wine glasses in a 45° angle and keep an eye distance of 40 cm to the poster. Data acquisition for all sensory experiments was carried out using FIZZ software (FIZZ network, version 2.47 B, Biosystems, Courtenon, France).

A.3.8 Statistical Analysis

Statistical analysis was performed using XLSTAT (Microsoft Office Professional Plus 2010, version 14.0.7194.5000, Redmond, WA, USA). T-tests were performed between RB (-) and RB (+) samples taken during ripening. All chemical, phenolic and volatile compound data were analyzed statistically for significance using univariate analyses of variance (ANOVA). Treatment effects were determined by Fisher's least significant differences (LSD). Sensory data were tested for significance by multivariate analysis of variance (MANOVA) for the overall treatment effect. Then ANOVA measuring the effects of judge, treatment and replicate was performed for those attributes that showed statistical differences for the overall treatment effect. Principal component analysis (PCA) was performed to compare and visualize the relations between RB (-), RB (+), RB (+) S, and RB (+) 2H wines graphically regarding volatile and sensory attributes. Multiple Factor Analysis (MFA) was performed to find relations among treatments, and wine chemical and phenolic composition, volatile compounds, and sensory descriptive analysis.

A.4 Results and Discussion:

A.4.1 Grape ripening

Juice analysis from grape samples collected from veraison to harvest demonstrated a significant ($p<0.05$) reduction in sugar loading (sugar per berry) and ºBrix (equivalent to the percentage of total soluble solids) in RB (+) grapes when compared to RB (-) grapes (Figures 1 and 2). The accumulation of sugar per berry basis, which was calculated as described by Deloire (2011), and ºBrix were significantly lower in 2016 during the entire maturation period, compared to 2017, especially at later stages of maturation. On the other hand, RB (+) grapes were higher in TA when compared with RB (-) grapes (Figures 1 and 2). The impact was clearer in the 2016 season when the differences in TA between RB (-) and RB (+) grapes were consistent from veraison until harvest. A similar trend was observed for pH. Thus, in the two seasons studied, GRBD decreased sugar accumulation during ripening with a simultaneous increased TA and a decreased pH. RB (+) grapes also consistently had lower anthocyanin accumulation during ripening than RB (-) grapes in both 2016 and 2017 seasons (Figure S1 – Supplementary Materials), as seen previously (Blanco-Ulate et al., 2017; Cauduro Girardello et al., 2019; Martínez-Lüscher et al., 2019).

Table A.1. Grape chemical and phenolic composition by RP-HPLC at harvest in the 2016 and 2017 seasons.

Variable	2016			2017			
	RB (-)[a]	**RB (+)[b]**	**RB (+) 2H[c]**	**RB (-)**	**RB (+)**	**RB (+) 2H**	**RB (+) S[d]**
Harvest Date	09/15/2016	09/15/2016	09/28/2021	09/09/2017	09/09/2017	09/29/2017	09/09/2017
Basic Composition							
Brix	25.2 ± 0.0 a	22.0 ± 0.0 c	24.5 ± 0.0 b	24.1 ± 0.0 a	21.3 ± 0.0 b	23.9 ± 0.2 a	21.4 ± 0.0 b [γ]
pH	4.15 ± 0.01 a	3.83 ± 0.02 c	3.98 ± 0.01 b	3.89 ± 0.02 a	3.45 ± 0.06 c	3.78 ± 0.04 b	3.50 ± 0.01 c
TA (g/L)	2.56 ± 0.05 b	3.35 ± 0.05 a	3.34 ± 0.02 a	4.95 ± 0.26 b	6.43 ± 0.32 a	4.70 ± 0.50 b	6.36 ± 0.07 a
YAN (mg/L)	125. 32 ± 4.26 b	95.97 ± 3.37 c	141.19 ± 1.41 a	181.80 ± 6.60 b	219.60 ± 13.24 a	138.20 ± 8.74 c	206.33 ± 3.37 a
Malic Acid (mg/L)	1188.6 ± 10.2 c	1561.3 ± 27.5 a	1737.3 ± 30.2 a	2119 ± 168.6 b	2381.3 ± 59.0 b	3315.3 ± 242.3 a	2385.6 ± 17.1 b
Phenolic Profile (mg/g of berry)							
Anthocyanins	0.638 ± 0.04 a	0.366 ± 0.04 b	0.152 ± 0.04 c	0.329 ± 0.03 a	0.166 ± 0.02 b	0.202 ± 0.05 b	**
Flavan-3-ols	0.534 ± 0.07 a	0.603 ± 0.06 a	0.311 ± 0.31 b	0.307 ± 0.05 b	0.392 ± 0.01 a	0.321 ± 0.04 b	**
Flavonols	0.095 ± 0.01 a	0.054 ± 0.01 b	0.039 ± 0.08 b	0.030 ± 0.00 a	0.021 ± 0.00 a	0.028 ± 0.00 a	**
Polymeric Phenols	5.948 ± 0.11 a	4.826 ± 0.22 b	4.716 ± 0.66 b	3.829 ± 0.54 a	2.840 ± 0.26 b	3.702 ± 0.15 a	**
Tannin*	4.08 ± 0.14 a	3.44 ± 0.19 b	3.50 ± 0.24 b	6.18 ± 1.16 a	4.96 ± 0.3 b	5.37 ± 0.27 ab	**

Values are the mean ± standard deviation expressed in mg/g of berry. Statistical differences are expressed as letters and indicate significant differences in the LSD test within each row for each year (n=5, $p \leq 0.05$). Means within a row followed by the same letter are not significantly different. A table presenting the phenolic composition per berry basis (mg/berry) is shown in the Supplementary Materials (Table S1). [a]RB (-) = Healthy grapes. [b]RB (+) = GRBD grapes harvested at the same time as RB (-). [c]RB (+) 2H = GRBD grapes with longer hanging time and harvested with similar [o]Brix as RB (-). [d]RB(+) S = GRBD grapes – must was chaptalized to 24 [o]Brix.* Analyzed by protein precipitation assay. [γ] Must be chaptalized to 24[o]Brix.

A.4.2 Grape composition at harvest

As previously described, RB (+) grapes were sequentially harvested, with the first harvest at the same time as healthy grapes (RB (-)) at 25°Brix, and the second harvest when RB (+) grapes reached 24 - 25 °Brix, approximately two weeks later (RB (+) 2H). Grape chemical and phenolic composition at harvest demonstrated that GRBD impacts not only °Brix, pH, and TA but also grape phenolic composition (Table A.1.). °Brix at harvest was lower by 13% and 12% in RB (+) grapes when compared to RB (-) grapes in 2016 and 2017 respectively. On the other hand, RB (+) grapes were higher in TA and as a consequence lower in pH when compared to RB (-). The decreased sugar accumulation and increased TA in RB (+) grapes was demonstrated previously in Cabernet Sauvignon and Merlot grapes (Cauduro Girardello et al., 2019; Martínez-Lüscher et al., 2019), and suggests that GRBD delays typical ripening events in grapes. Another indicator of slower ripening in GRBD grapes is the consistent higher malic acid content compared to healthy grapes. The third phase of grape berry ripening is characterized by sugar accumulation and the decline in juice acidity due to malic acid degradation (I. Jackson & B. Lombard, 1993). These results confirm the typical impact of grapevine viruses such as GRBV and grapevine leafroll virus (GLV) on grape chemical composition (Alabi et al., 2016; Calvi, 2011; Reynard & Gugerli, 2015; Vega, Gutiérrez, Pena-Neira, Cramer, & Arce-Johnson, 2011).

GRBD also had a significant impact on all grape phenolic classes for both seasons (Table A.1.). In the 2016 season, there was a significant decrease in all measured phenolics due to GRBD, except for the total flavan-3-ols. Phenolic concentrations either stayed the same or decreased further in the grapes impacted by GRBD but harvested later (RB (+) 2H). Similar trends were observed in 2017 with one exception. In 2017, the total flavan-3-ol concentration was higher in RB (+) compared to RB (-) grapes, but this difference was no longer apparent after longer hang

time (RB (+) 2H). In a previous study, GRBD caused the abnormal expression of transcription factors such as MYBs and hormone networks in Zinfandel grapes, which resulted in the inhibition of ripening pathways, specifically the phenylpropanoid pathway which is responsible for the biosynthesis of phenolic compounds (Blanco-Ulate et al., 2017). Thus, inhibition of the phenylpropanoid pathway can potentially explain the generally lower phenolic concentrations in GRBD affected grapes. Furthermore, our results also confirmed previous studies that found a decrease in grape anthocyanin concentration due to GRBD (Calvi, 2011; Reynard & Gugerli, 2015). However, it may not always be significant.

Regarding RB (+) 2H grapes, anthocyanin concentration was lower or similar to RB (+) grapes, even though the °Brix was significantly higher due to the extended hang time of the grapes (Table A.1.). The latter is due to dehydration as sugar accumulation has reached a plateau prior to harvest (Figures 1 and 2). It is known that sucrose derived from leaf photosynthesis is exported via the phloem to the berries. From veraison and throughout ripening the berries accumulate roughly equal amounts of glucose and fructose (B. Coombe, 1987). However, the accumulation of sugars photosynthesized in the leaves and transported to the berries stops at a certain point, and a further increase in berry sugar concentration at late stages of ripening is due to berry dehydration. A study performed in Shiraz grapes has demonstrated that sugar accumulation stops when the berry reaches maximum weight, which was observed in berries with 20-21°Brix, and without berry shrinkage, the juice °Brix would never rise above these concentrations (McCarthy & Coombe, 1999). It has been shown in Trebbiano Toscano and Rossetto cultivars that berry weight loss of 10% due to dehydration at late ripening stage may result in a 2°Brix increment (Muganu et al., 2011). In this study, the berry mass of RB (+) 2H grapes at harvest were 8% and 11% lower than

RB (+) grapes respectively in 2016 and 2017 due to berry dehydration as a result of longer hang time (data not shown), which agrees with Mugano et al. (2011)

Anthocyanin accumulation in grape berries starts at veraison after the onset of sugar accumulation approximately around 10°Brix, while the synthesis decreases around 30-40 days after veraison (Keller, 2015; Ryan & Revilla, 2003)[,]. Studies have found that sugar and anthocyanin have similar accumulation profiles during ripening (Boss et al., 1996) but that GRBD may disrupt it in Cabernet Sauvignon grapes (Cauduro Girardello et al., 2019). RB (+) 2H grapes had a similar or decreased total anthocyanin concentration when compared to RB (+) grapes. The decreased anthocyanin concentration observed in 2016 has been observed in previous studies on Shiraz and Cabernet Sauvignon harvested at late ripening stage (Keller & Hrazdina, 1998; Roggero, Coen, & Ragonnet, 1986). It is important to point out that during the 13 days that RB (+) 2H hung in the field after RB (-) and RB (+) were harvested in 2016, six days had maximum temperatures above 35°C. On the other hand, during the 20 days that RB (+) 2H grapes stayed longer in the field in 2017, only one day had a maximum temperature above 35°C. High temperatures were shown to stimulate peroxidase activity in grape berries, leading to anthocyanin degradation during ripening (Movahed et al., 2016), which was likely the case in the 2016 season.

Concerning polymeric phenols concentration, RB (+) 2H grapes were significantly lower than RB (-) and similar to RB (+) grapes in 2016. In 2017, RB (+) 2H did not differ from RB (-), and both had a higher concentration of polymeric phenols than RB (+). A similar trend was observed for tannins analyzed by protein precipitation assay (Table A.1.). Significant decreases in tannin concentrations were observed in RB (+) grapes when compared to RB (-) in both the 2016 and 2017 seasons. A similar decrease in tannin concentration has been observed in Pinot noir grapes infected by GLRV (Lee & Martin, 2009). Regarding GRBD, it was found that seven

enzymes that have essential roles in the phenylpropanoid pathway, which is responsible for the biosynthesis of anthocyanins and tannins, had reduced activity due to GRBV infections of berries at three ripening stages (Blanco-Ulate et al., 2017). Therefore, GRBV can potentially impact tannin accumulation in the berry.

In 2017, RB (+) 2H grapes had a similar concentration of polymeric phenols and tannins when compared to RB (-) grapes. Tannins are mostly accumulated in the berry before veraison. After veraison, their concentration declines due to berry growth (Adams, 2006), and therefore an increase of tannin concentration in the berry can be partially explained by berry dehydration (as observed in RB (+) 2H grapes in 2017 – Table A.1.). Another potential reason would be the activation of the plant's defense mechanism due to viral infection. Few previous studies have investigated the impacts of grapevine viruses on tannin content in grapes (Cauduro Girardello et al., 2019; Lee & Martin, 2009; Martínez-Lüscher et al., 2019). An increased concentration of proanthocyanidin (also known as condensed tannin) was observed in leaves of grapevines infected by GRLV when compared to healthy vines (Gutha et al., 2010). It is known that tannins are secondary metabolites synthesized as a stress response to biotic and abiotic factors such as fungal, bacterial, or viral infections (Scalbert, 1991). The impact of GRBV on grape composition was variable depending on the season and it has been demonstrated in previous studies, which suggested that in warmer seasons, plant's defense mechanism against viruses such as induced gene silencing impacts gene expression, resulting in decreases in viral DNA accumulation and decreases in symptoms and therefore, the impacts of GRBV in grapes (Cauduro Girardello et al., 2019; Chellappan, Vanitharani, Ogbe, & Fauquet, 2005; Rumbaugh et al., 2021). This is potentially the reason why RB grapes left for longer on the field were more similar to healthy grapes in the 2017 season when compared to the 2016 season.

A table presenting the phenolic composition per berry (mg/berry) is shown in the Supplementary Materials section (Table S1). In general, phenolic concentration (mg/g of berry) and content (mg/berry) followed similar trends.

A.4.3 Grape volatile compounds at harvest

In this study, 29 and 37 volatile compounds were identified in the grapes at harvest in the 2016 and 2017 seasons, respectively (Supplementary Materials - Table S2). In 2016, six volatile compounds were significantly different among the RB (-), RB (+), and RB (+) 2H grape treatments (ethyl acetate, geranial, β-ionone, octanal, β-linalool, and limonene). In 2017, 21 compounds were significantly different among the treatments (four of them were significantly different in 2016 in addition to 17 volatile compounds significantly different only in 2017).

Principal component analysis (PCA) was performed to determine the correlations between RB (-), RB (+), and RB (+) 2H grapes, and the volatile compounds found significantly different among the treatments (Figure A.1). In 2016, the first and second dimension explained 95% of the variance, showing a clear separation between RB (+) and RB (+) 2H, in which all the volatile compounds were found to be highly correlated to RB (+) 2H grapes on the right side of PC1, and weakly correlated to RB (+) grapes on the left side of PC1. RB (-) grapes did not show a clear separation either from RB (+) or RB (+) 2H. In 2017, RB (+) grapes had the lowest levels of volatile compounds again, showing a weak correlation with the volatile compounds found significantly different among the treatments, similarly to what was observed in 2016. However, in 2017, in general RB (+) 2H grapes were closely related to RB (+) grapes although with a small variation. On the opposite side of the PC1, RB (-) grapes were strongly correlated to all the volatile compounds.

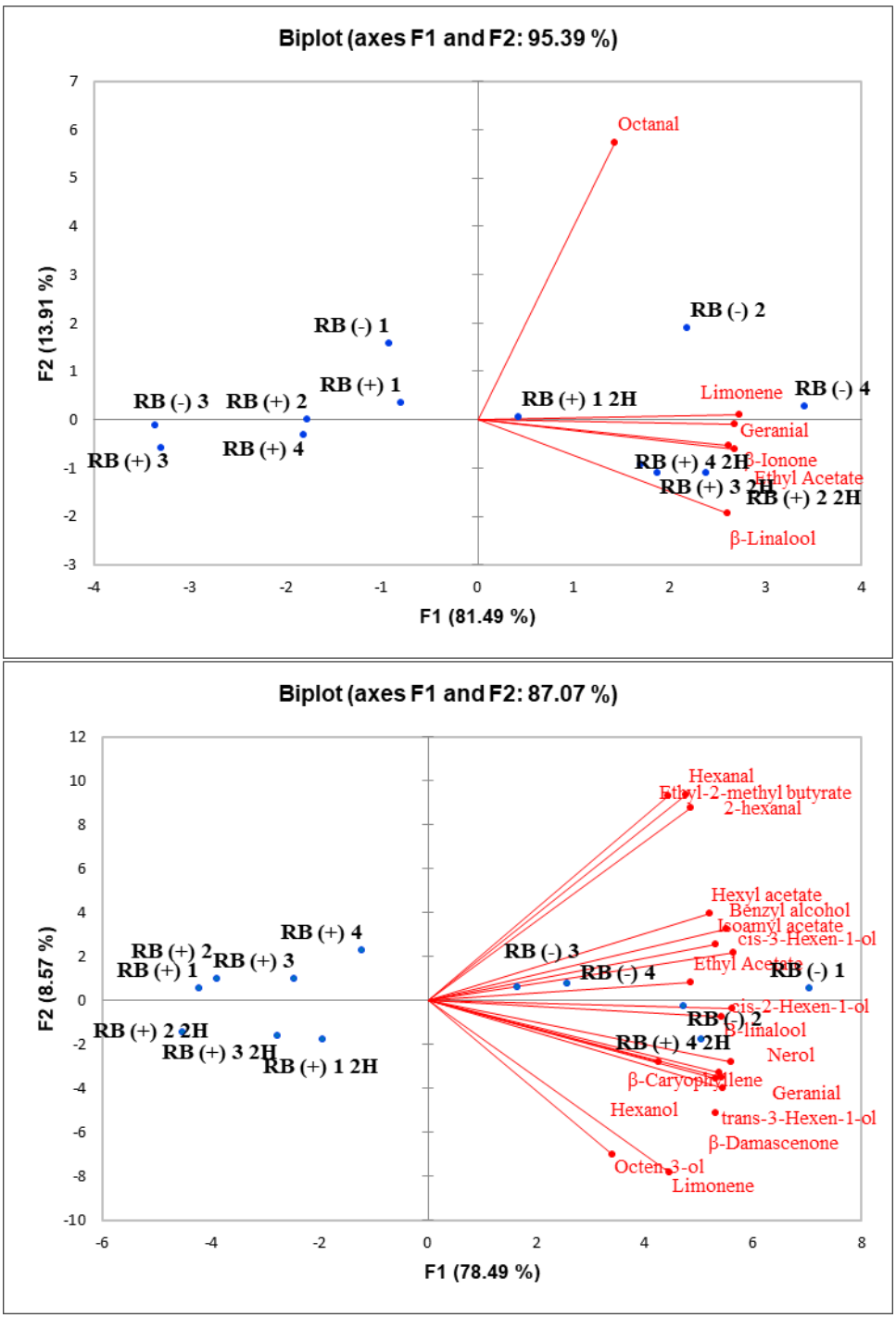

Figure A.1. Principal component analysis of berry volatile compounds at harvest in 2016 (top) and 2017 (bottom) (n=4). RB (-) = Healthy grapes. RB (+) = GRBD grapes harvested at the same time as RB (-). RB (+) 2H = GRBD grapes with longer hanging time and harvested with similar ºBrix as RB (-).

Monoterpenes such as linalool, geraniol, and nerol are synthesized in the mevalonate (MVA) pathway (Dunlevy, Kalua, Keyzers, & Boss, 2009). Linalool, nerol, ethyl 2-methyl butyrate, ethyl acetate levels were shown to increase during ripening in Moscato and table grapes reaching its maximum between 20-25°Brix and later declining at overripeness (Wilson, Strauss, & Williams, 1984; Yang, Wang, Wu, Fang, & Li, 2011). Another class of volatile compounds present in grapes, C_{13}-norisoprenoids are derived from carotenoids. In ripening grape berries, carotenoid levels decrease after véraison and the levels of the C_{13} norisoprenoids such as β-damascenone, β-ionone increase (Dunlevy et al., 2009). As discussed previously, extended grape hang time in RB (+) 2H were shorter in 2016 (13 days) when compared to 2017 (20 days), which may have reduced the volatile levels when compared to RB (-) grapes in 2017 (Table S2, Figure A.1). Therefore, these results demonstrated that GRBD can reduce the levels of volatile compounds in the berries. In addition, the longer hang time of diseased grapes was demonstrated to have variable effects on volatile compound levels depending on the season and environmental conditions such as temperature

A.4.4 Anthocyanin and tannin extraction during fermentation

The extraction of phenolics during fermentation was measured, and results demonstrated that all the wines followed similar extraction profiles in both 2016 and 2017 (Figures 4 and 5 and Supplementary Material - Table S4). Anthocyanin concentration increased rapidly from the second day of fermentation, reaching a plateau between days four and five and staying stable until pressing (Figures 4 and 5). For all the treatments, extraction profiles agree with previous studies (Bautista-Ortín, Busse-Valverde, Fernández-Fernández, Gómez-Plaza, & Gil-Muñoz, 2016; Smith, McRae,

& Bindon, 2015), in which extraction have a lag phase in the first two days followed by linear extraction until the last day of maceration.

Regarding the treatment differences, RB (-) wines had a significantly higher concentration of anthocyanin when compared to RB (+) 2H, and the latter was statistically higher than RB (+) wines. The higher anthocyanin content of wines made from healthy grapes agrees with the higher anthocyanin grape content of RB (-) grapes. However, the higher anthocyanin concentration in RB (+) 2H wines compared with RB (+) wines is contrary to grape anthocyanin concentration (Table A.1.), which indicated that RB (+) 2H had the lowest concentration of anthocyanins in the berry in 2016. This indicates that the extractability of anthocyanins was higher in RB (+) 2H musts than RB (+) musts during fermentation. This may partly be due to the higher ethanol content of RB (+) 2H musts due to higher sugar content in the second harvest GRBD grapes. In musts, anthocyanin extraction has been shown to increase with ethanol production during alcoholic fermentation (Lerno et al., 2015b) and anthocyanin solubility increases in hydroalcoholic solutions up to 20% ethanol content (Oancea, Stoia, & Coman, 2012). Additionally, it has been demonstrated that adsorption of anthocyanin onto grape cell walls decreased in the presence of 15% alcohol in comparison to water, due to a higher solubility of the pigments in this range of ethanol content (Medina-Plaza et al., 2020). However, chaptalization of must from diseased grapes was not effective in increasing anthocyanin concentration in RB (+) S wines in 2017. Furthermore, longer hang time could have influenced the extractability of skin phenolics, and will be discussed in further detail later. These findings suggest that both the ripening stage and ethanol content impact the extraction of color and phenolic compounds. It was shown that Tempranillo grapes harvested at an advanced stage of ripening combined with the higher ethanol content had an increased

anthocyanin and tannin extractability during fermentation than grapes harvested at an early ripening stage (Canals et al., 2005).

Tannin extraction followed a similar trend observed for anthocyanins in both 2016 and 2017, in which RB (-) and RB (+) 2H wines had a more similar extraction profile with similar concentrations between them, while RB (+) and RB (+) S wines presented lower tannin concentrations (Supplementary Materials - Figure S2). Similarly to what was observed for anthocyanins, these findings suggest that there was a higher tannin extractability due to the longer hang time of RB (+) 2H grapes when compared to RB (+) due to the higher ethanol content of the wines, which not only increases tannin extractability as shown by Canals et al (2005) but also enhances tannin solubility in the matrix (Beaver et al., 2020).

Table A.2. Basic chemical composition of RB (-), RB (+) and RB (+) 2H wines in 2016 and 2017

Year	Wine	Ethanol %	pH	TA[e] (g/L)	RS[e] (g/L)
2016	RB (-)[a]	14.52 ± 0.08 a	3.65 ± 0.01 b	5.40 ± 0.06 a	0.25 ± 0.01 a
	RB (+)[b]	12.28 ± 0.07 c	3.67 ± 0.01 b	5.31 ± 0.16 a	0.13 ± 0.01 b
	RB (+) 2H[c]	13.62 ± 0.10 b	3.76 ± 0.02 a	5.31 ± 0.05 a	0.25 ± 0.00 a
2017	RB (-)	14.22 ± 0.01 b	3.68 ± 0.02 c	5.61 ± 0.10 b	0.21 ± 0.01b
	RB (+)	12.21 ± 0.02 d	3.79 ± 0.00 b	5.54 ± 0.09 b	0.13 ± 0.01d
	RB (+) 2H	13.80 ± 0.03 c	3.67 ± 0.01 c	5.90 ± 0.08 a	0.18 ± 0.00 c
	RB (+) S[d]	14.79 ± 0.29 a	3.83 ± 0.00 a	4.95 ± 0.11 c	0.42 ± 0.01 a

Values are the mean of three biological replicates (n=3). Statistical differences are expressed as letters and indicate significant differences in the LSD test within each column for each year ($p \leq 0.05$). [a]RB (-) = Healthy grapes. [b]RB (+) = GRBD grapes harvested at the same time as RB (-). [c]RB (+) 2H = GRBD grapes with longer hanging time and harvested with similar [o]Brix as RB (-). [d]RB (+) S = GRBD grapes must was chaptalized to 24 [o]Brix. [e]TA = Titratable acidity. [e]RS = Residual sugar.

A.4.5 Wine chemical composition

Ethanol (EtOH) content (% v/v) was demonstrated to be significantly different among finished wines in both the 2016 and 2017 seasons (Table A.2.). It was observed for both years that RB (-) wines were significantly higher in EtOH content than RB (+) 2H, which, in turn, was significantly higher than RB (+). EtOH differences correlated with berry sugar content at harvest

for the different treatments (Table A.1.). In general, one gram of sugar in the berry equals 0.6% of ethanol after alcoholic fermentation (Ough & Amerine, 1963). Similar findings were demonstrated in wines made from Merlot grapevines affected by grapevine leafroll disease across three seasons (Alabi et al., 2016). However, longer hang time did decrease the chemical differences between wines made with GRBD and healthy grapes (Table A.2.).

In 2017, chaptalization was effective in mitigating the impact of GRBD on ethanol content as previously demonstrated in other studies (Cauduro Girardello, Cooper, et al., 2020; Cauduro Girardello, Rich, et al., 2020) (Table A.1.). Although ethanol content in RB (+) S wines was slightly higher than RB (-) wines (0.57 ethanol % difference), this difference was small and it is not considered large enough to have a significant sensory impact.

RB (+) 2H wines had higher pH values than RB (-) and RB (+) in 2016. In the following year, RB (+) wines had higher pH values than RB (-) and RB (+) 2H wines. Normally, TA and pH are inversely correlated in wines (Waterhouse et al., 2016). However, it is important to point out that TA concentrations in the wines were adjusted to similar levels (6 g/L) as part of the standard winemaking protocol. It is well known that pH in wines is also positively correlated to wine potassium (K) concentration (Kodur, 2011). Two factors may have influenced wine pH values in this study. K accumulation in the grape berry increases during ripening, in which the majority of K is located in the skins and is extracted during winemaking (B. Coombe, 1987). Grape skins at late ripening stages are more easily degraded during winemaking due to cell wall changes such as the weakening of primary cell walls and degradative changes to cell wall polysaccharides that occur during ripening (Brummell, 2006). This, in combination with high ethanol content, could explain why RB (+) 2H wines had higher pH values than the other two treatments in 2016, due to a possible higher extraction of K into the wines. In the 2017 season, another factor may have

contributed to the results found. It has been demonstrated in transgenic soybean plants (Glycine max (L.) Merr.), that the overexpressing of GmAKT2 potassium channel (soybean inner K+ transporter gene) and the addition of K+ fertilizer respectively increased resistance to soybean mosaic virus (SMV) and reduced its incidences (Zhou et al., 2014). Another study found that the concentration of potassium was significantly higher in fruits infected by GLRV than in healthy fruits (Kliewer & Lider, 1976). Therefore, one hypothesis is that grapevines infected with GRBV may accumulate more K in the berries in order to counter-attack virus infection and reduce its incidence. Unfortunately, the K content of the berries was not measured. This should be addressed in future studies. In the wines, no differences were found among the treatments regarding K concentration in 2016. However, in 2017, RB (+) wines had higher K concentrations (1,322 ± 34.01 mg/L) compared to RB (-) and RB (+) 2H wines (973 ± 34.93 mg/L and 1126 ± 129.60 mg/L, respectively).

Table A.3. Phenolic profiling (mg/L) of RB (-), RB (+) and RB (+) 2H wines in 2016 and 2017 by RP-HPLC analysis.

Phenolics	2016			2017			
	RB (-)[a]	RB (+)[b]	RB (+) 2H[c]	RB (-)	RB (+)	RB (+) 2H	RB (+) S[d]
(+)-Catechin	39.50 b	35.36 b	47.94 a	44.87 b	56.58 a	49.67 ab	55.38 a
B1	17.95 b	18.45 b	22.89 a	32.18 a	31.78 a	31.43 a	32.27 a
(-)-Epicatechin	20.94 b	18.99 b	29.88 a	1.60 b	1.84 a	1.88 a	1.76 a
Total flavan-3-ol	78.40 b	72.81 b	100.72 a	78.65 c	90.21 a	82.99 bc	89.42 ab
Caftaric acid	25.27 a	2.60 b	3.38 b	-	-	-	
Caffeic acid	0.00 c	22.89 b	27.03 a	-	-	-	
Coutaric acid	5.66 a	0.73 b	1.08 b	21.18 a	18.98 ab	20.07 a	16.60 b
p-Coumaric acid	-	-	-	5.09 a	5.54 a	5.42 a	4.93 a
Total hydroxycinnamic acid	30.94 a	26.23 a	31.50 a	26.28 a	24.52 a	25.50 a	21.54 b
Quer-galactoside	2.02 a	1.28 c	1.54 b	3.23 a	2.28 a	3.29 a	2.66 a
Quer-3-glucoside	10.97 a	6.52 c	7.47 b	3.77 a	1.80 b	4.70 a	2.08 b
Quer-glucuronide	24.99 a	20.61 b	27.23 a	6.93 b	6.00 b	9.57 a	6.04 b
Quer-rhamnoside	5.73 a	3.61 c	5.19 b	2.94 a	1.84 b	3.35 a	2.21 b
Quercetin	2.23 b	2.01 b	3.95 a	3.85 b	3.72 b	4.65 a	3.87 b
Total flavonol	45.98 a	34.06 b	45.40 a	20.74 b	15.66 c	25.57 a	16.88 c
Delph-3-gluc	25.71 a	12.82 b	14.63 b	9.56 a	5.82 b	8.50 a	4.92 b
Cya-3-gluc	1.63 a	0.74 b	0.87 b	0.59 a	0.34 b	0.58 a	0.33 b
Pet-3-gluc	32.35 a	17.97 b	20.94 b	13.26 a	9.66 bc	12.07 ab	8.42 c
Peo-3-gluc	10.47 a	5.65 c	6.88 b	4.73 a	3.05 b	4.72 a	2.89 b
Malv-3-gluc	182.24 a	140.29 b	157.29 b	86.98 b	87.07 b	101.31 a	79.07 b
Delph-3-acetylgluc	11.16 a	6.10 b	6.31 b	6.66 a	5.41 ab	5.30 ab	4.35 b
Pet-3-acetylgluc	12.14 a	7.26 b	7.43 b	5.50 a	4.68 ab	4.71 ab	3.89 b
Peo-3-acetylgluc	6.19 a	4.03 b	3.95 b	3.50 a	3.20 ab	3.38 a	2.84 b
Malv-3-acetylgluc	72.90 a	57.77 b	63.07 b	28.99 b	31.00 b	35.93 a	28,43 b
Malv-3-p-coumgluc	25.26 a	20.39 b	28.25 a	9.57 b	10.02 b	13.81 a	10.23 b
Total anthocyanin	390.94 a	279.72 b	317.37 b	169.38 ab	160.28 bc	190.34 a	145.41 c
Gallic acid	12.24 b	12.88 b	17.43 a	22.28 b	27.23 a	26.25 a	26.38 a
Polymeric pigments	8.09 a	7.64 a	8.97 a	8.23 b	6.71 c	9.27 a	6.96 c
Polymeric phenols	154.63 a	133.86 b	158.56 a	134.99 ab	115.55 b	153.94 a	123.58 b

Values are the mean of three biological replicates (n=3). Statistical differences are expressed as letters and different letters indicate significant differences in the LSD test within each row for each year ($p \leq 0.05$). [a]RB (-) = Healthy grapes . [b]RB (+) = GRBD grapes harvested at the same time as RB (-). [c]RB (+) 2H = GRBD grapes with longer hanging time and harvested with similar [o]Brix as RB (-). [d]RB (+) S = GRBD grapes must was chaptalized to 24 [o]Brix.

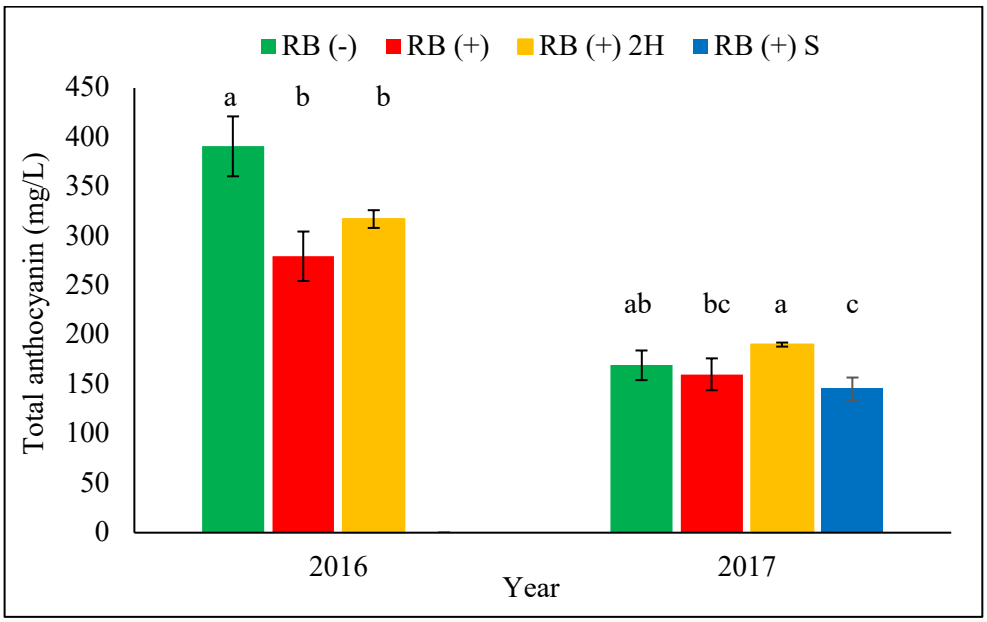

Figure A.2. Total anthocyanin concentration of RB (-), RB (+) and RB (+) 2H and RB (+) S wines in the 2016 and 2017 seasons. Each bar represents the mean ± standard deviation of three biological replicates (n=3, $p \leq 0.05$). Means within a column followed by the same letter are not significantly different within a year.

A.4.6 Phenolic composition in final wines

Analysis of anthocyanins in the final wines demonstrated that RB (-) wines were significantly higher for all monomeric anthocyanins when compared to RB (+) wines in 2016 (Table A.3.). In the 2017 season, a similar significant decrease in the concentration of four out of ten of the monomeric anthocyanins was found in the RB (+) wines when compared to RB (-); however, the total anthocyanin concentration was not significantly different. On the other hand, RB (+) 2H wines generally showed an increase in concentration for total anthocyanins when compared to RB (+) wines, although it was not significantly different in 2016. In 2017, the anthocyanin concentration of RB (+) 2H wines was significantly higher than RB (-) and RB (+) wines (Figure A.2). Chaptalization of must from diseased grapes did not have any effect on anthocyanin concentration in the RB (+) S wines, which were not statistically different from the RB (+) wines. The higher concentration of anthocyanins in RB (+) 2H wine compared to RB (+) and RB (+) S wines demonstrated that higher ethanol content associated with extended grape

ripening facilitated anthocyanin extraction from grapes into the wines. This is due to grape extractability differences during alcoholic fermentation as grape berry concentration does not show this trend.

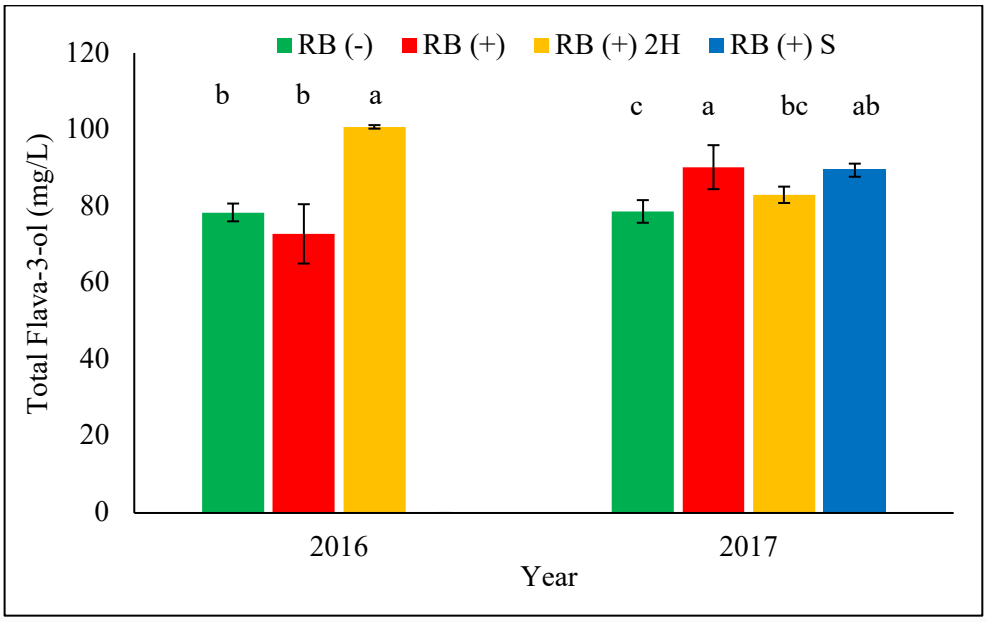

Figure A.3. Total flavan-3-ols concentration of RB (-), RB (+) and RB (+) 2H and RB (+) S wines in the 2016 and 2017 seasons. Each bar represents the mean ± standard deviation of three biological replicates (n=3, $p \leq 0.05$). Means within a column followed by the same letter are not significantly different within a year.

The total flavan-3-ol concentrations were significantly higher in RB (+) 2H than RB (-) and RB (+) wines in 2016. Whereas in 2017, the concentration of flavan-3-ols in RB (+) and RB (+) S wines were statistically higher than in RB (-) wines, with RB (+) 2H wines being statistically similar to RB (+) S and RB (-) (Figure A.3). Catechin made the main contributions to the total concentration of flavan-3-ols in all the treatments (Table A.3). In both seasons, RB (-) wines had lower flavan-3-ol concentration when compared to RB (+) 2H (2016), and RB (+), RB (+) 2H, and RB (+) S (2017) even though this was not the case for the grapes (Table A.1). The combination of longer hang time of RB (+) 2H, and higher ethanol content (RB (+) 2H and RB (+) S) possibly facilitated the extraction of flavan-3-ols, resulting in wines with higher flavan-3-ol concentration than RB (-) and RB (+) in 2016 and 2017. Extraction of flavan-3-ols from seeds and skins was

shown to be positively correlated to ethanol content in model wine solution (González-Manzano, Rivas-Gonzalo, & Santos-Buelga, 2004). In fruits, the degradation of polysaccharides and alterations in the bonding between polymers cause an increase in cell separation and softening of the cell wall. The depolymerization of pectins is usually most pronounced late in ripening when it increases cell wall porosity allowing the access of degradative enzymes (Brummell, 2006). No significant differences were found among the treatments in hydroxycinnamic acid concentration (Table A.3.).

Regarding total flavonols and polymeric phenols concentration, RB (-) and RB (+) 2H were significantly higher than RB (+) wines in 2016. On the other hand, in 2017, RB (+) 2H wines were similar to RB (-), but higher than RB (+) and RB (+) S (Figures 8-9). Quercetin-glucuronide followed by quercetin-3-glucoside were the main flavonols found in all the treatments (Table A.3.), which is in agreement with the findings of Castillo-Muñoz et al. (Castillo-Muñoz, Gómez-Alonso, García-Romero, & Hermosín-Gutiérrez, 2007) in Merlot grapes. These results indicated the impact of a longer hang time of which the significance depended on the season. In 2017, ripening was slower, and slightly lower ^{o}Brix levels were obtained at harvests compared with 2016 (Table A.1.). RB (+) 2H grapes spent seven days longer on the vine in 2017 than in 2016 in order to reach the same ^{o}Brix as RB (-) grapes. This could have impacted flavonol and polymeric phenol concentration in the grapes and extractability due to cell wall degradation during ripening. It has been found that flavonol concentration increases during ripening and its concentration is directly related to sun-exposure (Czemmel et al., 2009). In addition, it has been found that the increase in polymeric anthocyanins in wines from sun-exposed clusters is directly related to quercetin levels and that the high wine quercetin levels may increase the rate of polymerization with potential stability and quality implications (Downey, Dokoozlian, & Krstic, 2006; Price et al., 1995). As the

data show, wines made with grapes that were left for longer on the field (RB (+) 2H) had a higher polymeric pigment (2017) and flavonol concentration than those wines from chaptalized must (RB (+) S) due to the long sun exposure on the grapes and more advanced ripening stage, which facilitated flavonol extraction and formation of polymeric pigments in the RB (+) 2H wines.

In general, the delayed harvest of diseased grapes (RB (+) 2H) yielded wines more similar to RB (-) wines than RB (+) and RB (+) S wines. These findings may be attributed to the combination of high ethanol content in the wines (due to the higher sugar content in the berries as a result of dehydration) and the more advanced ripening stage of RB (+) 2H grapes. The high ethanol concentration of RB (+) S wines did not result in wines with increased concentrations of flavonols and polymeric pigments, which indicated that increased extractability due to increased ripening and cell wall degradation played a larger role than increased solubility due to higher ethanol concentration. During ripening, a substantial weakening of the primary cell wall and degradative changes to cell wall polysaccharides occur. These changes in cell wall architecture, combined with the increased pore size, make the cell wall a much more open structure, increasing accessibility of enzymes responsible for cell wall degradation at later ripening stages, and decreasing limitation to cell wall disassembly (K. A. Bindon, Madani, Pendleton, Smith, & Kennedy, 2014; Brummell, 2006).

Total phenolics, tannins, and anthocyanin concentration in the wines measured by protein precipitation assay (James F. Harbertson et al., 2015) are presented in the Supplementary Materials section (Table S3) and followed similar trends (except for tannins in RB (-) wines in 2016) to HPLC determination of phenolics.

A.4.7 Wine Volatile Compounds

Similar to the grape and wine phenolic composition, the volatile composition of the grapes and wine did not agree entirely. Wine matrix and its components such as ethanol, catechin, glucose, and glycerol, which differed among RB (-), RB (+), RB (+) S, and RB (+) 2H wines have been demonstrated to influence headspace concentration of aroma volatile compounds (Robinson et al., 2009).

Table A.4 indicates that 24 out of 29, and 26 out of 28 volatile compounds analyzed in the wines were significantly different among treatments in the 2016 and 2017 seasons, respectively. The odor description for each of the volatile compounds is presented in Table S5. In 2016, RB (-) had higher levels than RB (+) and RB (+) 2H wines for the following compounds: ethyl acetate, ethyl isobutyrate, isobutanol, isoamyl acetate, α-terpinene, limonene, ethyl hexanoate, hexyl acetate, ethyl lactate, ethyl octanoate, isobutyric acid, myrcene, diacetyl, p-cymene, ethyl isoval, acetoin, and rose oxide. Some compounds such as ethyl-2-methylbutyrate, isoamyl alcohol, isobutyric acid, and 2-phenylentil alcohol were not significantly different between RB (-) and RB (+) 2H wines but were significantly different with RB (+) wines, indicating a small decrease in volatile compositional differences with the longer hang time of GRBD fruit. In 2017, levels of ethyl acetate, ethyl isobutyrate, ethyl-2-methyl butyrate, isobutanol, limonene, isoamyl alcohol, ethyl lactate, nerol, ethyl hexanoate, and 2-phenylenthyl alcohol were similar among RB (-), RB (+) S, and RB (+) 2H wines and higher than RB (+) wines.

Table A.4. Peaks areas of volatile compounds identified by GC-MS analysis in RB (-), RB (+), RB (+) S and RB (+) 2H wines in 2016 and 2017.

Volatile Compounds	2016			Volatile Compounds	2017			
	RB (-)[a]	RB (+)[b]	RB (+) 2H[c]		RB (-)	RB (+)	RB (+) 2H	RB (+) S[d]
Ethyl Acetate	2.440 a	1.215 b	1.526 b	Ethyl Acetate	2.383 a	1.852 b	2.569 a	2.852 a
Ethyl Isobutyrate	0.132 a	0.071 b	0.088 b	Ethyl Isobutyrate	0.012 a	0.008 c	0.010 ab	0.010 b
Ethyl 2-methylbutyrate	0.011 a	0.008 b	0.010 ab	Ethyl 2-methylbutyrate	0.006 a	0.004 c	0.006 ab	0.005 bc
Isobutanol	0.089 a	0.057 b	0.070 b	Isobutanol	0.069 a	0.056 b	0.067 ab	0.074 a
Isoamyl Acetate	1.005 a	0.448 b	0.471 b	Isoamyl Acetate	0.525 b	0.426 b	0.720 a	0.722 a
α-Terpinene	0.001 a	0.001 c	0.001 b	α-Terpinene	0.000 ab	0.000 b	0.001 a	0.000 ab
Limonene	0.003 a	0.002 c	0.002 b	Limonene	0.008 a	0.005 b	0.008 a	0.009 a
Isoamyl Alcohol	2.747 a	1.733 b	2.436 a	Isoamyl Alcohol	2.201 a	1.656 b	2.288 a	2.256 a
Ethyl Hexanoate	1.656 a	1.426 b	1.349 b	Ethyl Hexanoate	1.531 ab	1.332 b	1.607 a	1.649 a
Hexyl Acetate	0.111 a	0.066 b	0.047 b	Hexyl Acetate	0.058 b	0.056 b	0.087 a	0.084 a
Ethyl Lactate	0.164 a	0.108 c	0.143 b	Ethyl Lactate	0.104 a	0.074 b	0.099 a	0.084 a
Hexanol	0.031 a	0.025 ab	0.023 b	Hexanol	0.029 a	0.030 a	0.021 b	0.029 a
Ethyl Octanoate	13.249 a	10.005 b	10.516 b	Ethyl Octanoate	10.666 a	9.659 a	12.546 a	14.097 a
Isobutyric Acid	0.002 a	0.001 b	0.001 ab	Isobutyric Acid	0.002 a	0.002 a	0.002 a	0.002 a
Ethyl decanoate	4.342 a	3.668 a	3.831 a	Ethyl decanoate	3.010 b	3.403 b	3.749 b	4.890 a
b-Citronellol	0.005 b	0.006 a	0.005 ab	b-Citronellol	0.003 c	0.004 a	0.003 b	0.003 b
Nerol	0.001 a	0.001 a	0.001 a	Nerol	0.002 a	0.001 b	0.002 a	0.002 a
Damascenone	0.008 ab	0.009 a	0.007 b	Damascenone	0.011 b	0.013 a	0.013 a	0.011 b
Benzyl Alchool	0.009 a	0.014 a	0.010 a	Benzyl Alchool	0.013 b	0.020 a	0.011 b	0.012 b
2-Phenylethyl alcohol	2.635 a	1.975 b	2.654 a	2-Phenylethyl alcohol	2.649 a	1.869 b	2.417 a	2.393 a
Nerolidol	0.006 b	0.017 a	0.010 ab	Nerolidol	0.002 b	0.003 a	0.003 a	0.002 ab
Linalool	0.007 a	0.006 b	0.007 a	Linalool	0.005 b	0.004 bc	0.006 a	0.004 c
Only in 2016				**Only in 2017**				
2-3-Hexenol	0.004 a	0.004 a	0.003 a	Ethyl Butanoate	0.118 a	0.089 b	0.126 a	0.130 a
Hexenol 2	0.001 a	0.001 a	0.001 a	Ethyl dehydrocinnamate	0.001 c	0.001 b	0.001 d	0.002 a
Myrcene	0.000 a	0.000 c	0.000 b	β-Ionone	0.000 b	0.000 ab	0.000 b	0.000 a
Diacetil	0.026 a	0.018 b	0.019 b	γ-Nonalactone	0.001 ab	0.000 b	0.001 a	0.001 ab
p-Cymene	0.002 a	0.001 c	0.002 b	Farnesol	0.001 b	0.001 b	0.001 ab	0.001 a
Ethyl Isoval	0.015 a	0.009 b	0.011 b	Ethyl vanillate	0.000 a	0.000 b	0.000 b	0.000 a
Acetoin	0.004 a	0.002 b	0.003 b					
Rose Oxide	0.001 a	0.001 b	0.000 b					

Values are the mean of three biological replicates (n=3). Statistical differences are expressed as letters and indicate significant differences in the LSD test within each row for each year ($p \leq 0.05$). [a]RB (-) = Healthy grapes. [b]RB (+) = GRBD grapes harvested at the same time as RB (-). [c]RB (+) 2H = GRBD grapes with longer hanging time and harvested with similar [o]Brix as RB (-). [d]RB (+) S = GRBD grapes must was chaptalized to 24 [o]Brix.

Based on the differences among the wines regarding their must sugar content at the onset of fermentation as a direct impact of GRBD on grapes, one can conclude that GRBD indirectly impacted major volatile compound groups present in wines such as esters and high alcohols. Esters such as ethyl-2-methylbutyrate and ethyl isobutyrate are formed through the reaction of a carboxylic acid (R-COOH) and an alcohol (R'-OH), which is referred to as esterification (Waterhouse et al., 2016). It is known that esterification occurs to a higher degree in wines with high levels of alcohol and lower pH, which correlates more with RB (-) wine treatments when compared to the other two wine treatments in 2016 and with RB (-), RB (+) S and RB (+) 2H when compared to RB (+) wines in 2017.

Higher alcohol compounds such as isobutanol and isoamyl alcohol are formed as a byproduct of amino acid yeast metabolism (Gonzalez & Morales, 2017). RB (-), RB (+) S, and RB (+) 2H musts were ~24°Brix at the onset of fermentation, 12% higher than RB (+) must, which was 21.4°Brix (Table A.1.). Therefore, yeast activity and reproduction were likely extended due to the higher sugar content at the onset of fermentation and longer fermentation in RB (-), RB (+) S, and RB (+) 2H wines, resulting in higher biosynthesis of yeast-derived volatile compounds. It has been shown that increasing must sugar concentration resulted in significant effects on yeast metabolism during fermentation. As the production of ethanol by yeast increased, there were concomitant increases in most yeast-derived metabolites (K. Bindon, Varela, Kennedy, Holt, & Herderich, 2013).

On the other hand, a few volatile compounds were higher in RB (+) wines when compared to RB (-) and RB (+) 2H wines. This was observed for nerolidol and citronellol in 2016, and for damascenone, nerolidol, citronellol, and benzyl alcohol in 2017. Even though RB (+) wines had higher levels of damascenone than RB (-), it was not significantly different from RB (+) 2H wines

in 2017. The C13-norisoprenoid damascenone is a volatile compound derived from the degradation of carotenoids in the isoprenoid biosynthetic pathway (Kanasawud, Crouzet, & Chemistry, 1990). Carotenoid concentration has been demonstrated to decrease after veraison during grape ripening in Merlot grapes and its concentration in grapes has shown to be highly correlated to C13-norisoprenoid concentrations in wines (Crupi, Coletta, & Antonacci, 2010). Although carotenoid concentration was not measured in this study, the higher concentration of damascenone in RB (+) wines compared to RB (-) wines may be explained due to the delay of grape ripening caused by GRBD (Cauduro Girardello et al., 2019; Martínez-Lüscher et al., 2019), and due to the reduced grapevine vigor caused by the disease (Calvi, 2011; Cauduro Girardello, Rich, et al., 2020). This could have increased grape berry exposure to the sunlight, which has been demonstrated to increase carotenoid concentration in grapes at early ripening stages and thus delaying the decrease of grape carotenoid content (Mendes-Pinto, 2009).

Monoterpenes such as nerolidol have been shown to protect many species of plants, animals, and microorganisms against predators, pathogens, and competitors (Gershenzon & Dudareva, 2007). Although nerolidol was not measured in the grapes, it is possible that wines from RB (+) grapes had a higher content of this specific terpene due to its role in plant defense.

Principle component analysis (PCA) was performed in both 2016 and 2017 to analyze the relationship between the volatile compounds and the different wine treatments (Figures 10 and 11). In the 2016 season, the first and second dimensions explained 82% of the variance, with clear separation among wine treatments being observed. RB (+) wines are located on the left and RB (-) wines on the right, with RB (+) 2H wines in the center. Most of the volatile compounds were highly correlated to RB (-) wines and weakly correlated to RB (+) wines. Also, RB (+) 2H were more similar to RB (-) wines than RB (+) wines. In 2017, the similarities among RB (-), RB

(+) S, and RB (+) 2H wines became even more evident. The first and second dimensions explained 68% of the variance. RB (-), RB (+) S, and RB (+) 2H wines were clustered together on the right of the PCA, and most of the volatile compounds analyzed were highly correlated with these wines. On the other hand, RB (+) wines were negatively correlated to RB (-), RB (+) S, and RB (+) 2H wines, and strongly correlated to a smaller amount of volatile compounds (benzyl alcohol, nerolidol, damascenone, hexanol). Volatile compositional analysis indicated that GRBD significantly impacted the aroma profiles of wines when harvested at the same time as healthy grapes. However, when diseased grapes were harvested at a later date to extend ripening, or chaptalized, the impact of GRBD was reduced, resulting in wines with more similar volatile profiles to wines made from healthy fruit. In summary, data suggest that the higher sugar levels of RB (+) S and RB (+) 2H compared to RB (+) at the onset of fermentation resulted in longer fermentations and more yeast metabolism during fermentation. It resulted in wines with more ethanol content, which enhanced the formation of volatile compounds through encouraging chemical reactions and yeast metabolism-derived compounds. Therefore, these observations indicate that a delayed harvest of diseased grapes can potentially mitigate some of the impacts of GRBD on wine volatile profile.

Table A.5. Aroma, taste, and mouthfeel attributes rated in the RB (-), RB (+) and RB (+) 2H wines and their respective overall score means obtained by descriptive analysis in 2016 and 2017. Rating scale: 0 (not present) to 10 (very intense).

2016				2017				
Attributes	**RB (-)[a]**	**RB (+)[b]**	**RB (+) 2H[c]**	**Attributes**	**RB (-)**	**RB (+)**	**RB (+) 2H**	**RB (+) S[d]**
Ethanol	**4.316 a**	**3.500 b**	**4.035 ab**	Raspberry	1.232 a	1.034 a	1.148 a	1.198 a
Vanilla	1.930 a	1.974 a	1.641 a	Blackberry	1.441 a	1.231 a	1.379 a	1.490 a
Cherry	2.728 a	2.902 a	2.265 a	Plum	1.556 a	1.658 a	1.396 a	1.553 a
Floral	2.369 a	2.483 a	1.901 a	Cherry	1.276 a	1.332 a	1.396 a	1.323 a
Earthy	1.017 a	0.886 a	0.947 a	Strawberry	1.206 a	1.073 a	1.022 a	1.249 a
Apple	**1.521 ab**	**1.978 a**	**1.230 b**	Fresh Veg.	0.982 a	1.102 a	0.918 a	0.849 a
Rubber	1.737 a	1.191 a	1.281 a	Vinegar	0.512 a	0.614 a	0.658 a	0.707 a
Strawberry	1.457 a	1.647 a	1.538 a	Alcohol	3.460 a	3.470 a	3.358 a	3.433 a
Tropical Fruit	0.933 a	1.158 a	0.956 a	Floral	1.003 a	1.013 a	0.916 a	0.952 a
Leather	1.721 a	1.486 a	1.948 a	Mineral	0.870 a	0.841 a	1.020 a	1.009 a
Ripe Fruit	1.807 a	1.978 a	1.773 a	Vanilla	1.027 a	0.950 a	1.038 a	0.936 a
Leafy	0.454 a	0.685 a	0.588 a	Oak	1.584 a	1.491 a	1.331 a	1.274 a
Raspberry	1.669 a	1.560 a	1.419 a	Other	0.110 a	0.074 a	0.046 a	0.020 a
Black current	2.679 a	2.322 a	2.643 a	Sweet	2.611 a	2.229 a	2.169 a	2.458 a
Blackberry	2.040 a	2.112 a	2.172 a	Bitter	2.266 a	2.134 a	2.137 a	2.159 a
Mint	0.759 a	0.644 a	0.690 a	Salty	0.230 a	0.287 a	0.264 a	0.217 a
Black pepper	0.828 a	0.705 a	0.695 a	**Sour**	**2.710 b**	**3.207 a**	**2.957 ab**	2.952 ab
Chocolate	0.620 a	0.615 a	0.701 a	Astringency	2.997 a	2.816 a	2.698 a	2.851 a
Bitter	**2.946 ab**	**2.304 b**	**3.296 a**	Viscosity	2.628 a	2.582 a	2.533 a	2.498 a
Sweet	1.702 a	1.333 a	1.368 a	**Hot**	**2.048 ab**	**1.931 ab**	**1.808 b**	**2.293 a**
Salty	1.272 a	0.933 a	0.889 a	**Peppery**	**1.020 a**	**0.681 b**	**0.867 ab**	0.922 ab
Sour	3.904 a	3.500 a	3.759 a	Grippy	1.440 a	1.537 a	1.491 a	1.563 a
Hot Burning	**3.717 a**	**2.619 b**	**3.268 a**					
Flat	3.630 a	4.272 a	3.815 a					
Viscosity	2.567 a	2.565 a	2.407 a					
Astringency	2.506 a	2.188 a	2.251 a					
Effervescence	0.553 a	0.535 a	0.706 a					

Statistical differences are expressed as letters and indicate significant differences in LSD test within each row for each year (n=27 in 2016 and n=30 in 2017, $p \leq 0.05$). Bold attributes were found significantly different among the wines. [a]RB (-) = Healthy grapes. [b]RB (+) = GRBD grapes harvested at the same time as RB (-). [c]RB (+) 2H = GRBD grapes with longer hanging time and harvested with similar [o]Brix as RB (-). [d]RB (+) S = GRBD grapes must was chaptalized to 24 [o]Brix.

A.4.8 Descriptive sensory analysis

Table 5 shows sensory attribute means and their respective Fisher's LSD test for wines treatments in 2016 and 2017. Tables S5 and S6 (Supplementary Materials) list the corresponding reference standards used for each attribute in 2016 and 2017. From the 27 attributes generated to describe the wines in 2016, statistical analysis indicated that four attributes were significantly different among the wines. RB (-) and RB (+) 2H wines were rated similarly regarding "hot/burning" mouthfeel and significantly higher than RB (+) wines. These results agree with the chemical analysis presented in Table A.2., which shows that RB (-) and RB (+) 2H had significantly higher ethanol content when compared to RB (+) wines. Also, RB (+) 2H was similar to RB (-) and higher than RB (+) regarding "bitter" taste. Phenolic composition presented in Table A.3. demonstrated that RB (+) 2H wines had a higher concentration of flavan-3-ols than RB (-) and RB (+), which includes catechin and epicatechin, compounds that were shown to be responsible for bitterness in model wine solution (Kallithraka, Bakker, & Clifford, 1997). Although RB (-) had a lower flavan-3-ol concentration than RB (+) 2H, they were rated similarly for "bitter" taste, likely because the difference in flavan-3-ol concentration was not large enough to be detectable. Also, the similarities between RB (-) and RB (+) 2H wines concerning ethanol content may have played an essential role since ethanol content has been shown to enhance bitterness perception in wine (Fontoin et al., 2008; Ellena S King, Dunn, & Heymann, 2014).

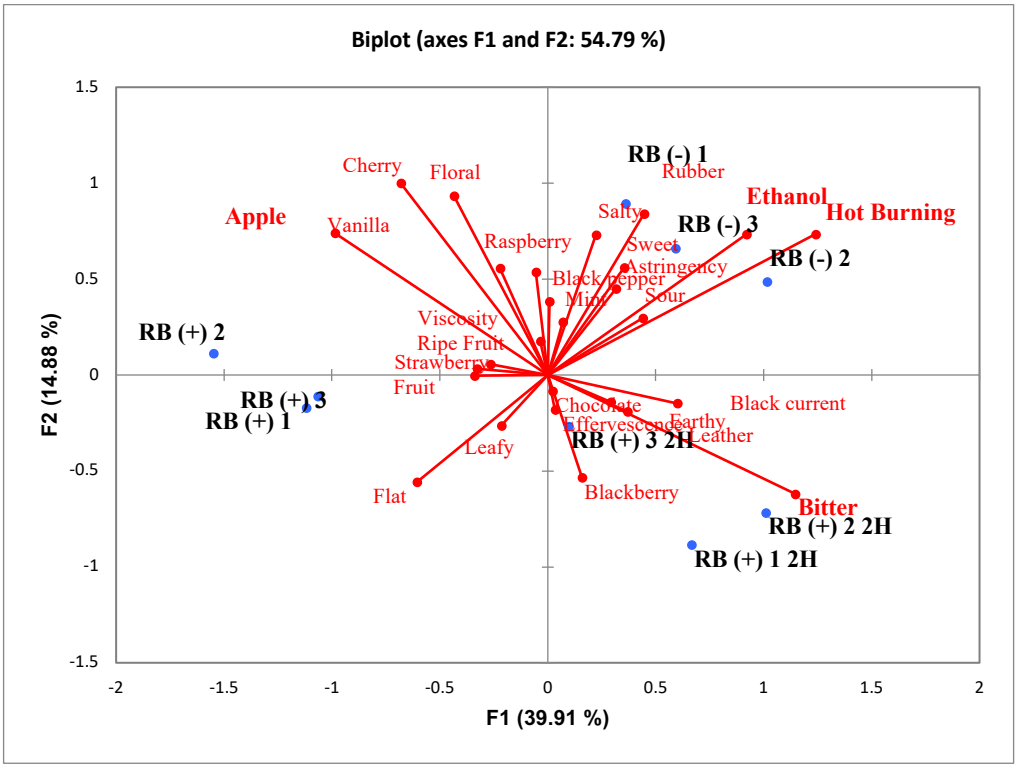

Figure A.4. Score (black) and loadings (red) plots of a principal component analysis (PCA) of wines analyzed by descriptive analysis in the 2016 season. RB (-) = Healthy grapes. RB (+) = GRBD grapes harvested at the same time as RB (-). RB (+) 2H = GRBD grapes with longer hanging time and harvested with similar ºBrix as RB (-).

The only attribute rated higher for RB (+) wines in comparison to RB (+) 2H and similar to RB (-) was "apple aroma". PCA was performed to find correlations between the wines and the sensory attributes evaluated by judges in 2016 (Figure A.4). RB (-) and RB (+) 2H were grouped at the right side of the principal component 1 (F1), confirming their strong correlation with attributes "ethanol" aroma, "hot/burning" mouthfeel and "bitter" taste. On the other hand, RB (+) wines were grouped on the left side of F1, demonstrating their negative correlation with RB (-) and RB (+) 2H wines.

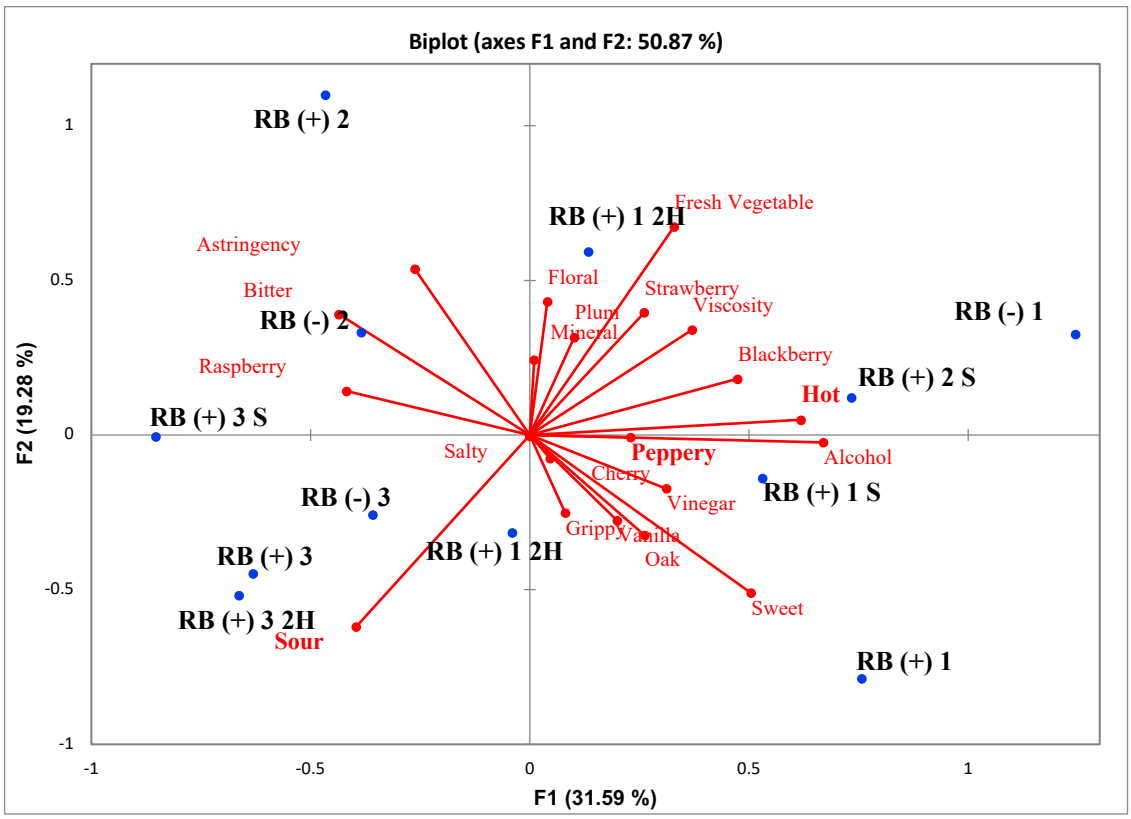

Figure A.5. Score (black) and loadings (red) plots of a principal component analysis (PCA) of wines analyzed by descriptive analysis in 2017. RB (-) = Healthy grapes. RB (+) = GRBD grapes harvested at the same time as RB (-). RB (+) 2H = GRBD grapes with longer hanging time and harvested with similar ºBrix as RB (-). RB (+) S = GRBD grapes - must was chaptalized to 24 ºBrix.

Descriptive analysis performed in 2017 did not find a clear separation among treatments as observed in 2016 (Figure A.5). Only 3 out of 22 attributes were significantly different: RB (+) wines were rated significantly more "sour" than RB (-) wines, while RB (+) 2H and RB (+) S wines were rated intermediately between RB (+) and RB (-). Although chemical analysis (Table A.2.) showed similar TA concentrations among the wines, ethanol plays an important role in the perception of "sourness" in wines. It has been demonstrated that "sourness" decreases as ethanol content increases due to its masking action (Fischer & Noble, 1994), which partially explains why RB (+) wines were rated more "sour". RB (+) wines were also rated significantly lower than RB (-) and RB (+) 2H for "peppery" aroma. The volatile compound rotundone is known for being responsible for the "peppery" aroma in wines. The concentration of this compound was found to

increase in grapes during ripening (Caputi et al., 2011). Even though rotundone was not measured in the grapes and wines in this study, one hypothesis is that RB (+) wines had lower "peppery" aroma due to the delayed ripening caused by GRBD, which potentially impacted rotundone accumulation. "Hot" mouthfeel was also found to be higher in RB (+) S wines when compared to RB (+) 2H and RB (+) wines, which is highly correlated to the ethanol content of the wines presented in Table A.2. It what has been demonstrated that judges rated the attribute "heat" higher in wines with 13.6% (v/v) ethanol than in wines with 12.6% (v/v), demonstrating that a difference of 1% (v/v) in ethanol content in wines is large enough to be perceived by a trained consumer panel in Riesling wines (Gawel, Sluyter, & Waters, 2007).

Figure S3 (Supplementary Materials) displays the wines color evaluations performed by judges in 2016 and 2017. In both years, judges were not able to distinguish between RB (-) and RB (+) 2H wines, which had similar color scores. On the other hand, RB (+) wines had lower scores when compared to RB (-) and RB (+) 2H, agreeing with the trends observed for anthocyanin concentration (Table A.3.).

Multiple factor analyses (MFA) were performed to investigate the relationships among wines and their respective compositional and sensory data for the 2016 and 2017 seasons (Figures 14-17). For 2016 wines, principal components one and two explain 65.8% of the variance (Figures 14 and 15). The score plot shows a clear separation among the three treatments for 2016. Comparing the loading plot (Figure A.6) to the score plot (Figure A.7), it is possible to see the stronger relation between RB (-) and RB (+) 2H wines with most of the compounds analyzed, which includes most of the phenolic compounds and volatile compounds. Ethanol content (EtOH%) also plays an important role in this separation, since it is located between RB (-) and RB (+) 2H wines and on the opposite side of RB (+) wines. RB (+) wines were strongly related to a

few key volatile compounds as discussed previously. In 2017, MFA was able to separate the 2017 RB (+) wines from RB (-), RB (+) 2H, and RB (+) S wines. Here the latter, RB (+) S, was separated from RB (-) and RB (+) 2H wines. Sensory results agree with chemical data. confirming that the more advanced ripening stages due to the longer grape hangtime helped to mitigate the impacts of GRBD, which in general, resulted in wines more similar to those made with grapes from healthy grapevines (Figures 16 and 17).

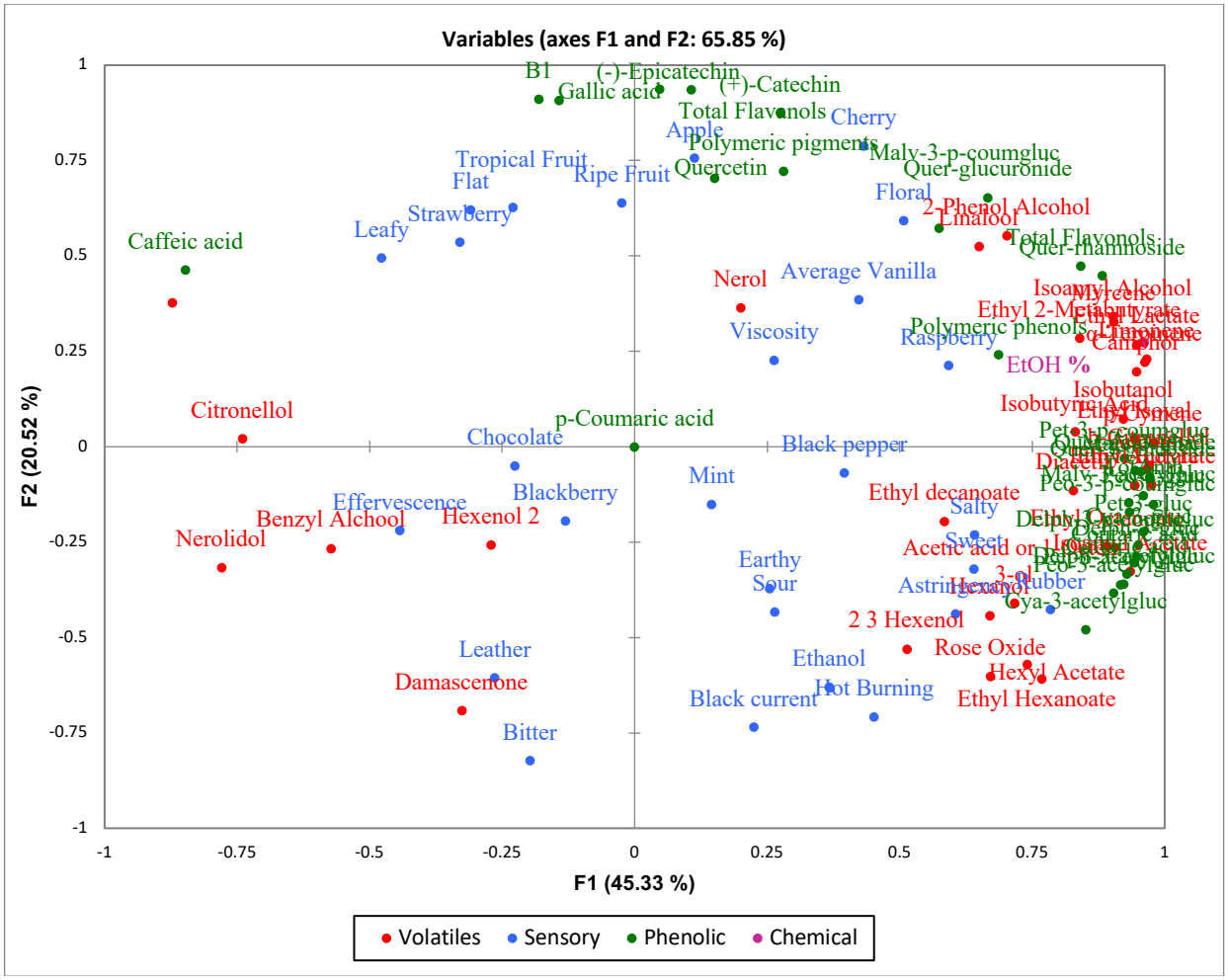

Figure A.6. Multiple Factor Analysis (MFA) loading plots of 2016 wines. Volatile compounds (red), sensory attributes (blue), phenolic compounds are in (green) and ethanol (purple).

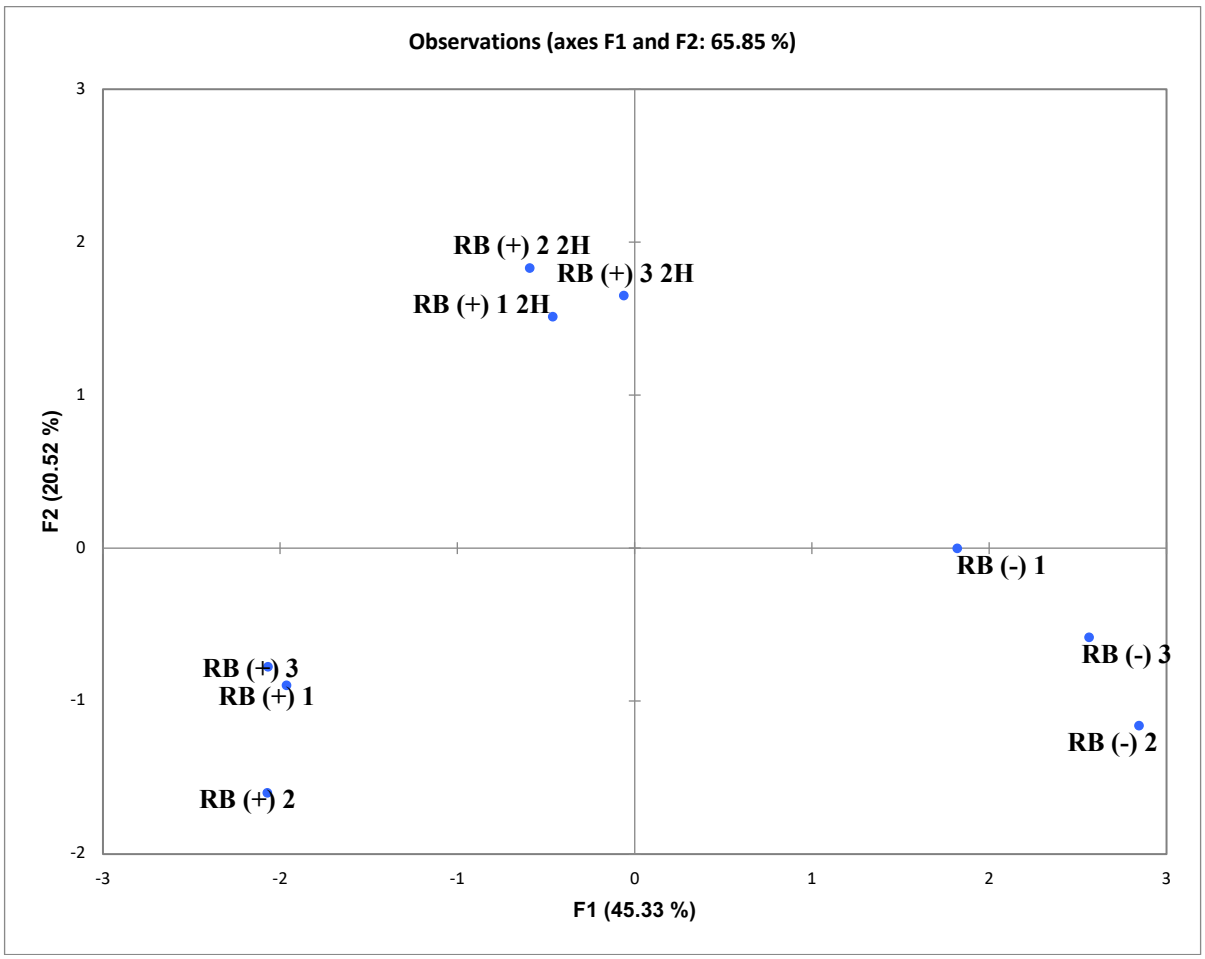

Figure A.7. Multiple Factor Analysis (MFA) score plots of RB (-), RB (+) and RB (+) 2H 2016 wines. RB (-) = Healthy grapes. RB (+) = GRBD grapes harvested at the same time as RB (-). RB (+) 2H = GRBD grapes with longer hanging time and harvested with similar ºBrix as RB (-).

A.5 Conclusions:

Grape compositional analysis during ripening confirmed previous studies that found that GRBV delays ripening. Longer hang time was successful in increasing sugar content in diseased grapes and making wines with more similar ethanol as well as phenolic and volatile aroma content to those made from healthy grapes. This is in contrast with grape data that, in general, did not indicate higher phenolic concentrations with longer hang time. Potentially, the higher ethanol concentration and greater degradation of grape cell walls due to the more advanced ripening stage aided

extractability of phenolics in to the RB (+) 2H wines. Chaptalization helped to decrease the differences between the wines made with grapes from diseased and healthy grapevines regarding some volatile compounds. However, this was not true for phenolic compounds, such as tannins and anthocyanins. Final wine analysis, as well as descriptive analysis, indicated that RB (+) 2 H wines were more similar to RB (-) wines than RB (+) wines. The current study indicated that ethanol content along with more advanced grape berry ripening plays a synergetic role to mitigate the impacts of GRBD in wines.

Conflicts of Interest: The authors declare no conflict of interest.

Use of Human Subjects: Authors inform that consent was obtained for experimentation with human subjects by the Institutional Review Board (IRB) Administration and each of the wine sensory panelists.

Funding: This research was funded by American Vineyard Foundation (AVF) grant number 2016-1953 and 2017-1675 as well as J. Lohr Vineyards and Wines.

Acknowledgements: We would like to thank the Brazilian Government through Coordination for the Improvement of Higher Education Personnel (CAPES), the Henry A. Jastro Scholarship, and the Horticulture and Agronomy Graduate Group at UC Davis for the scholarships, which enabled this study to be performed.

Authors contributions: R.C.G. performed experiments, analyzed data, and wrote the manuscript. A.R. helped with performing the experiments, data analysis and reviewed the manuscript. A.O. designed experiments, evaluated data, and reviewed and edited the manuscript. C.B. advised and supported winemaking. H.H. designed sensorial experiments. A. P. gave vineyard support and helped design the experiments. All authors have read and agreed to the published version of the manuscript.

A.6 Supplemental Figures:

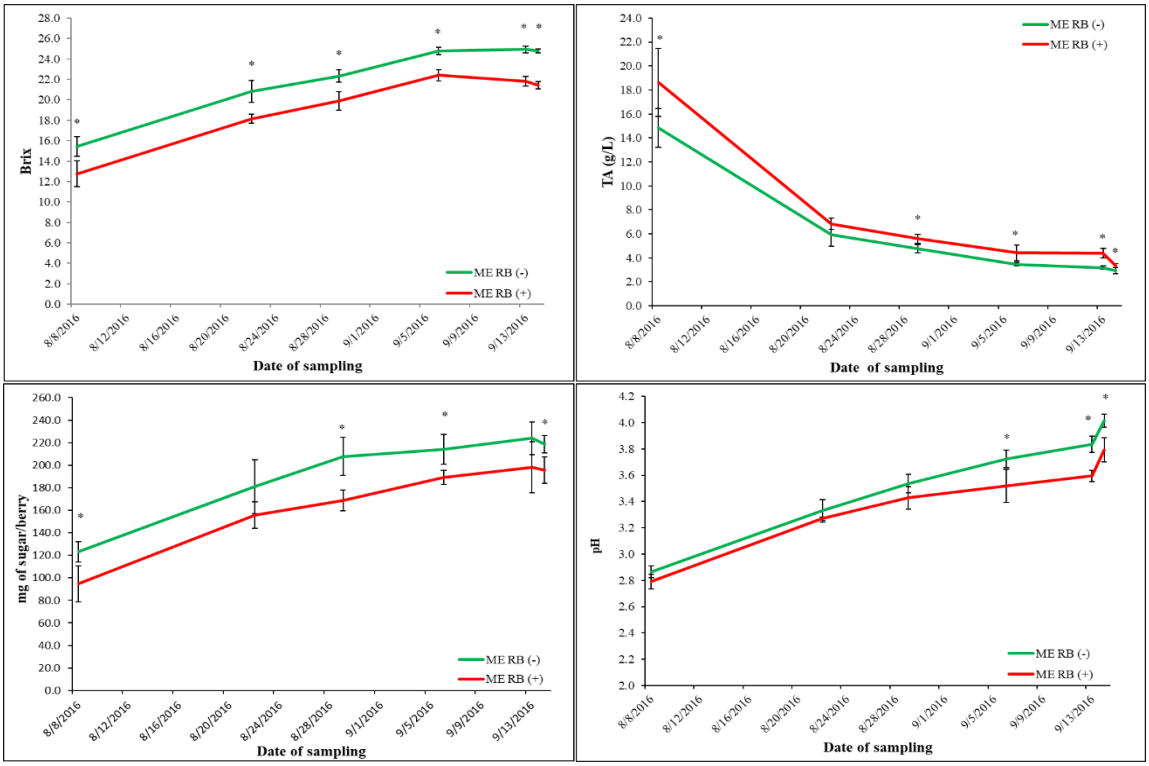

Figure A.S1. Analysis of the impact of GRBD on ºBrix, sugar loading, TA and pH during ripening in 2016. RB (-) is represented in green while RB (+) is shown in red. Each data point represents the mean of 5 biological repetitions of 4 vines each and its respective standard deviation bars (n=5). The first data point was taken at veraison and the last at harvest. Statistical differences were determined by T-test (*$p \leq 0.05$).

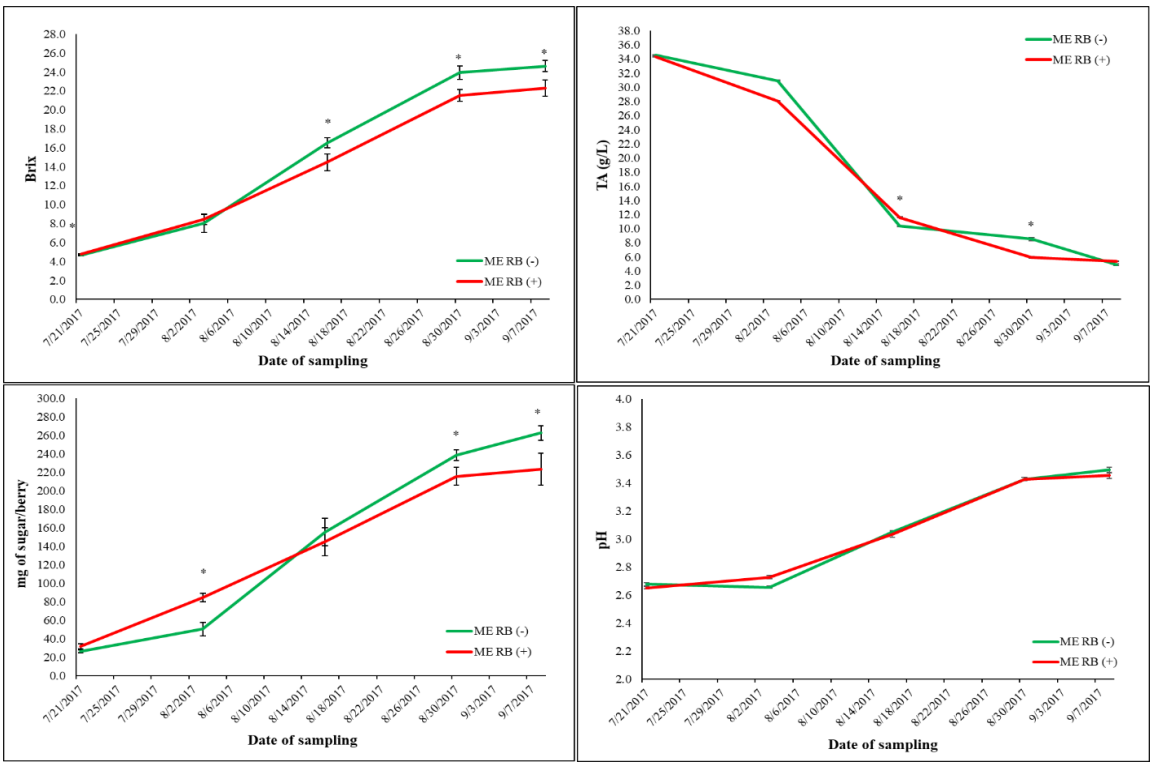

Figure A.S2. Analysis of the impact of GRBD on ºBrix, sugar loading, TA, and pH during ripening in 2017. RB (-) is represented in green while RB (+) is shown in red. Each data point represents the mean of 5 biological repetitions of 5 vines each and its respective standard deviation bars (n=5). The first data point was taken at veraison and the last at harvest. Statistical differences were determined by T-test (*$p \leq 0.05$).

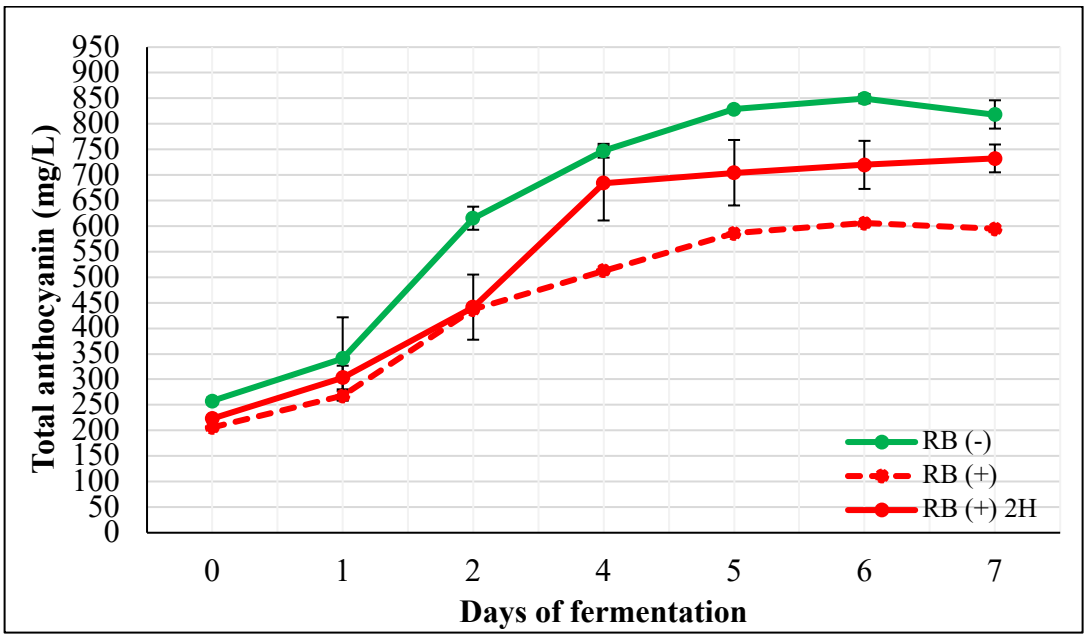

Figure A.S3. Extraction profile of total anthocyanin during alcoholic fermentation of wines in the 2016 season (n=3). RB (-) = Healthy grapes. RB (+) = GRBD grapes harvested at the same time as RB (-). RB (+) 2H = GRBD grapes with longer hanging time and harvested with similar ºBrix as RB (-).

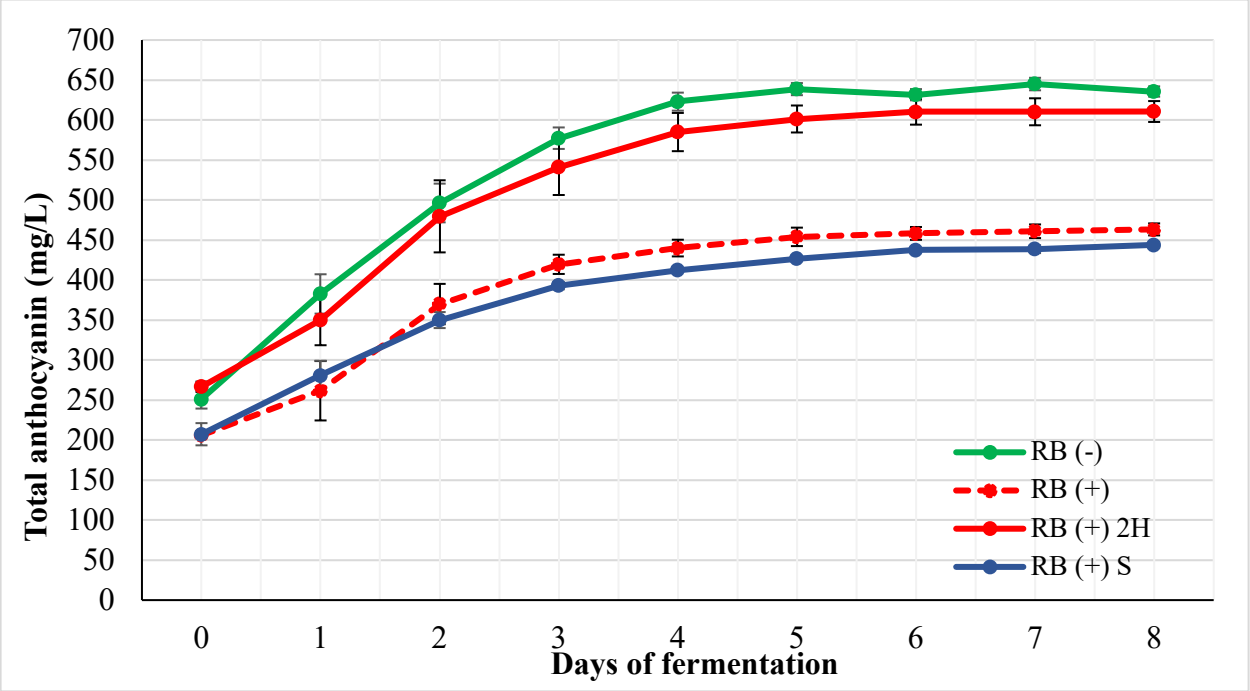

Figure A.S4. Extraction profile of total anthocyanin during alcoholic fermentation of wines in the 2017 season (n=3). RB (-) = Healthy grapes. RB (+) = GRBD grapes harvested at the same time as RB (-). RB (+) 2H = GRBD grapes with longer hanging time and harvested with similar ºBrix as RB (-). RB (+) S = GRBD grapes - must was chaptalized to 24 ºBrix.

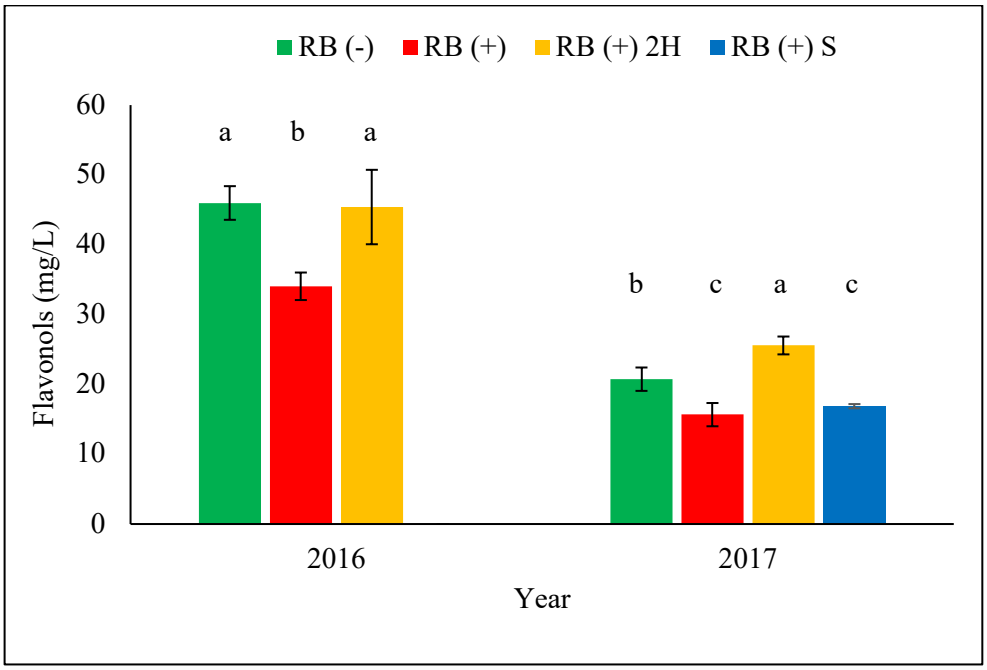

Figure A.S5. Total flavonols concentration of RB (-), RB (+) and RB (+) 2H and RB (+) S wines in the 2016 and 2017 seasons. Each bar represents the mean ± standard deviation of three biological replicates (n=3, $p \leq 0.05$). Means within a column followed by the same letter are not significantly different within a year.

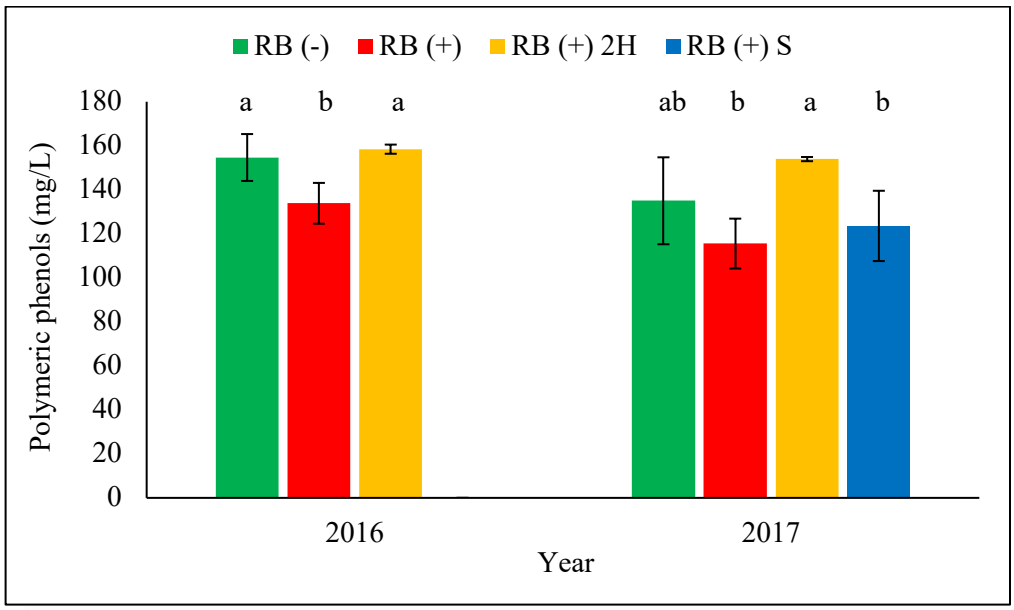

Figure A.S6. Total polymeric phenols concentration of RB (-), RB (+) and RB (+) 2H and RB (+) S wines in the 2016 and 2017 seasons. Each bar represents the mean ± standard deviation of three biological replicates (n=3, $p \leq 0.05$). Means within a column followed by the same letter are not significantly different within a year.

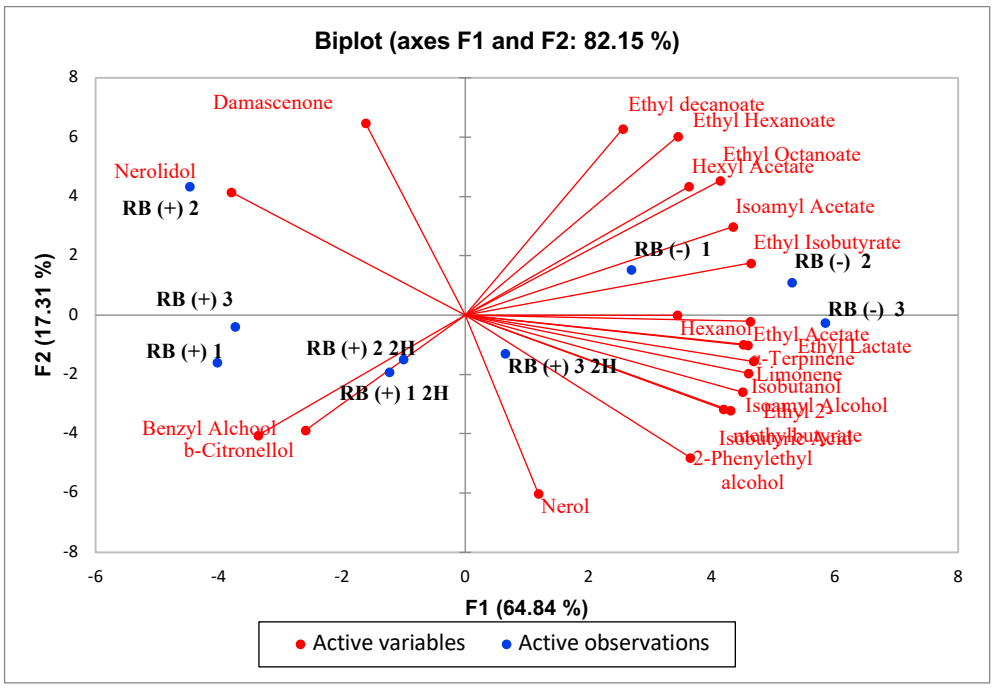

Figure A.S7. Score (black) and loadings plots (red) of a principal component analysis (PCA) of volatile compounds analyzed by GC-MS in wines in the 2016 season (n=3). RB (-) = Healthy grapes. RB (+) = GRBD grapes harvested at the same time as RB (-). RB (+) 2H = GRBD grapes with longer hanging time and harvested with similar ºBrix as RB (-).

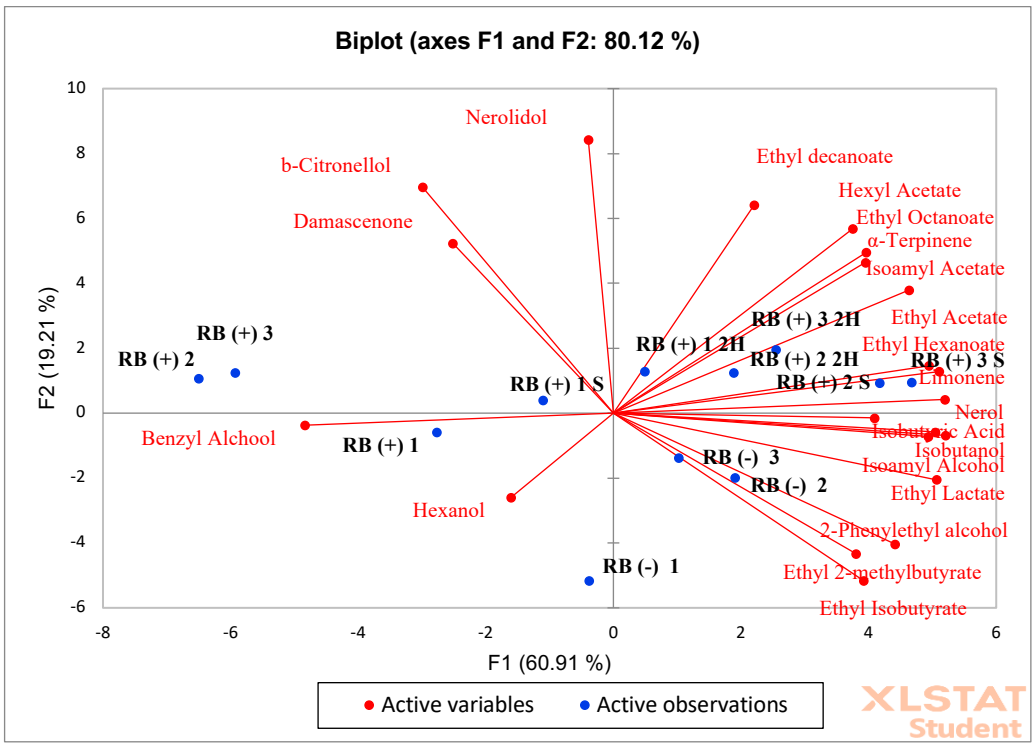

Figure A.S8. Score (black) and loadings (red) plots of a principal component analysis (PCA) of volatile compounds analyzed by GC-MS in wines in the 2017 season (n=3). RB (-) = Healthy grapes. RB (+) = GRBD grapes harvested at the same time as RB (-). RB (+) 2H = GRBD grapes with longer hanging time and harvested with similar ºBrix as RB (-). RB (+) S = GRBD grapes - must was chaptalized to 24 ºBrix.

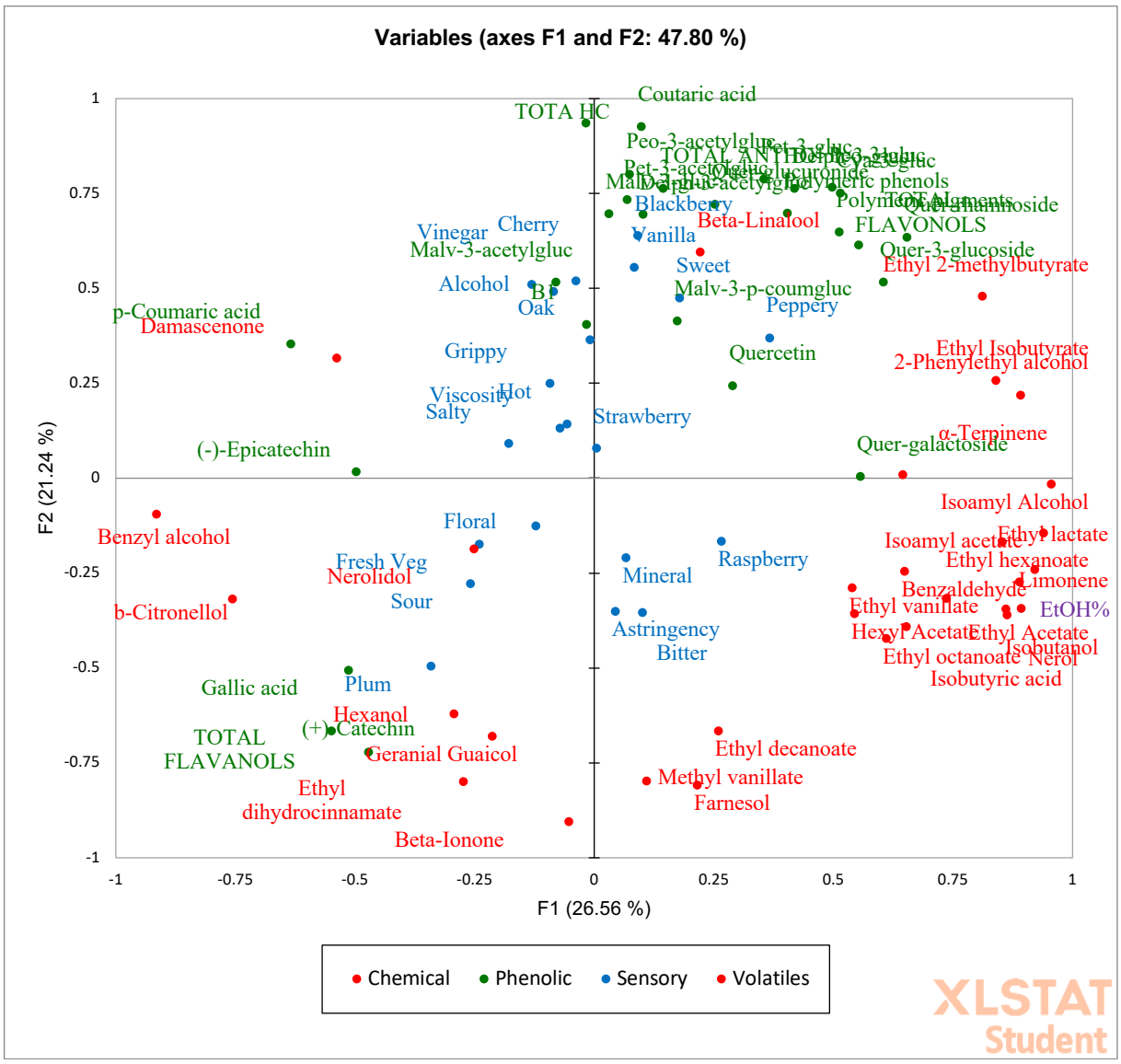

Figure A.S9. Multiple Factor Analysis (MFA) loading plots of 2017 wines. Volatile compounds (red), sensory attributes (blue), phenolic compounds are in (green) and ethanol (purple).

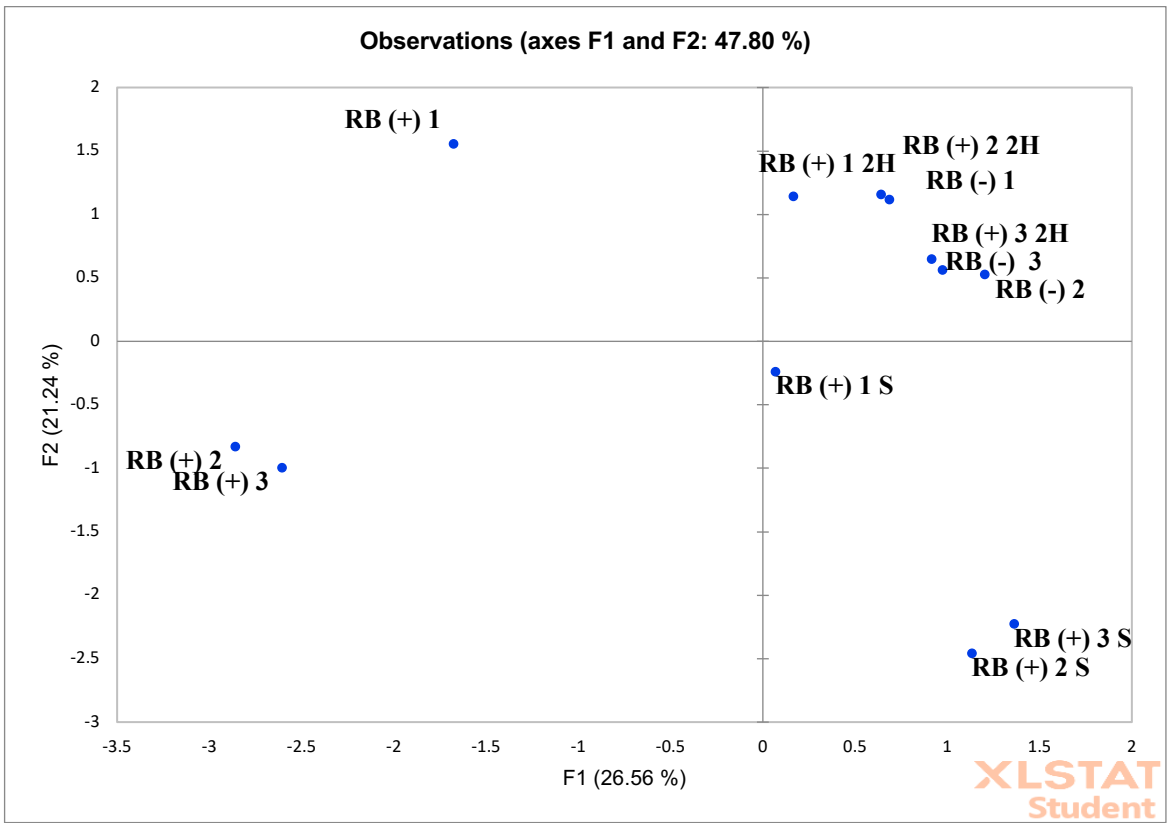

Figure A.S10. Multiple Factor Analysis (MFA) score plots of RB (-), RB (+), and RB (+) 2H 2017 wines. RB (-) = Healthy grapes. RB (+) = GRBD grapes harvested at the same time as RB (-). RB (+) 2H = GRBD grapes with longer hanging time and harvested with similar ºBrix as RB (-). RB (+) S = GRBD grapes - must was chaptalized to 24 ºBrix.

A.7 References

Adams, D. O. (2006). Phenolics and ripening in grape berries. *American Journal of Enology and Viticulture, 57* (3), 249-256.

Alabi, O. J., Casassa, L. F., Gutha, L. R., Larsen, R. C., Henick-Kling, T., Harbertson, J. F., & Naidu, R. A. (2016). Impacts of Grapevine Leafroll Disease on Fruit Yield and Grape and Wine Chemistry in a Wine Grape (Vitis vinifera L.) Cultivar. *PLOS ONE, 11* (2), e0149666.

Bahder, B. W., Zalom, F. G., Jayanth, M., & Sudarshana, M. R. (2016). Phylogeny of Geminivirus Coat Protein Sequences and Digital PCR Aid in Identifying Spissistilus festinus as a Vector of Grapevine red blotch-associated virus. *Phytopathology, 106* (10), 1223-1230.

Bautista-Ortín, A. B., Busse-Valverde, N., Fernández-Fernández, J. I., Gómez-Plaza, E., & Gil-Muñoz, R. (2016). The extraction kinetics of anthocyanins and proanthocyanidins from grape to wine in three different varieties. *OENO One, 50* (2).

Beaver, J. W., Medina-Plaza, C., Miller, K., Dokoozlian, N., Ponangi, R., Blair, T., Block, D., & Oberholster, A. (2020). Effects of the Temperature and Ethanol on the Kinetics of Proanthocyanidin Adsorption in Model Wine Systems. *Journal of Agricultural and Food Chemistry, 68* (10), 2891-2899.

Bindon, K., Varela, C., Kennedy, J., Holt, H., & Herderich, M. (2013). Relationships between harvest time and wine composition in Vitis vinifera L. cv. Cabernet Sauvignon 1. Grape and wine chemistry. *Food Chemistry, 138* (2), 1696-1705.

Bindon, K. A., Madani, S. H., Pendleton, P., Smith, P. A., & Kennedy, J. A. (2014). Factors Affecting Skin Tannin Extractability in Ripening Grapes. *Journal of Agricultural and Food Chemistry, 62* (5), 1130-1141.

Blanco-Ulate, B., Hopfer, H., Figueroa-Balderas, R., Ye, Z., Rivero, R. M., Albacete, A., Pérez-Alfocea, F., Koyama, R., Anderson, M. M., Smith, R. J., Ebeler, S. E., & Cantu, D. (2017). Red blotch disease alters grape berry development and metabolism by interfering with the transcriptional and hormonal regulation of ripening. *Journal of Experimental Botany, 68* (5), 1225-1238.

Boss, P. K., Davies, C., & Robinson, S. P. (1996). Analysis of the expression of anthocyanin pathway genes in developing Vitis vinifera L. cv Shiraz grape berries and the implications for pathway regulation. *Plant physiology, 111* (4), 1059-1066.

Brummell, D. A. (2006). Cell wall disassembly in ripening fruit. *Functional Plant Biology, 33* (2), 103-119.

Calvi, B. L. (2011). *Effects of red-leaf disease on Cabernet Sauvignon at the Oakville experimental vineyard and mitigation by harvest delay and crop adjustment*: University of California, Davis.

Canals, R., Llaudy, M., Valls, J., Canals, J., & Zamora, F. (2005). Influence of ethanol concentration on the extraction of color and phenolic compounds from the skin and seeds of Tempranillo grapes at different stages of ripening. *Journal of Agricultural and Food Chemistry, 53* (10), 4019-4025.

Caputi, L., Carlin, S., Ghiglieno, I., Stefanini, M., Valenti, L., Vrhovsek, U., & Mattivi, F. (2011). Relationship of Changes in Rotundone Content during Grape Ripening and

Winemaking to Manipulation of the 'Peppery' Character of Wine. *Journal of Agricultural and Food Chemistry, 59* (10), 5565-5571.
Castellarin, S. D., Gambetta, G. A., Wada, H., Krasnow, M. N., Cramer, G. R., Peterlunger, E., Shackel, K. A., & Matthews, M. A. (2015). Characterization of major ripening events during softening in grape: turgor, sugar accumulation, abscisic acid metabolism, colour development, and their relationship with growth. *Journal of Experimental Botany*, erv483.
Castillo-Muñoz, N., Gómez-Alonso, S., García-Romero, E., & Hermosín-Gutiérrez, I. (2007). Flavonol Profiles of Vitis vinifera Red Grapes and Their Single-Cultivar Wines. *Journal of Agricultural and Food Chemistry, 55* (3), 992-1002.
Cauduro Girardello, R., Cooper, M. L., Lerno, L. A., Brenneman, C., Eridon, S., Sokolowsky, M., Heymann, H., & Oberholster, A. (2020). Impact of Grapevine Red Blotch Disease on Cabernet Sauvignon and Merlot Wine Composition and Sensory Attributes. *Molecules, 25* (14), 3299.
Cauduro Girardello, R., L Cooper, M., J Smith, R., Lerno, L., Clifton Bruce, R., Eridon, S., & Oberholster, A. (2019). Impact of Grapevine Red Blotch disease on grape composition of Vitis vinifera Cabernet Sauvignon, Merlot and Chardonnay. *Journal of Agricultural and Food Chemistry*.
Cauduro Girardello, R., Rich, V., Smith, R. J., Brenneman, C., Heymann, H., Oberholster, A. J. J. o. t. S. o. F., & Agriculture. (2020). The impact of grapevine red blotch disease on Vitis vinifera L. Chardonnay grape and wine composition and sensory attributes over three seasons. *100* (4), 1436-1447.
Chellappan, P., Vanitharani, R., Ogbe, F., & Fauquet, C. M. (2005). Effect of Temperature on Geminivirus-Induced RNA Silencing in Plants. *Plant physiology, 138* (4), 1828-1841.
Cieniewicz, E., Thompson, J. R., McLane, H., Perry, K. L., Dangl, G. S., Corbett, Q., Martinson, T., Wise, A., Wallis, A., & O'Connell, J. (2018). Prevalence and Genetic Diversity of Grabloviruses in Free-Living Vitis spp. *Plant Disease*, PDIS-03-18-0496-RE.
Coombe, B. (1987). Distribution of solutes within the developing grape berry in relation to its morphology. *American Journal of Enology and Viticulture, 38* (2), 120-127.
Coombe, B. G. (1992). Research on Development and Ripening of the Grape Berry. *American Journal of Enology and Viticulture, 43* (1), 101-110.
Crupi, P., Coletta, A., & Antonacci, D. (2010). Analysis of Carotenoids in Grapes To Predict Norisoprenoid Varietal Aroma of Wines from Apulia. *Journal of Agricultural and Food Chemistry, 58* (17), 9647-9656.
Czemmel, S., Stracke, R., Weisshaar, B., Cordon, N., Harris, N. N., Walker, A. R., Robinson, S. P., & Bogs, J. (2009). The Grapevine R2R3-MYB Transcription Factor VvMYBF1 Regulates Flavonol Synthesis in Developing Grape Berries. *151* (3), 1513-1530.
Dalton, D. T., Hilton, R. J., Kaiser, C., Daane, K. M., Sudarshana, M. R., Vo, J., Zalom, F. G., Buser, J. Z., & Walton, V. M. J. P. D. (2019). Spatial associations of vines infected with grapevine red blotch virus in Oregon vineyards. (ja).
Deloire, A. (2011). *The concept of berry sugar loading* (Vol. 257).
Downey, M. O., Dokoozlian, N. K., & Krstic, M. P. (2006). Cultural practice and environmental impacts on the flavonoid composition of grapes and wine: a review of recent research. *American Journal of Enology and Viticulture, 57* (3), 257-268.

Dunlevy, J. D., Kalua, C. M., Keyzers, R. A., & Boss, P. K. (2009). The Production of Flavour & Aroma Compounds in Grape Berries. In K. A. Roubelakis-Angelakis (Ed.), *Grapevine Molecular Physiology & Biotechnology* (pp. 293-340). Dordrecht: Springer Netherlands.

Fischer, U., & Noble, A. C. (1994). The Effect of Ethanol, Catechin Concentration, and pH on Sourness and Bitterness of Wine. *American Journal of Enology and Viticulture, 45* (1), 6-10.

Fontoin, H., Saucier, C., Teissedre, P.-L., & Glories, Y. (2008). Effect of pH, ethanol and acidity on astringency and bitterness of grape seed tannin oligomers in model wine solution. *Food Quality and Preference, 19* (3), 286-291.

Gasperin-Bulbarela, J., Licea-Navarro, A. F., Pino-Villar, C., Hernández-Martínez, R., & Carrillo-Tripp, J. (2018). First report of grapevine red blotch virus in Mexico. *Plant Disease*, PDIS-07-18-1227-PDN.

Gawel, R., Sluyter, S. V., & Waters, E. J. (2007). The effects of ethanol and glycerol on the body and other sensory characteristics of Riesling wines. *13* (1), 38-45.

Gershenzon, J., & Dudareva, N. (2007). The function of terpene natural products in the natural world. *Nature Chemical Biology, 3*, 408.

González-Barreiro, C., Rial-Otero, R., Cancho-Grande, B., & Simal-Gándara, J. (2015). Wine Aroma Compounds in Grapes: A Critical Review. *Critical Reviews in Food Science and Nutrition, 55* (2), 202-218.

González-Manzano, S., Rivas-Gonzalo, J. C., & Santos-Buelga, C. (2004). Extraction of flavan-3-ols from grape seed and skin into wine using simulated maceration. *Analytica Chimica Acta, 513* (1), 283-289.

Gonzalez, R., & Morales, P. J. M. b. (2017). Wine secondary aroma: understanding yeast production of higher alcohols. *10* (6), 1449.

Gutha, L. R., Casassa, L. F., Harbertson, J. F., & Naidu, R. A. (2010). Modulation of flavonoid biosynthetic pathway genes and anthocyanins due to virus infection in grapevine (Vitis viniferaL.) leaves. *BMC Plant Biology, 10* (1), 187.

Harbertson, J. F., Mireles, M., & Yu, Y. (2014). Improvement of BSA tannin precipitation assay by reformulation of resuspension buffer. *American Journal of Enology and Viticulture*, ajev. 2014.14082.

Harbertson, J. F., Mireles, M., & Yu, Y. (2015). Improvement of BSA Tannin Precipitation Assay by Reformulation of Resuspension Buffer. *American Journal of Enology and Viticulture, 66* (1), 95-99.

Hendrickson, D. A., Lerno, L. A., Hjelmeland, A. K., Ebeler, S. E., Heymann, H., Hopfer, H., Block, K. L., Brenneman, C. A., & Oberholster, A. (2016). Impact of Mechanical Harvesting and Optical Berry Sorting on Grape and Wine Composition. *American Journal of Enology and Viticulture*, ajev. 2016.14132.

I. Jackson, D., & B. Lombard, P. (1993). *Environmental and Management Practices Affecting Grape Composition and Wine Quality - A Review* (Vol. 44).

Kallithraka, S., Bakker, J., & Clifford, M. (1997). Evaluation of Bitterness and Astringency of (+)-Catechin and (-)-Epicatechin in Red Wine and in Model Solution. *Journal of Sensory Studies, 12* (1), 25-37.

Kanasawud, P., Crouzet, J. C. J. J. o. A., & Chemistry, F. (1990). Mechanism of formation of volatile compounds by thermal degradation of carotenoids in aqueous medium. 1.. beta.-Carotene degradation. *38* (1), 237-243.

Keller, M. (2015). *The science of grapevines: anatomy and physiology*: Academic Press.

Keller, M., & Hrazdina, G. (1998). Interaction of nitrogen availability during bloom and light intensity during veraison. II. Effects on anthocyanin and phenolic development during grape ripening. *American Journal of Enology and Viticulture, 49* (3), 341-349.
Kennedy, J. A. (2008). Grape and wine phenolics: Observations and recent findings. *Ciencia e investigación agraria, 35* (2), 107-120.
King, E. S., Dunn, R. L., & Heymann, H. (2013). The influence of alcohol on the sensory perception of red wines. *Food Quality and Preference, 28* (1), 235-243.
King, E. S., Dunn, R. L., & Heymann, H. (2014). The influence of alcohol on the sensory perception of red wines. *Wine and viticulture journal* (2), 5.
Kliewer, W. M., & Lider, L. A. (1976). Influence of Leafroll Virus on Composition of Burger Fruits. *27* (3), 118-124.
Kodur, S. (2011). Effects of juice pH and potassium on juice and wine quality, and regulation of potassium in grapevines through rootstocks (Vitis): a short review. *VITIS Journal of Grapevine Research, 50* (1), 1-6.
Krenz, B., Thompson, J., McLane, H., Fuchs, M., & Perry, K. (2014). Grapevine red blotch-associated virus is widespread in the United States. *Phytopathology, 104* (11), 1232-1240.
Lamikanra, O., Inyang, I. D., & Leong, S. (1995). Distribution and effect of grape maturity on organic acid content of red muscadine grapes. *Journal of Agricultural and Food Chemistry, 43* (12), 3026-3028.
Lee, J., & Martin, R. R. (2009). Influence of grapevine leafroll associated viruses (GLRaV-2 and -3) on the fruit composition of Oregon Vitis vinifera L. cv. Pinot noir: Phenolics. *Food Chemistry, 112* (4), 889-896.
Lerno, L., Reichwage, M., Ponangi, R., Hearne, L., Block, D. E., & Oberholster, A. (2015a). Effects of Cap and Overall Fermentation Temperature on Phenolic Extraction in Cabernet Sauvignon Fermentations. *American Journal of Enology and Viticulture*.
Lerno, L., Reichwage, M., Ponangi, R., Hearne, L., Block, D. E., & Oberholster, A. (2015b). Effects of Cap and Overall Fermentation Temperature on Phenolic Extraction in Cabernet Sauvignon Fermentations. *American Journal of Enology and Viticulture, 66* (4), 444-453.
Lim, S., Igori, D., Zhao, F., Moon, J., Cho, I.-S., & Choi, G.-S. (2016). First report of Grapevine red blotch-associated virus on grapevine in Korea. *Plant Disease, 100* (9), 1957-1957.
Luna, F., Debat, H., Moyano, S., Zavallo, D., Asurmendi, S., & Gomez-Talquenca, S. (2019). First report of grapevine red blotch virus infecting grapevine in Argentina. *Journal of Plant Pathology, 101* (4), 1239-1239.
Martelli, G. P. (2014). Directory of virus and virus-like diseases of the grapevine and their agents. *Journal of Plant Pathology, 96* (1sup), 1-136.
Martínez-Lüscher, J., Plank, C. M., Brillante, L., Yu, R., AlRwahnih, M., Cooper, M. L., Smith, R., Girardello, R., Oberholster, A., Kurtural, S. K. J. J. o. a., & chemistry, f. (2019). Grapevine Red Blotch Virus May Reduce Carbon Translocation Leading to Impaired Grape Berry Ripening.
McCarthy, M. G., & Coombe, B. G. (1999). Is weight loss in ripening grape berries cv. Shiraz caused by impeded phloem transport? *, 5* (1), 17-21.
Medina-Plaza, C., Beaver, J. W., Miller, K. V., Lerno, L., Dokoozlian, N., Ponangi, R., Blair, T., Block, D. E., & Oberholster, A. (2020). Cell Wall–Anthocyanin Interactions during Red Wine Fermentation-Like Conditions. *71* (2), 149-156.

Mendes-Pinto, M. M. (2009). Carotenoid breakdown products the—norisoprenoids—in wine aroma. *Archives of Biochemistry and Biophysics, 483* (2), 236-245.
Movahed, N., Pastore, C., Cellini, A., Allegro, G., Valentini, G., Zenoni, S., Cavallini, E., D'Incà, E., Tornielli, G. B., & Filippetti, I. J. J. o. p. r. (2016). The grapevine VviPrx31 peroxidase as a candidate gene involved in anthocyanin degradation in ripening berries under high temperature. *129* (3), 513-526.
Muganu, M., Bellincontro, A., Barnaba, F. E., Paolocci, M., Bignami, C., Gambellini, G., & Mencarelli, F. (2011). Influence of Bunch Position in the Canopy on Berry Epicuticular Wax during Ripening and on Weight Loss during Postharvest Dehydration. *American Journal of Enology and Viticulture, 62* (1), 91-98.
Oancea, S., Stoia, M., & Coman, D. (2012). Effects of Extraction Conditions on Bioactive Anthocyanin Content of Vaccinium Corymbosum in the Perspective of Food Applications. *Procedia Engineering, 42*, 489-495.
Ough, C., & Amerine, M. (1963). Use of grape concentrate to produce sweet table wines. *American Journal of Enology and Viticulture, 14* (4), 194-204.
Peng, Z., Iland, P. G., Oberholster, A., Sefton, M. A., & Waters, E. J. (2002). Analysis of pigmented polymers in red wine by reverse phase HPLC. *Australian Journal of Grape and Wine Research, 8* (1), 70-75.
Pirie, A., & Mullins, M. G. (1977). Interrelationships of Sugars, Anthocyanins, Total Phenols and Dry Weight in the Skin of Grape Berries during Ripening. *American Journal of Enology and Viticulture, 28* (4), 204-209.
Poojari, S., Alabi, O. J., Fofanov, V. Y., & Naidu, R. A. (2013). A leafhopper-transmissible DNA virus with novel evolutionary lineage in the family geminiviridae implicated in grapevine redleaf disease by next-generation sequencing. *PLOS ONE, 8* (6), e64194.
Price, S., Breen, P., Valladao, M., & Watson, B. (1995). Cluster sun exposure and quercetin in Pinot noir grapes and wine. *American Journal of Enology and Viticulture, 46* (2), 187-194.
Reynard, J., & Gugerli, P. (2015). Effects of Grapevine red blotch-associated virus on vine physiology and fruit composition of field grown grapevine cv. In: Gamay.
Robinson, A. L., Ebeler, S. E., Heymann, H., Boss, P. K., Solomon, P. S., & Trengove, R. D. (2009). Interactions between Wine Volatile Compounds and Grape and Wine Matrix Components Influence Aroma Compound Headspace Partitioning. *Journal of Agricultural and Food Chemistry, 57* (21), 10313-10322.
Roggero, J., Coen, S., & Ragonnet, B. (1986). High performance liquid chromatography survey on changes in pigment content in ripening grapes of Syrah. An approach to anthocyanin metabolism. *American Journal of Enology and Viticulture, 37* (1), 77-83.
Rumbaugh, A. C., Girardello, R. C., Cooper, M. L., Plank, C., Kurtural, S. K., & Oberholster, A. (2021). Impact of Rootstock and Season on Red Blotch Disease Expression in Cabernet Sauvignon (V. vinifera). *Plants, 10* (8), 1583.
Ryan, J.-M., & Revilla, E. (2003). Anthocyanin Composition of Cabernet Sauvignon and Tempranillo Grapes at Different Stages of Ripening. *Journal of Agricultural and Food Chemistry, 51* (11), 3372-3378.
Scalbert, A. (1991). Antimicrobial properties of tannins. *Phytochemistry, 30* (12), 3875-3883.
Smith, P. A., McRae, J. M., & Bindon, K. A. (2015). Impact of winemaking practices on the concentration and composition of tannins in red wine. *Australian Journal of Grape and Wine Research, 21* (S1), 601-614.

Song, J., Shellie, K. C., Wang, H., & Qian, M. C. (2012). Influence of deficit irrigation and kaolin particle film on grape composition and volatile compounds in Merlot grape (Vitis vinifera L.). *Food Chemistry, 134* (2), 841-850.

Sudarshana, M. R., Perry, K. L., & Fuchs, M. F. (2015). Grapevine red blotch-associated virus, an emerging threat to the grapevine industry. *Phytopathology, 105* (7), 1026-1032.

Vega, A., Gutiérrez, R. A., Pena-Neira, A., Cramer, G. R., & Arce-Johnson, P. (2011). Compatible GLRaV-3 viral infections affect berry ripening decreasing sugar accumulation and anthocyanin biosynthesis in Vitis vinifera. *Plant molecular biology, 77* (3), 261.

Waterhouse, A. L., Sacks, G. L., & Jeffery, D. W. (2016). *Understanding Wine Chemistry*: John Wiley & Sons.

Wilson, B., Strauss, C. R., & Williams, P. J. (1984). Changes in free and glycosidically bound monoterpenes in developing muscat grapes. *Journal of Agricultural and Food Chemistry, 32* (4), 919-924.

Yang, C., Wang, Y., Wu, B., Fang, J., & Li, S. (2011). Volatile compounds evolution of three table grapes with different flavour during and after maturation. *Food Chemistry, 128* (4), 823-830.

Zhou, L., He, H., Liu, R., Han, Q., Shou, H., & Liu, B. (2014). Overexpression of GmAKT2potassium channel enhances resistance to soybean mosaic virus. *BMC Plant Biology, 14* (1), 154.